Chapter-5

Part-I

Synthesis and mesomorphic properties of

(i) **5-Cyano-1,3-phenylene bis [4-(4-n-alkylbiphenyl-4-carbonyloxy) 2-fluorobenzoates] (Series-5.I)**

(ii) **5-Cyano-1,3-phenylene bis [4-(4-n-alkylbiphenyl-4-carbonyloxy) 3-fluorobenzoates] (Series-5.II)**

Part-II

Synthesis and mesomorphic properties of

(iii) **2-Cyano-1,3-phenylene bis [4-(4-n-alkylbiphenyl-4-carbonyloxy) 2-fluorobenzoates] (Series-5.III)**

(iv) **2-Cyano-1,3-phenylene bis [4-(4-n-alkylbiphenyl-4-carbonyloxy) 3-fluorobenzoates] (Series-5.IV)**

A brief introduction to banana-shaped mesogens exhibiting B_7 and SmC_G phases

One of the most interesting features of liquid crystalline phases is the fascinating and the beautiful optical textures that they exhibit. The different textural characteristics have been used to identify the mesophases of compounds made up of rod-like and disk-like molecules. These include compounds composed of both chiral and achiral molecules. The relationship between the chemical structure of the bent-core compounds and the mesomorphic behaviour is not comparable to those known for calamitics. The bent-core compounds containing four phenyl rings do not appear to be liquid crystalline, and most of the compounds reported so far contain five phenyl rings [32]. In addition, both six and seven phenyl ring esters have also been reported and the seven-ring compounds broaden the thermal range of the mesophases [36, 42, 61].

Compounds composed of banana-shaped molecules are quite sensitive to lateral substituents especially on the central and the outer phenyl rings. The occurrence of mesophases in such compounds containing lateral substituents greatly depends on the number of phenyl rings present in the bent-core structure [61] and also the nature and position of the lateral substituents. For example, compounds substituted at position-5 of the central phenyl ring such as 5-cyano, 5-methoxy, or 5-methyl inhibit the formation of liquid crystalline phases [32]. However, compounds derived from 2-methyl- and 2-nitro-resorcinol are known to exhibit very interesting mesophases [32].

Although one of the most fascinating mesophases exhibited by banana-shaped compounds which is structurally complicated is the B_7 phase which was first reported [32, 44] in some Schiff's base derivatives of 2-nitroresorcinol. This mesophase exhibits several beautiful optical textures when cooled slowly from the isotropic phase and none of these variants is seen in any of the other banana phases. One such characteristic texture of this phase is that of helical or spiral filaments resembling telephone wires [44]. Such filamentary growth patterns have also been observed in some sulphur containing compounds [55, 68] which show antiferroelectric switching behaviour, and a ferroelectric liquid crystal conglomerate exhibited by compounds composed of racemic molecules [54], some novel halogen substituted banana-shaped mesogens [51, 56, 57] and a salicylaldimine ester [107] with a two- or three-dimensional structure exhibiting antiferroelectric switching behaviour and all of these are derived from resorcinol. Also, some fluorine substituted compounds [51] do exhibit these

two- or three-dimensional periodic patterns which have been observed for B_7 phase and this mesophase shows ferroelectric switching behaviour and is designated as B_{7bis}. In all these cases, the observation of spiral growth domains in the samples is the dominant feature and based on this, the symbol B_7 has been assigned. This assignment is purely based on optical textures and is independent of the XRD and the electro-optical switching behaviour.

Though the B_7 phase was discovered in 1997 [32], till now there is no complete understanding about the structure of this mesophase. Recently, Clark *et al.* [114] speculated that B_7 phase might have a three-dimensional modulated structure (having a polarization splay) based on some experimental studies which they have carried out on B_7 materials synthesized by several groups. The proposed structural model for this mesophase is some what similar to a B_1 phase, except that there is polarization splay and modulation as found for the standard materials synthesized by the Halle group. A different model has been proposed for the remaining B_7 phases which are switchable. According to this model, these switchable phases can have antiferroelectric ordering within the layers and there by changing its polarization sign at the modulation via leaning of the molecules. They also suggest that the polarization splay defects drive the modulation. It should also be emphasized here that the number of compounds exhibiting this phase is small in number. To arrive at any meaningful description regarding the relationship between molecular structure and the occurrence of B_7 phase, more compounds have to be synthesized and hence the present investigations which are described in Part-**II** of this chapter.

The possibility of smectic phases with triclinic symmetry (chiral C_1 symmetry) which is referred to as SmC_G phase (G stands for generalized) was predicted by de Gennes [46]. This has not been possible so far to obtain in calamitic liquid crystals. This phase is characterized by two tilt directions with respect to the layer normal in BC compounds: (i) tilt of the molecular plane in which smectic layers will have in-layer polarizations and may form both ferro- and or antiferro-electric phases and (ii) tilt of the molecular kink direction (leaning) in which smectic layers can have out-of-layer polarization and may form both ferro- and or antiferro-electric phases. In otherwords, SmC_G phase shows synleaning and antileaning structures in addition to synclinic and anticlinic configurations. A pair of adjacent layers (synclinic or anticlinic) can have the rotation of synleaning or antileaning and hence the SmC_G phase can exist in eight diasteriomeric forms [100]. Among these, four are chiral conglomerates: (i) synleaning or antileaning of synclinic ferroelectric and (ii) synleaning or

antileaning of anticlinic antiferroelectric states. The remaining four are macroscopic racemates: (i) synleaning or antileaning of synclinic antiferroelectric and (ii) synleaning or antileaning of anticlinic ferroelectric states. Although a compound exhibiting the SmC_G phase has not been proved unambiguously, recently Jakli *et al.* [100], Walba *et al.* [108] and Rauch *et al.* [91] have claimed some mesophase structures which exhibit out-of-layer polarization in addition to in-layer polarization with triclinic symmetry. The investigations carried out on the mesophases exhibited by compounds derived from 5-cyanoresorcinol and described in Part-**I** of this chapter, suggest the existence of a SmC_G phase in some of these compounds.

Part-I

Results and discussion

In 1998, Weissflog *et al.* [30, 32] reported a bent-core compound derived from 5-cyanoresorcinol without any liquid crystalline phase. They also suggested that the cyano group substitution at position-5 prevents the formation of any mesophase in such five-ring compounds [48]. Until now, there is no bent-core compound derived from 5-cyanoresorcinol exhibiting a mesophase that has been reported. Herein, we report detailed synthetic procedures as well as the mesomorphic behaviour of two new homologous series of seven-ring compounds derived from 5-cyanoresorcinol. These are symmetrical seven-ring esters containing a fluorine on the middle phenyl ring of the arms of the bent-core as shown in structure **5.I**.

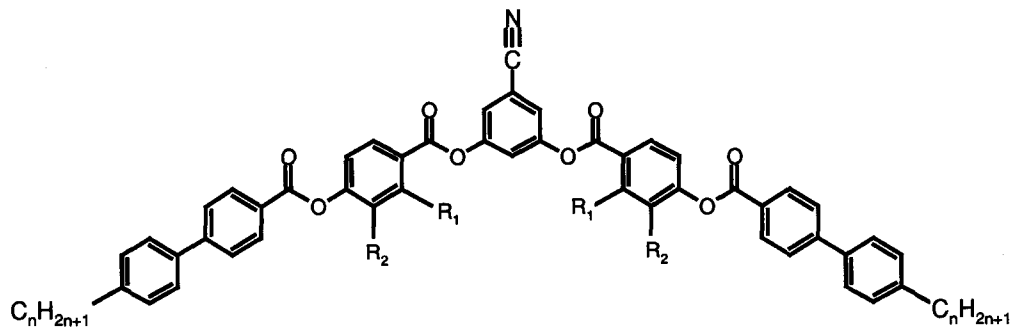

n=5, 6,.....12, 14, 16, 18

R_1=F, R_2=H Series-**5.I**

R_1=H, R_2=F Series-**5.II**

Structure 5.I

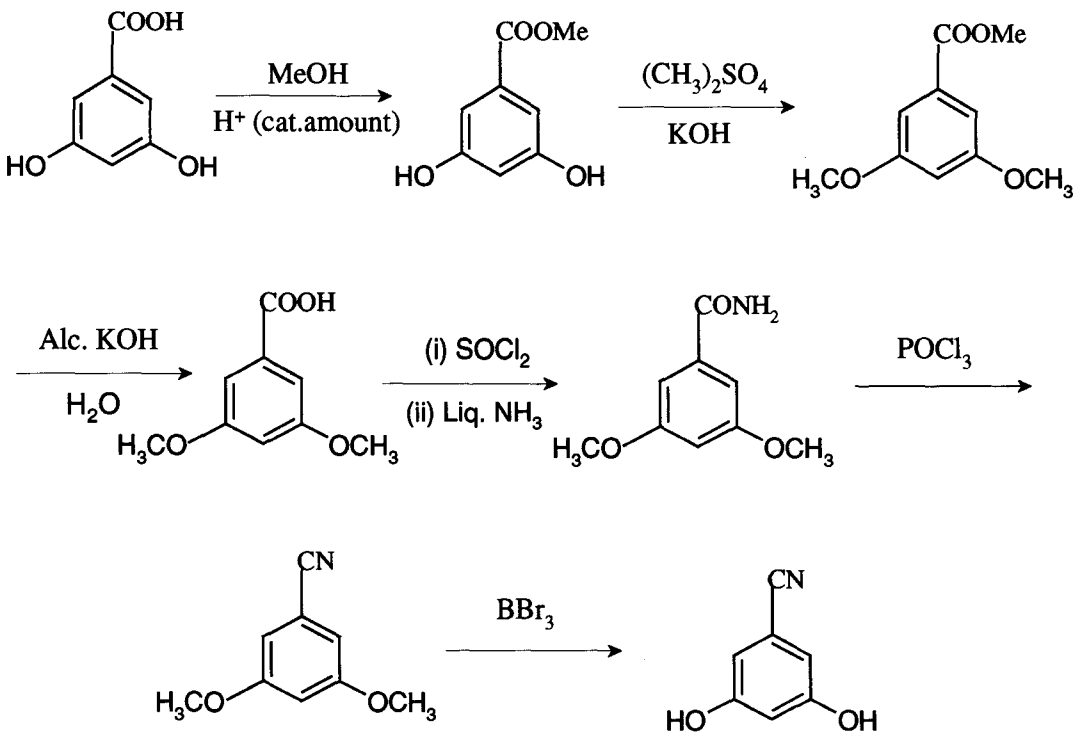

Fig. 5.1. Synthetic pathway employed for the preparation of 5-cyanoresorcinol.

The synthesis of the two homologous series of compounds composed of achiral symmetrical bent-core molecules containing a cyano substituent at position-5 on the central phenyl ring and a fluorine substituent on the phenyl ring adjacent to it in the arms of the seven-ring esters was carried out as shown in scheme **5.1**. The synthesis of 5-cyanoresorcinol from 3,5-dihydroxybenzoic acid was achieved following a route shown in figure **5.1**. Methyl 3, 5-dimethoxybenzoate was obtained by the esterification of commercially available 3, 5-dihydroxybenzoic acid followed by methylation using dimethyl sulphate. 3,5-Dimethoxybenzoic acid was obtained by the hydrolysis of the ester thus obtained. The resultant carboxylic acid was converted to its amide by refluxing it in thionyl chloride and after removal of excess thionyl chloride treating it with liquid ammonia. The dehydration of amide gave the corresponding 3,5-dimethoxybenzonitrile which on demethylation gave 5-cyanoresorcinol [109]. The synthesis of 2-fluoro-4-benzyloxybenzoic acid and 3-fluoro-4-benzyloxybenzoic acids have already been described in Chapter-**2**. 4-n-Alkylbiphenyl-4-carboxylic acids were synthesized according to a procedure described earlier [111] and the transition temperatures obtained agree well with the literature values.

The synthesis of 5-cyano-1,3-phenylene bis [4-(4-n-alkylbiphenyl-4-carbonyloxy)2- or 3-fluorobenzoates] were carried out as follows. 2- or 3-Fluoro-4-benzyloxybenzoic acid was

esterified with 5-cyanoresorcinol using N, N^{l}-dicyclohexylcarbodiimide (DCC) in the presence of a small quantity of 4-(N,N-dimethylamino)pyridine (DMAP) in anhydrous dichloromethane at room temperature. The product, 5-cyano-1,3-phenylene bis (2- or 3-fluoro-4-benzyloxybenzoate) was purified and subjected to hydrogenolysis with 5% Pd-C in 1,4-dioxane. The bis-phenol obtained viz. 5-cyano-1,3-phenylene bis (2- or 3-fluoro-4-hydroxybenzoate) was again esterified with an appropriate 4-n-alkylbiphenyl-4-carboxylic acids using DCC and DMAP. The desired products were purified by column chromatography on silica gel using chloroform as an eluent and finally by repeated crystallization using suitable solvents.

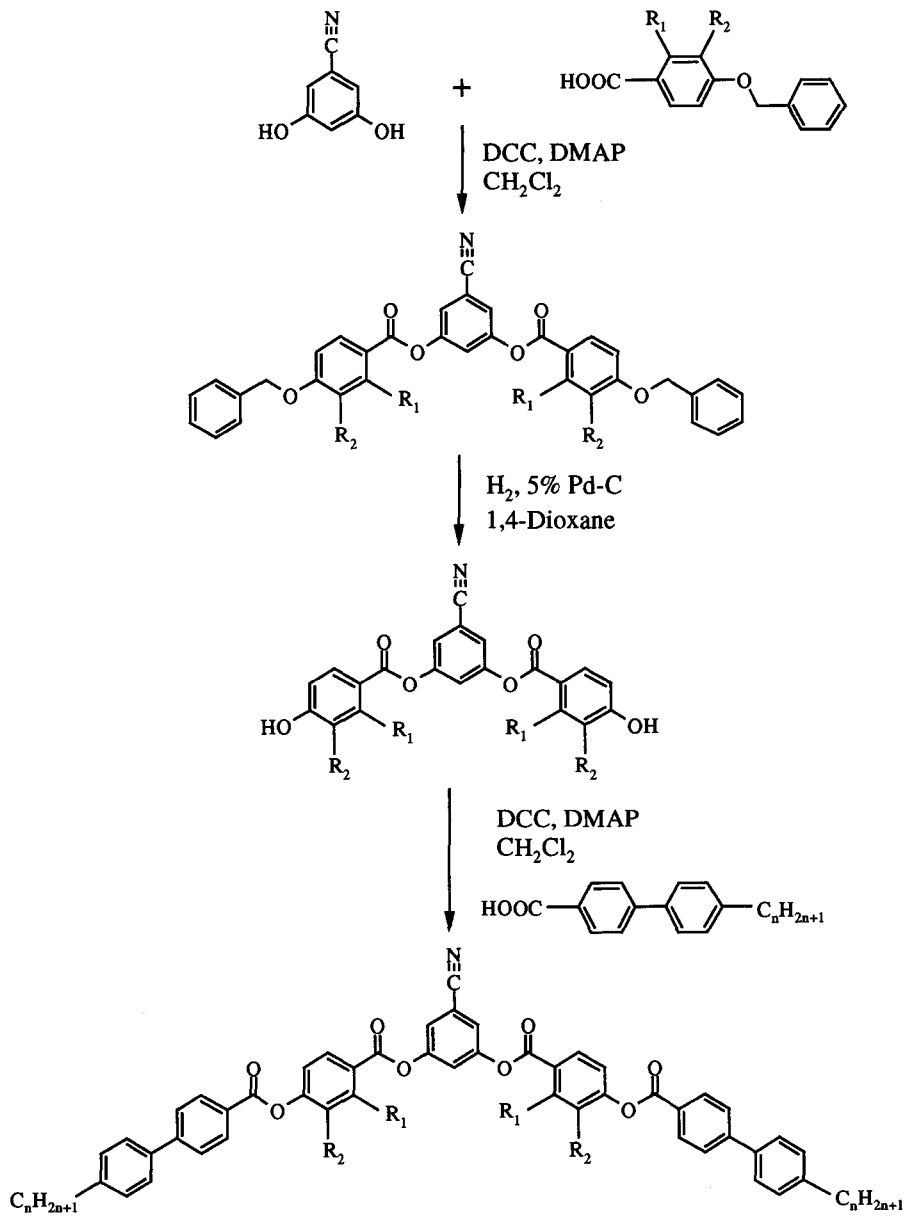

Scheme 5.1. General pathway used to synthesize the seven-ring symmetrical banana-shaped mesogens.

Mesomorphic properties of compounds derived from 5-cyanoresorcinol: series 5.I and 5.II.

Two new homologous series (**5.I** and **5.II**) of bent-core compounds containing a highly polar cyano group on the central phenyl ring in the direction of polar axis and a fluorine substituent on the middle phenyl ring of the arms of the bent-core compounds have been synthesized and their mesomorphic properties are reported here.

The two homologous series of compounds, series **5.I** and **5.II** differ only in the position of the fluorine substituent. In compounds of series **5.I**, a fluorine is substituted at *ortho* position while in series **II** it is at *meta* position w.r.t. the carboxylate group of the phenyl ring adjacent to the central phenyl ring. In both series of compounds only two kinds of mesophases are observed. The transition temperatures and the associated enthalpy values obtained for compounds of series **5.I** and **5.II** are summarized in tables **5.1** and **5.2** respectively. Let us look at the mesomorphic properties of the lower homologues of series **5.I**. On slow cooling of the isotropic liquid of compound **5.A.3,** a dendritic pattern develops which coalesce to form a mosaic texture. Sometimes spherulitic growth could also be seen which is the signature for a two-dimensional structure. These textural features strongly point towards a two-dimensional rectangular columnar phase, namely a B_1 mesophase. Similar textural features are observed for the other homologues viz. **5.A.1**, **5.A.2** and **5.A.4**. The clearing transition enthalpy value obtained for this mesophase is in the range of 25-27 $kJmol^{-1}$ and the corresponding melting transition enthalpy is also in the range of 26-28 $kJmol^{-1}$. This value increases gradually on increasing the n-alkyl chain length. Surprisingly, compound **5.A.5** is not liquid crystalline and this is the homologue where a cross over from B_1 to B_2-like phase occurs. Similarly, the lower homologues of series **5.II** (**5.B.1**, **5.B.2**, **5.B.3** and **5.B.4**) also show a B_1 phase, the melting and clearing enthalpy values obtained are about 20-32 $kJmol^{-1}$ and 21-27 kJ mol^{-1} respectively. Both the melting and clearing transition enthalpies increase on ascending the series. The structure of the B_1 phase was further confirmed by XRD studies which showed a rectangular lattice. The d-spacings and the corresponding lattice parameter values obtained for compounds **5.A.2** and **5.B.1** are given in table **5.3**. In addition, both the compounds show a wide-angle diffuse peak at about 4.8 Å indicating the fluidity of the alkyl chains in the mesophase.

The higher homologues of series **5.I** (**5.A.6** to **5.A.10**) and **5.II** (**5.B.5** to **5.B.8**) show similar textural features and are completely different from the textures observed for the lower

Table 5.1. Transition temperatures (°C) and enthalpies ($kJmol^{-1}$) (*in italics*) for compounds of series 5.I.

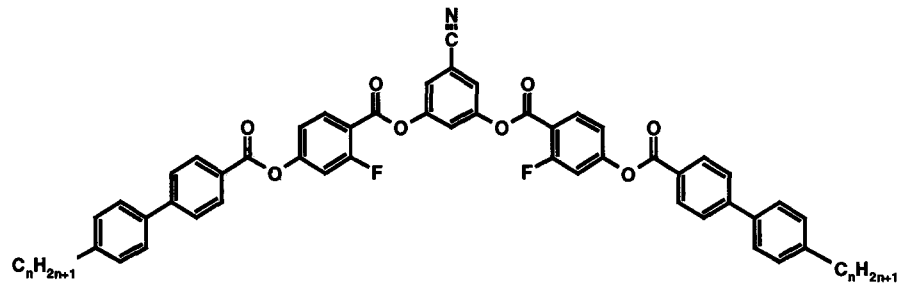

Compound	n	Cr		B_2-like		B_1		I
5.A.1	5	.	177.5	-		.	216.0	.
			25.2				*23.5*	
5.A.2	7	.	179.0	-		.	206.0	.
			28.4				*26.1*	
5.A.3	8	.	182.0	-		.	195.5	.
			27.9				*26.5*	
5.A.4	9	.	189.0	-		.	192.0	.
			29.0				*26.5*	
5.A.5	10	.	189.5	-		-		.
			48.1					
5.A.6	11	.	183.5	.	188.0	-		.
			28.8		*29.1*			
5.A.7	12	.	178.0	.	188.0	-		.
			27.4		*29.9*			
5.A.8	14	.	172.5	.	188.5	-		.
			33.8		*30.1*			
5.A.9	16	.	166.5	.	188.0	-		.
			40.2		*30.6*			
5.A.10	18	.	161.0	.	187.0	-		.
			46.4		*30.9*			

Cr=Crystalline phase; B_2-like=Variant of a B_2 phase; B_1=Two-dimensional rectangular columnar phase; I= Isotropic phase; . Phase exists; - Phase does not exist.

Table 5.2. Transition temperatures (°C) and enthalpies ($kJmol^{-1}$) (*in italics*) for compounds of series 5.II.

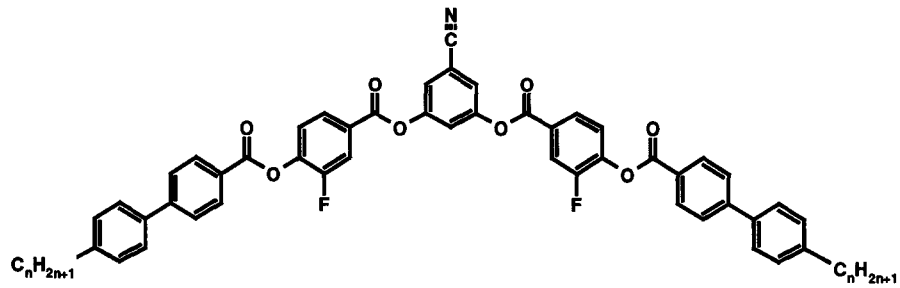

Compound	n	Cr		B_2-like		B_1		I
5.B.1	8	.	155.0	-		.	205.0	.
			19.9				*25.5*	
5.B.2	9	.	157.0	-		.	201.0	.
			19.9				*27.4*	
5.B.3	10	.	156.0	-		.	195.0	.
			22.1				*27.4*	
5.B.4	11	.	156.0	-		.	189.5	.
			23.9				*27.5*	
5.B.5	12	.	158.0	.	184.3	.	184.5[c]	.
			30.3				*27.2*	
5.B.6	14	.	152.0	.	184.0	-		.
			38.4		*27.3*			
5.B.7	16	.	145.0	.	182.0	-		.
			34.9		*27.6*			
5.B.8	18	.	141.5	.	181.0	-		.
			38.0		*28.4*			

c: enthalpy denoted is the sum of both the phase transitions.

homologues. Compound **5.B.6** shows the following textural features. Upon cooling the isotropic liquid, a schlieren texture with beaded filaments as well as a fingerprint pattern which is normally seen for a B_2 phase is obtained and is shown in figure **5.2.** The appearance of the schlieren texture suggests an inhomogeneous in-plane orientation of the director field. However, on very slow cooling of the isotropic liquid, this mesophase grows as filaments, long in size and coalesce to an undefined texture (bright) as shown in figures **5.3a** and **5.3b.** Sometimes these filaments transform to a helical pattern. A photomicrograph showing this transition is shown in figure **5.3c.** In addition, short single-spiral helix can be seen to grow directly from the isotropic liquid. No other textural patterns were observed for these materials that are normally seen for a B_7 phase. Sometimes the mesophase also exhibits circular domains in which the dark brushes are oriented parallel to the directions of crossed polarizers

(domain 1) and in some other domains they rotate in clock-wise (domain 2) and anticlock-wise (domain 3) directions. A typical photomicrograph obtained in a homogeneously aligned cell (thickness of 5.5 μm) showing these features is shown in figures **5.4a** and **5.4b**. Some of these circular domains exhibit equidistant concentric stripes which are indicative of helicoidal periodicity for the mesophase as shown in figure **5.5**. Also, this mesophase exhibits very unusual textures as shown in figures **5.3c** and **5.6a**. The schlieren texture obtained shows both s= ± 1/2 and s= ±1 dark brushes as shown in figure **5.6b**. Though the mesophase appears with some textural features of a B_2 phase, the additional complex textural patterns indicate that this may be a variant of B_2 phase which will be discussed later. Hence, this mesophase has been considered as B_2-like phase. Similar textural complexity could be observed for the other homologues in the series. The clearing transition enthalpy values increase from 27.9 to 30.9 $kJmol^{-1}$ on ascending the homologous series. It is interesting to note that the clearing enthalpy value is rather high. The corresponding melting enthalpy value is in the range of 28-47 $kJmol^{-1}$. Similarly, for series **5.II**, clearing transition enthalpy value obtained increases from 25.6 to 26.3 $kJmol^{-1}$ and the corresponding melting enthalpy value is in the range of 30-33 $kJmol^{-1}$. A DSC thermogram obtained in the B_2-like phase exhibited by compound **5.B.6** is shown in figure **5.7**. Many crystal-crystal transitions are seen in both heating and cooling cycles.

Fig. 5.2. Optical photomicrograph of a typical B_2-like phase texture obtained for compound 5.B.6.

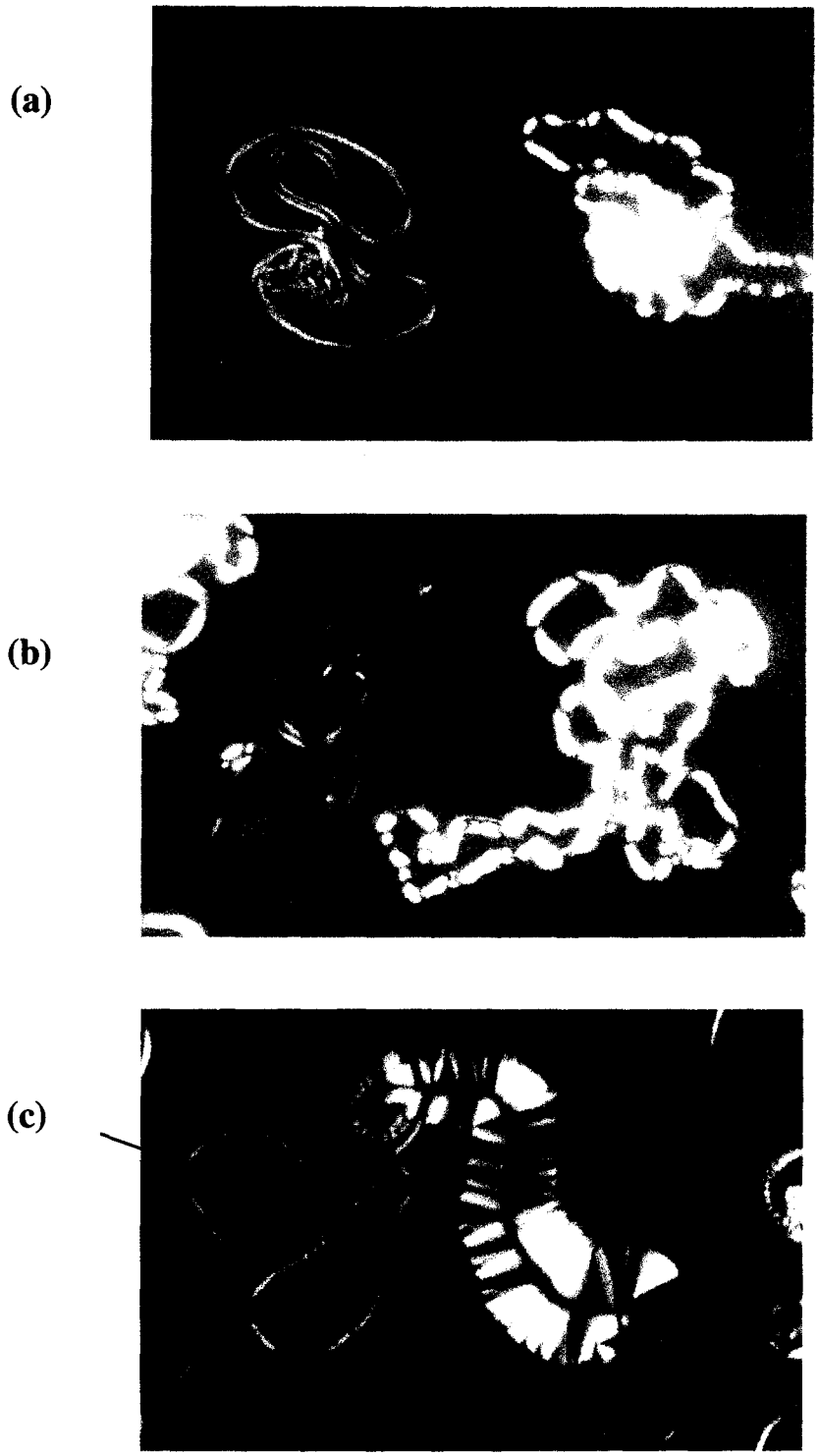

Fig. 5.3. Optical photomicrographs of the growth of filaments from the isotropic phase of compound 5.B.6. In both (a) and (b), the left hand side shows the growth of the filaments and adjacent to these the collapsed filaments can be seen. In (c), the transition from a filamentary pattern to a helical pattern (as indicated by the arrow) can be seen.

(a)

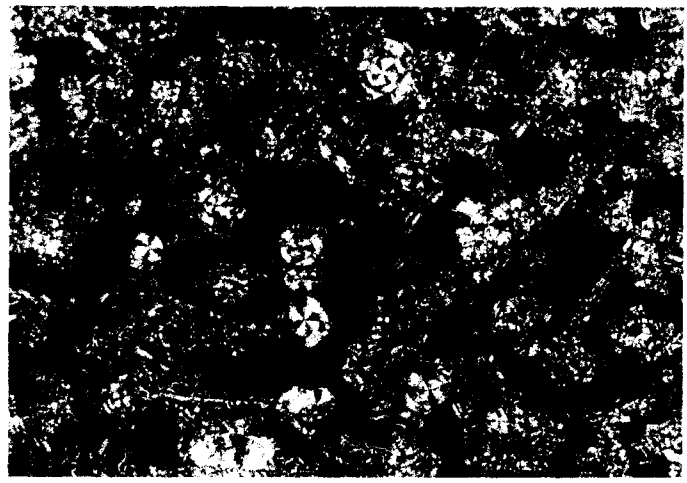

(b)

domain 3

domain 2

domain 1

Fig. 5.4. Optical photomicrographs (a) and (b) obtained in a homogeneously aligned cell of a sample of compound 5.B.6 showing single-winded helical pattern, circular domains and schlieren texture on cooling the isotropic liquid.

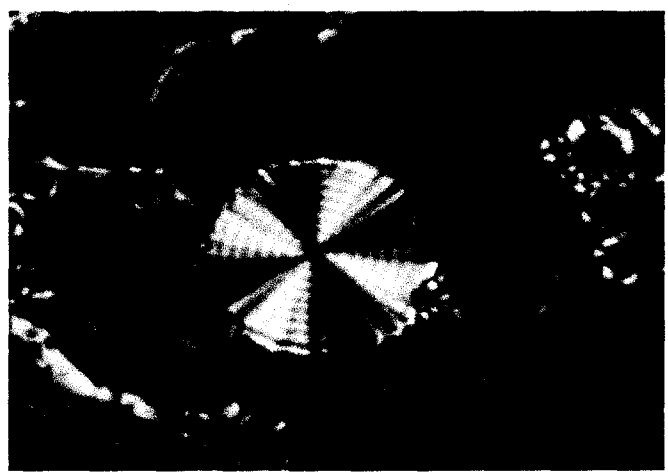

Fig. 5.5. Photomicrograph showing a circular domain in which equidistant circular stripes indicative of helical periodicity for the mesophase of compound 5.B.6.

(a)

(b)

Fig. 5.6. Photomicrographs showing (a) the appearance of a complicated textural pattern in which both helical as well as filamentary patterns are obtained on cooling the isotropic liquid of compound 5.B.6 and (b) a schlieren texture comprising both 4- and 2-brush defects for the same compound.

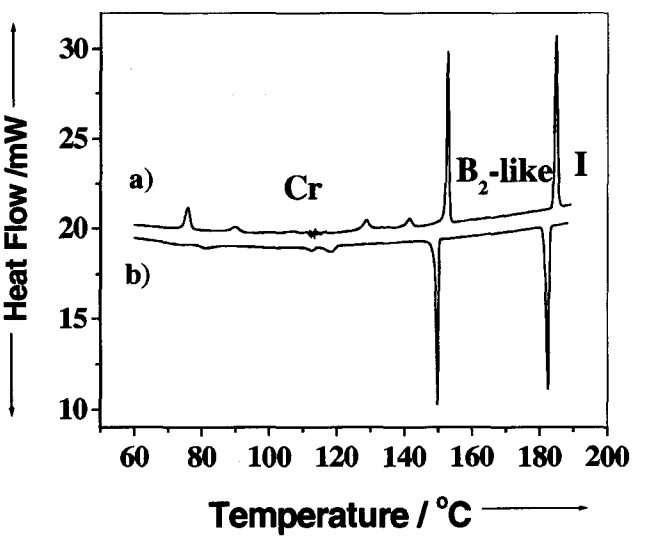

Fig. 5.7. A DSC thermogram obtained for compound 5.B.6; a) heating cycle; b) cooling cycle; rate 5°C min^{-1}.

The understanding of the occurrence of these filaments is again a complex problem. Meyer *et al.* [112] reported the filamentary growth pattern at the I-SmA phase transition and recently it has been observed even at I-SmC phase transition in a single component system [113] for the first time. According to Meyer *et al.*[112], the negative surface tension anisotropy ($\Delta\gamma < 0$) is a necessary condition for the formation of filaments. $\Delta\gamma = \gamma^{\parallel} - \gamma\perp$, where $\gamma\parallel$ and $\gamma\perp$ are the surface tensions for interfaces parallel and perpendicular to the smectic layers. For a number of systems ($\Delta\gamma > 0$, but filaments can be produced only for those materials in which $\Delta\gamma < 0$. The surface tension associated with the interface separating the isotropic liquid and mesophase is anisotropic (formation of filaments). On further cooling, the filaments formed transform to chiral helical structures as shown in figure **5.3c**. One of the possible explanations is as follows. In general, synclinic antiferroelectric (racemic) structure appears at high temperatures when compared with an anticlinic antiferroelectric (chiral) structure in a given mesophase [108] and this is thermodynamically and entropically favoured. In this manner, the transformation of filaments to helical structure may be due to a phase transition from SmC_SP_A to SmC_AP_A on lowering the temperature. The origin of the helical filaments is perhaps due to the leaning of molecules on lowering the temperature, which cannot be excluded.

Interestingly, only one compound **5.B.5** exhibits two mesophases. On very slow cooling a thin film of the sample to a temperature of 182.5°C, the textures obtained (mosaic as well as the spherulites) are indicative of a two-dimensional B_1 phase. On further cooling to 182.3 °C, along with the B_1 phase texture, schlieren texture as well as fingerprint patterns are observed. This indicates the phase transition from B_1 to a B_2-like phase. On further cooling, the texture of a B_2-like phase dominates but the B_1 phase features could also be seen. The textural photomicrograph obtained at this transition is shown in figure **5.8**. However, no indication of such a transition could be observed in a DSC thermogram and the enthalpy denoted in table **5.2** is the sum of both the transitions.

In table **5.3**, the XRD data is given for many compounds exhibiting the B_2-like mesophase which suggests a tilted smectic phase. The calculated tilt angle is about 42-45°. In all these cases, a wide-angle diffuse maxima is obtained at about 4.8 Å indicating the absence of in-plane order. The X-ray angular intensity profile obtained in the B_2-like mesophase exhibited by compound **5.B.8** is shown in figure **5.9**.

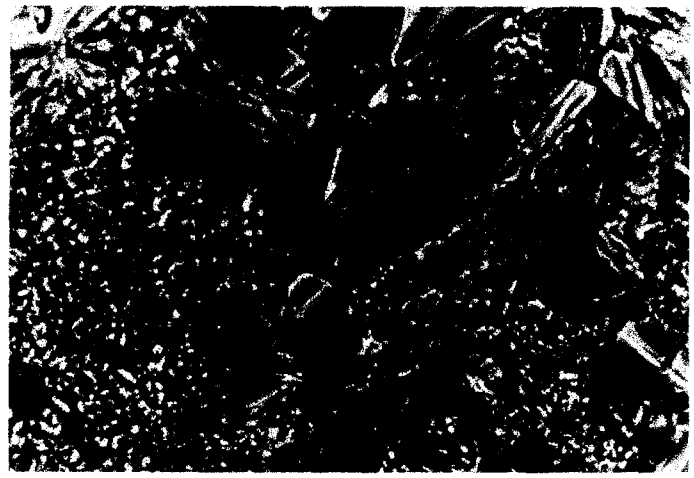

Fig. 5.8. Optical photomicrograph showing the co-existence (0.2°C) of both spherulites (B_1 phase) and the texture of a B_2-like phase exhibited by compound 5.B.5.

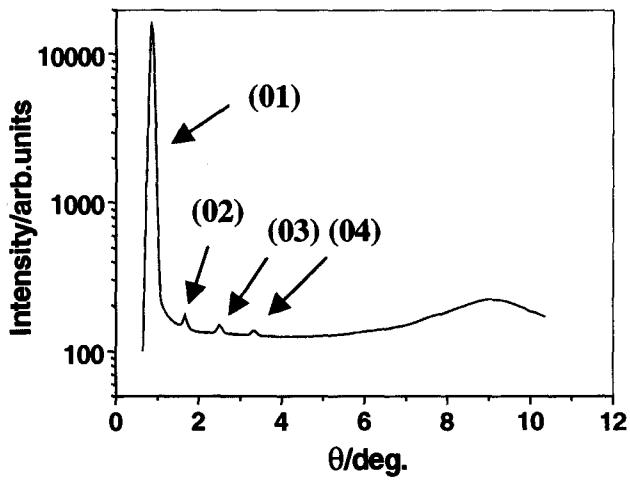

Fig. 5.9. X-Ray angular intensity profile obtained in the mesophase of compound 5.B.8 at 150°C indicating a lamellar ordering.

Table 5.3. The measured spacings (d/Å) in the small angle region for the mesophases of different compounds.

Compound	d-spacings Å / Miller indices	Phase type	T/°C
5.A.2	27.4(11), 22.4(02); **a**=34.5 Å, **b**=45 Å	B_1	185
5.A.6	40.0 (01), 20.0 (02)	B_2-like	184
5.A.8	42.9 (01), 21.4 (02), 14.3 (03)	B_2-like	175
5.A.9	45.5 (01)	B_2-like	170
5.B.1	31.7 (11), 23.5 (02); **a**=43 Å, **b**=47 Å	B_1	160
5.B.5	40.4 (01), 20.2 (02)	B_2-like	165
5.B.8	52.0 (01), 26.0 (02), 17.3 (03), 13.0 (04)	B_2-like	145

The electro-optical studies were carried out for the mesophase of several compounds under investigation and in detail for compound **5.B.6**. The mesophase of this compound shows the following unusual switching behaviour. A sample of this compound was taken between two ITO coated glass plates which were coated with polyimide and unidirectionally rubbed to get a homogeneous alignment. The cell thickness was measured to be 8.5 μm. On very slow cooling of the isotropic liquid under a dc electric field of about 50V, the mesophase appears as circular domains in which the extinction cross makes an angle with respect to the directions of the crossed polarizers as observed under a polarizing microscope. On reversing the polarity of the applied field, the domains with extinction cross rotating in a clock-wise direction now rotate in an anticlock-wise direction and vice-versa. On switching off the electric field (0V), the extinction cross obtained in these circular domains reorient along the directions of the crossed polarizers. For example, consider the domains **I** and **II** in figure **5.10**, **a**, **b** and **c**. In the absence of the electric field (0V), the extinction cross obtained orient along the directions of the crossed polarizers as shown in figure **5.10a**. By the application of an electric field (figure **5.10b**) the extinction cross in domain **I**, rotates in an anticlock-wise direction while domain **II** rotates in a clock-wise direction with respect to the crossed polarizers. This clearly suggests the existence of chiral domains of opposite handedness. The dark extinction cross obtained at zero electric field (figure **5.10a**) is an evidence for the anticlinic-antiferroelectric (SmC_AP_A) ordering of the bent-core molecules in adjacent layers in these circular domains. At a saturated dc field, the domains (**b** and **c**) exist in a synclinic-ferroelectric state (SmC_SP_F) and these are chiral states. The saturated optical tilt angle estimated is about $\pm$ 36°. A schematic representation of the arrangement of molecules in adjacent layers in each domain that are responsible for the occurrence of heterochiral domains (opposite polarity and tilt) are also shown in figure **5.10**. Interestingly, the dark brushes obtained rotate linearly (electro-clinic effect) from SmC_AP_A state to SmC_SP_F state on increasing the dc electric field and saturates at 7 $V\mu m^{-1}$. However, no bistabilty could be observed in this mesophase even for small cell thickness of about 4.5μm and the dark brushes always relax by turning off the applied field. In addition, racemic ground state domains could also be seen in which the dark brushes obtained exist along the directions of the crossed polarizers. No change in position of the dark brushes is observed either by reversing the polarity of the applied field or in the absence of the field as shown in figure **5.11**. These observations suggest that these domains must be having a macroscopic racemic structure.

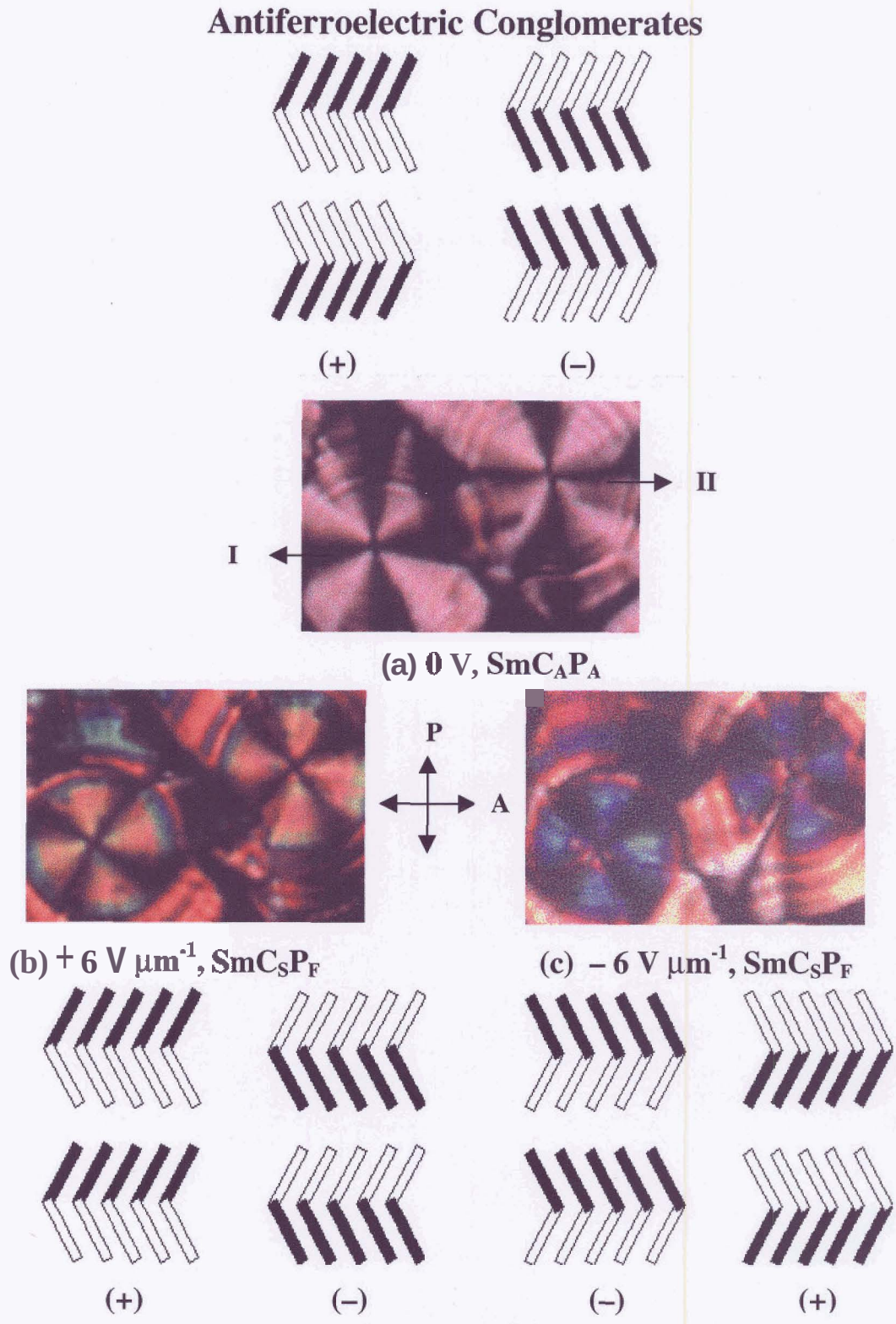

Fig. 5.10. Focal-conic circular domains of opposite handedness (I, II) obtained under a polarizing microscope for the mesophase of compound 5.B.6. (a) 0 V, (b) + 6 Vμm^{-1} and (c) − 6Vμm^{-1}. A schematic representation of the molecular organization (tilt and polarity) in such heterochiral domains exhibiting tristable switching is also presented. The solid line of the BC molecules represents the orientation above the plane and the other is below the plane. The (+) and (–) sign indicate the two chiral domains of opposite handedness

Even more interestingly, the birefringence changes with the variation of the dc field as shown in figure **5.12** and this is reversible. The colour of the texture changes gradually from purple red (2 $V\mu m^{-1}$) to violet (4 $V\mu m^{-1}$) and from violet (4 $V\mu m^{-1}$) to green (6 $V\mu m^{-1}$) on increasing the electric field. These change take place in two steps. Based on these observations, one can estimate that the wavelength reduces initially (from red to violet) and then increases (violet to green) gradually on increasing the field. From the available data it is difficult to explain this mechanism. One possibility could be that a phase transition takes place from SmC_SP_A to SmC_AP_A on application of the electric field. This phase transition could reduce the average birefringence. On increasing the voltage further, the phase transition into the SmC_SP_F takes place and that could increase the birefringence. However, this mechanism may also be due to the leaning of molecules, which cannot be excluded.

As shown in figure **5.4**, on cooling the isotropic liquid and viewing under a polarizing microscope, some circular domains are obtained in which the dark brushes make an angle with respect to the directions of the crossed polarizers (for example domains 2 and 3). At lower voltages no effect could be observed. However, at high electric fields (> 5$V\mu m^{-1}$) the dark brushes rotate along the orientation directions of the crossed polarizers. No switching could be observed by reversing the polarity of the electric field. On turning off the electric field the dark brushes remain unchanged and the additional circular striped pattern could be

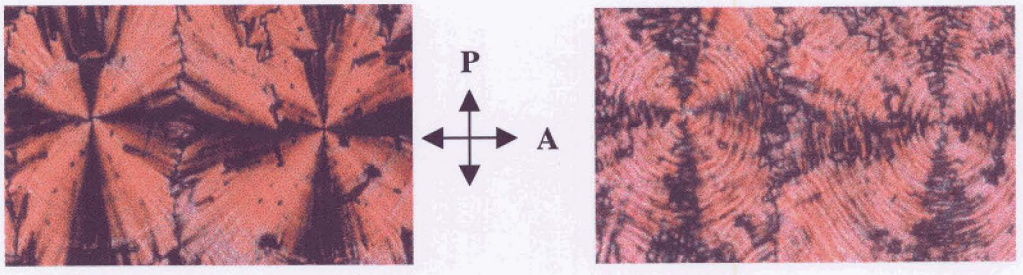

(a) ± 10 V μm^{-1} **(b)** 0 V μm^{-1}

Fig. 5.11. Photomicrographs showing (a) the racemic ferroelectric state obtained in the B_2-like phase of compound 5.B.6 by the application of dc field and (b) texture obtained on turning off the electric field, clearly indicating the racemic nature of the domains. Note that the dark brushes obtained exist along the directions of the crossed polarizers.

observed as shown in figure **5.11b**. This indicates the existence of synclinic-antiferroelectric (SmC_SP_A) ground state racemic domains. Under the electric field a racemic anticlinic-

ferroelectric state (SmC_AP_F) is produced and is probably stabilized by the surface. In any case, the anticlinic ferro- and antiferro-electric structures are stabilized under these conditions.

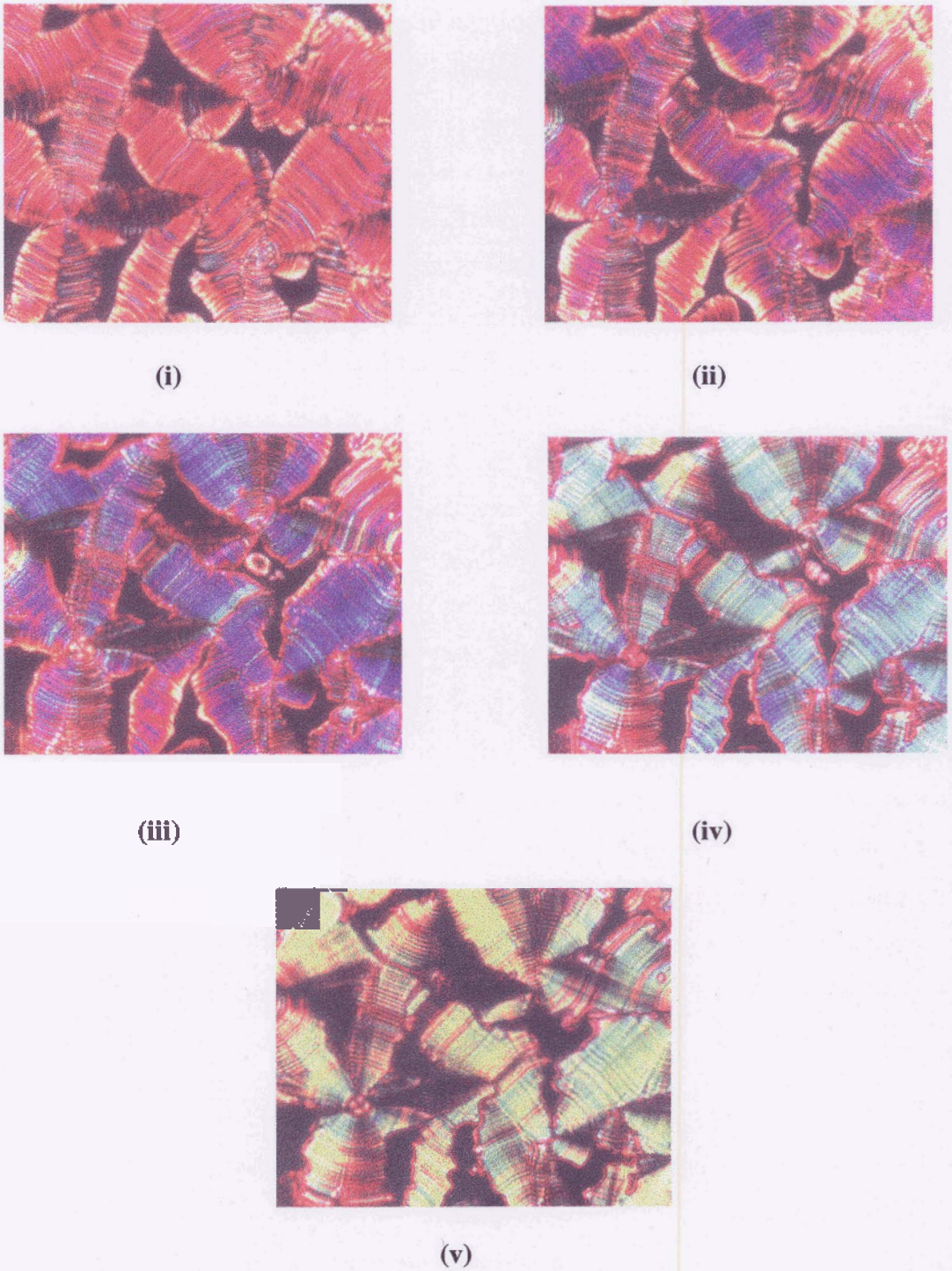

Fig. 5.12. Photomicrographs of the mesophase of compound 5.B.6 showing change in colour (birefringence) with the variation of dc field (increasing voltage). (i) 2 Vμm^{-1}, purple red; (ii) 3 Vμm^{-1}, dark violet; (iii) 4 Vμm^{-1}, blue & violet; (iv) 5 Vμm^{-1}, cyanish blue; (v) 6 Vμm^{-1}, yellowish green.

In addition, triangular-wave electric field experiments were carried out in order to confirm the antiferroelectric ground state and also to measure the polarization value for the mesophase of the same compound. The sample was taken in a 10 μm thick cell as described above for dc field experiments. On application of a triangular-wave electric field of about ± 75 V (threshold voltage is about ± 50 V) and at a frequency of 50 Hz, a broad single polarization current peak was observed for each half cycle indicating a ferroelectric-type switching behaviour for the mesophase. The polarization current peak obtained completely disappears in the isotropic phase and reappears on cooling. This clearly confirms that the polarization peak obtained is not due to ionic impurities or the cell. The calculated polarization value obtained is about 490 nC cm^{-2} and the current response trace obtained is shown in figure **5.13a.** However, on increasing the voltage further, at a second threshold voltage of about ± 110 V, a second polarization current peak appears (origin of the peak is shown by arrow in figure **5.13b**) and saturates at about ±150 V. This is the signature for the antiferroelectric ground state of the mesophase. The saturated polarization value obtained by integrating the area under the two current peaks is about 885 nC cm^{-2}. The resultant triangular-wave current response is shown in figure **5.13b.** The high polarization value may be attributed to the polar cyano group which is present and whose dipole is along the direction of the polar axis. The optical photomicrographs obtained at zero field, after the first and the second threshold voltages are shown in figure **5.14.** It can be seen that at zero electric field, a striped pattern could be observed and at the first threshold voltage, part of this pattern disappears. At higher voltages, these stripes completely disappear and exhibit a smooth fan-shaped texture. This complicated switching behaviour perhaps suggests a strong influence of the surface on the existing mesophase. Since this compound has a highly polar cyano group along the direction of the polar axis, the influence of the surface can be high. Observation of a single polarization broad current peak at lower voltages may be due to switching of a partially unwound state of the antiferroelectric structure.

As pointed out by Jakli *et al.* [100], in the B_2 phase where the polarization has only in-plane component, the equidistant circular smectic layers (fan-shaped texture) can satisfy this requirement. In the SmC_G or B_7 phase, the compensation of divergence of the out-of-layer polarization requires an additional coiling of the filaments or ribbons. The formation of helical filaments can average out the out-of-layer polarization and stabilizes. The out-of-layer polarization is due to the leaning of BC molecules within the smectic layers. Thus, in the present investigations, the formation of helical filaments as well as the spontaneously

obtained chiral circular domains (fig. **5.5**) clearly indicate the possibility of leaning of the molecules which produces the out-of-layer polarization. The leaning angle may be small and hence the electro-optical switching behaviour is observed. Since, this is a smectic phase, the possibility of a B_7 phase can safely be ruled out. These findings point towards a SmC_G phase and hence this mesophase is designated as B_2-like phase to differentiate it from a normal B_2 phase.

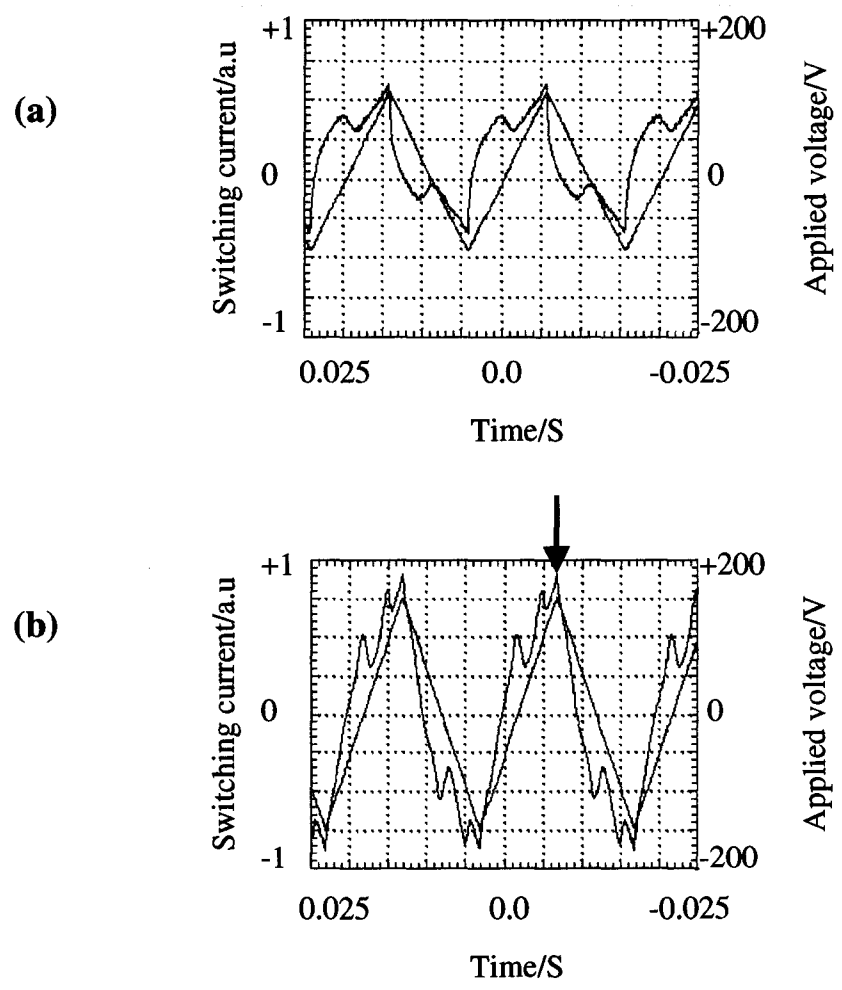

Fig. 5.13. Switching current response obtained for the mesophase exhibited by compound 5.B.6 by applying a triangular-wave voltage at 160°C. Cell thickness 10 *μm*; (a) ± 75 V, 50 Hz, $P_S \approx 490$ nC cm^{-2}; (b) ± 150 V, 50 Hz, $P_S \approx 885$ nC cm^{-2}.

(a)

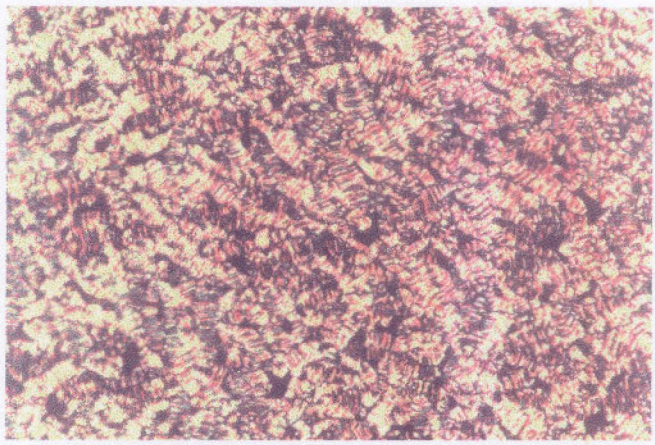

(b)

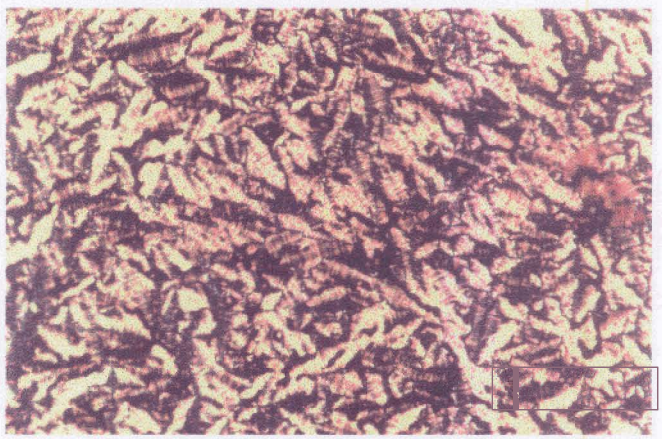

(c)

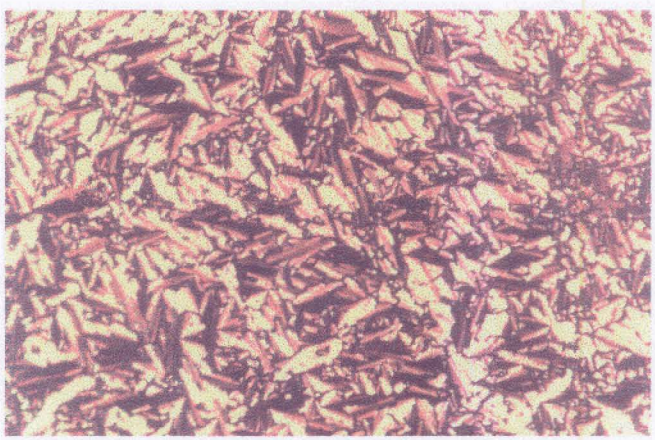

Fig. 5.14. The change in textural pattern observed by the application of a triangular-wave electric field of (a) 0 V, (b) ± 75 V, 50 Hz (above the first threshold voltage), and (c) ± 150 V, 50 Hz (above the second threshold voltage) for compound 5.B.6.

Influence of the position of fluorine substituent (series 5.I and 5.II):

The two homologous series of compounds differ from one another by the position of the fluorine substituent. The position of fluorine substituent strongly influences the transition temperatures, especially the melting points and also the stability of both the mesophases. When a fluorine is substituted at *meta* position w.r.t. the carboxylate group on the middle phenyl ring (series **5.II**) of the arms of the bent-core, both melting and clearing temperatures are reduced and the thermal range of the mesophase also increase when compared with the other series of compounds(series **5.I**). The B_1 mesophase is stabilized even for the higher homologues (**5.B.3**, **5.B.4** and **5.B.5**) if a fluorine is at *meta* position (series **5.II**). The stability of the individual mesophases may also depend on the orientation directions of the polar fluorine (F) substituent w.r.t. the polar axis. A plot of the melting as well as the clearing transition temperatures as a function of n-alkyl chain length obtained for the homologues of series **5.I** is shown in figure **5.15a**. A steep decreasing trend is observed for B_1-I transition temperatures while the B_2-like to I transition temperatures curve is almost horizontal. The melting points also increase for the shorter chain lengths and then gradually decrease on ascending the homologous series **5.I** and hence the mesophases are completely suppressed for the middle homologues. For example, compound **5.A.5** does not show a mesophase and perhaps this is a cross over homologue in which the lower homologues exhibit a B_1 phase and the higher homologues show a B_2-like mesophase as shown in figure **5.15a**. Similar trend could be observed for the homologues of series **5.II**, but the effect is minimal as shown in figure **5.15b**. The B_1-I and B_2-like to I transition point curves show similar trends in both the series of compounds.

(a)

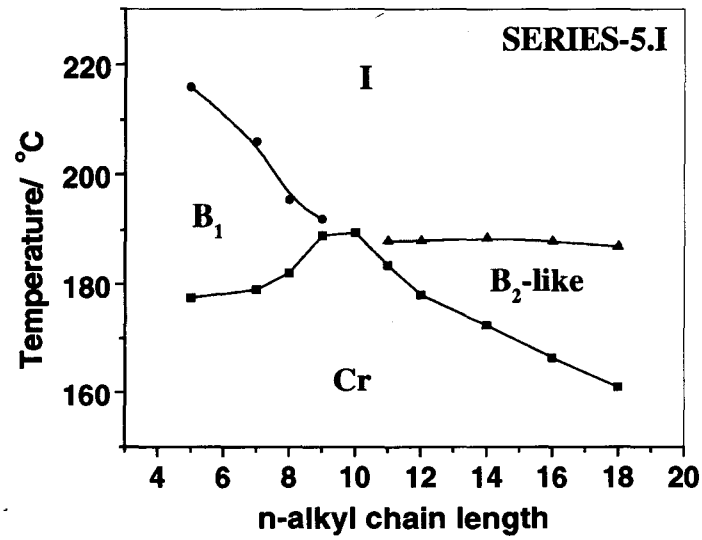

(b)

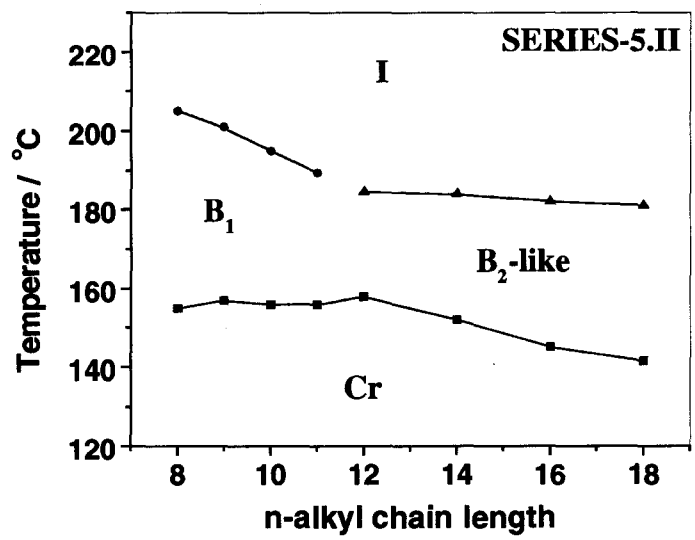

Fig. 5.15. Plots of the transition temperatures as a function of the number of carbon atoms in the n-alkyl chain obtained for (a) series 5.I and (b) series 5.II.

Part-II

In this part, the synthesis, characterization and mesomorphic properties of two homologous series of compounds derived from 2-cyanoresorcinol have been reported. These are the first banana-shaped mesogens derived from 2-cyanoresorcinol. The side wings of these bent-core molecules contain a fluorine substituent (R_1 / R_2=F) as shown in the general molecular structure **5.II.**

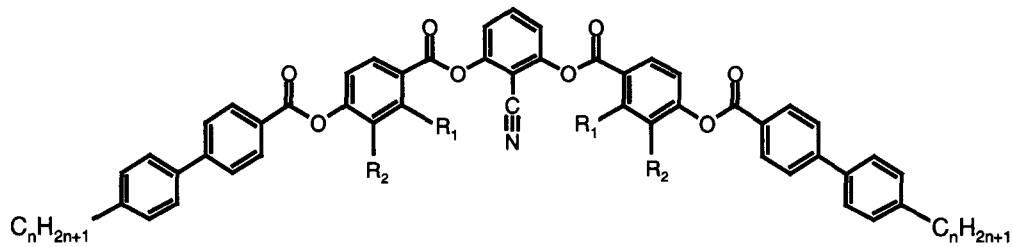

n=5, 6,.....12, 14, 16, 18

R_1=F, R_2=H Series-**5.III**

R_1=H, R_2=F Series-**5.IV**

Structure 5.II

2-Cyanoresorcinol [110] was prepared from commercial 2,6-dimethoxybenzonitrile by demethylation using borontribromide. Using this 2-cyanoresorcinol, two homologous series of compounds (series **5.III** and **5.IV**) having the general molecular structure **5.II** have been synthesized following the synthetic pathway shown in scheme **5.2.** 2- or 3-Fluoro-4-benzyloxybenzoic acid was esterified with 2-cyanoresorcinol using N, N^{I}-dicyclohexylcarbodiimide (DCC) in the presence of a catalytic quantity of 4-(N,N-dimethylamino)pyridine (DMAP) in anhydrous dichloromethane at room temperature. The product, 2-cyano-1,3-phenylene bis (2- or 3-fluoro-4-benzyloxybenzoate) obtained was purified and subjected to hydrogenolysis using 5% Pd-C as catalyst and 1,4-dioxane as solvent. The bis-phenol obtained viz. 2-cyano-1,3-phenylene bis (2- or 3-fluoro-4-hydroxybenzoate) was further esterified with an appropriate 4-n-alkylbiphenyl-4-carboxylic acid in the presence of DCC and DMAP. The desired product was purified by column chromatography on silica gel using chloroform as an eluent and finally by repeated crystallization using a suitable solvent.

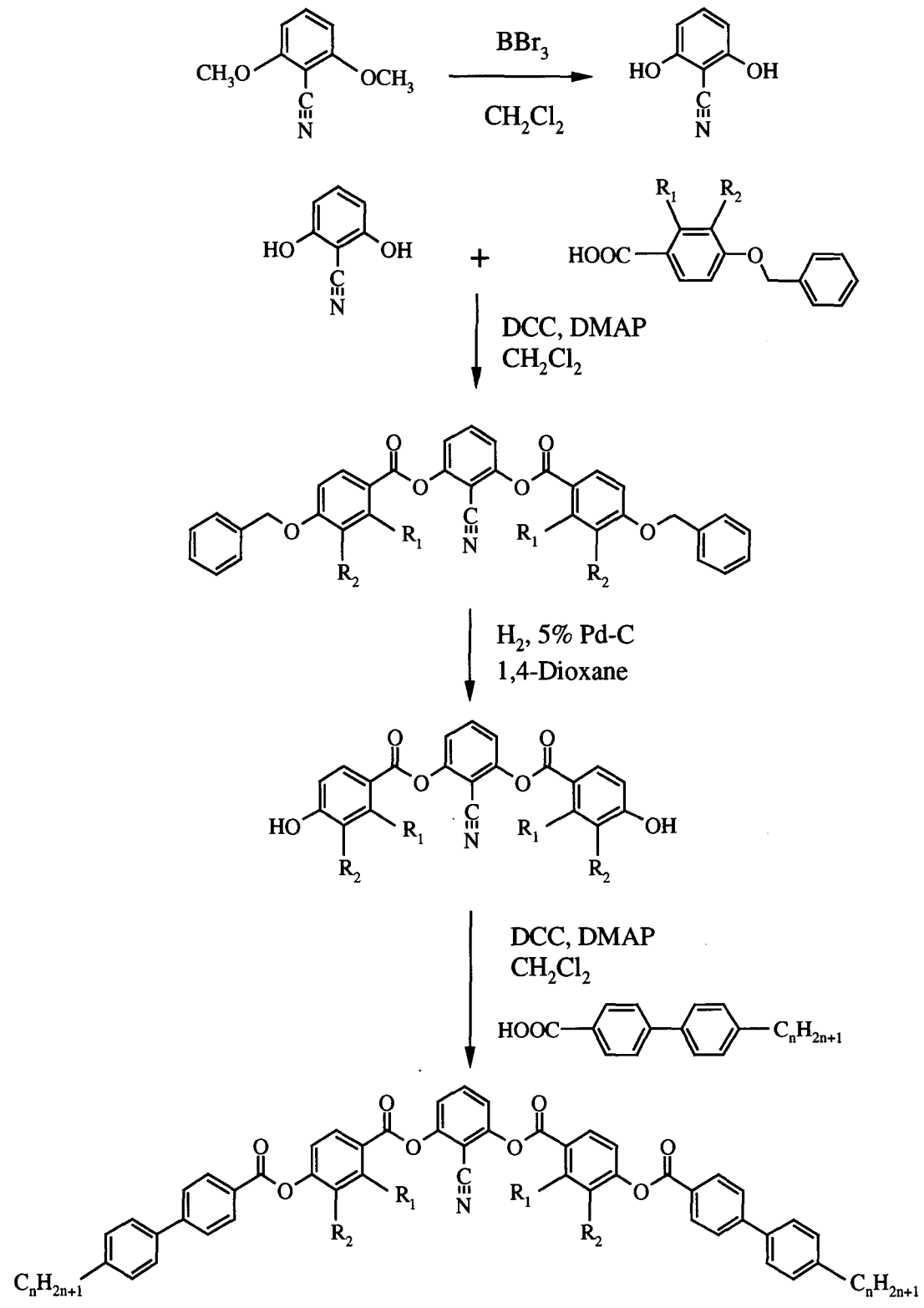

Scheme 5.2. General pathway used to synthesize the seven-ring symmetrical banana-shaped mesogens.

Mesomorphic properties of compounds derived from 2-cyanoresorcinol: series 5.III and 5.IV.

The phase transition temperatures and the associated enthalpies for the two homologous series (series **5.III** and **5.IV**) of symmetrically substituted compounds about the central phenyl ring are summarized in tables **5.4** and **5.5** respectively. In series **5.III**, a fluorine is substituted *ortho* to the carboxylate group while in series **5.IV** it is in *meta* position. Of a total of twenty compounds synthesized and investigated, eighteen are monomesomorphic, one is dimesomorphic and one compound does not show any mesophase. Compounds **5.C.1** to **5.C.4** exhibit a monotropic mesophase, compounds **5.D.2** and **5.D.3** are enantiotropic mesomorphic and all these six compounds exhibit the same type of mesophase. On cooling the isotropic liquid of these compounds, as thin films between two glass plates, and observed under a polarizing microscope, colourful circular domains appear which grow in size and coalesce. Sometimes they also show a mosaic texture. Typical textures obtained for compound **5.D.3** is shown in figure **5.16**. The enthalpy of the clearing transition for this mesophase is about 20 $kJmol^{-1}$. The textures of this mesophase resemble those of the two-dimensional B_1 phase.

However, for two-dimensional structures, X-ray diffraction studies give conclusive evidence. The mesophase of compound **5.D.3** shows a diffuse maxima in the wide-angle region at about 4.7 Å indicating a liquid-like in-plane order. In the small angle region three sharp reflections at d_1=31.8 Å, d_2=20.2 Å and d_3=15.9 Å are obtained. These cannot be indexed as due to reflections from a simple layered structure but is indicative of a two-dimensional structure. On the basis of the assignment for the structure of B_1 phase, the reflection at d_1=31.8 Å can safely be excluded as due to half molecular length of this compound assuming that the chains are in a fully stretched all *trans* conformation (58 Å). If we assume the second reflection d_2=20.2 Å as due to half molecular length (02), then the other two reflections $d_1$and d_3 can be indexed as (11) and (22) respectively for a B_1 phase with a two-dimensional rectangular lattice. From this assumption, the obtained lattice parameters are **a**=51.5 Å and **b**=40.4 Å as shown in table **5.6**. However, this would mean a very large tilt of the molecules (tilt angle 45°) in the B_1 phase and such a large tilt has not been observed in the usual two-dimensional rectangular B_1 phase reported for a number of other compounds. Hence, this mesophase is designated as B_1'. The angular intensity profile of the mesophase of this compound is shown in figure **5.17**. It has not been possible to get a perfectly oriented monodomain sample to confirm the exact structure of this mesophase.

Table 5.4. Transition temperatures (°C) and enthalpies (kJmol^{-1}) (*in italics*) for compounds of series 5.III.

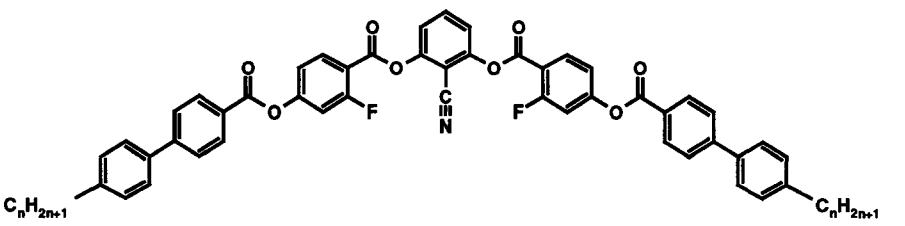

Compound	n	Cr		B_7		B_1^l		I
5.C.1	5	.	149.0 *39.0*	-		(.	143.0)[a]	.
5.C.2	6	.	144.0 *41.8*	-		(.	140.0) *17.0*	.
5.C.3	7	.	146.0 *53.7*	-		(.	138.0) *19.4*	.
5.C.4	8	.	141.5 *52.5*	-		(.	134.5) *21.3*	.
5.C.5	9	.	136.5 *30.2*	.	137.5 *23.4*	-		.
5.C.6	10	.	130.5 *33.7*	.	141.0 *25.0*	-		.
5.C.7	11	.	138.0 *38.5*	.	144.5 *26.6*	-		.
5.C.8	12	.	134.5 *36.7*	.	146.0 *26.7*	-		.
5.C.9	14	.	131.0 *40.0*	.	148.0 *28.5*	-		.
5.C.10	16	.	124.0[b] *58.6*	.	149.0 *28.7*	-		.
5.C.11	18	.	123.0[b] *59.4*	.	149.5 *30.2*	-		.

a: temperature obtained on cooling; enthalpy could not be determined as the sample crystallizes immediately.

b : compound has crystal-crystal transition; enthalpy denoted is the sum of all previous transitions.

Cr=Crystalline phase; B_7=Two- or Three-dimensional banana phase with helical super-structure; B_X=Unidentified two- or three-dimensional banana phase; B_1^l= Variant of B_1 phase; I= Isotropic phase; . Phase exists; - Phase does not exist.

Table 5.5. Transition temperatures (°C) and enthalpies (kJmol^{-1}) (*in italics*) for compounds of series 5.IV.

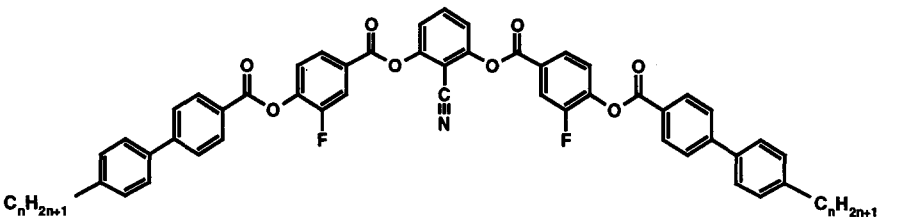

Compound	n	Cr		B_x		B_7		B_1'		I
5.D.1	5	.	162.0	-		-		-		.
			47.8							
5.D.2	8	.	142.0	-		-		.	147.0	.
			24.6						*20.9*	
5.D.3	9	.	140.5	-		-		.	146.0	.
			45.6						*21.8*	
5.D.4	10	.	125.0	(.	95.0)	.	148.0	-		.
			31.2		*1.3*		*25.2*			
5.D.5	11	.	128.0	-		.	151.0	-		.
			28.1				*25.7*			
5.D.6	12	.	131.0	-		.	152.5	-		.
			44.6				*26.6*			
5.D.7	14	.	122.5	-		.	154.0	-		.
			35.9				*27.4*			
5.D.8	16	.	117.0	-		.	155.0	-		.
			47.5				*29.1*			
5.D.9	18	.	112.0	-		.	154.5	-		.
			38.4				*29.9*			

The contact preparation of the mesophase of compound **5.D.3** with one of the standard compounds which exhibits a B_1 phase (compound **51** in ref. 61), shows the boundary between the two phases as shown in figure **5.18**. On cooling the isotropic liquid of both compounds, at the contact, a depression in clearing temperature of about 6°C was seen indicating that the ground state structures of these two phases may not be the same.

The mesophases of compounds **5.C.5** to **5.C.11** and **5.D.4** to **5.D.9** exhibit several different textures similar to those observed for 2-nitro-1,3-phenylene bis [4-(4-n-alkoxyphenylimino-methyl)benzoates] (n-OPIMB-NO_2) [44] for which the symbol B_7 has been assigned and represent the standard materials for such a mesophase. It is interesting to note that in both the standard as well as the present series of compounds, the temperature range of the B_7 phase increases on ascending the series. Also, the thermal range is larger for *meta* fluorine

substituted compounds (series **5.IV**) with compound **5.D.9** having a thermal range of about 42.5 °C. The clearing transition enthalpy values obtained for this mesophase in both the series are quite high (about 25 to 30 $kJmol^{-1}$) when compared with the other known B-phases and are comparable to that of the standard compound exhibiting the B_7 phase. A DSC thermogram obtained for one of the compounds exhibiting a B_7 phase is shown in figure **5.19**.

The microscopic textures of the B_7 phase exhibited by the present series of compounds is not only fascinating but interesting. When a thin film of isotropic liquid of compound **5.D.4** is cooled slowly, several different textural variants can be seen. One of the common textural features seen for this mesophase is the growth of single- and double-spiral structures, filaments etc., and a photomicrograph of this is shown in figure **5.20**. Sometimes domains containing equidistant concentric bands are seen and this is indicative of helical periodicity in the mesophase. The various other complex textures that are obtained for this B_7 mesophase is shown in figure **5.21**. These textural variants observed in the above two series of compounds are very similar to those reported for the B_7 mesophase of the standard n-OPIMB-NO_2 series of compounds.

The XRD of an unoriented sample of compound **5.C.8** at 138°C shows the following reflections. As usual, in the wide-angle region a diffuse maxima at 4.8 Å was seen indicating the absence of an in-plane order. In the small angle region five reflections were obtained. These are d_1=57.8 Å, d_2=37.6 Å, d_3=18.8 Å, d_4=12.6 Å and d_5=7.7 Å. This complex pattern rules out a lamellar structure and indicates a two- or three-dimensional ordering of the molecules for the mesophase. The angular intensity profile of the mesophase of this compound is shown in figure **5.22**. Similar X-ray diffraction pattern has been obtained for the B_7 phase of some n-OPIMB-NO_2 derivatives [48]. As a consequence of this and from the characteristic textural features, we have identified the mesophases of compounds **5.C.5** to **5.C.11** and **5.D.4** to **5.D.9** as B_7. Since perfectly oriented samples are difficult to obtain, the exact structural features of the B_7 phase are not yet understood completely.

We have carried out electric field experiments on the B_7 mesophase of the two series of compounds under investigation. For example compound **5.D.6** was taken in a cell (thickness 6.5 μm) which was constructed for planar alignment. On application of a triangular-wave electric field up to ± 40 $V\mu m^{-1}$, there was no evidence of switching seen under a polarizing microscope. This was carried out at different temperatures of the mesophase and varying frequencies from 1 Hz to 100 Hz.

Fig. 5.16. The different textural patterns obtained in the B_1' phase of compound 5.D.3 on cooling the isotropic liquid.

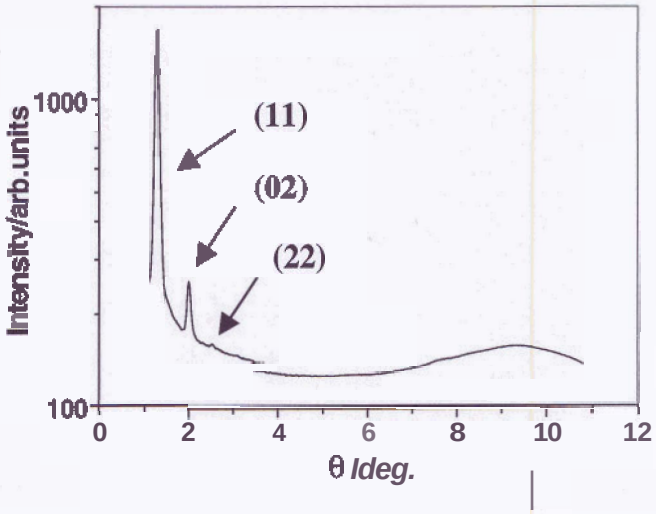

Fig. 5.17. The X-ray angular intensity profile obtained in the B_1^l mesophase of compound 5.D.3 at 142°C.

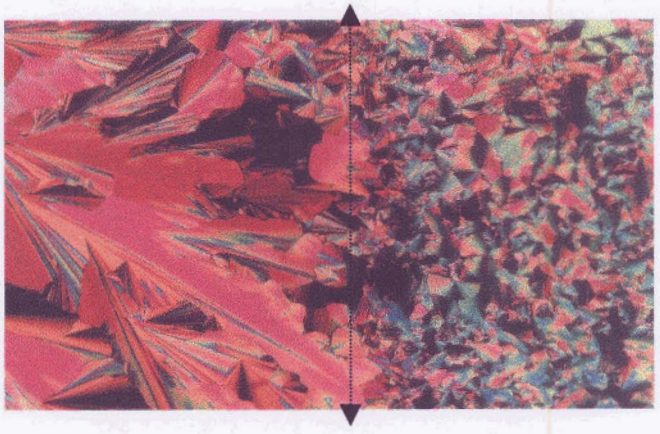

Fig. 5.18. The contact preparation between the B_1^l mesophase (left-side)of compound 5.D.3 and a B_1 mesophase (right-side) of a standard (compound 51 in ref. 61) showing the boundary between the two mesophases which is indicated by a dotted line.

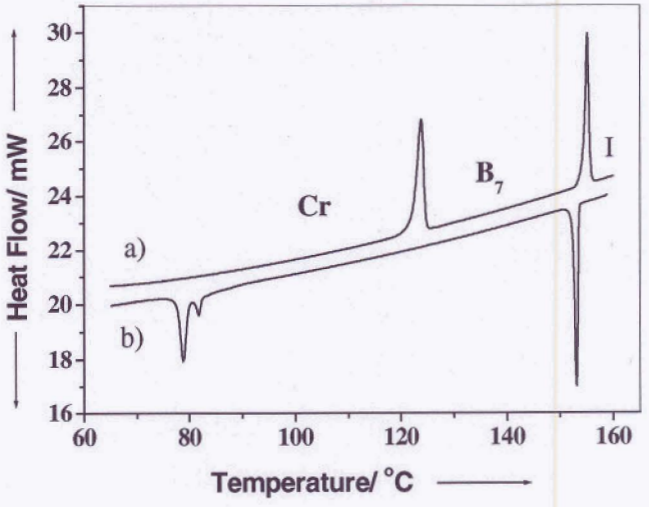

Fig. 5.19. Differential *scanning* calorimetric scan of compound 5.D.7; a) heating cycle, b) cooling cycle; rate 5°C min^{-1}.

Similarly, when a dc electric field was applied to the same cell, up to 16 $V\mu m^{-1}$ no change, either in the position of the dark brushes or the colour of the circular domains was visible.

In order to verify if the B_7 mesophase does switch, we carried out triangular-wave electric field experiments with one of the standard compounds viz. 12-OPIMB-NO_2 using the same experimental procedure described above. We did not observe any switching up to ± 40 $V\mu m^{-1}$. This supports our view that the mesophase exhibited by compounds of the n-OPIMB-NO_2 series [32] as well as the present series of compounds (**5.C.5** to **5.C.11** and **5.D.4** to **5.D.9**) containing a strongly polar cyano group at position-2 in the central phenyl ring belong to the same mesophase type. In contrast, Jakli *et al.* [45] have reported evidence for electro-optical switching in 2-nitro-1,3-phenylene bis [4-(4-n-octyloxyphenyliminomethyl)benzoate.

Interestingly compound **5.D.4** shows a highly metastable phase on supercooling the B_7 phase at 95°C. The textural changes at the transition are minimal and it is difficult to see the same under a polarizing microscope. But this transition can be clearly seen on a DSC thermogram as the change is accompanied by a small enthalpy (1.3 $kJmol^{-1}$). Since the phase is metastable and we are unable to obtain a perfectly oriented sample for X-ray diffraction studies, it has not been possible to characterize this mesophase completely and hence we have designated this mesophase as a B_X phase. The XRD of this highly metastable phase shows the following reflections. The wide-angle peak at 4.8 Å is retained and a change in the pattern in the small angle region is seen. These reflections correspond to d_1=45 Å, d_2 =34 Å, d_3=22.6 Å, d_4=11.4 Å, d_5=7.3 Å and d_6=6.9 Å. Since the structure of the higher temperature B_7 phase itself has not been understood, it is difficult to speculate the structure of this higher ordered mesophase. Hence we have designated this as B_X phase. Surprisingly this B_X phase has been observed in only one homologue. The XRD data obtained in the B_7 mesophase for the other homologues is recorded in table **5.6**.

Plots of the transition temperatures as a function of the number of carbon atoms in the n-alkyl chain for the two series (**5.III** and **5.IV**) of compounds are shown in figure **5.23**. While the clearing points for B_1 phase shows a downward trend in both the series, that for the B_7 clearing points rise initially and appear to level off as the chain length is increased. These two plots represent the first example of B_7-I transition point curves for homologous series of compounds.

In order to confirm that the mesophase exhibited by the higher homologues of the two series of compounds (**5.C.5** to **5.C.11** and **5.D.4** to **5.D.9**) is the same, we have carried out miscibility studies with a standard material, viz. 2-nitro-1,3-phenylene bis [4-(4-n-dodecyloxyphenyliminomethyl)benzoate] (12-OPIMB-NO_2). This compound was synthesized and has the following transition temperatures: Cr 85.5 B_7 173.0 I; these temperatures agree well with what is reported in the literature [32]. Compound **5.D.6** and the standard material were mixed well in the isotropic phase as weight % compositions and investigated using POM, DSC and XRD methods. The isomorphous binary phase diagram thus obtained is shown in figure **5.24**. One can see that the clearing temperatures are not very sharp and varies from 1°C to about 8°C. This is probably due to the incompatibility of the two systems which are made up of five and seven phenyl rings. Also, the standard compound is a Schiff's base ester while compound **5.D.6** is an ester. The eutectic temperature is obtained for about 60 weight % of compound **5.D.6**. Apart from this, it is clear from this diagram that there is complete miscibility between the mesophases of these two compounds over the entire composition range indicating that the mesophase exhibited by compound **5.D.6** is indeed B_7.

Table 5.6. The measured spacings (d/Å) from XRD in the small angle region for the mesophases of different compounds.

Compound	d-spacings Å / Miller indices	Phase type	T/°C
5.C.5	49.9, 33.1, 22.1, 17.4, 16.2, 7.7	B_7	135
5.C.8	57.8, 37.6, 18.8, 12.6, 7.7	B_7	138
5.C.10	59.7, 41.9, 20.6, 14.0	B_7	130
5.D.3	31.8 (11), 20.2 (02), 15.9 (22); **a**=51.5 Å, **b**=40.4 Å	B_1'	142
5.D.4	57.8, 35.0, 25.7, 18.6, 17.6	B_7	130
	45, 34, 22.6, 11.4, 7.3, 6.9	B_x	92
5.D.6	65.3, 52.2, 38.9, 19.5, 13.0, 7.7	B_7	135
5.D.7	65.2, 40.6, 20.3, 13.5, 10.8, 7.7	B_7	130
5.D.9	64.1, 45.1, 22.9, 15.3, 11.5, 7.7	B_7	120

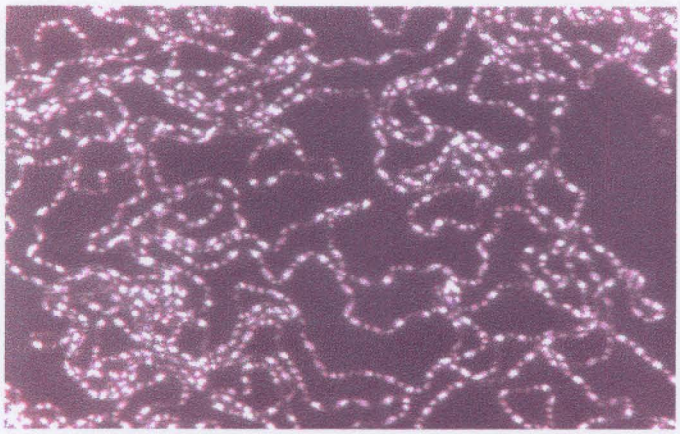

(a)

(b)

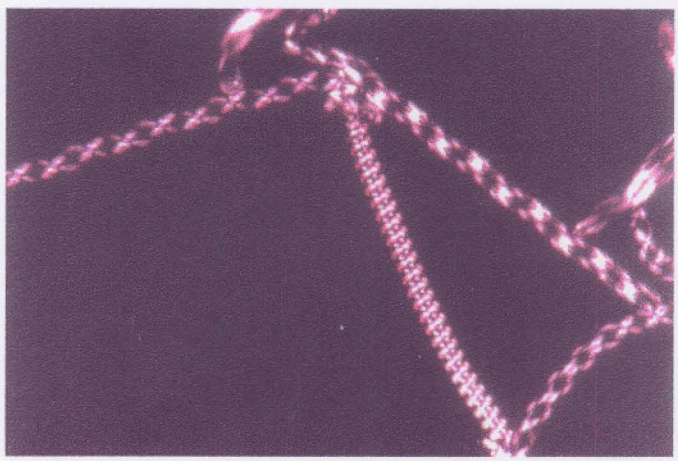

(c)

Fig. 5.20. Observation of (a) filamentary growth pattern, (b) single-spiral helical pattern and (c) the double-winded loosely packed helm in the B_7 mesophase of compound 5.D.4.

Textural variants of B_7 phase

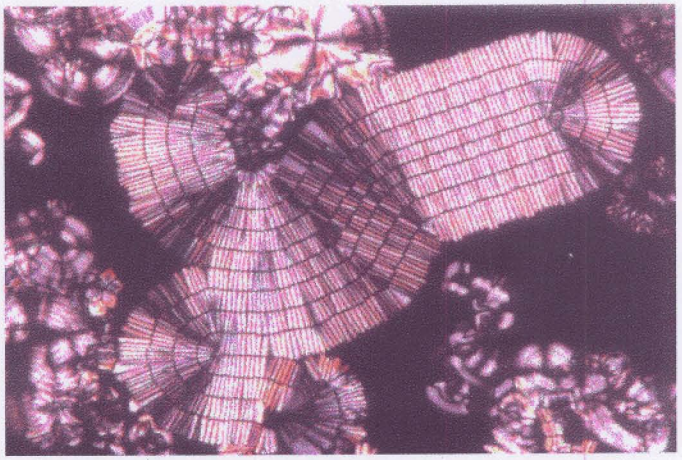

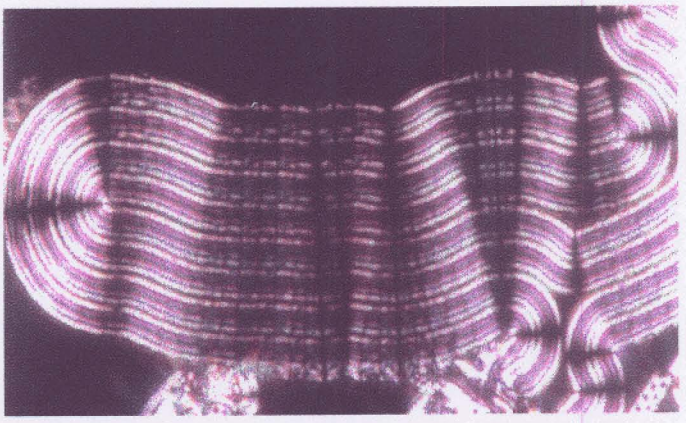

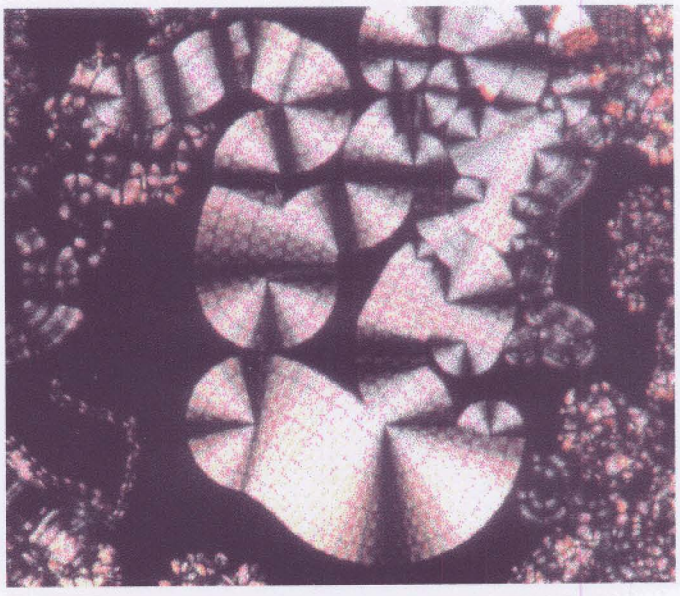

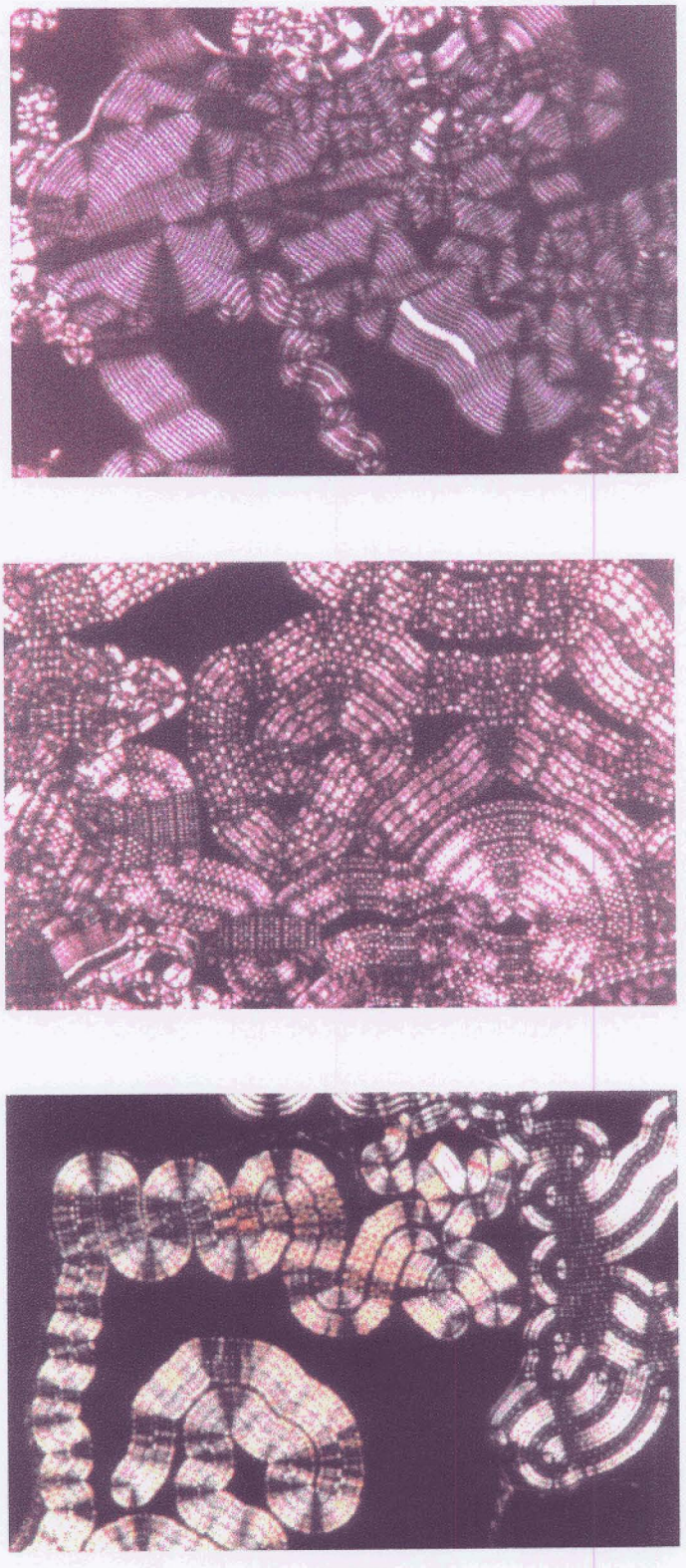

Fig. 5.21

Fig. 531. Other textural variants of the B_7 mesophase obtained.

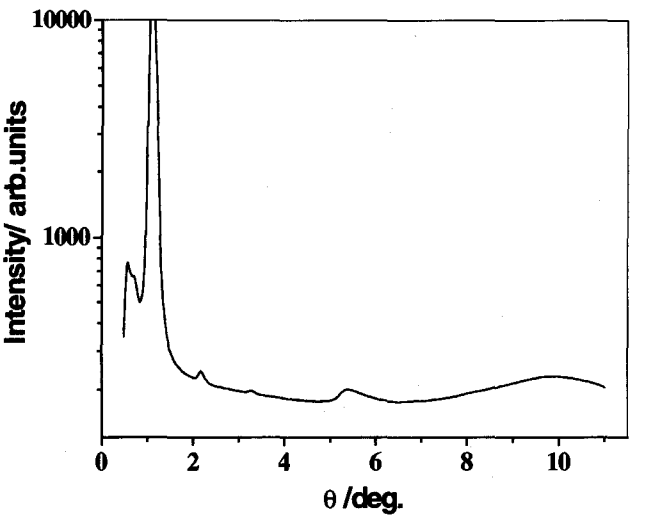

Fig. 5.22. X-Ray angular intensity profile of the B_7 phase of compound 5.C.8 at 138°C.

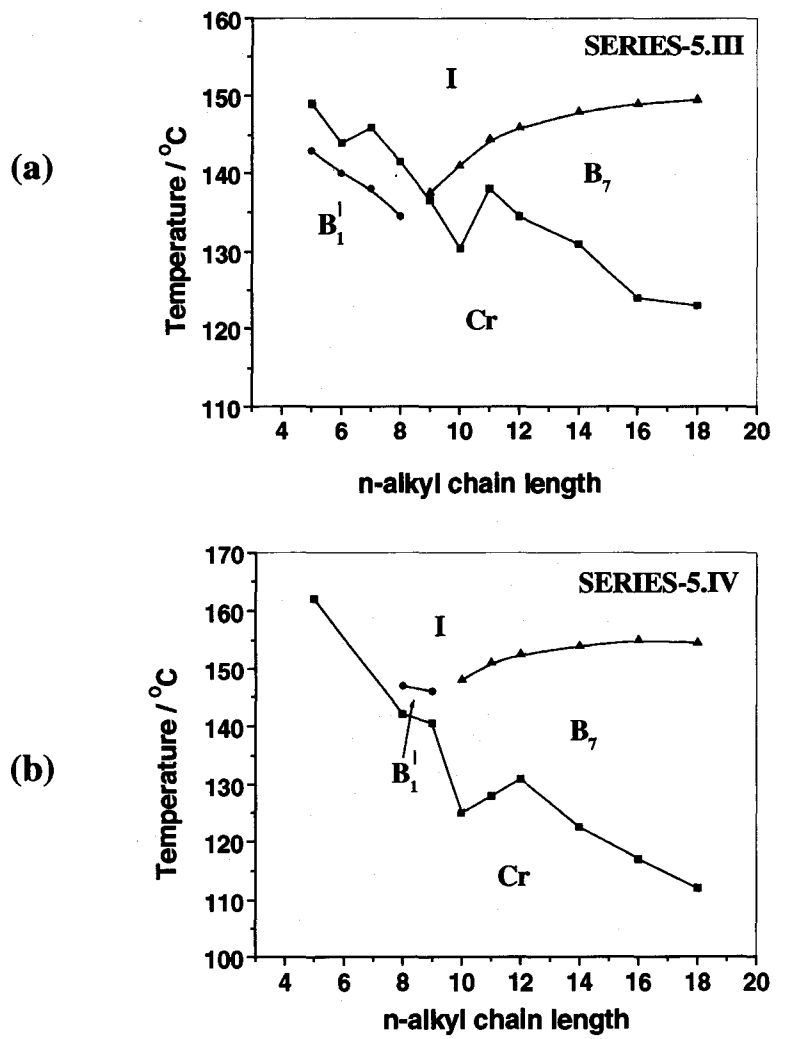

Fig. 5.23. Plots of the transition temperatures as a function of the number of carbon atoms in the n-alkyl chain obtained for (a) series 5.III and (b) series 5.IV.

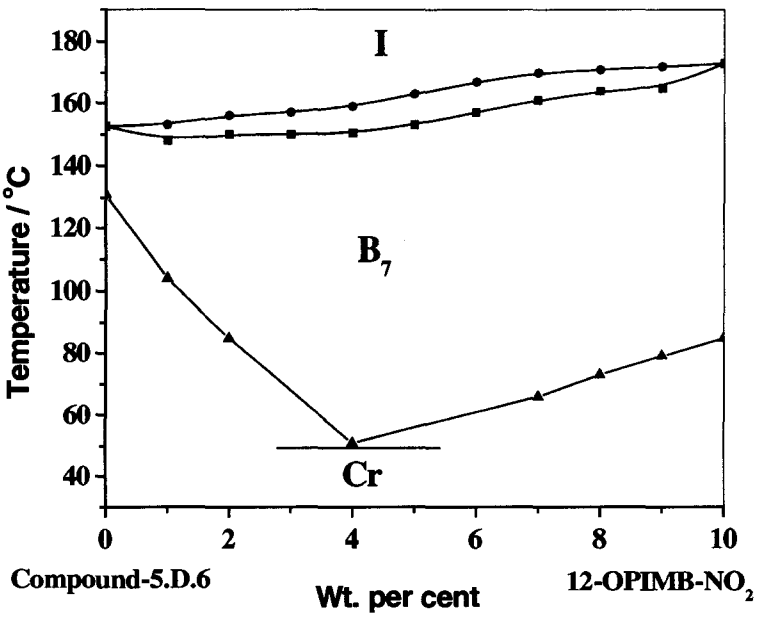

Fig. 5.24. Phase diagram of the binary mixtures of compound 5.D.6 and the standard compound 12-OPIMB-NO_2.

It is appropriate to consider the mesophases of different compounds, which have been assigned the symbol B_7. Since the observation of fascinating helical textures and other two-dimensional patterns by Pelzl *et al.* [44] in the n-OPIMB-NO_2 compounds, attempts have been made to understand the structure of this phase. Single- and double-spiral domains have been observed by a number of groups on different types of compounds. Heppke *et al.* [55,68] studied the mesomorphic properties of a series of novel sulphur containing banana-shaped liquid crystals. These materials exhibit spiral-domain texture indicating the chiral nature of the mesophase and they speculated that this smectic mesophase is B_7. From electro-optical investigations they have indicated that the mesophase is antiferroelectric in nature. Walba *et al.* [54] have described a ferroelectric liquid crystal composed of racemic molecules and based on characteristic textural features have indicated that the mesophase of this Schiff's base ester is indeed B_7. Bedel *et al.* [51] reported the synthesis and characterization of a homologous series of Schiff's base achiral banana-shaped mesogens. The compounds contain a lateral fluorine substituent on the outer phenyl ring *ortho* to the terminal n-alkoxy chain. The higher homologues of this series (n-alkoxy chain $\geq$ n-nonyloxy) show microscopic textures as well as X-ray diffraction patterns which are somewhat similar to that of the B_7

phase of the standard n-OPIMB-NO_2 compounds. The electro-optical studies show that this phase is ferroelectric in nature.

During the last one year or so, Shankar Rao *et al.* [107] described the mesomorphic behaviour of a salicylaldimine derivative which exhibited spiral domains. No other textural variants have been reported for this two-dimensional antiferroelectric phase and the symbol B_7 was assigned to the mesophase. Also, Dierking *et al.* [57] observed spiral filamentary growth patterns in a Schiff's base containing a fluorine substituent *ortho* to the terminal n-alkoxy chain. The phase ordering process was investigated by means of fractal dimensional analysis and the mesophase has been assigned the symbol B_7.

Lee *et al.* [56] reported a switchable banana phase in a Schiff's base containing a chlorine substituent *ortho* to the terminal n-alkoxy chain and assigned the symbol B_7 to the mesophase. From the XRD data, they showed the mesophase to be lamellar and from electro-optical switching experiments it has been characterized as ferroelectric. A re-examination of the mesophase of one of these compounds by Weissflog *et al.* [48] showed that the mesophase does switch weakly and that it is not a B_7 phase.

From the above reports it is clear that for the mesophase which has been assigned the symbol B_7, both ferroelectric and antiferroelectric switching properties are described. However, the standard B_7 compounds viz. n-OPIMB-NO_2 derivatives do not switch atleast upto about ± 40 $V\mu m^{-1}$, although Jakli *et al.* [45] report a minor optical effect under an electric field for one of these compounds. They also suggest that this effect is too complex for any quantitative conclusions to be drawn. Very recently, Clark *et al.* [114] have shown that the phase structure of the B_7 phase is either two- or three-dimensional using synchrotron based X-ray diffraction and freeze fracture electron microscopy measurements on a B_7 material synthesized by the Halle group. Hence, one can rule out a simple lamellar structure for a B_7 phase, for example, as reported for the sulphur containing compounds [55, 68]. One common feature in all the above cases is the observation of the growth of helical- or spiral-domains as the isotropic liquid is cooled slowly. Therefore, the optical textures and the switching behaviour (ferro- or antiferro-electric) do not provide sufficient proof for the assignment of the B_7 phase. Obviously, careful high-resolution X-ray diffraction measurements coupled with other physical investigations are necessary to unambiguously arrive at the structure of this fascinating B_7 mesophase.

Experimental

Methyl-3, 5-dihydroxybenzoate, (5.1)

Commercial 3, 5-dihydroxybenzoic acid (10 g), methanol (100 ml) and concentrated sulphuric acid (1 ml) were taken in a 250 ml RB flask. The reaction mixture was refluxed for about 40 hours and excess methanol was distilled off. The resultant reaction mixture was cooled in an ice-bath and extracted with solvent ether (3 × 100 ml). The combined organic solution was washed with ice-cold aqueous sodium bicarbonate solution (2 × 75 ml) and several times with distilled water and dried (anhydrous Na_2SO_4). The removal of solvent yielded a solid material, which was purified by column chromatography on silica gel using a mixture of 10% acetone in chloroform as eluent. The product so obtained after removal of solvent from the eluate was crystallized using water. Yield, 9.5 g (87%); m.p. 165-166°C (Reported [109a] 163-164°C).

Methyl-3, 5-dimethoxybenzoate, (5.2)

Methyl-3, 5-dihydroxybenzoate (9.0 g, 53.57 mmol) was added to a solution of KOH (6 g, 107.14 mmol) in water (50 ml) and cooled in an ice-bath. The mixture was stirred and dimethyl sulphate (12.96 g, 117.85 mmol) was added dropwise over a period of 1 hour and stirring was continued overnight. Then, the reaction mixture was gently refluxed for about 2 hours using an oil-bath. The resultant reaction mixture was cooled in an ice-bath, neutralized with diluted sulphuric acid and extracted using solvent ether (3 × 100 ml). The combined organic solution was washed with 5% ice-cold aqueous sodium hydroxide (2 × 50 ml) and several times with distilled water. The solvent was removed and the residue was passed through a column of silica gel using a mixture of 1:1 chloroform and petroleum ether (b.p. 60-80°C) as eluent. The product obtained after the removal of solvent was crystallized from petroleum ether (b.p. 60-80°C). Yield, 7.0 g (68%); m.p. 42-43°C (Reported [109a] 42-44°C).

3, 5-Dimethoxybenzoic acid, (5.3)

A mixture of methyl-3,5-dimethoxybenzoate (6.5 g), alcoholic 10 % potassium hydroxide solution (10g KOH in water and ethanol) was refluxed for 8 hours. Excess ethanol distilled off, the reaction mixture was cooled in an ice-bath and neutralized with diluted hydrochloric acid. The white precipitate obtained was filtered off, washed several times with water until the washings were neutral and dried. The solid compound so obtained was crystallized from ethanol. Yield 5.6g (93%); m.p. 184-185°C (Reported [109a] 185-186°C).

3, 5-Dimethoxybenzamide, (5.4)

A mixture of 3, 5-dimethoxybenzoic acid (6.0 g), thionyl chloride (15 ml) and dry toluene (20 ml) was refluxed for 8 hours. Excess thionyl chloride and toluene were completely distilled off under anhydrous conditions. Excess liquid ammonia (180 ml) was added to the reaction mixture and the stirring continued overnight at room temperature. The precipitated benzamide was filtered off and washed with water to remove the excess of ammonia. The solid material so obtained was crystallized from toluene. Yield, 4.9g (82%); m.p. 147-148°C (Reported [109a] 148-149°C).

3, 5-Dimethoxybenzonitrile, (5.5)

A mixture of 3, 5-dimethoxybenzamide (4.5 g), phosphorus oxychloride ($POCl_3$) (30 ml) and dry toluene (50 ml) was refluxed for 45 hours. Excess of phosphorus oxychloride and toluene were removed under vacuum. The solid residue obtained was dissolved in an excess of ether (100 ml) and the resultant solution was washed with water until the washings were free from acid. The solid compound obtained after the removal of solvent was passed through a column of silica gel and eluted using a mixture of chloroform and petroleum ether (b.p. 60-80°C). The product obtained after removal of solvent was crystallized from petroleum ether (b.p. 60-80°C). Yield, 3.4g (84%); m.p. 87-88°C (Reported [109b] 87-89 °C).

3, 5-Dihydroxybenzonitrile, (5.6)

A solution of 3,5-dimethoxybenzonitrile (3.0 g, 18.75 mmol) in dry dichloromethane (20 ml) was cooled to -78°C using alcohol and liquid nitrogen. To this, a solution of boron tribromide (18.78 g, 75 mmol) in dichloromethane (20 ml) was added dropwise over a period of 1 hour and the temperature was maintained for about 2-3 hours and allowed slowly to attain room temperature. The reaction mixture was then stirred for about 10 hours at room temperature. The excess of boron tribromide was decomposed carefully by the addition of moist chloroform. This was extracted with chloroform (3 × 50 ml) and the combined organic solution was washed several times with water and dried (anhydrous Na_2SO_4). Removal of solvent gave a solid material, which was passed through a column of silica gel using 5% acetone in chloroform as eluent. The light brown colour solid obtained after removal of solvent from the eluate was crystallized from a minimum amount of water to yield 3, 5-dihydroxybenzonitrile, 1.9 g (79%); m.p. 191-193°C (Reported [109c] m.p. 164-170°C); ν_{max}(KBr):3502, 3454, 3260, 2239, 1600, 1358, 1180 cm^{-1}; δ_H:9.3 (s, 2H, 2 × Ar-OH, exchangeable with D_2O), 6.8-6.79(m, ^4J 2.2 Hz, 2H, Ar-H), 6.77-6.76 (m, ^4J 2.1 Hz, 1H, Ar-

H). Elemental analysis: $C_7H_5O_2N$ requires, C, 62.22; H, 3.73; N, 10.37%; found, C, 62.06; H, 3.78; N, 10.35%.

2, 6-Dihydroxybenzonitrile, (5.7)

This was prepared following a procedure similar to the one used for the preparation of compound **5.6**, except the reaction mixture was gently refluxed for about 10 hours using an oil-bath. Yield, 76%; m.p. 206-208°C (dec.), sublimes ≈ 155°C at 2 mm of Hg (Reported [110] m.p. 203-204°C, sublimation raises the melting point to 209°C); ν_{max}(KBr):3452, 3331, 2226, 2239, 1612, 1472, 1022 cm^{-1}; δ_H:9.89 (s, 2H, 2 × Ar-OH, exchangeable with D_2O), 7.39-7.35(t, 1H, ^{3}J8.28 Hz, Ar-H), 6.65-6.63 (d, 2H, ^{3}J8.28 Hz, Ar-H). Elemental analysis: $C_7H_5O_2N$ requires, C, 62.22; H, 3.73; N, 10.37%; found, C, 62.13; H, 3.71; N, 10.43%.

5-Cyano-1,3-phenylene bis(2-fluoro-4-benzyloxybenzoate), (5.8)

5-Cyanoresorcinol (1.33g, 10 mmol) and 2-fluoro-4-benzyloxybenzoic acid, (4.92g, 20 mmol) were dissolved in dry dichloromethane (50 ml). After the addition of N, N' - dicyclohexylcarbodiimide (DCC), (4.5g, 22 mmol) and a catalytic amount of 4-(N, N - dimethylamino)pyridine (DMAP), the mixture was stirred at room temperature for about 15 hours. The dicyclohexylurea which precipitated was filtered off and washed with excess of chloroform (100 ml). This combined organic solution was washed with 2% aqueous acetic acid (3 × 50 ml) and 5% ice-cold aqueous sodium hydroxide solution (3 × 50 ml) and finally washed with water and dried (anhydrous Na_2SO_4). The solid material obtained after removal of solvent was chromatographed on silica gel using chloroform as an eluent. Removal of solvent from the eluate afforded a white material which was crystallized from acetonitrile. Yield, 3.8g (65%); m.p. 144.5-145.5°C; ν_{max}:2924, 2854, 2235, 1751, 1620, 1600, 1466, 1250, 1135 cm^{-1}; δ_H:8.05-8.01 (t, 2H, ^{3}J8.64 Hz, Ar-H), 7.48-7.36 (m, 13H, Ar-H), 6.89-6.86 (dd, 2H, ^{3}J8.9 Hz, ^{4}J2.36 Hz, Ar-H), 6.80-6.77 (dd, 2H, ^{3}J12.6 Hz, ^{4}J2.36 Hz, Ar-H), 5.15 (s, 4H, 2 × $ArCH_2O$-).

5-Cyano-1,3-phenylene bis(2-fluoro-4-hydroxybenzoate), (5.9)

5-Cyano-1,3-phenylene bis (2-fluoro-4-benzyloxybenzoate) (3.5g) was dissolved in 1,4-dioxane (40 ml) and 5% Pd-C catalyst (0.7 g) was added to it. The mixture was stirred at 50°C in an atmosphere of hydrogen till the required quantity of hydrogen was absorbed. The resultant mixture was filtered hot and the solvent removed under reduced pressure. The solid material so obtained was passed through a column of silica gel and eluted with a mixture of

6% acetone in chloroform. Removal of solvent from the eluate gave a white material, which was crystallized using a mixture of butan-2-one and petroleum-ether(b.p. 60-80°C). Yield, 2.2 g (90%); m.p. 229-231°C; ν_{max}:3340, 3315, 2924, 2854, 2245, 1734, 1707, 1622, 1600, 1465, 1252, 1139 cm^{-1}; δ_H:10.24(s, 2H, 2 × Ar–OH, exchangeable with D_2O), 8.20-8.15(t, 2H, ^{3}J8.68 Hz, Ar-H), 7.87-7.86(d, 2H, ^{4}J2.08 Hz, Ar-H), 7.80-7.79(t, 1H, ^{4}J2.12 Hz, Ar-H), 7.01-6.98 (dd, 2H, ^{3}J8.76 Hz, ^{4}J2.4 Hz, Ar-H), 6.89-6.85(dd, 2H, ^{3}J12.82 Hz, ^{4}J2.28 Hz, Ar-H).

5-Cyano-1,3-phenylene bis(3-fluoro-4-benzyloxybenzoate), (5.10)

This was synthesized following a procedure similar to that given for compound **5.8** using 3-fluoro-4-benzyloxybenzoic acid instead of 2-fluoro-4-benzyloxybenzoic acid.

Yield, 68%; m.p. 176-177°C; ν_{max}(KBr):3066, 2914, 2228, 1738, 1732, 1612, 1591, 1433, 1230, 1142 cm^{-1}; δ_H:7.93-7.87 (m, 4H, Ar-H), 7.47-7.36 (m, 13H, Ar-H), 7.12-7.08 (t, 2H, ^{3}J8.04 Hz, Ar-H), 5.25 (s, 4H, 2 × $ArCH_2O$-).

5-Cyano-1,3-phenylene bis(3-fluoro-4-hydroxybenzoate), (5.11)

This was prepared following a procedure similar to that given for compound **5.9**

Yield, 88%; m.p. 220-222°C; ν_{max}(KBr):3385, 3103, 2924, 2241, 1744, 1720, 1618, 1593, 1437, 1281, 1180 cm^{-1}; δ_H:10.25(s, 2H, 2 × Ar–OH, exchangeable with D_2O), 8.06-8.02(m, 4H, Ar-H), 7.907-7.902(d, 2H, ^{4}J2.12 Hz, Ar-H), 7.85-7.84(t, 1H, ^{4}J2.12 Hz, Ar-H), 7.36-7.31 (m, 2H, Ar-H).

2-Cyano-1,3-phenylene bis(2-fluoro-4-benzyloxybenzoate), (5.12)

This was prepared following a procedure similar to that given for compound **5.8** using 2-cyanoresorcinol instead of 5-cyanoresorcinol.

Yield, 62%; m.p. 164.5-165.5°C; ν_{max}:2924, 2854, 2235, 1751, 1622, 1600, 1466, 1250, 1121 cm^{-1}; δ_H:8.15-8.11 (t, 2H, ^{3}J8.6 Hz, Ar-H), 7.71-7.67 (t, 1H, ^{3}J8.4 Hz, Ar-H), 7.47-7.35 (m, 12H, Ar-H), 6.9-6.87 (dd, 2H, ^{3}J8.9 Hz, ^{4}J2.4 Hz, Ar-H), 6.81-6.78 (dd, 2H, ^{3}J12.52 Hz, ^{4}J2.36 Hz, Ar-H), 5.15 (s, 4H, 2 × $ArCH_2O$-).

2-Cyano-1,3-phenylene bis(2-fluoro-4-hydroxybenzoate), (5.13)

This was prepared following a procedure similar to that given for compound **5.9**

Yield, 91%; m.p. 230-232° C; ν_{max}:3329, 2924, 2854, 2243, 1755, 1740, 1626, 1595, 1466, 1232, 1122 cm^{-1}; δ_H:10.29(s, 2H, 2 × Ar–OH, exchangeable with D_2O), 8.25-8.20(t, 2H, ^{3}J8.68 Hz, Ar-H), 7.08-7.04(t, 1H, ^{3}J8.48 Hz, Ar-H),7.69-7.67(d, 2H, ^{3}J8.4 Hz, Ar-H), 7.04-7.01 (dd, 2H, ^{3}J8.76 Hz, ^{4}J2.24 Hz, Ar-H), 6.94-6.90(dd, 2H, ^{3}J12.8 Hz, ^{4}J2.28 Hz, Ar-H).

2-Cyano-1,3-phenylene bis(3-fluoro-4-benzyloxybenzoate), (5.14)

This was prepared following a synthetic procedure similar to that given for compound **5.8**.

Yield, 70%; m.p. 171-172°C; ν_{max}:2924, 2854, 2229, 1740, 1611, 1460, 1283, 1134 cm^{-1}; δ_H:8.0-7.98 (d, 2H, ^{3}J8.68 Hz, Ar-H), 7.96-7.93 (dd, 2H, ^{3}J11.24 Hz, ^{4}J2.08 Hz, Ar-H), 7.72-7.68(t, 1H, ^{3}J8.48 Hz, Ar-H), 7.47-7.34(m, 12H, Ar-H), 7.13-7.09 (t, 2H, ^{3}J8.28 Hz, Ar-H), 5.26 (s, 4H, 2 × $ArCH_2O$-).

2-Cyano-1,3-phenylene bis(3-fluoro-4-hydroxybenzoate), (5.15)

This was prepared following a procedure similar to that given for compound **5.9**

Yield, 92%; m.p. 221-223°C; ν_{max}:3344, 2924, 2854, 2247, 1747, 1728, 1618, 1595, 1466, 1286, 1139 cm^{-1}; δ_H:10.22(s, 2H, 2 × Ar–OH, exchangeable with D_2O), 8.11-8.06(m, 5H, Ar-H), 7.73-7.71(d, 2H, ^{3}J8.4 Hz, Ar-H), 7.38-7.34(m, 2H, Ar-H).

5-Cyano-1,3-phenylene bis [4-(4-n-pentylbiphenyl-4-carbonyloxy)2-fluorobenzoate], (5.A.1)

Yield, 41%; m.p. 177.5°C; ν_{max}:2924, 2854, 2241, 1747, 1728, 1615, 1607, 1460, 1252, 1124 cm^{-1}; δ_H:8.26-8.18(m, 6H, Ar-H), 7.77-7.75(d, 4H, ^{3}J8.28 Hz, Ar-H), 7.6-7.55(m, 7H, Ar-H), 7.32-7.23(m, 8H, Ar-H), 2.7-2.65(t, 4H, ^{3}J7.52 Hz, 2 × Ar-CH_2-), 1.66-1.64(quin, 4H, ^{3}J6.64 Hz, 2 × Ar-CH_2-$C\underline{H}_2$-), 1.35-1.29(m, 8H, 4 × -$C\underline{H}_2$-), 0.9-0.87(t, 6H, ^{3}J6.24 Hz, 2 × -CH_2-$C\underline{H}_3$).

5-Cyano-1,3-phenylene bis [4-(4-n-heptylbiphenyl-4-carbonyloxy)2-fluorobenzoate], (5.A.2)

Yield, 40%; m.p. 179°C; ν_{max}:2924, 2854, 2239, 1749, 1726, 1618, 1608, 1458, 1252, 1126 cm^{-1}; δ_H:8.26-8.17(m, 6H, Ar-H), 7.77-7.75(d, 4H, ^{3}J8.26 Hz, Ar-H), 7.6-7.55(m, 7H, Ar-H), 7.32-7.23(m, 8H, Ar-H), 2.7-2.64(t, 4H, ^{3}J7.5 Hz, 2 × Ar-CH_2-), 1.66-1.64(quin, 4H, ^{3}J7.62 Hz, 2 × Ar-CH_2-$C\underline{H}_2$-), 1.35-1.28(m, 16H, 8 × -$C\underline{H}_2$-), 0.9-0.87(t, 6H, ^{3}J6.24 Hz, 2 × -CH_2-$C\underline{H}_3$).

5-Cyano-1,3-phenylene bis [4-(4-n-octylbiphenyl-4-carbonyloxy)2-fluorobenzoate], (5.A.3)

Yield, 44%; m.p. 182°C; ν_{max}:2924, 2854, 2241, 1749, 1730, 1618, 1608, 1461, 1252, 1126 cm^{-1}; δ_H:8.26-8.18(m, 6H, Ar-H), 7.77-7.74(d, 4H, ^{3}J8.28 Hz, Ar-H), 7.6-7.55(m, 7H, Ar-H), 7.32-7.23(m, 8H, Ar-H), 2.7-2.65(t, 4H, ^{3}J7.64 Hz, 2 × Ar-CH_2-), 1.68-1.64(quin, 4H, ^{3}J7.6

Hz, 2 × Ar-CH_2-$C\underline{H}_2$-), 1.34-1.28(m, 20H, 10 × -$C\underline{H}_2$-), 0.9-0.87(t, 6H, ^{3}J6.48 Hz, 2 × -CH_2-$C\underline{H}_3$).

5-Cyano-1,3-phenylene bis [4-(4-n-nonylbiphenyl-4-carbonyloxy)2-fluorobenzoate], (5.A.4)

Yield, 46%; m.p. 189°C; ν_{max}:2924, 2854, 2239, 1747, 1726, 1615, 1608, 1458, 1252, 1126 cm^{-1}; δ_H:8.26-8.18(m, 6H, Ar-H), 7.77-7.74(d, 4H, ^{3}J8.26 Hz, Ar-H), 7.6-7.55(m, 7H, Ar-H), 7.32-7.23(m, 8H, Ar-H), 2.7-2.65(t, 4H, ^{3}J7.6 Hz, 2 × Ar-CH_2-), 1.68-1.64(quin, 4H, ^{3}J7.64 Hz, 2 × Ar-CH_2-$C\underline{H}_2$-), 1.34-1.28(m, 24H, 12 × -$C\underline{H}_2$-), 0.9-0.87(t, 6H, ^{3}J6.5 Hz, 2 × -CH_2-$C\underline{H}_3$).

5-Cyano-1,3-phenylene bis [4-(4-n-decylbiphenyl-4-carbonyloxy)2-fluorobenzoate], (5.A.5)

Yield, 43%; m.p. 189.5°C; ν_{max}:2924, 2854, 2239, 1747, 1726, 1615, 1608, 1458, 1252, 1126 cm^{-1}; δ_H:8.26-8.18(m, 6H, Ar-H), 7.77-7.74(d, 4H, ^{3}J8.36 Hz, Ar-H), 7.6-7.55(m, 7H, Ar-H), 7.32-7.23(m, 8H, Ar-H), 2.7-2.65(t, 4H, ^{3}J7.6 Hz, 2 × Ar-CH_2-), 1.69-1.62(quin, 4H, ^{3}J7.56 Hz, 2 × Ar-CH_2-$C\underline{H}_2$-), 1.34-1.27(m, 28H, 14 × -$C\underline{H}_2$-), 0.9-0.86(t, 6H, ^{3}J6.6 Hz, 2 × -CH_2-$C\underline{H}_3$).

5-Cyano-1,3-phenylene bis [4-(4-n-undecylbiphenyl-4-carbonyloxy)2-fluorobenzoate], (5.A.6)

Yield, 42%; m.p. 183.5°C; ν_{max}:2922, 2853, 2239, 1747, 1726, 1615, 1608, 1460, 1252, 1126 cm^{-1}; δ_H:8.26-8.18(m, 6H, Ar-H), 7.77-7.74(d, 4H, ^{3}J8.32 Hz, Ar-H), 7.6-7.55(m, 7H, Ar-H), 7.32-7.23(m, 8H, Ar-H), 2.7-2.65(t, 4H, ^{3}J7.56 Hz, 2 × Ar-CH_2-), 1.68-1.62(quin, 4H, ^{3}J7.32 Hz, 2 × Ar-CH_2-$C\underline{H}_2$-), 1.34-1.27(m, 32H, 16 × -$C\underline{H}_2$-), 0.9-0.86(t, 6H, ^{3}J6.44 Hz, 2 × -CH_2-$C\underline{H}_3$).

5-Cyano-1,3-phenylene bis [4-(4-n-dodecylbiphenyl-4-carbonyloxy)2-fluorobenzoate], (5.A.7)

Yield, 43%; m.p. 178°C; ν_{max}:2922, 2851, 2239, 1747, 1726, 1615, 1608, 1464, 1252, 1124 cm^{-1}; δ_H:8.26-8.18(m, 6H, Ar-H), 7.77-7.74(d, 4H, ^{3}J8.36 Hz, Ar-H), 7.7-7.55(m, 7H, Ar-H), 7.32-7.23(m, 8H, Ar-H), 2.7-2.65(t, 4H, ^{3}J7.64 Hz, 2 × Ar-CH_2-), 1.69-1.62(quin, 4H, ^{3}J7.64 Hz, 2 × Ar-CH_2-$C\underline{H}_2$-), 1.34-1.27(m, 36H, 18 × -$C\underline{H}_2$-), 0.9-0.86(t, 6H, ^{3}J6.48 Hz, 2 × -CH_2-$C\underline{H}_3$).

5-Cyano-1,3-phenylene bis [4-(4-n-tetradecylbiphenyl-4-carbonyloxy)2-fluorobenzoate], (5.A.8)

Yield, 46%; m.p. 172.5°C; ν_{max}:2922, 2851, 2237, 1749, 1734, 1615, 1608, 1466, 1252, 1126 cm^{-1}; δ_H:8.26-8.18(m, 6H, Ar-H), 7.77-7.74(d, 4H, ^{3}J8.32 Hz, Ar-H), 7.6-7.55(m, 7H, Ar-H), 7.32-7.23(m, 8H, Ar-H), 2.7-2.65(t, 4H, ^{3}J7.56 Hz, 2 × Ar-CH_2-), 1.66-1.62(quin, 4H, ^{3}J7.28 Hz, 2 × Ar-CH_2-$C\underline{H}_2$-), 1.34-1.26(m, 44H, 22 × -$C\underline{H}_2$-), 0.9-0.86(t, 6H, ^{3}J6.4 Hz, 2 × -CH_2-$C\underline{H}_3$).

5-Cyano-1,3-phenylene bis [4-(4-n-hexadecylbiphenyl-4-carbonyloxy)2-fluorobenzoate], (5.A.9)

Yield, 45%; m.p. 166.5°C; ν_{max}:2920, 2851, 2235, 1736, 1718, 1615, 1608, 1458, 1252, 1126 cm^{-1}; δ_H:8.26-8.18(m, 6H, Ar-H), 7.77-7.74(d, 4H, ^{3}J8.32 Hz, Ar-H), 7.6-7.55(m, 7H, Ar-H), 7.32-7.23(m, 8H, Ar-H), 2.7-2.65(t, 4H, ^{3}J7.64 Hz, 2 × Ar-CH_2-), 1.67-1.62(quin, 4H, ^{3}J6.68 Hz, 2 × Ar-CH_2-$C\underline{H}_2$-), 1.34-1.21(m, 52H, 26 × -$C\underline{H}_2$-), 0.9-0.86(t, 6H, ^{3}J6.44 Hz, 2 × -CH_2-$C\underline{H}_3$).

5-Cyano-1,3-phenylene bis [4-(4-n-octadecylbiphenyl-4-carbonyloxy)2-fluorobenzoate], (5.A.10)

Yield, 48%; m.p. 161°C; ν_{max}:2920, 2851, 2237, 1747, 1724, 1612, 1608, 1458, 1252, 1124 cm^{-1}; δ_H:8.26-8.18(m, 6H, Ar-H), 7.77-7.74(d, 4H, ^{3}J8.30 Hz, Ar-H), 7.6-7.54(m, 7H, Ar-H), 7.32-7.23(m, 8H, Ar-H), 2.7-2.65(t, 4H, ^{3}J7.64 Hz, 2 × Ar-CH_2-), 1.67-1.63(quin, 4H, ^{3}J6.6 Hz, 2 × Ar-CH_2-$C\underline{H}_2$-), 1.34-1.25(m, 60H, 30 × -$C\underline{H}_2$-), 0.89-0.86(t, 6H, ^{3}J6.4 Hz, 2 × -CH_2-$C\underline{H}_3$).

5-Cyano-1,3-phenylene bis [4-(4-n-octylbiphenyl-4-carbonyloxy)3-fluorobenzoate], (5.B.1)

Yield, 40%; m.p. 155°C; ν_{max}:2924, 2852, 2247, 1747, 1740, 1615, 1608, 1458, 1286, 1128 cm^{-1}; δ_H:8.29-8.26(d, 4H, ^{3}J8.44 Hz, Ar-H), 8.09-8.04(m, 4H, Ar-H), 7.77-7.75(d, 4H, ^{3}J8.48 Hz, Ar-H), 7.6-7.48(m, 9H, Ar-H), 7.32-7.30(d, 4H, ^{3}J8.16 Hz, Ar-H), 2.7-2.66(t, 4H, ^{3}J7.48 Hz, 2 × Ar-CH_2-), 1.68-1.63(quin, 4H, ^{3}J6.68 Hz, 2 × Ar-CH_2-$C\underline{H}_2$-), 1.35-1.29(m, 20H, 10 × -$C\underline{H}_2$-), 0.9-0.87(t, 6H, ^{3}J6.68 Hz, 2 × -CH_2-$C\underline{H}_3$).

5-Cyano-1,3-phenylene bis [4-(4-n-nonylbiphenyl-4-carbonyloxy)3-fluorobenzoate], (5.B.2)

Yield, 43%; m.p. 157°C; ν_{max}:2922, 2851, 2247, 1748, 1740, 1608, 1458, 1286, 1121 cm^{-1}; δ_H:8.29-8.26(d, 4H, ^{3}J8.48 Hz, Ar-H), 8.09-8.04(m, 4H, Ar-H), 7.77-7.75(d, 4H, ^{3}J8.44 Hz, Ar-H), 7.6-7.48(m, 9H, Ar-H), 7.32-7.30(d, 4H, ^{3}J8.12 Hz, Ar-H), 2.7-2.66(t, 4H, ^{3}J7.48 Hz, 2 × Ar-CH_2-), 1.68-1.63(quin, 4H, ^{3}J6.72 Hz, 2 × Ar-CH_2-C$\underline{H_2}$), 1.35-1.28(m, 24H, 12 × -C$\underline{H_2}$-), 0.9-0.87(t, 6H, ^{3}J6.72 Hz, 2 × -CH_2-C$\underline{H_3}$).

5-Cyano-1,3-phenylene bis [4-(4-n-decylbiphenyl-4-carbonyloxy)3-fluorobenzoate], (5.B.3)

Yield, 46%; m.p. 156°C; ν_{max}:2922, 2853, 2247, 1750, 1740, 1608, 1458, 1286, 1121 cm^{-1}; δ_H:8.29-8.26(d, 4H, ^{3}J8.44 Hz, Ar-H), 8.09-8.04(m, 4H, Ar-H), 7.77-7.75(d, 4H, ^{3}J8.44 Hz, Ar-H), 7.6-7.48(m, 9H, Ar-H), 7.32-7.30(d, 4H, ^{3}J8.16 Hz, Ar-H), 2.7-2.65(t, 4H, ^{3}J7.52 Hz, 2 × Ar-CH_2-), 1.68-1.63(quin, 4H, ^{3}J6.88 Hz, 2 × Ar-CH_2-C$\underline{H_2}$), 1.34-1.27(m, 28H, 14 × -C$\underline{H_2}$-), 0.9-0.87(t, 6H, ^{3}J6.68 Hz, 2 × -CH_2-C$\underline{H_3}$).

5-Cyano 1,3-phenylene bis [4-(4-n-undecylbiphenyl-4-carbonyloxy)3-fluorobenzoate], (5.B.4)

Yield, 41%; m.p. 156°C; ν_{max}:2922, 2851, 2247, 1752, 1740, 1608, 1458, 1286, 1121 cm^{-1}; δ_H:8.29-8.26(d, 4H, ^{3}J8.32 Hz, Ar-H), 8.09-8.04(m, 4H, Ar-H), 7.77-7.75(d, 4H, ^{3}J8.32 Hz, Ar-H), 7.6-7.48(m, 9H, Ar-H), 7.32-7.30(d, 4H, ^{3}J8.04 Hz, Ar-H), 2.7-2.65(t, 4H, ^{3}J7.48 Hz, 2 × Ar-CH_2-), 1.66-1.64(quin, 4H, ^{3}J6.9 Hz, 2 × Ar-CH_2-C$\underline{H_2}$-), 1.34-1.27(m, 32H, 16 × -C$\underline{H_2}$-), 0.9-0.87(t, 6H, ^{3}J6.64 Hz, 2 × -CH_2-C$\underline{H_3}$).

5-Cyano-1,3-phenylene bis [4-(4-n-dodecylbiphenyl-4-carbonyloxy)3-fluorobenzoate], (5.B.5)

Yield, 44%; m.p. 158°C; ν_{max}:2922, 2852, 2247, 1747, 1736, 1608, 1458, 1288, 1121 cm^{-1}; δ_H:8.29-8.26(d, 4H, ^{3}J8.4 Hz, Ar-H), 8.09-8.04(m, 4H, Ar-H), 7.77-7.75(d, 4H, ^{3}J8.44 Hz, Ar-H), 7.6-7.48(m, 9H, Ar-H), 7.32-7.30(d, 4H, ^{3}J8.12 Hz, Ar-H), 2.7-2.65(t, 4H, ^{3}J7.52 Hz, 2 × Ar-CH_2-), 1.66-1.64(quin, 4H, ^{3}J6.86 Hz, 2 × Ar-CH_2-C$\underline{H_2}$), 1.34-1.27(m, 36H, 18 × -C$\underline{H_2}$-), 0.9-0.87(t, 6H, ^{3}J6.64 Hz, 2 × -CH_2-C$\underline{H_3}$).

5-Cyano-1,3-phenylene bis [4-(4-n-tetradecylbiphenyl-4-carbonyloxy)3-fluorobenzoate], (5.B.6)

Yield, 45%; m.p. 152°C; ν_{max}:2922, 2851, 2247, 1748, 1736, 1608, 1458, 1288, 1121 cm^{-1}; δ_H:8.29-8.27(d, 4H, ^{3}J8.4 Hz, Ar-H), 8.09-8.04(m, 4H, Ar-H), 7.77-7.75(d, 4H, ^{3}J8.4 Hz, Ar-H), 7.6-7.48(m, 9H, Ar-H), 7.32-7.30(d, 4H, ^{3}J8.08 Hz, Ar-H), 2.7-2.65(t, 4H, ^{3}J7.48 Hz, 2 × Ar-CH_2-), 1.66-1.64(quin, 4H, ^{3}J6.82 Hz, 2 × Ar-CH_2-C$\underline{H_2}$), 1.34-1.26(m, 44H, 22 × -C$\underline{H_2}$-), 0.9-0.87(t, 6H, ^{3}J6.68 Hz, 2 × -CH_2-C$\underline{H_3}$).

5-Cyano-1,3-phenylene bis [4-(4-n-hexadecylbiphenyl-4-carbonyloxy)3-fluorobenzoate], (5.B.7)

Yield, 48%; m.p. 145°C; ν_{max}:2920, 2851, 2241, 1744, 1735, 1608, 1597, 1466, 1288, 1117 cm^{-1}; δ_H:8.29-8.27(d, 4H, ^{3}J8.32 Hz, Ar-H), 8.09-8.04(m, 4H, Ar-H), 7.77-7.75(d, 4H, ^{3}J8.32 Hz, Ar-H), 7.6-7.48(m, 9H, Ar-H), 7.32-7.30(d, 4H, ^{3}J8.08 Hz, Ar-H), 2.7-2.65(t, 4H, ^{3}J7.48 Hz, 2 × Ar-CH_2-), 1.66-1.64(quin, 4H, ^{3}J7.36 Hz, 2 × Ar-CH_2-C$\underline{H_2}$), 1.34-1.26(m, 52H, 26 × -C$\underline{H_2}$-), 0.9-0.86(t, 6H, ^{3}J6.32 Hz, 2 × -CH_2-C$\underline{H_3}$).

5-Cyano-1,3-phenylene bis [4-(4-n-octadecylbiphenyl-4-carbonyloxy)3-fluorobenzoate], (5.B.8)

Yield, 43%; m.p. 141.5°C; ν_{max}:2920, 2851, 2241, 1744, 1736, 1607, 1597, 1466, 1286, 1119 cm^{-1}; δ_H:8.29-8.27(d, 4H, ^{3}J8.4 Hz, Ar-H), 8.09-8.04(m, 4H, Ar-H), 7.77-7.75(d, 4H, ^{3}J8.44 Hz, Ar-H), 7.6-7.48(m, 9H, Ar-H), 7.32-7.30(d, 4H, ^{3}J8.16 Hz, Ar-H), 2.7-2.65(t, 4H, ^{3}J7.6 Hz, 2 × Ar-CH_2-), 1.66-1.64(quin, 4H, ^{3}J6.72 Hz, 2 × Ar-CH_2-C$\underline{H_2}$), 1.34-1.21(m, 60H, 30 × -C$\underline{H_2}$-), 0.9-0.86(t, 6H, ^{3}J6.6 Hz, 2 × -CH_2-C$\underline{H_3}$).

2-Cyano-1,3-phenylene bis [4-(4-n-pentylbiphenyl-4-carbonyloxy)2-fluorobenzoate], (5.C.1)

Yield, 34%; m.p. 149°C; ν_{max}:2924, 2854, 2235, 1742, 1718, 1605, 1460, 1229, 1119 cm^{-1}; δ_H:8.32-8.24(m, 4H, Ar-H), 7.77-7.73(m, 6H, Ar-H), 7.6-7.58(m, 4H, Ar-H), 7.49-7.43(m, 4H, Ar-H), 7.32-7.24(m, 7H, Ar-H), 2.69-2.65(t, 4H, ^{3}J7.64 Hz, 2 × Ar-CH_2-), 1.68-1.65(quin, 4H, ^{3}J7.2 Hz, 2 × Ar-CH_2-C$\underline{H_2}$-), 1.37-1.33(m, 8H, 4 × -C$\underline{H_2}$-), 0.93-0.89(t, 6H, ^{3}J6.64 Hz, 2 × -CH_2-C$\underline{H_3}$).

2-Cyano-1,3-phenylene bis [4-(4-n-hexylbiphenyl-4-carbonyloxy)2-fluorobenzoate], (5.C.2)

Yield, 37%; m.p. 144°C; ν_{max}:2924, 2854, 2235, 1740, 1733, 1607, 1458, 1232, 1122 cm^{-1}; δ_H:8.32-8.24(m, 4H, Ar-H), 7.77-7.73(m, 6H, Ar-H), 7.6-7.58(m, 4H, Ar-H), 7.49-7.43(m, 4H, Ar-H), 7.32-7.22(m, 7H, Ar-H), 2.69-2.65(t, 4H, ^{3}J7.56 Hz, 2 × Ar-CH_2-), 1.68-1.63(quin, 4H, ^{3}J7.08 Hz, 2 × Ar-CH_2-C$\underline{H}_2$-), 1.37-1.32(m, 12H, 6 × -C$\underline{H}_2$), 0.93-0.89(t, 6H, ^{3}J6.64 Hz, 2 × -CH_2-C$\underline{H}_3$).

2-Cyano-1,3-phenylene bis [4-(4-n-heptylbiphenyl-4-carbonyloxy)2-fluorobenzoate], (5.C.3)

Yield, 35%; m.p. 146°C; ν_{max}:2924, 2854, 2237, 1745, 1736, 1607, 1458, 1229, 1122 cm^{-1}; δ_H:8.32-8.24(m, 4H, Ar-H), 7.77-7.75(m, 6H, Ar-H), 7.6-7.58(m, 4H, Ar-H), 7.49-7.43(m, 4H, Ar-H), 7.32-7.22(m, 7H, Ar-H), 2.69-2.65(t, 4H, ^{3}J7.84 Hz, 2 × Ar-CH_2-), 1.66-1.64(quin, 4H, ^{3}J7.08 Hz, 2 × Ar-CH_2-C$\underline{H}_2$-), 1.37-1.29(m, 16H, 8 × -C$\underline{H}_2$), 0.90-0.87(t, 6H, ^{3}J6.16 Hz, 2 × -CH_2-C$\underline{H}_3$).

2-Cyano-1,3-phenylene bis [4-(4-n-octylbiphenyl-4-carbonyloxy)2-fluorobenzoate], (5.C.4)

Yield, 36%; m.p. 141.5°C; ν_{max}:2924, 2854, 2235, 1745, 1736, 1607, 1458, 1230, 1122 cm^{-1}; δ_H:8.32-8.24(m, 4H, Ar-H), 7.77-7.75(m, 6H, Ar-H), 7.6-7.58(m, 4H, Ar-H), 7.49-7.43(m, 4H, Ar-H), 7.32-7.30(m, 7H, Ar-H), 2.69-2.65(t, 4H, ^{3}J7.84 Hz, 2 × Ar-CH_2-), 1.66-1.64(quin, 4H, ^{3}J7.0 Hz, 2 × Ar-CH_2-C$\underline{H}_2$-), 1.37-1.28(m, 20H, 10 × -C$\underline{H}_2$), 0.90-0.87(t, 6H, ^{3}J6.56 Hz, 2 × -CH_2-C$\underline{H}_3$).

2-Cyano-1,3-phenylene bis [4-(4-n-nonylbiphenyl-4-carbonyloxy)2-fluorobenzoate], (5.C.5)

Yield, 32%; m.p. 136.5°C; ν_{max}:2924, 2854, 2230, 1745, 1734, 1607, 1458, 1236, 1124 cm^{-1}; δ_H:8.32-8.24(m, 4H, Ar-H), 7.77-7.75(m, 6H, Ar-H), 7.6-7.58(m, 4H, Ar-H), 7.49-7.43(m, 4H, Ar-H), 7.32-7.30(m, 7H, Ar-H), 2.69-2.65(t, 4H, ^{3}J7.84 Hz, 2 × Ar-CH_2-), 1.66-1.64(quin, 4H, ^{3}J7.16 Hz, 2 × Ar-CH_2-C$\underline{H}_2$-), 1.37-1.28(m, 24H, 12 × -C$\underline{H}_2$), 0.90-0.87(t, 6H, ^{3}J6.56 Hz, 2 × -CH_2-C$\underline{H}_3$).

2-Cyano-1,3-phenylene bis [4-(4-n-decylbiphenyl-4-carbonyloxy)2-fluorobenzoate], (5.C.6)

Yield, 33%; m.p. 130.5°C; ν_{max}:2924, 2854, 2232, 1742, 1734, 1606, 1458, 1236, 1126 cm^{-1}; δ_H:8.32-8.24(m, 4H, Ar-H), 7.77-7.75(m, 6H, Ar-H), 7.6-7.58(m, 4H, Ar-H), 7.49-7.43(m, 4H, Ar-H), 7.32-7.30(m, 7H, Ar-H), 2.69-2.65(t, 4H, ^{3}J7.68 Hz, 2 × Ar-CH_2-), 1.67-1.64(quin, 4H, ^{3}J6.56 Hz, 2 × Ar-CH_2-C$\underline{H_2}$-), 1.37-1.27(m, 28H, 14 × -C$\underline{H_2}$), 0.90-0.86(t, 6H, ^{3}J6.12 Hz, 2 × -CH_2-C$\underline{H_3}$).

2-Cyano-1,3-phenylene bis [4-(4-n-undecylbiphenyl-4-carbonyloxy)2-fluorobenzoate], (5.C.7)

Yield, 34%; m.p. 138°C; ν_{max}:2924, 2854, 2232, 1742, 1734, 1606, 1458, 1236, 1126 cm^{-1}; δ_H:8.32-8.24(m, 4H, Ar-H), 7.77-7.74(m, 6H, Ar-H), 7.6-7.57(m, 4H, Ar-H), 7.49-7.43(m, 4H, Ar-H), 7.32-7.30(m, 7H, Ar-H), 2.69-2.65(t, 4H, ^{3}J7.68 Hz, 2 × Ar-CH_2-), 1.67-1.64(quin, 4H, ^{3}J6.56 Hz, 2 × Ar-CH_2-C$\underline{H_2}$-), 1.37-1.26(m, 32H, 16 × -C$\underline{H_2}$), 0.90-0.86(t, 6H, ^{3}J6.48 Hz, 2 × -CH_2-C$\underline{H_3}$).

2-Cyano-1,3-phenylene bis [4-(4-n-dodecylbiphenyl-4-carbonyloxy)2-fluorobenzoate], (5.C.8)

Yield, 36%; m.p. 134.5°C; ν_{max}:2924, 2854, 2227, 1755, 1738, 1607, 1460, 1238, 1124 cm^{-1}; δ_H:8.32-8.24(m, 4H, Ar-H), 7.77-7.73(m, 6H, Ar-H), 7.6-7.58(m, 4H, Ar-H), 7.49-7.43(m, 4H, Ar-H), 7.32-7.30(m, 7H, Ar-H), 2.69-2.65(t, 4H, ^{3}J7.64 Hz, 2 × Ar-CH_2-), 1.66-1.64(quin, 4H, ^{3}J6.5 Hz, 2 × Ar-CH_2-C$\underline{H_2}$-), 1.37-1.26(m, 36H, 18 × -C$\underline{H_2}$), 0.89-0.86(t, 6H, ^{3}J6.4 Hz, 2 × -CH_2-C$\underline{H_3}$).

2-Cyano-1,3-phenylene bis [4-(4-n-tetradecylbiphenyl-4-carbonyloxy)2-fluorobenzoate], (5.C.9)

Yield, 38%; m.p. 131°C; ν_{max}:2920, 2851, 2227, 1752, 1740, 1606, 1458, 1235, 1122 cm^{-1}; δ_H:8.32-8.24(m, 4H, Ar-H), 7.77-7.73(m, 6H, Ar-H), 7.6-7.58(m, 4H, Ar-H), 7.49-7.43(m, 4H, Ar-H), 7.32-7.30(m, 7H, Ar-H), 2.69-2.65(t, 4H, ^{3}J7.68 Hz, 2 × Ar-CH_2-), 1.66-1.63(quin, 4H, ^{3}J6.52 Hz, 2 × Ar-CH_2-C$\underline{H_2}$-), 1.34-1.26(m, 44H, 22 × -C$\underline{H_2}$), 0.89-0.86(t, 6H, ^{3}J6.0 Hz, 2 × -CH_2-C$\underline{H_3}$).

2-Cyano-1,3-phenylene bis [4-(4-n-hexadecylbiphenyl-4-carbonyloxy)2-fluorobenzoate], (5.C.10)

Yield, 35%; m.p. 124°C; ν_{max}:2922, 2851, 2237, 1749, 1732, 1724, 1610, 1466, 1238, 1126 cm^{-1}; δ_H:8.32-8.24(m, 4H, Ar-H), 7.77-7.75(m, 6H, Ar-H), 7.6-7.58(m, 4H, Ar-H), 7.49-7.43(m, 4H, Ar-H), 7.32-7.30(m, 7H, Ar-H), 2.69-2.65(t, 4H, ^{3}J7.6 Hz, 2 × Ar-CH_2-), 1.66-1.62(quin, 4H, ^{3}J6.56 Hz, 2 × Ar-CH_2-C$\underline{H}_2$-), 1.34-1.26(m, 52H, 26 × -C$\underline{H}_2$), 0.89-0.86(t, 6H, ^{3}J6.08 Hz, 2 × -CH_2-C$\underline{H}_3$).

2-Cyano-1,3-phenylene bis [4-(4-n-octadecylbiphenyl-4-carbonyloxy)2-fluorobenzoate], (5.C.11)

Yield, 31%; m.p. 123°C; ν_{max}:2922, 2851, 2233, 1747, 1734, 1718, 1610, 1466, 1238, 1122 cm^{-1}; δ_H:8.32-8.24(m, 4H, Ar-H), 7.77-7.75(m, 6H, Ar-H), 7.6-7.58(m, 4H, Ar-H), 7.49-7.43(m, 4H, Ar-H), 7.32-7.30(m, 7H, Ar-H), 2.69-2.65(t, 4H, ^{3}J7.4 Hz, 2 × Ar-CH_2-), 1.65-1.63(quin, 4H, ^{3}J6.52 Hz, 2 × Ar-CH_2-C$\underline{H}_2$-), 1.34-1.20(m, 60H, 30 × -C$\underline{H}_2$), 0.89-0.86(t, 6H, ^{3}J6.32 Hz, 2 × -CH_2-C$\underline{H}_3$).

2-Cyano-1,3-phenylene bis [4-(4-n-pentylbiphenyl-4-carbonyloxy)3-fluorobenzoate], (5.D.1)

Yield, 31%; m.p. 162°C; ν_{max}:2924, 2854, 2235, 1753, 1743, 1607, 1466, 1288, 1124 cm^{-1}; δ_H:8.32-8.27(t, 4H, ^{3}J8.28 Hz, Ar-H), 8.16-8.10(m, 2H, Ar-H), 7.77-7.75(d, 6H, ^{3}J7.44 Hz, Ar-H), 7.6-7.58(d, 6H, ^{3}J7.84 Hz, Ar-H), 7.52-7.48(t, 1H, ^{3}J8.64 Hz, Ar-H), 7.45-7.43(d, 2H, ^{3}J8.44 Hz, Ar-H), 7.32-7.3(d, 4H, ^{3}J7.72 Hz, Ar-H), 2.69-2.65(t, 4H, ^{3}J7.6 Hz, 2 × Ar-CH_2-), 1.66-1.64(quin, 4H, ^{3}J7.4 Hz, 2 × Ar-CH_2-C$\underline{H}_2$-), 1.37-1.27(m, 8H, 4 × -C$\underline{H}_2$-), 0.9-0.87(t, 6H, ^{3}J6.78 Hz, 2 × -CH_2-C$\underline{H}_3$).

2-Cyano-1,3-phenylene bis [4-(4-n-octylbiphenyl-4-carbonyloxy)3-fluorobenzoate], (5.D.2)

Yield, 34%; m.p. 142°C; ν_{max}:2924, 2854, 2235, 1753, 1743, 1607, 1466, 1288, 1124 cm^{-1}; δ_H:8.32-8.27(t, 4H, ^{3}J9.2 Hz, Ar-H), 8.17-8.10(m, 2H, Ar-H), 7.77-7.75(d, 6H, ^{3}J8.04 Hz, Ar-H), 7.6-7.58(d, 6H, ^{3}J7.8 Hz, Ar-H), 7.52-7.48(t, 1H, ^{3}J8.62 Hz, Ar-H), 7.45-7.43(d, 2H, ^{3}J8.44 Hz, Ar-H), 7.32-7.3(d, 4H, ^{3}J7.72 Hz, Ar-H), 2.69-2.65(t, 4H, ^{3}J7.6 Hz, 2 × Ar-CH_2-), 1.66-1.64(quin, 4H, ^{3}J7.4 Hz, 2 × Ar-CH_2-C$\underline{H}_2$-), 1.37-1.27(m, 20H, 10 × -C$\underline{H}_2$-), 0.9-0.87(t, 6H, ^{3}J6.8 Hz, 2 × -CH_2-C$\underline{H}_3$).

2-Cyano-1,3-phenylene bis [4-(4-n-nonylbiphenyl-4-carbonyloxy)3-fluorobenzoate], (5.D.3)

Yield, 33%; m.p. 140.5°C; ν_{max}:2924, 2854, 2230, 1757, 1736, 1607, 1466, 1288, 1124 cm^{-1}; δ_H:8.32-8.27(t, 4H, ^{3}J8.48 Hz, Ar-H), 8.17-8.10(m, 2H, Ar-H), 7.77-7.75(d, 6H, ^{3}J8.04 Hz, Ar-H), 7.6-7.58(d, 6H, ^{3}J7.8 Hz, Ar-H), 7.52-7.48(t, 1H, ^{3}J8.62 Hz, Ar-H), 7.45-7.43(d, 2H, ^{3}J8.44 Hz, Ar-H), 7.32-7.3(d, 4H, ^{3}J7.72 Hz, Ar-H), 2.69-2.65(t, 4H, ^{3}J7.6 Hz, 2 × Ar-CH_2-), 1.66-1.64(quin, 4H, ^{3}J7.4 Hz, 2 × Ar-CH_2-C$\underline{H_2}$-), 1.37-1.27(m, 24H, 12 × -C$\underline{H_2}$-), 0.9-0.87(t, 6H, ^{3}J7.0 Hz, 2 × -CH_2-C$\underline{H_3}$).

2-Cyano-1,3-phenylene bis [4-(4-n-decylbiphenyl-4-carbonyloxy)3-fluorobenzoate], (5.D.4)

Yield, 36%; m.p. 125°C; ν_{max}:2924, 2854, 2230, 1757, 1738, 1605, 1462, 1288, 1128 cm^{-1}; δ_H:8.32-8.27(t, 4H, ^{3}J8.6 Hz, Ar-H), 8.17-8.11(m, 2H, Ar-H), 7.77-7.75(d, 6H, ^{3}J7.88 Hz, Ar-H), 7.6-7.58(d, 6H, ^{3}J7.6 Hz, Ar-H), 7.52-7.48(t, 1H, ^{3}J8.4 Hz, Ar-H), 7.45-7.43(d, 2H, ^{3}J8.36 Hz, Ar-H), 7.32-7.3(d, 4H, ^{3}J7.76 Hz, Ar-H), 2.69-2.65(t, 4H, ^{3}J7.68 Hz, 2 × Ar-CH_2-), 1.66-1.62(quin, 4H, ^{3}J7.4 Hz, 2 × Ar-CH_2-C$\underline{H_2}$-), 1.34-1.27(m, 28H, 14 × -C$\underline{H_2}$-), 0.9-0.86(t, 6H, ^{3}J6.12 Hz, 2 × -CH_2-C$\underline{H_3}$).

2-Cyano-1,3-phenylene bis [4-(4-n-undecylbiphenyl-4-carbonyloxy)3-fluorobenzoate], (5.D.5)

Yield, 38%; m.p. 128°C; ν_{max}:2922, 2853, 2230, 1757, 1738, 1605, 1462, 1288, 1128 cm^{-1}; δ_H:8.32-8.27(t, 4H, ^{3}J8.66 Hz, Ar-H), 8.17-8.11(m, 2H, Ar-H), 7.77-7.75(d, 6H, ^{3}J7.8 Hz, Ar-H), 7.6-7.58(d, 6H, ^{3}J7.6 Hz, Ar-H), 7.52-7.48(t, 1H, ^{3}J8.4 Hz, Ar-H), 7.45-7.43(d, 2H, ^{3}J8.32 Hz, Ar-H), 7.32-7.3(d, 4H, ^{3}J7.7 Hz, Ar-H), 2.69-2.65(t, 4H, ^{3}J7.62 Hz, 2 × Ar-CH_2-), 1.66-1.62(quin, 4H, ^{3}J7.4 Hz, 2 × Ar-CH_2-C$\underline{H_2}$-), 1.34-1.27(m, 32H, 16 × -C$\underline{H_2}$-), 0.9-0.86(t, 6H, ^{3}J6.2 Hz, 2 × -CH_2-C$\underline{H_3}$).

2-Cyano-1,3-phenylene bis [4-(4-n-dodecylbiphenyl-4-carbonyloxy)3-fluorobenzoate], (5.D.6)

Yield, 36%; m.p. 131°C; ν_{max}:2922, 2853, 2230, 1757, 1738, 1605, 1462, 1284, 1128 cm^{-1}; δ_H:8.32-8.27(t, 4H, ^{3}J9.36 Hz, Ar-H), 8.17-8.11(m, 2H, Ar-H), 7.77-7.75(d, 6H, ^{3}J7.92 Hz, Ar-H), 7.6-7.58(d, 6H, ^{3}J7.72 Hz, Ar-H), 7.52-7.48(t, 1H, ^{3}J8.36 Hz, Ar-H), 7.45-7.43(d, 2H, ^{3}J7.96 Hz, Ar-H), 7.32-7.3(d, 4H, ^{3}J7.76 Hz, Ar-H), 2.69-2.65(t, 4H, ^{3}J7.62 Hz, 2 × Ar-CH_2-),

1.66-1.62(quin, 4H, ^{3}J7.4 Hz, 2 × Ar-CH_2-C$\underline{H}_2$-), 1.34-1.27(m, 36H, 18 × -C$\underline{H}_2$-), 0.89-0.86(t, 6H, ^{3}J6.0 Hz, 2 × -CH_2-C$\underline{H}_3$).

2-Cyano-1,3-phenylene bis [4-(4-n-tetradecylbiphenyl-4-carbonyloxy)3-fluorobenzoate], (5.D.7)

Yield, 35%; m.p. 122.5°C; ν_{max}:2922, 2853, 2228, 1757, 1740, 1605, 1460, 1284, 1128 cm^{-1}; δ_H:8.32-8.27(t, 4H, ^{3}J8.56 Hz, Ar-H), 8.17-8.11(m, 2H, Ar-H), 7.77-7.75(d, 6H, ^{3}J7.04 Hz, Ar-H), 7.6-7.58(d, 6H, ^{3}J6.64 Hz, Ar-H), 7.52-7.48(t, 1H, ^{3}J8.2 Hz, Ar-H), 7.45-7.43(d, 2H, ^{3}J8.4 Hz, Ar-H), 7.32-7.3(d, 4H, ^{3}J7.68 Hz, Ar-H), 2.69-2.65(t, 4H, ^{3}J7.04 Hz, 2 × Ar-CH_2-), 1.66-1.62(quin, 4H, ^{3}J7.4 Hz, 2 × Ar-CH_2-C$\underline{H}_2$-), 1.34-1.27(m, 44H, 22 × -C$\underline{H}_2$-), 0.89-0.86(t, 6H, ^{3}J6.88 Hz, 2 × -CH_2-C$\underline{H}_3$).

2-Cyano-1,3-phenylene bis [4-(4-n-hexadecylbiphenyl-4-carbonyloxy)3-fluorobenzoate], (5.D.8)

Yield, 34%; m.p. 117°C; ν_{max}:2922, 2853, 2228, 1755, 1740, 1605, 1460, 1284, 1128 cm^{-1}; δ_H:8.32-8.27(t, 4H, ^{3}J8.68 Hz, Ar-H), 8.17-8.10(m, 2H, Ar-H), 7.77-7.75(d, 6H, ^{3}J7.2 Hz, Ar-H), 7.6-7.58(d, 6H, ^{3}J8.0 Hz, Ar-H), 7.50-7.48(t, 1H, ^{3}J8.56 Hz, Ar-H), 7.45-7.43(d, 2H, ^{3}J8.52 Hz, Ar-H), 7.32-7.3(d, 4H, ^{3}J7.92 Hz, Ar-H), 2.69-2.65(t, 4H, ^{3}J7.36 Hz, 2 × Ar-CH_2-), 1.66-1.64(quin, 4H, ^{3}J7.4 Hz, 2 × Ar-CH_2-C$\underline{H}_2$-), 1.34-1.27(m, 52H, 26 × -C$\underline{H}_2$-), 0.89-0.86(t, 6H, ^{3}J6.88 Hz, 2 × -CH_2-C$\underline{H}_3$).

2-Cyano-1,3-phenylene bis [4-(4-n-octadecylbiphenyl-4-carbonyloxy)3-fluorobenzoate], (5.D.9)

Yield, 31%; m.p. 112°C; ν_{max}:2922, 2853, 2230, 1753, 1743, 1605, 1460, 1284, 1126 cm^{-1}; δ_H:8.32-8.27(t, 4H, ^{3}J8.62 Hz, Ar-H), 8.17-8.10(m, 2H, Ar-H), 7.77-7.75(d, 6H, ^{3}J7.24 Hz, Ar-H), 7.6-7.58(d, 6H, ^{3}J8.08 Hz, Ar-H), 7.50-7.48(t, 1H, ^{3}J8.56 Hz, Ar-H), 7.45-7.43(d, 2H, ^{3}J8.52 Hz, Ar-H), 7.32-7.3(d, 4H, ^{3}J7.9 Hz, Ar-H), 2.69-2.65(t, 4H, ^{3}J7.36 Hz, 2 × Ar-CH_2-), 1.66-1.64(quin, 4H, ^{3}J7.4 Hz, 2 × Ar-CH_2-C$\underline{H}_2$-), 1.34-1.27(m, 60H, 30 × -C$\underline{H}_2$-), 0.89-0.86(t, 6H, ^{3}J6.88 Hz, 2 × -CH_2-C$\underline{H}_3$).

Chapter-6

Part-I

Synthesis and mesomorphic properties of

(i) 4-Cyanophenyl-4-[3-{4-(4-n-alkoxybenzoyloxy)benzoyloxy} benzoyloxy]benzoate (Series - 6.I)

(ii) 4-Cyanophenyl-4-[3-{4-(4-n-alkoxybenzoyloxy)2-fluorobenzoyloxy} benzoyloxy]benzoate (Series - 6.II)

(iii) 4-Cyanophenyl-4-[3-{4-(4-n-alkoxybenzoyloxy)3-fluorobenzoyloxy} benzoyloxy]benzoate (Series - 6.III)

Part-II

Synthesis and mesomorphic properties of

(iv) 4-Cyanophenyl-4-[3-{4-(4-n-alkylbiphenyl-4-carbonyloxy) benzoyloxy} benzoyloxy]benzoate (Series - 6.IV)

(v) 4-Cyanophenyl-4-[3-{4-(4-n-alkylbiphenyl-4-carbonyloxy)2-fluoro-benzoyloxy}benzoyloxy]benzoate (Series - 6.V)

(vi) 4-Cyanophenyl-4-[3-{4-(4-n-alkylbiphenyl-4-carbonyloxy)3-fluoro-benzoyloxy}benzoyloxy]benzoate (Series- 6.VI)

Theoretical prediction of biaxial smectic A phase:

In conventional calamitic smectic phases such as SmA phase, the molecules are aligned parallel and in SmC phase they are tilted with respect to the layer normal. The uniaxial smectic A phase exhibits the local symmetry $D_{\infty h}$ and the biaxial SmC phase has a C_{2h} symmetry. However, in 1974 de Gennes [115,116] predicted quite an unusual smectic phase with D_{2h} point group symmetry namely, a biaxial smectic A phase. In this phase, also designated as C_M phase where M refers to McMillan [117, 118], the molecules align parallel to the layer normal as in the case of conventional SmA phase, but the properties in this direction are different when compared with the in-plane directions. According to the theoretical predictions, the C_M phase should exist if one of the principal axes of the magnetic susceptibility tensor $Q_{\alpha,\beta}$ is along the layer normal and the transverse components of the tensors $Q_{\varepsilon,\varepsilon}$ and $Q_{\eta,\eta}$ are non-equivalent.

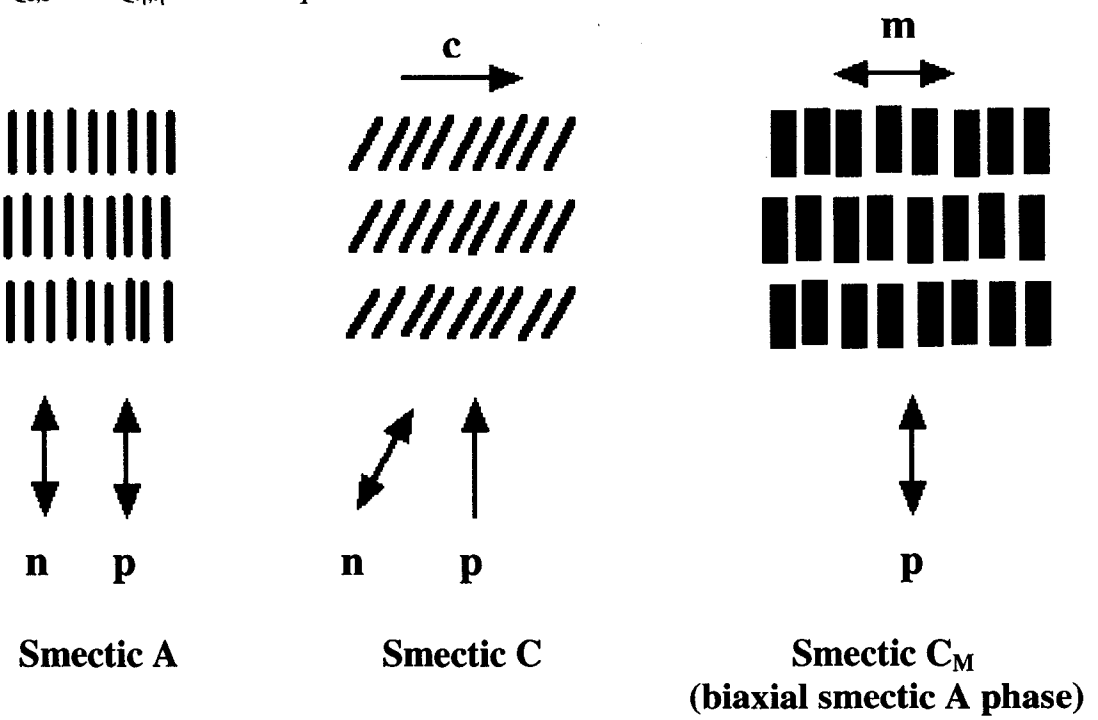

Fig. 6.1. A schematic representation of layer normal (p), long molecular axes (n), c vector (projection of n) and the in-plane director (m) for the three different mesophase structures.

Later in 1992, Brand *et al.* [119] suggested that the C_M phase (biaxial smectic A phase) can be obtained in board-like molecules in which $Q_{\varepsilon,\varepsilon} \neq Q_{\eta,\eta}$ due to steric reasons. They also discuss about the defects allowed by the symmetry of this phase and the distinguishing features in microscopic textures from the other biaxial and fluid smectic phases such as smectic C and anticlinic smectic C phases.

As pointed out by Brand *et al.* [119], the nematic phase has the indistinguishable director (**n**) along a preferred direction. In SmA phase also the layer normal is a unit vector **p** that is indistinguishable from $-\mathbf{p}$ (because $\mathbf{n} \parallel \mathbf{p}$) and hence the in-plane properties are the same. However, in classical SmC phase, since the director **n** is tilted with respect to the layer normal **p** and hence the inequivalence in $\mathbf{p} \longrightarrow -\mathbf{p}$ as well as the **c** vector (projection of **n** in the plane) $\mathbf{c} \longrightarrow -\mathbf{c}$. In contrast to classical smectic C phase, the biaxial smectic A phase has no tilt and $\mathbf{p} \parallel \mathbf{n}$. The in-plane preferred directions are indicated by a director **m** and is perpendicular to the layer normal **P**. Thus, the equivalency in $\mathbf{p} \longrightarrow -\mathbf{p}$ and also $\mathbf{m} \longrightarrow -\mathbf{m}$ is shown in figure **6.1**. Due to the equivalency in $\mathbf{m} \longrightarrow -\mathbf{m}$, the biaxial smectic A phase can have ±1/2 strength defects in addition to ± 1 strength defects, just as in the uniaxial nematic phase. In contrast to classical smectic C phase in which **c** is not equivalent to **–c** (because of tilt) and as such no ± 1/2 strength defects (unequivalency by π rotation) are allowed and only ± 1 strength defects (due to equivalency by 2π rotation) are allowed by its symmetry. These differences help to distinguish the classical smectic C phase from the biaxial smectic A phase under a polarizing microscope.

One of the important features the smectic phases is the occurrence of fan or focal-conic texture which is due to the fact that the layer curvature energy is small and also they conserve microscopic layer spacing when the layers are curved. When a transition takes place from SmA to SmC phase, because of the mismatch in the layer spacing the focal-conics become broken focal-conics. However, while going from SmA to SmA_b phase, because of the equivalency in in-plane directions (**m** is equivalent to **–m**) there is no mismatch in the layer spacings and hence no broken focal-conic texture is observed. Perhaps, these qualitative distinguishable microscopic observations help to distinguish the biaxial smectic A phase from the classical SmC phase.

The inequivalence in **m** to **–m** can be achieved from the bow- or banana- or bent-shaped molecules which can be considered as biaxial objects as shown in figure **6.2**.

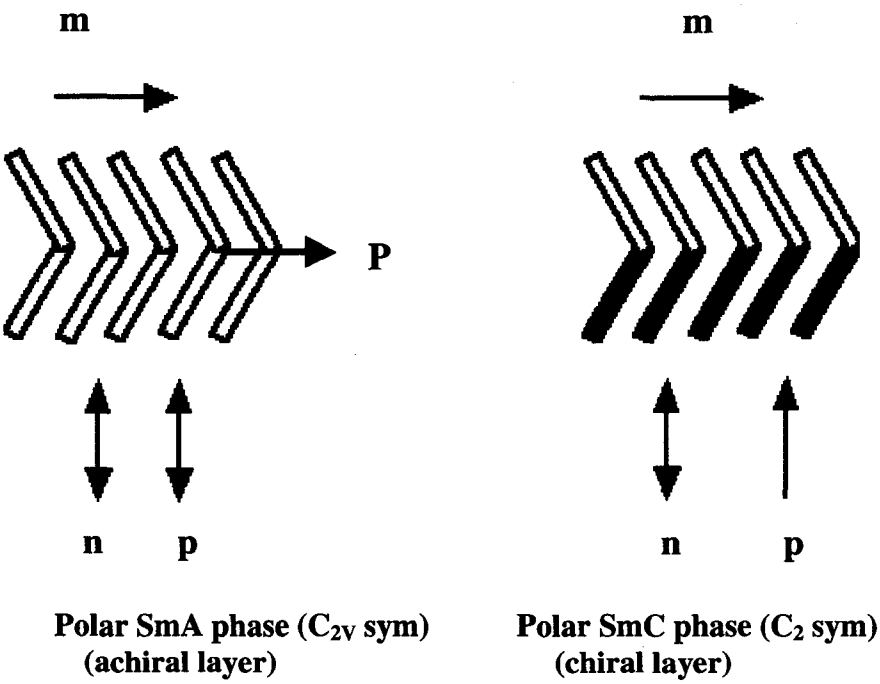

Fig. 6.2. A schematic representation of achiral and chiral layers containing biaxial BC molecules which induce a polar packing within the layers resulting in a polarization along the bent direction.

Experimental evidence for biaxial smectic A phase:

There has been a claim for the observation of the biaxial smectic A phase in a binary mixture of a liquid crystalline side chain polymer laterally substituted with naphthalene groups in the mesogenic moiety and a monomeric material [120]. The binary phase diagram indicates that both the polymer and the monomer are completely miscible throughout the concentration range. Mixtures with up to 50 mole % of the monomeric liquid crystal show a nematic phase and the lower temperature phase has been claimed to be a biaxial smectic A phase.

In 1998, Semmler *et al.* [121] claimed to have observed the biaxial smectic A phase in a low molecular mass liquid crystal composed of boomerang-shaped molecules. Since the smectic A phase occurs at very high temperatures, higher than 235°C, no other experiments have been carried out for this compound. Also, the conoscopic experiments reveal the uniaxial interference pattern for the smectic A phase in the absence of electric field. On application of an electric field perpendicular to the layer normal, the separation of isogyres was observed and is perhaps a field induced biaxiality. As pointed out by Hegmann *et al.* [122] in the latter

two cases [120, 121], the textural features of non-aligned samples resemble the uniaxial smectic A phase and unambiguous proof for the existence of the biaxial smectic A phase has not been provided.

In 2000, Pratibha *et al.* [123] examined binary mixtures of a compound exhibiting the B_2 phase [36] with one composed of lath-like molecules [124] exhibiting the bilayer smectic A_2 phase which resulted in a very interesting phase diagram. At certain concentrations of the bent-core molecules (4-13 mole %) a new biaxial smectic A_2 (SmA_{2b}) phase is induced in which the BC molecules undergo an orientational transition as the temperature is lowered from the uniaxial smectic A_2 phase. The biaxial smectic A phase obtained in this binary mixture is evident with ± 1 and ± 1/2 brush defects seen under a polarizing microscope. Perhaps this is the first experimental evidence for the existence of biaxial smectic A phase in low molecular weight compounds though in a mixture.

The biaxial smectic A phase has also been reported in a binary mixture of a metallomesogen and 2,4,7-trinitrofluorenone [122]. From the molecular structure point of view, though the metallomesogen itself has the required molecular shape to exhibit the biaxial smectic A phase, the rotation about the long molecular axis is perhaps fast and exhibit only a uniaxial smectic A phase. However, the mixtures with TNF (trinitrofluorenone) exhibit the biaxial smectic A phase. This may be due to the strong face-to-face interactions between TNF and the metallomesogen which reduces the molecular rotation around the long molecular axis, leading to the biaxiality. The XRD studies on oriented samples, confirm the orthogonal arrangement of flat molecules within the smectic layers.

Recently, Prehm *et al.* [125, 126] reported the biaxial smectic A phase in a single component system. In contrast to all conventional smectic phases, the calamitic core parts are organized parallel to the layer planes and the lateral alkyl chains are strongly disordered (liquid-like) but with a certain preferred direction which is perpendicular to the layer planes. In contrast to the high temperature SmA phase, in the low temperature biaxial smectic A phase, the aromatic cores adopt a long-range orientational order within the aromatic sub-layers. The individual layers are orientationally correlated with each other, so that macroscopic optical biaxiality results. This phase can be considered as a smectic phase built up of quasi 2D layers with nematic order, separated by isotropic layers of the lateral chains.

In addition, Eremin *et al.* [127] also reported an achiral orthogonal biaxial smectic A phase exhibiting antiferroelectric switching behaviour. This mesophase was observed in a compound composed of banana-shaped molecules derived from 4-cyanoresorcinol and containing a fluorine substituent at *ortho* position with respect to the terminal n-alkoxy chains on the outer phenyl rings. In this mesophase, the orthogonal arrangement of molecules in smectic layers have C_{2V} symmetry and the polar director which alternates from layer to layer gives rise to an antiferroelectric structure. The polar biaxial smectic A phase has also been reported [128] in a binary mixture of banana-shaped molecules with TNF. The pure banana-shaped compound exhibits a B_2 phase and the mixture with TNF shows the uniaxial SmA phase, antiferroelectric biaxial SmA phase and a B_2 phase on lowering the temperature.

Part-I

Results and discussion

In this part, we describe the synthesis and characterization of three new homologous series of compounds composed of highly polar unsymmetrically substituted BC molecules. The unsymmetrical molecule contains an n-alkoxy chain in one of the arms of the bent-core, while the other arm is terminally substituted with a highly polar cyano group. Interestingly, these compounds exhibit a partial bilayer biaxial smectic A (SmA_{db}) phase in which the bent cores of two neighbouring molecules overlap in an antiparallel orientation as in the case of highly polar lath-like molecules [129, 130]. In fact, this compound exhibits a direct transition from uniaxial smectic A to biaxial smectic A phase on lowering the temperature. More interestingly, the lower temperature biaxial smectic A phase shows an antiferroelectric switching behaviour. This represents the first example of a bent-core compound with partial bilayer structure and showing an antiferroelectric switching behaviour. These five-ring compounds are esters having the general molecular structure **6.1**.

The unsymmetrically substituted bent-core compounds belonging to three different homologous series were synthesized following a general synthetic pathway shown in scheme **6.1**. 3-Hydroxybenzoic acid and 4-cyanophenol were obtained commercially and used without further purification. 3-Benżyloxybenzoic acid was prepared using 3-hydroxybenzoic acid following a procedure described in the literature [80]. 4-Benzyloxybenzoic acid, 2-fluoro-4-benzyloxybenzoic acid and 3-fluoro-4-benzyloxybenzoic acids were prepared as described in Chapter-**2**.

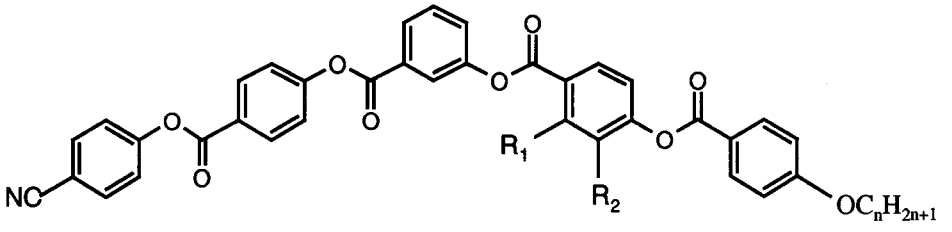

R_1=H, R_2=H **Series-6.I**

R_1=F, R_2=H **Series-6.II**

R_1=H, R_2=F **Series-6.III**

Structure-6.1

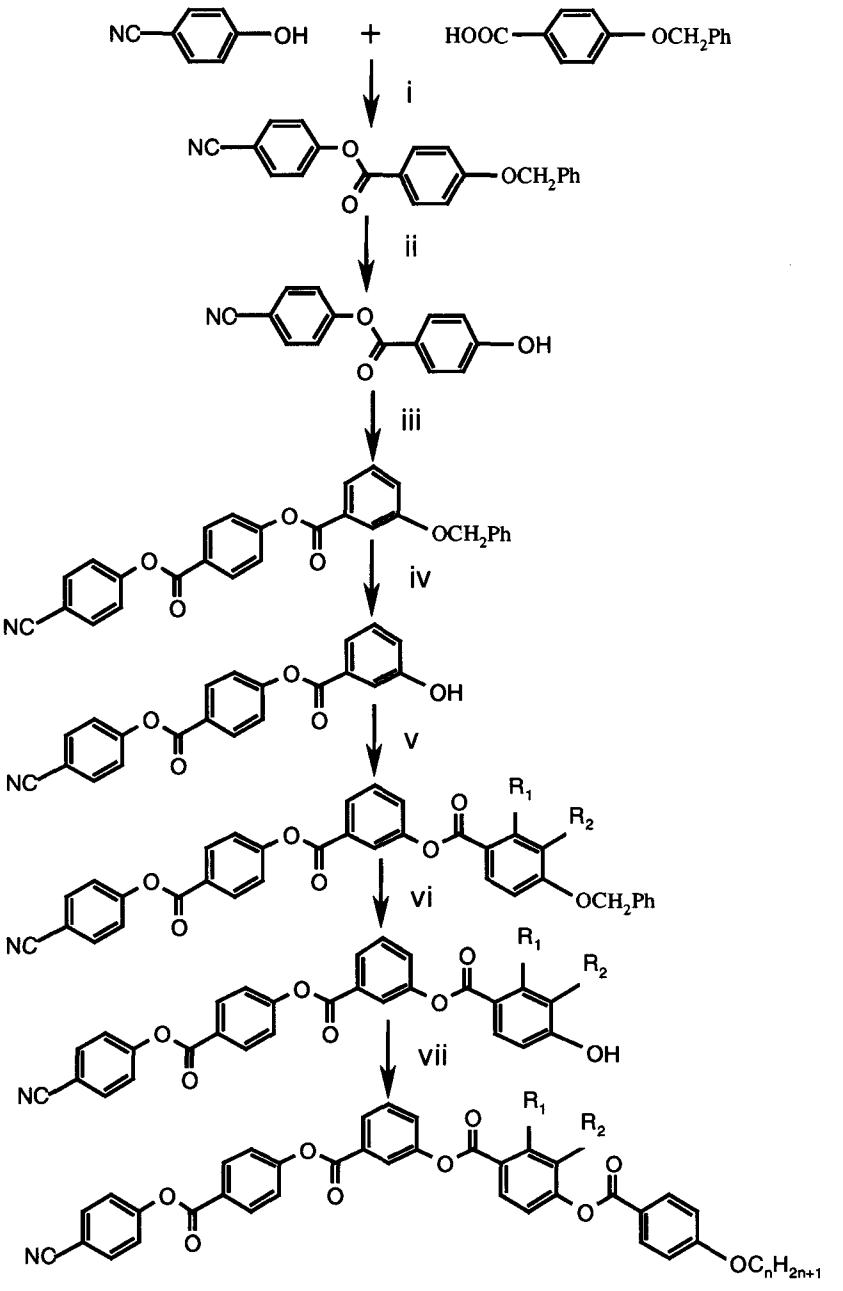

Reagents and conditions: (i) DCC, cat. DMAP, dry $CHCl_3$, room temp., 15h, 81%; (ii) cat. 5% Pd-C, H_2, 1,4-dioxane, 55°C, 75%; (iii) 3-benzyloxybenzoic acid, DCC, cat. DMAP, dry $CHCl_3$, room temp., 15h, 72%; (iv) cat. 5% Pd-C, H_2, 1,4-dioxane, 55°C, 73%; (v) 4-benzyloxybenzoic acid or 2-fluoro- or 3-fluoro-4-benzyloxybenzoic acid, DCC, cat. DMAP, dry $CHCl_3$, room temp., 20h, 68%; (vi) cat. 5% Pd-C, H_2, 1,4-dioxane, 55°C, 80%; (vii) 4-n-alkoxybenzoic acids, DCC, cat. DMAP, dry $CHCl_3$, room temp., 20h, 61%.

Scheme 6.1. General synthetic pathway used for the preparation of unsymmetrically substituted banana-shaped mesogens.

Mesomorphic properties of compounds of series 6.I, 6.II and 6.III:

The phase transition temperatures and the associated enthalpies obtained for the highly polar unsymmetrically substituted compounds belonging to three new homologous series, viz. **6.I, 6.II** and **6.III** are summarized in tables **6.1**, **6.2** and **6.3** respectively. The compounds of series **6.I** are unsubstituted while in series **6.II** and **6.III**, a fluorine is introduced in *ortho* and *meta* positions respectively with respect to the carboxylate group of the middle phenyl ring of the arm containing the n-alkoxy chain. In series **6.I**, a total of nine compounds were prepared. The lower three homologues namely, **6.A.1**, **6.A.2** and **6.A.3** are non-mesomorphic and the remaining six compounds are dimesomorphic and enantiotropic. On cooling the isotropic liquid of a sample (compounds **6.A.4** to **6.A.9**) sandwiched between a glass slide and a coverslip and viewed under a polarizing microscope, a well aligned homeotropic texture is obtained. However, in some regions a focal-conic texture could also be seen. This mesophase has been identified as uniaxial smectic A_d phase. As the temperature is lowered further, a phase transition takes place in which the homeotropic regions exhibit a schlieren texture with both two- and four-brush defects as shown in figure **6.3**. At this transition the homeotropic alignment is lost which indicates the introduction of biaxial director for the lower temperature phase. The presence of two-brush defects in the low temperature mesophase indicates one of the following structures: (i) a biaxial smectic A phase in which the two orthogonal directors in the plane of smectic layers are also *apolar* in nature, (ii) a packing of the BC molecules such that each layer is polarized, but with a mutually antiferroelectric arrangement in neighbouring layers. The two-brush defects in such a case were dispirations which are combinations of 1/2 strength disclinations and screw dislocations. This structure can also be described as a biaxial SmA phase. (iii) Another possibility would be for the molecules to tilt with an anticlinic arrangement in successive layers, in which case again dispirations can produce two-brush defects. As pointed out by Brand *et al.* [119] a distinguishing feature of the biaxial smectic A phase is the occurrence of $\pm$ ½ strength defects, unlike in the smectic C phase with tilted molecules which allows only disclinations of strength $\pm$ 1. The strong fluctuations in intensity seen in the lower temperature phase is also observed in the binary mixture [123] and this phase has been identified as a biaxial smectic A_d phase. The focal-conic texture obtained in the uniaxial smectic A_d phase changes over to a focal-conic texture with stripes, and no broken focal-conic texture is observed. The textural changes obtained in the uniaxial and biaxial smectic phases are shown in figure **6.4.** Sometimes the lower temperature mesophase also exhibits a striped texture as shown in figure **6.5** and further studies have to be carried out

to understand the origin of such patterns. A differential scanning calorimetric (DSC) thermogram obtained for compound **6.A.8** is shown in figure **6.6** and all the transitions can be seen clearly. While the clearing transition enthalpy ranges from 3.5 to 6 $kJmol^{-1}$, that for the

Table 6.1. Transition temperatures (°C) and enthalpies ($kJmol^{-1}$) for compounds of series 6.I.

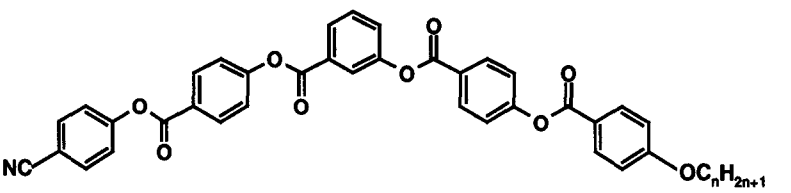

Compound	n	Cr		$SmA_{db}P_A$		SmA_d		I
6.A.1	8	.	140.5	.		-		.
			48.5					
6.A.2	10	.	133.5	.		-		.
			63.8					
6.A.3	11	.	131.0	.		-		.
			43.3					
6.A.4	12	.	129.5	.	130.5	.	130.8	.
			41.1		*0.17*		*3.48*	
6.A.5	13	.	129.0[b]	.	135.0	.	135.5	.
			80.9		*0.09*		*4.24*	
6.A.6	14	.	129.5[b]	.	138.0	.	140.2	.
			77.3		*0.13*		*4.81*	
6.A.7	15	.	129.5[b]	.	140.2	.	144.0	.
			89.1		*0.09*		*5.27*	
6.A.8	16	.	130.0[b]	.	141.9	.	147.5	.
			86.7		*0.08*		*5.79*	
6.A.9	18	.	129.5[b]	.	143.2	.	153.5	.
			60.6		*0.11*		*6.17*	

b: compound has crystal-crystal transition; enthalpy denoted is the sum of all previous transitions.

Key: Applicable to all the tables: Cr=Crystalline phase; SmA_d=Partial bilayer uniaxial smectic A phase; $SmA_{db}P_A$=Partial bilayer biaxial antiferroelectric smectic A phase; I= Isotropic phase. . Phase exists; - Phase does not exist; Temperature in parentheses indicate monotropic transitions.

Table 6.2. Transition temperatures (°C) and enthalpies (kJmol^{-1}) for compounds of series 6.II.

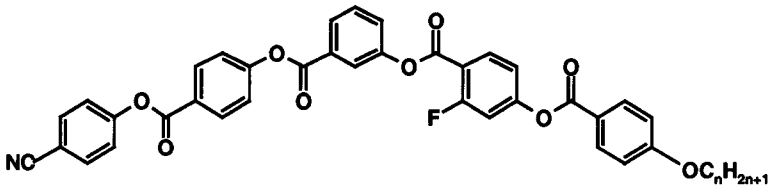

Compound	n	Cr		$SmA_{db}P_A$		SmA_d		I
6.B.1	12	.	130.0	-		-		.
			66.8					
6.B.2	14	.	132.0	-		(.	130.5)	.
			68.3				*4.2*	
6.B.3	16	.	131.5	(.	130.0)	.	137.5	.
			60.3		*0.12*		*5.0*	
6.B.4	18	.	131.0	.	132.5	.	143.5	.
			60.3		*0.06*		*5.95*	

Table 6.3. Transition temperatures (°C) and enthalpies (kJmol^{-1}) for compounds of series 6.III.

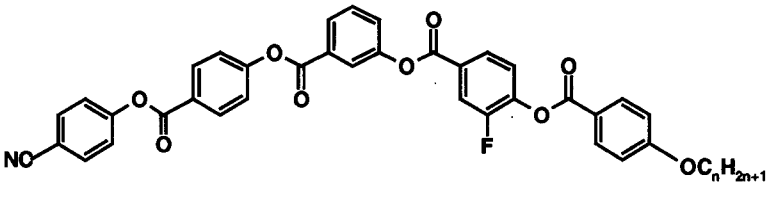

Compound	n	Cr		$SmA_{db}P_A$		SmA_d		I
6.C.1	6	.	161.0	.		.		.
			70.3					
6.C.2	12	.	119.5	(.	119.2)	.	120.0	.
			80.7		*0.02*		*3.86*	
6.C.3	13	.	120.0	.	123.4	.	125.5	.
			82.7		*0.02*		*4.22*	
6.C.4	14	.	120.5	.	126.2	.	130.0	.
			85.5		*0.04*		*4.77*	
6.C.5	15	.	121.0	.	128.0	.	133.8	.
			72.6		*0.09*		*4.95*	
6.C.6	16	.	121.0	.	129.0	.	137.0	.
			67.1		*0.08*		*5.47*	
6.C.7	18	.	120.0	.	130.0	.	142.3	.
			44.8		*0.11*		*5.85*	

(a)

(b)

Fig. 6.3. Optical photomicrographs of (a) a perfectly aligned homeotropic texture obtained in the SmA_d phase and (b) schlieren texture obtained in the $SmA_{db}P_A$ phase for compound 6.A.6.

biaxial smectic A_d to uniaxial smectic A_d phase transition is quite low and is of *the* order of 0.1 $kJmol^{-1}$. A plot of the transition temperatures against the number of carbon atoms in the n-alkoxy chain for this series is shown in figure 6.7. One can see smooth curve relationships for like transitions and both the mesophase-mesophase and mesophase-isotropic transition point curves rise gradually on ascending the *series,* while the melting points remain more or less constant.

Only four compounds were synthesized in series 6.11. Compound 6.B.1 is non-mesomorphic and compound 6.B.2 does not exhibit the biaxial smectic A_d phase. Though compounds 6.B.3 and 6.B.4 do exhibit the polar biaxial smectic A_d phase, the former is monotropic. The characteristic textural features observed in series 6.1 were observed for these two compounds

as well. In series **6.III**, seven homologues were synthesized and the transition temperatures and the associated enthalpies are shown in table **6.3.** The first homologue (**6.C.1**) is not liquid crystalline and the others do exhibit both the uniaxial as well as the polar biaxial smectic A_d phases. Again the textural characteristics and the DSC data are similar to those observed for homologues of series **6.I.** A plot of the transition temperatures versus the number of carbon atoms in the n-alkoxy chain for the homologues of series **6.III** is shown in figure **6.8**. Again, a rising trend is obtained for like transitions and the melting points lie practically on a horizontal line on ascending the series. It is interesting to note that the near constancy of the melting points in each of the three homologous series of compounds is rather unusual. A comparison of the transition temperatures of the three series of compounds **6.I, 6.II** and

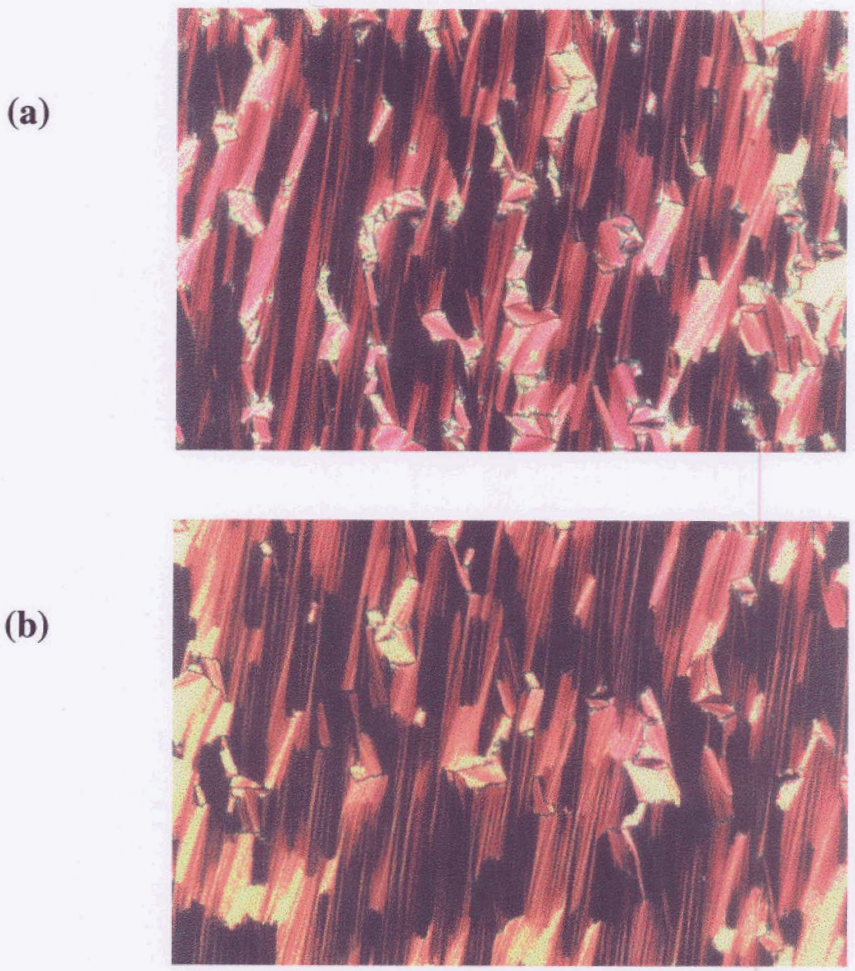

Fig. 6.4. Photomicrographs obtained (a) focal-conic texture of SmA_d phase (b) focal-conic texture with stripes in $SmA_{db}P_A$ phase of compound 6.A.6.

reveal the following features. The introduction of an *ortho* fluoro substituent (series **6.II**) lowers the clearing temperatures by about 10°C while the melting points are increased

marginally. Also, the compound with n-dodecyloxy chain (6.B.1) is rendered non-mesogenic. However, in the case of *meta* fluoro substituted compounds (series 6.III), both the melting and clearing points are reduced by about 10°C. This suggests that the position of the fluoro substituent (dipolar interactions) has an influence on the stability of the mesophase in such bent-core compounds.

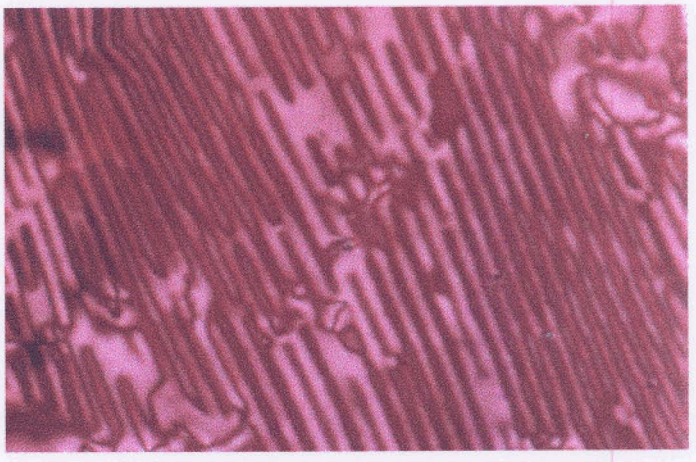

Fig. 6.5. A photomicrograph of the striped pattern obtained for compound 6.A.6 at 132°C.

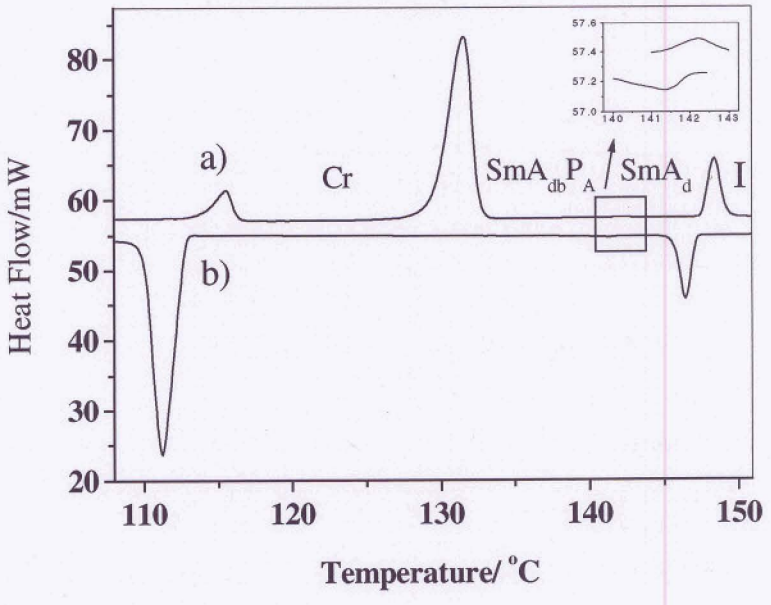

Fig. 6.6. Differential scanning calorimetric scans for compound 6.A.8: a) heating cycle, b) cooling cycle; rate 5°C mid^{-1}. The inset shows the SmA$_{db}$P$_A$ → SmA$_d$ phase transition.

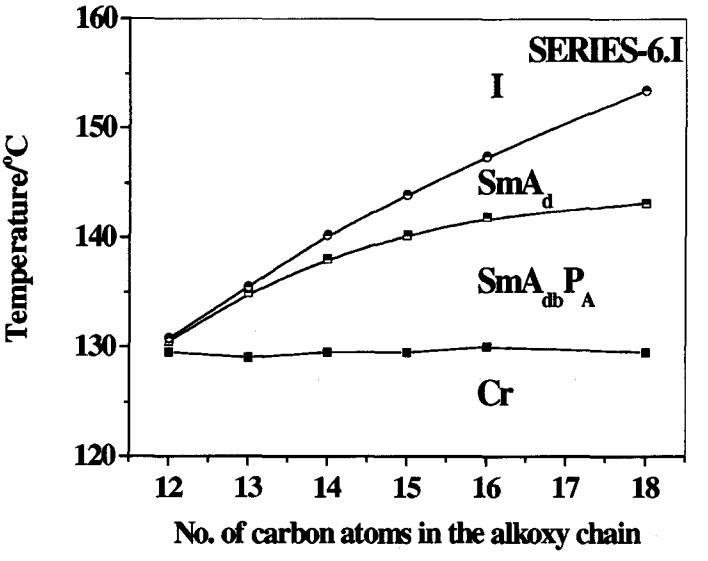

Fig. 6.7. A plot of the transition temperatures as a function of the number of carbon atoms in n-alkoxy chain obtained for compounds of series 6.I.

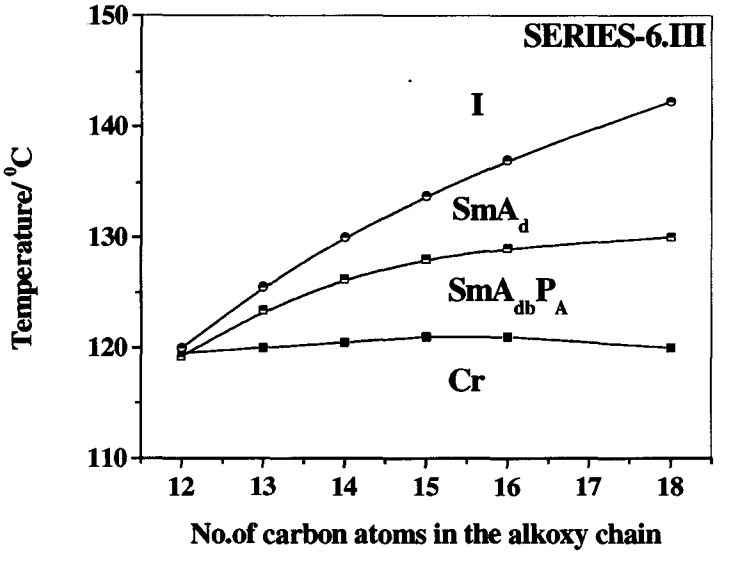

Fig. 6.8. A plot of transition temperatures as a function of the number of carbon atoms in n-alkoxy chain obtained for compounds of series 6.III.

In order to confirm the optical biaxiality of the lower temperature smectic A_d phase, conoscopic experiments were carried out. For this purpose, well aligned samples have to be used and the same was achieved in the following way. A cell was constructed in which one of the glass plates has an ITO conducting coating with a gap of 1 *mm* between the electrodes that is etched out. The other plate was an ordinary glass slide and both were pretreated with

octadecyltriethoxysilane (ODSE) which facilitates a homeotropic alignment of the smectic A liquid crystal. The thickness of the sample (usually ~ 30 μm) was controlled by using appropriate spacers and this was measured using an interference technique before filling the sample. In such a cell, one of the directors (long axes, n) could be aligned along the layer normal due to the ODSE coating of the glass plates and one of the in-layer directors (bent-direction) was aligned by the application of an external electric field perpendicular to the layer normal. Since the two directors have been aligned, the third gets aligned automatically. For compound **6.A.7,** the conoscopic observations between crossed polarizers which were set at 45° to the direction of the electric field (178V, 10kHz) showed the uniaxial interference pattern in the smectic A_d phase (140.5°C). As the temperature was lowered to 139.5°C this splits and gave the biaxial pattern. On lowering the temperature (139.2°C) further the separation between the isogyres increased continuously. On reducing the temperature (139°C) further the isogyres went out of the field of view. All the three conoscopic patterns obtained are shown in figure **6.9**. However, this behaviour could be seen even in the absence of the external electric field confirming the biaxiality of the lower temperature phase.

X-Ray diffraction studies were carried out on ten compounds. For all the samples, in the small angle region, a sharp reflection corresponding to the smectic layer spacing could be seen. The second order reflection was found to be rather weak. The values obtained for both the first order as well as the second order reflections and the calculated molecular length L in their most extended form with an all *trans* conformation of the alkoxy chain are given in table **6.4**. In addition, the X-ray diffraction pattern showed a diffuse scattering in the wide-angle region with a peak around 4.6Å indicating a liquid-like in-plane order. A significant point to note is that the *d* values are almost temperature independent (within an experimental error of ± 0.2 Å) in the entire range of both smectic phases. It can be clearly seen that the layer spacing *d*, in most of the cases is significantly larger than the calculated molecular length. This evidently implies a partial bilayer structure of the smectic layers in both the higher and lower temperature smectic phases. Interestingly, the lower temperature phase switches (which will be described later) and hence we have designated them as SmA_d and $SmA_{db}P_A$ phases respectively. However, it is seen that for very long n-alkoxy chains such as n-octadecyloxy chain, the *d* values are closer to those of L. This perhaps implies that the long chains adopt *gauche* conformations for which there is sufficient space to fill.

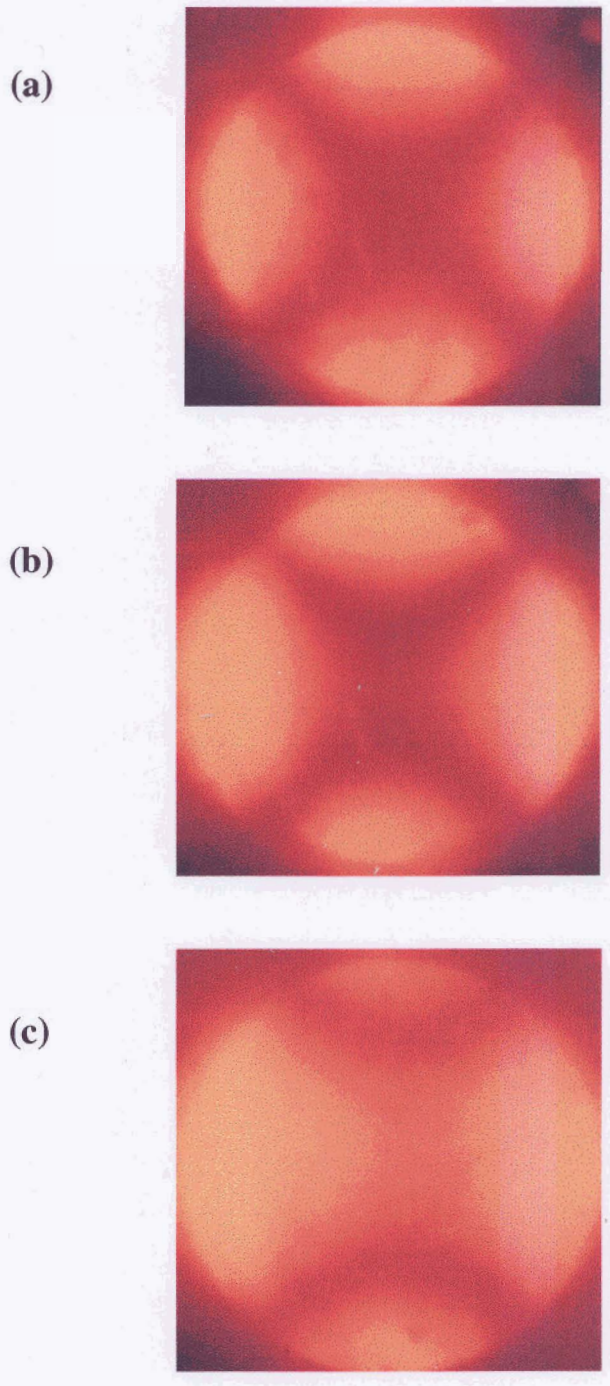

Fig. *6.9.* Photomicrographs of the conoscopic patterns from a homeotropically aligned sample of compound 6.A.7: (a) the uniaxial smectic A_d phase at T=140.5°C, (b) polar biaxial smectic A_d phase at T = 139.5°C, (c) polar biaxial smectic A_d phase at T= 139.2°C.

One can also see from this table that the *d* values increase as the terminal alkyl chain length is increased. The X-ray angular intensity profile obtained i the $SmA_{db}P_A$ phase of compound 6.C.4 is shown in figure 6.10. X-Ray diffraction experiments have also been carried out using samples mounted on a horizontal glass plate pretreated with ODSE, In the

$SmA_{db}P_A$ phase, equatorial spots are seen corresponding to the layer order and the diffuse scattering is now confined to arcs centered at an angle to the horizontal plane. The biaxial director is not aligned, but it may be noted that the two spacings in the layer will not be very different for BC molecules unlike in the biaxial phase made of board-like molecules [122]. Hegmann *et al.* [122] report additional reflections in a monodomain sample for a mixture composed of a metallomesogen and trinitrofluorenone in the lower temperature biaxial smectic A phase.

From the molecular structure of these compounds (series **6.I**, **6.II** and **6.III**), it is clear that all the four ester groups in the aromatic core have dipole moments whose long axis components are parallel to that of the cyano end group. In the case of compounds of series **6.II** and **6.III,** the C-F bond on one of the phenyl rings has a dipole moment which is almost exactly orthogonal to the long axis of the molecule. The dipolar interactions between two neighbouring molecules in all these cases favour an antiparallel configuration, and in view of the distribution of dipoles in the core, a complete overlap between the aromatic cores can be expected. The mutual configuration of a molecular pair can then be expected to be as shown in figure **6.11**, which maximizes dispersion interaction and allows for a better packing of the molecules. The length of the molecular core is ~ 32Å along the 'bow string axis' between the

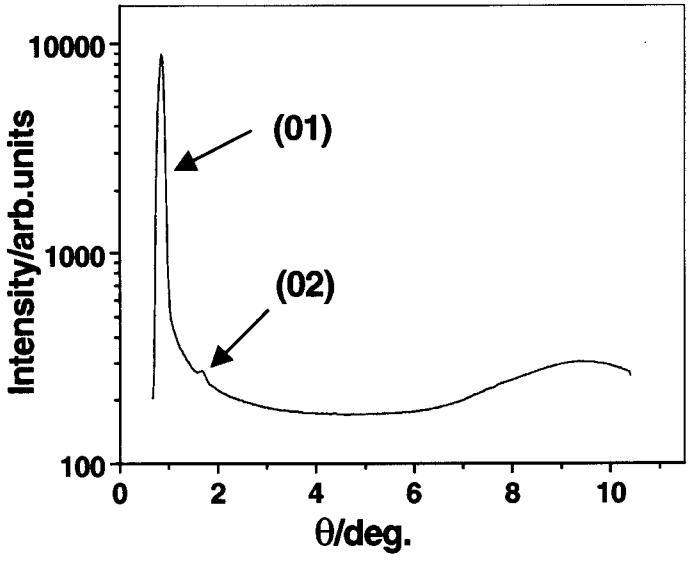

Fig. 6.10. Intensity profile of the X-ray diffraction pattern in the $SmA_{db}P_A$ phase of compound 6.C.4 at 123°C as a function of the Bragg angle θ. The sharp reflection corresponds to a layer spacing of 54 Å. A very weak second order reflection can also be seen. The diffuse maximum corresponds to 4.6 Å, which is typically due to intermolecular separation in the liquid-like layers.

Table 6.4. The layer spacings d obtained from XRD for the smectic phases of several compounds investigated and the molecular length L, measured in the most extended form with an all *trans* conformation of the chain.

Compound	d/Å		L/Å
	First order	Second order	
6.A.5	50.8	25.4	47.9
6.A.6	52.3	26.1	49.2
6.A.8	54.0	27.0	51.9
6.A.9	55.7	27.9	54.5
6.B.3	53.0	26.5	51.9
6.B.4	54.8	27.4	54.5
6.C.3	52.4	26.2	47.9
6.C.4	53.9	27.0	49.2
6.C.6	55.5	27.7	51.9
6.C.7	56.6	28.3	54.5

nitrogen atom of the cyano group and the oxygen atom of the n-alkoxy chain. In the case of compound **6.C.4,** this would imply that each tetradecyl chain contributes about 11Å to the layer thickness. The fully stretched all *trans* chain length is ~ 17Å, but as the lowest temperature at which the $SmA_{db}P_A$ phase occurs is above 120°C or so, the chain can be expected to have considerable conformational flexibility. The effective length of the chain is then smaller than that of a fully stretched conformation, probably by 1 or 2 Å. Further, the chain is attached to the arm of a bent aromatic core which makes an angle of 30° with the bow-string axis. The chain-axis makes an angle of ~ 36° with the axis of the arm of the core to which it is attached, and the effective contribution of chain to the layer thickness depends on the angle between the chain axis and the plane of the aromatic core. In the usual BC molecules in which both ends have alkyl chains, packing efficiency would favour the chains to be in the plane defined by the central core. In the SmA_d and $SmA_{db}P_A$ structures, the

number of chains in the aliphatic parts of the layer is only half the number of aromatic cores in the densely packed central part. This in turn gives rise to a relative orientational freedom for the chains to increase the entropy. The final effect is that the chain contributes about 11 Å to the effective thickness of the partial bilayer.

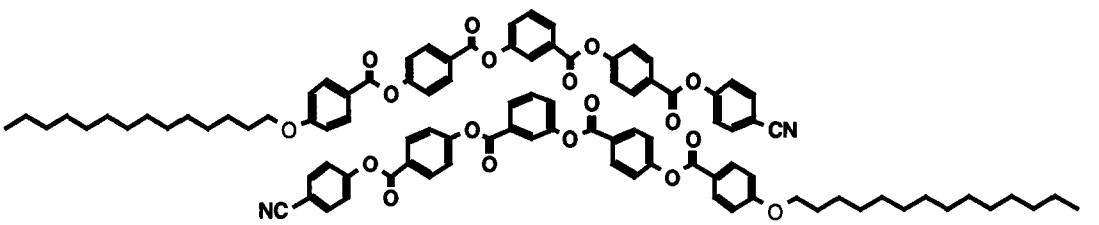

Fig. 6.11. The antiparallel configuration of a pair of highly polar BC molecules showing the complete overlap of the aromatic cores.

The switching behaviour of the mesophase of compound **6.A.8** was examined as follows. On cooling the isotropic liquid in a homogeneously aligned cell (cell thickness, 9.4 μm), the uniaxial smectic A_d phase appeared with a focal-conic texture under a triangular-wave electric field of about ± 150 V and at a frequency of about 500 Hz. No polarization current peak/s could be observed in the high temperature SmA_d phase. On lowering the temperature into the biaxial smectic A_d phase, growth of two polarization current peaks for each half period could be clearly seen. The current was measured across 1 kΩ resistance. The saturated polarization value was calculated at ± 190 V (threshold, ± 125 V at 500 Hz) is about 125 nC cm^{-2}. The electro-optical response trace obtained is shown in figure **6.12a**. The optical photomicrograph obtained under these conditions is shown in figure **6.12b**. No optical switching could be observed under a polarizing microscope which is due to the absence of layer chirality. The texture of the switched states obtained is independent of the polarity of the applied field. These experimental observations reveal that the molecular plane is orthogonal to the layer planes and the polarization is antiparallel in adjacent layers.

In the high temperature SmA_d phase, the BC molecules are stacked on top of each other in a disordered manner and these layers can form the usual non-polar uniaxial smectic A phase as shown in figure **1.9**, Chapter-**1**. On lowering the temperature, it is likely that the molecules will spontaneously form a polar, non-tilted smectic layer. This is due to the strong anisotropic interactions, caused by the very specific shape of the molecules. The energetically more probable structure is antiferroelectric ordering of the dipoles in adjacent layers which agree well with the observed experimental results. Based on these experimental observations, a

(a)

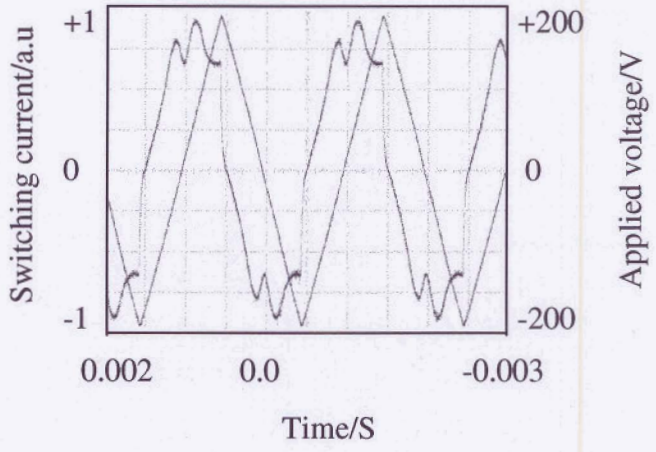

(b)

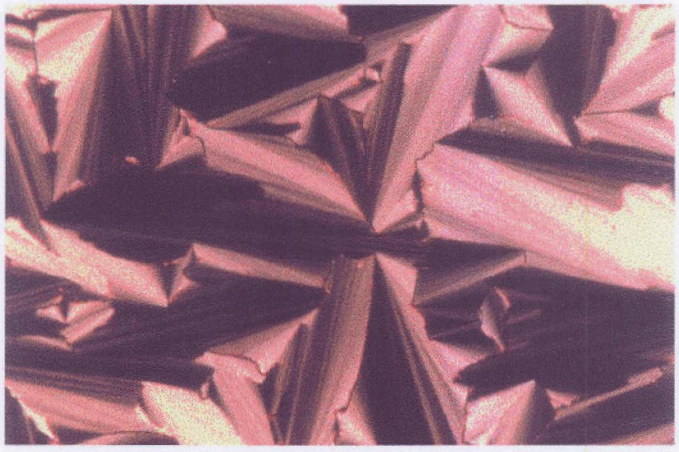

Fig. 6.12. (a) Switching current response obtained in the $SmA_{db}P_A$ phase at 132°C exhibited by compound 6.A.8 by applying a triangular-wave voltage ± 190 V at 500 Hz (threshold *a* 125 V); polarization value, P ≈ 125 nC cm^{-2} and (b) the optical photomicrograph obtained under these conditions. Cell thickness, 9.4 *μm*.

molecular model has been proposed for the $SmA_{db}P_A$ phase and is shown in figure 6.13. This is some what similar to the proposed model for polar smectic A phase observed by Eremin *et al.* [127]. The mesophase structure is apolar in adjacent layers as well as in the longitudinal directions. These preliminary observations are compatible with a C_M phase. However, the observation of antiferroelectric switching behaviour indicates the presence of a polar packing, which reduces the symmetry of the mesophase to C_{2V} (achiral smectic layers). Hence from the symmetry point of view, $SmA_{db}P_A$ phase is different from D_{2h} symmetry of the C_M phase.

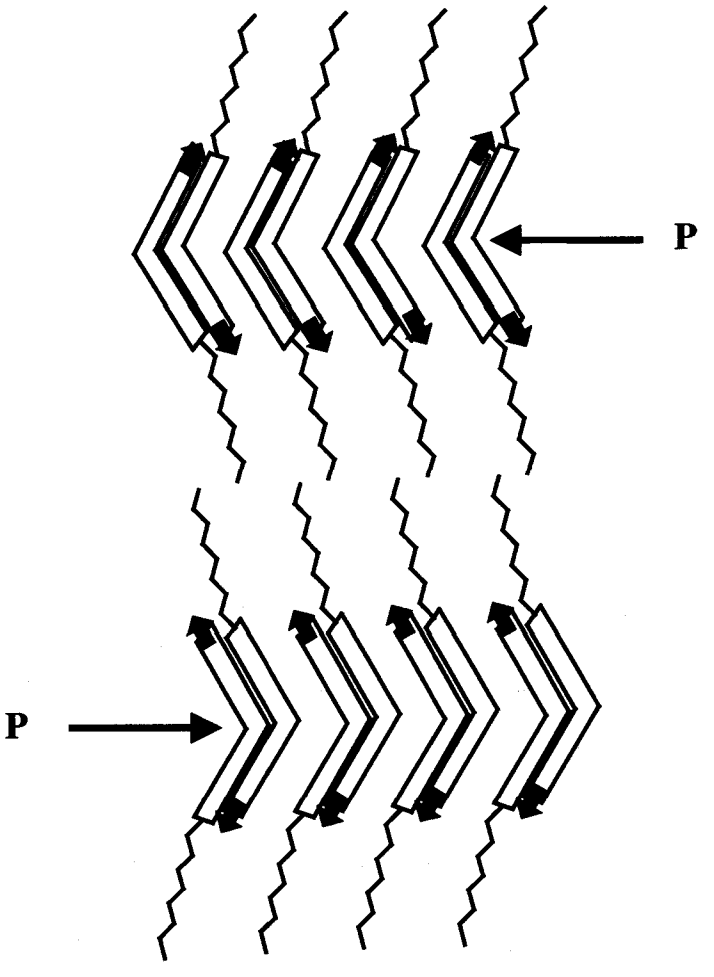

Fig. 6.13. A schematic representation of a polar packing of molecular pairs within the layer with an antiferroelectric ordering between successive layers.

The steric hindrance around the long molecular axis caused by the molecular geometry prefers a polar packing within the layers, which causes a polarization along the bent direction. This mesophase exhibits defects of strength ±1 and ±1/2, which agrees well with the experimental findings. The observation of 4-brush defects (±1) is due to the equivalency in the layers only by 2π-rotation (**m** is inequivalent to –**m** by π-rotation due to the bent-shape, **m** is the in-plane director). This is some what similar to the occurrence of ±1 strength defects in SmC phase and the inequivalency of **m** is due to the tilt of the molecules. The occurrence of 2-brush defects is due to the alternation of polar axis from layer to layer and is an evidence for the ground state antiferroelectric structure. Unlike in the B_2 phase where the layers are chiral due to the tilt of molecules, no homochiral or racemic domains could be observed in the $SmA_{db}P_A$ phase in which the molecular bow plane is parallel to the optic axis. Similar electro-optical

switching behaviour could be observed in the $SmA_{db}P_A$ phase of compound **6.C.4**. The polarization value obtained is about 150 nC cm^{-2}. The current response traces obtained in both SmA_d and $SmA_{db}P_A$ phases are shown in figures **6.14a** and **6.14b** respectively.

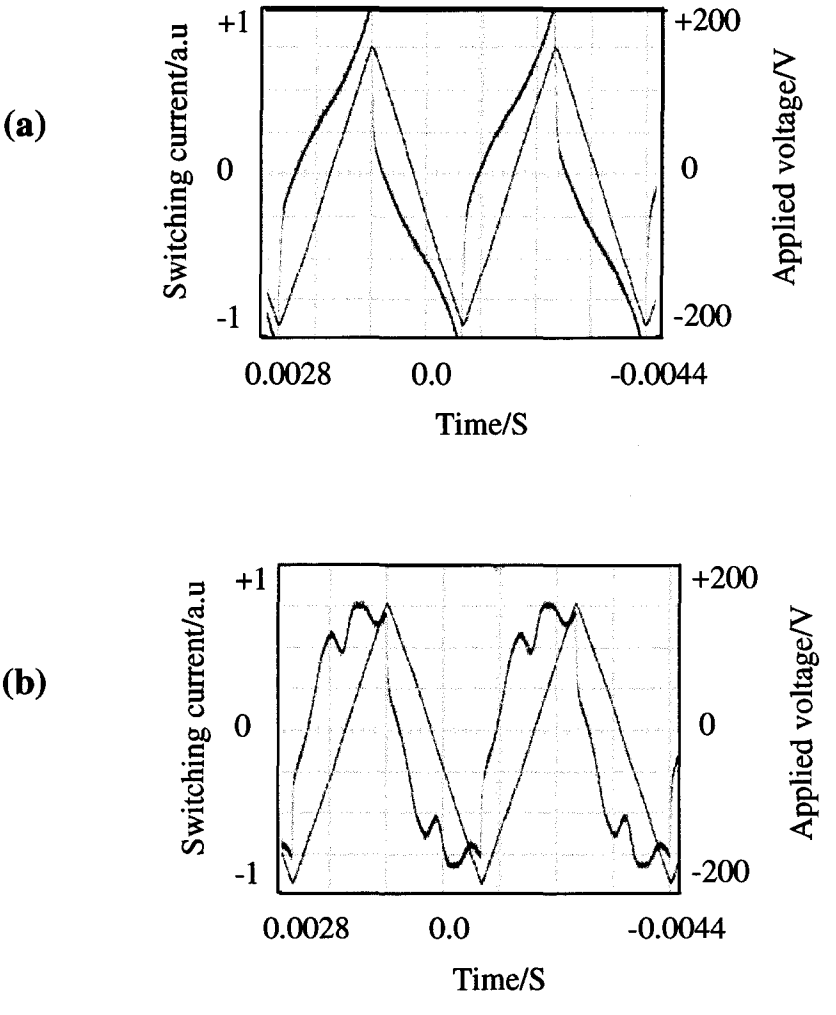

Fig. 6.14. Switching current response obtained by applying a triangular-wave voltage of about ± 169 V at 300Hz (a) in SmA_d phase at 128°C and (b) in $SmA_{db}P_A$ phase at 122°C exhibited by compound 6.C.4. Cell thickness 7 μm; polarization value P ≈ 150 nC cm^{-2}.

The quantitative measurement of the in-layer birefringence ($\Delta\mu$) of the $SmA_{db}P_A$ phase of compound **6.C.4** was carried out at λ 5893 Å by using a quarter wave plate as a compensator. The oven temperature was maintained to an accuracy of about 5 mK. However, a strong electric field ($0.4V\mu m^{-1}$) was applied to get an aligned sample, the temperature of the latter was found to increase by about 1°C, due to dissipation caused by ion flow. Hence the optical measurements were made on cooling the sample under a continuous application of the field and the temperatures indicated in figure **6.15** correspond to those of the oven. Though the

DSC thermograms indicate a very weak first order transition between SmA_d and $SmA_{db}P_A$ phases (with $\Delta H \sim 0.4$ $kJmol^{-1}$), the local heating problem mentioned above prevented from measuring any small jump in $\Delta\mu$ at the transition point. $\Delta\mu$ increases continuously as the temperature is lowered in the $SmA_{db}P_A$ phase. The data can be fitted to an equation of the form $\Delta\mu = A\ (T_{ub} - T)^{\beta}$ giving an index $\beta = 0.5$ (figure **6.15**). The local heating problem perhaps has an influence on the measured value.

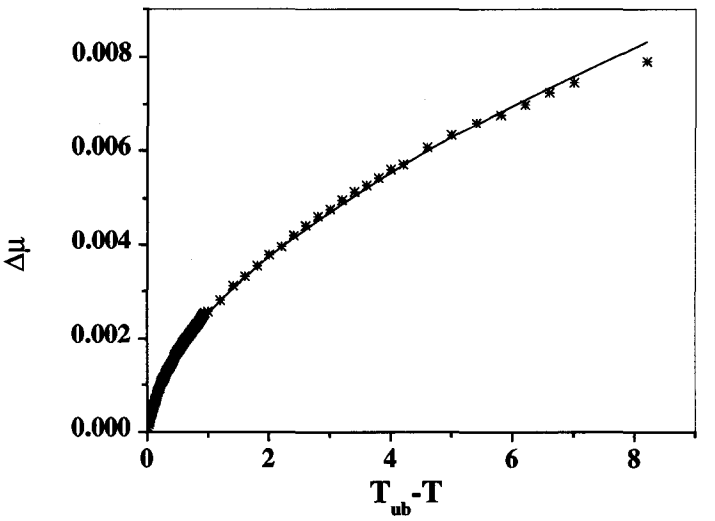

Fig. 6.15. Temperature variation of the layer birefringence in the polar biaxial smectic A_d phase of compound 6.C.4. Stars are experimental data and the continuous line is the theoretical fit referred to in the text.

To summarize this part, we have synthesized twenty compounds belonging to three new homologous series of unsymmetrically substituted compounds composed of bent-core molecules which contain a highly polar cyano group at one terminal position. A total of fourteen compounds exhibit the $SmA_{db}P_A$ phase. The mesophase-mesophase and mesophase-isotropic transition points follow smooth curves as functions of the n-alkoxy chain length. However, the melting points are about the same for all the homologues in each of the three series which is somewhat unusual. X-Ray diffraction studies show that both the smectic A phases are partially bilayer in nature. This is the first example of a bent-core compound exhibiting a partial bilayer structure and exhibiting an antiferroelectric switching behaviour.

Part-II

In this part, the synthesis and characterization of another three new homologous series of unsymmetrical compounds derived from 3-hydroxybenzoic acid are described. Apart from the laterally unsubstituted parent compounds, the mesomorphic properties of two other series of compounds which contain a fluorine substituent on the middle phenyl ring are also discussed. The general molecular structure of these compounds is shown as structure **6.2**. These compounds contain a highly polar cyano group at one end of the arms and the other arm is extended using a biphenyl moiety. The synthesis of these six phenyl ring unsymmetrical compounds is similar to the one described in scheme **6.1** (Part-I), except that in the final step (vii), 4-n-alkylbiphenyl-4-carboxylic acids were used instead of 4-n-alkoxybenzoic acids.

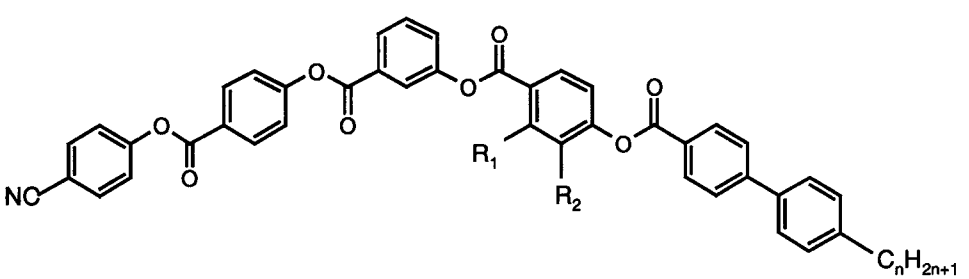

R_1=H, R_2=H **Series-6.IV**

R_1=F, R_2=H **Series-6.V**

R_1=H, R_2=F **Series-6.VI**

Structure 6.2.

Mesomorphic properties of compounds of series 6.IV, 6.V and 6.VI:

The transition temperatures and the associated enthalpy values obtained for the compounds of series **6.IV**, **6.V** and **6.VI** are summarized in tables **6.5**, **6.6** and **6.7** respectively. As can be seen in structure **6.2**, the compounds of series **6.IV** are unsubstituted while the compounds of series **6.V** and **6.VI** are substituted at *ortho* and *meta* positions respectively with a fluorine on the middle phenyl ring. All the compounds of series **6.IV** are mesomorphic. On slow cooling a thin film of the isotropic liquid of compound **6.D.1** and observing under a polarizing microscope, birefringent droplets which develop initially, transform to a homeotropic texture subsequently. However, some regions display the characteristic features of 2- and 4-brush defects of the uniaxial nematic phase. Similar textural features could be seen for the compounds **6.D.2** to **6.D.5** indicating a uniaxial nematic phase. The N-I transition enthalpy value is in the range of 0.4 to 0.6 $kJmol^{-1}$. In order to confirm the exact nature of the nematic phase, conoscopic experiments were carried out in the nematic phase of compound **6.D.3** which indicated the uniaxial nature of the mesophase.

On increasing the chain length, compounds **6.D.2** and **6.D.3** were obtained which show an additional mesophase. On slow cooling the homeotropically aligned nematic phase of compound **6.D.3**, a schlieren texture was obtained indicating the biaxiality of the lower temperature phase. The textural features of this lower temperature phase resemble the biaxial smectic A phase ($SmA_{db}P_A$) obtained in the other three homologous series (**6.I**, **6.II** and **6.III**). On slow cooling the homogeneously aligned nematic phase into the lower temperature phase of the same compound, a fan-shaped texture was obtained with sharp lines over the fans as shown in figure **6.16 (b)**. This excludes the possibility of the phase being a SmC phase which shows normally a broken fan-shaped texture. The XRD measurements obtained in the lower temperature phase of compound **6.D.3** indicated a partial bialyer structure for the mesophase. Further, the conoscopic experiments show the uniaxial interference pattern in the nematic phase which splits as the temperature was lowered as shown in figure **6.17.** On further cooling, the isogyres obtained move away from the field of view. These observations clearly indicate that the lower temperature phase is in fact a biaxial smectic A phase ($SmA_{db}P_A$) and is obtained directly from the uniaxial nematic phase. The N-$SmA_{db}P_A$ phase transition enthalpy value is in the range of 0.2 to 0.5 $kJmol^{-1}$. Perhaps, this is the first example of a compound showing a direct transition from the uniaxial nematic phase to a polar biaxial smectic A_d phase.

Table 6.5. Transition temperatures (°C) and enthalpies ($kJmol^{-1}$) for compounds of series 6.IV.

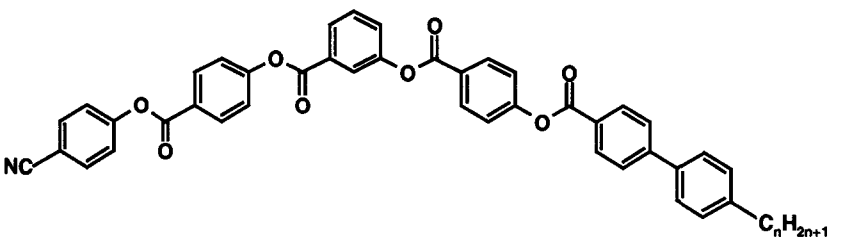

Compound	n	Cr		$SmA_{db}P_A$		SmA_d		N		I
6.D.1	6	.	156.0	-		-		.	204.0	.
			46.7						*0.48*	
6.D.2	8	.	170.0	(.	151.5)[a]	-		.	195.0	.
			50.2						*0.45*	
6.D.3	9	.	160.0	(.	158.0)	-		.	189.8	.
			39.2		*0.48*				*0.43*	
6.D.4	10	.	169.0	.	171.3	.	174.8	.	189.0	.
			56.8		*0.15*		*0.2*		*0.47*	
6.D.5	11	.	169.0	.	176.5	.	185.3	.	187.5	.
			44.7		*0.13*		*0.4*		*0.57*	
6.D.6	12	.	158.0	.	181.0	.	192.0	-		.
			53.6		*0.25*		*2.9*			
6.D.7	14	.	157.0	.	184.3	.	199.2	-		.
			58.5		*0.16*		*4.76*			
6.D.8	16	.	156.0	.	185.0	.	204.5	-		.
			38.4		*0.1*		*5.8*			
6.D.9	18	.	154.0	.	184.0	.	206.7	-		.
			65.4		*0.09*		*6.6*			

Cr=Crystalline phase; N=Nematic phase; SmA_d=Partial bilayer uniaxial smectic A phase; $SmA_{db}P_A$=Partial bilayer biaxial antiferroelectric smectic A phase; SmX=Unidentified antiferroelectric smectic phase; I=isotropic phase; . Phase exists; - Phase does not exist; Temperature in parentheses indicate monotropic transitions.

a: enthalpy could not be determined as the sample crystallizes immediately.

Table 6.6. Transition temperatures (°C) and enthalpies ($kJmol^{-1}$) for compounds of series 6.V.

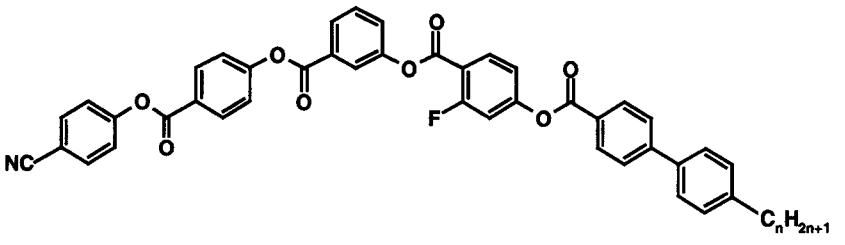

Compound	n	Cr		$SmA_{db}P_A$		SmA_d		N		I
6.E.1	6	.	175.5	-		-		.	197.2	.
			57.8						*0.42*	
6.E.2	8	.	155.0	-		-		.	184.9	.
			53.1						*0.4*	
6.E.3	9	.	160.0	(.	152.5)	-		.	183.0	.
			52.3		*0.5*				*0.4*	
6.E.4	10	.	161.5	.	162.5	.	166.0	.	179.8	.
			48.2		*0.2*		*0.1*		*0.38*	
6.E.5	11	.	161.5	.	168.0	.	177.0	.	180.2	.
			58.9		*0.18*		*0.3*		*0.57*	
6.E.6	12	.	160.0	.	172.5	.	183.0	-		.
			45.6		*0.1*		*2.7*			
6.E.7	14	.	159.5	.	176.8	.	191.0	-		.
			42.8		*0.14*		*4.54*			
6.E.8	16	.	158.0	.	178.2	.	197.0	-		.
			48.9		*0.06*		*5.8*			
6.E.9	18	.	157.5	.	179.2	.	202.0	-		.
			49.9		*0.05*		*6.6*			

Table 6.7. Transition temperatures (°C) and enthalpies (kJ mol^{-1}) (*in italics*) for compounds of series 6.VI.

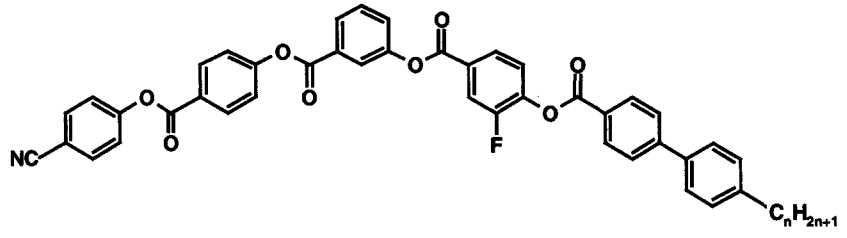

Compound	n	Cr		SmX		$SmA_{db}P_A$		SmA_d		N		I
6.F.1	6	.	159.5	-		-		-		.	197.5	.
			54.0								*0.6*	
6.F.2	8	.	157.0	-		-		-		.	186.4	.
			40.2								*0.5*	
6.F.3	9	.	154.0	-		(.	149.0)	-		.	183.1	.
			35.9				*0.2*				*0.3*	
6.F.4	10	.	158.0	-		.	162.0	.	166.9	.	179.8	.
			40.2				*0.1*		*0.1*		*0.7*	
6.F.5	11	.	158.0	-		.	167.0	.	177.6	.	179.8	.
			37.4				*0.1*		*0.5*		*0.6*	
6.F.6	12	.	154.5	-		.	170.3	.	182.0	-		.
			38.7				*0.1*		*3.1*			
6.F.7	14	.	153.0	-		.	174.0	.	189.5	-		.
			43.4				*0.1*		*4.8*			
6.F.8	16	.	148.5	.	160.0	.	176.2	.	195.0	-		.
			47.0		*0.34*		*0.2*		*5.8*			
6.F.9	18	.	149.0	.	166.0	.	176.5	.	199.5	-		.
			44.5		*0.1*		*0.1*		*6.4*			

(a)

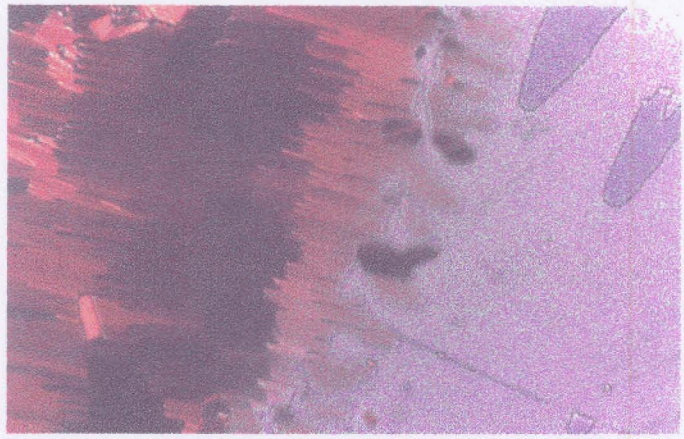

(b)

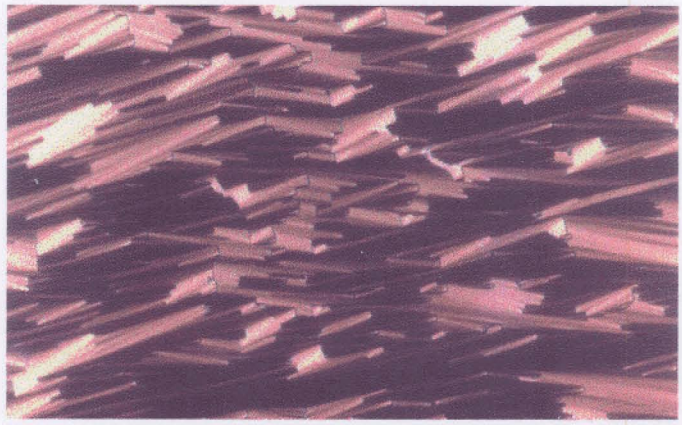

Fig. 6.16. Photomicrographs showing (a) a transition from nematic to polar biaxial smectic A_d phase and (b) polar biaxial smectic A_d phase obtained in a homogeneously aligned cell for compound 6.D.3.

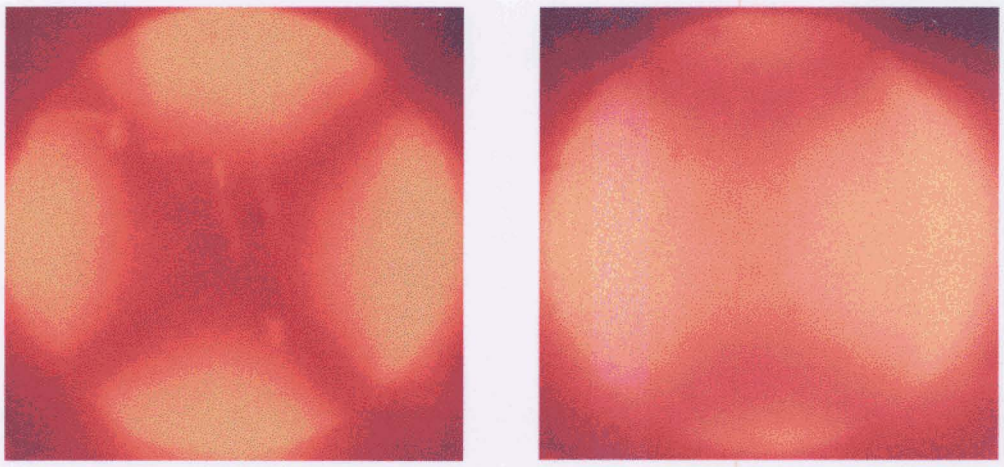

(i) N ⟶ $SmA_{db}P_A$ (ii)

Fig. 6.17. Photomicrographs of conoscopic patterns obtained from a homeotropically aligned sample of compound 6.D.3, (i) a uniaxial pattern in the nematic phase at 162°C, and (ii) a biaxial pattern in the $SmA_{db}P_A$ phase at 156°C.

On ascending the homologous series, the polar biaxial smectic A_d phase gets stabilized and the uniaxial smectic A_d phase is induced, and these exist even for a compound with n-octadecyl chain. For example, compounds **6.D.4** and **6.D.5** show trimesomorphism namely, uniaxial nematic, uniaxial smectic A_d and polar biaxial smectic A_d phases on cooling the isotropic liquid. As expected, on ascending a homologous series, the nematic phase gets eliminated and only uniaxial and biaxial smectic A_d phases are retained.

In series **6.V**, the lower homologues viz. compounds **6.E.1** and **6.E.2** exhibit only uniaxial nematic phase while compound **6.E.3** exhibits a direct transition from uniaxial nematic phase to a polar biaxial smectic A_d phase. Compounds **6.E.4** and **6.E.5** show nematic, SmA_d and $SmA_{db}P_A$ phases on lowering the temperature and the higher homologues exhibit only SmA_d and $SmA_{db}P_A$ phases. The textural features and the enthalpies are similar to those observed for the compounds of series **6.IV**. The conoscopic patterns obtained in the uniaxial and the biaxial smectic A_d phases for compound **6.E.6** is shown in figure **6.18.**

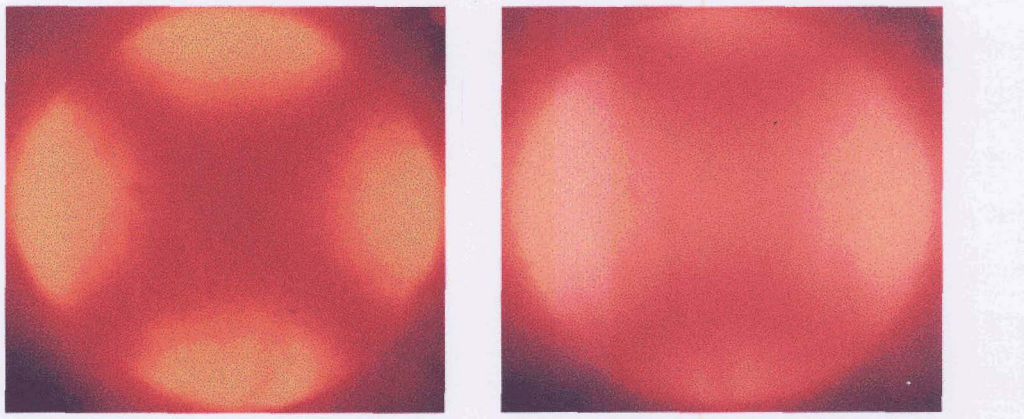

Fig. 6.18. Photomicrographs of conoscopic patterns obtained for a homeotropically aligned sample of compound 6.E.6, (i) the uniaxial smectic A_d phase at 175 °C, and (ii) the polar biaxial smectic A_d phase at 171°C.

Similarly, for series **6.VI**, the lower homologues exhibit a nematic phase and on increasing the chain length $SmA_{db}P_A$ phase is induced (for compound 6.F.3). The SmA_d phase appears on increasing the chain length further (for compound 6.F.4) while the nematic phase is still retained. However, for compounds 6.F.6 to 6.F.9 both the SmA_d and $SmA_{db}P_A$ phases are stabilized and the nematic phase gets eliminated. The textural transformation observed in a homogeneously aligned cell, from N to SmA_d phase is shown in figure **6.19a**. The textures of

SmA_d and $SmA_{db}P_A$ phases obtained for compound **6.F.5** is shown in figure **6.19 b** and **c** respectively. A schlieren texture obtained in the $SmA_{db}P_A$ phase on cooling the homeotropic texture of the SmA_d phase for compound **6.F.5** is shown in figure **6.20**. Interestingly, compounds **6.F.8** and **6.F.9** show trimesomorphism. On slow cooling the isotropic liquid of compound **6.F.8**, a homeotropic alignment of SmA_d phase is obtained. On cooling this mesophase to a temperature of about 175°C, a schlieren texture is obtained, which exhibit both 4- and 2-brush strength defects indicating a polar biaxial smectic A_d phase as observed for the lower homologues (**6.F.3** to **6.F.7**). A photomicrograph of this is shown in figure **6.21a**. However, on cooling further to a temperature of about 158°C, a transition takes place with a gradual increase in the birefringence as shown in figure **6.21b.** This is followed by a small transition enthalpy in DSC (0.1-0.3 $kJmol^{-1}$). This is probably due to the tilt of BC molecules in the lower temperature phase which has been designated as SmX phase. The 4- and 2-brush defects observed in the high temperature phase ($SmA_{db}P_A$) is retained even in the lower temperature SmX phase. Similar mesophase behaviour is observed for compound **6.F.9** also. The enthalpy values obtained for the SmA_d-N phase transition varies from 0.2 to 0.5 $kJmol^{-1}$ and for the SmA_d-I transition it varies from 2 to 7 $kJmol^{-1}$. However, for the biaxial smectic A_d to uniaxial smectic A_d phase, the transition enthalpy is quite low and is of the order of 0.1 to 0.25 $kJmol^{-1}$. All the compounds (series **6.IV**, **6.V** and **6.VI**) exhibiting SmA_d and $SmA_{db}P_A$ phases show a partial bilayer structure as determined from XRD studies and a model of antiparallel arrangement of molecules is shown in figure **6.22**. The layer spacings obtained for the mesophases of different compounds of series **6.IV**, **6.V** and **6.VI** are summarized in table **6.8**. The X-ray angular intensity profile obtained in the $SmA_{db}P_A$ phase of compound **6.F.8** is shown in figure **6.23**.

Electro-optical studies have been carried out for several compounds of different homologous series. Compound **6.F.9** shows the following switching behaviour. A cell having a thickness of about 18 μm was constructed as usual which is used for the polarization measurements. The isotropic liquid was cooled slowly under a triangular-wave electric field of about ± 280 V at a frequency of 1 kHz. No polarization current peak/s could be observed in the high temperature uniaxial smectic A_d phase. However, on cooling to a temperature of about 174°C (the temperature was found to increase by about 2° due to the dissipation caused by ion flow), two polarization current peaks appeared for each half period indicating an antiferroelectric ground state structure for the lower temperature $SmA_{db}P_A$ phase. The current response trace obtained in the $SmA_{db}P_A$ phase is shown in figure **6.24a**.

(a)

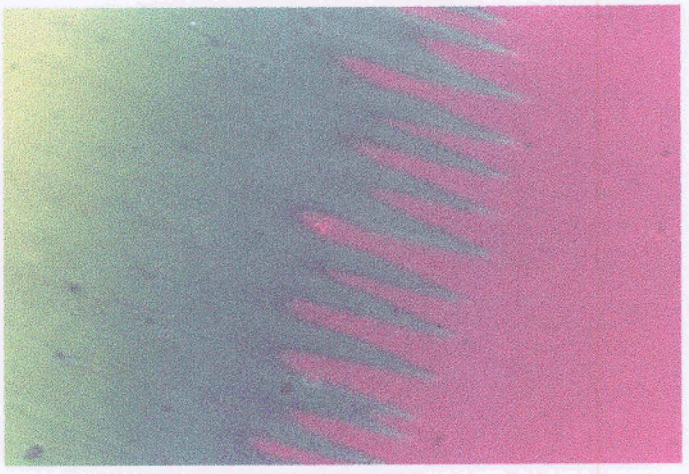

(b)

(c)

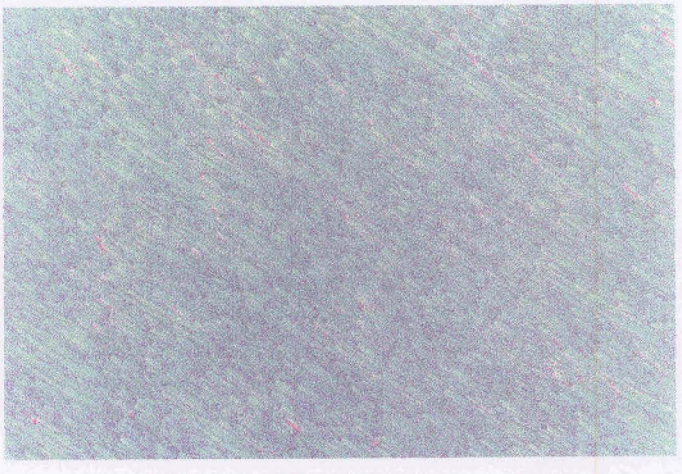

Fig. 6.19. Photomicrographs showing (a) transition from nematic phase to a uniaxial smectic A_d phase, (b) a uniaxial smectic A_d phase and (c) a polar biaxial smectic A_d phase in a homogeneously aligned cell of a sample of compound 6.F.5.

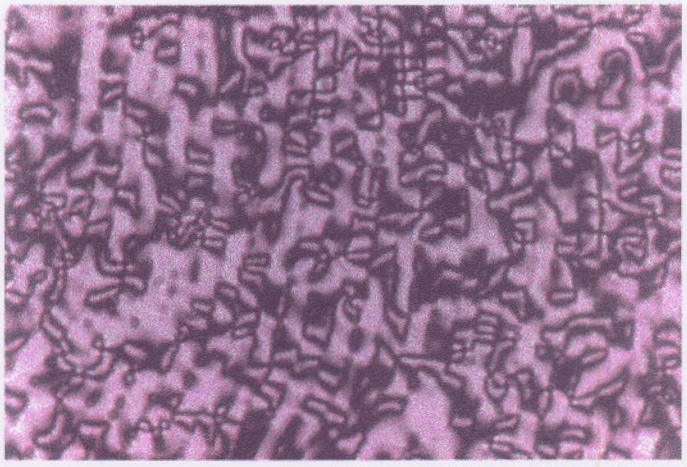

Fig. 6.20. Photomicrograph of st schlieren texture obtained in the polar biaxial smectic A_d phase exhibited by compound 6.F.5 at 160°C.

(a)

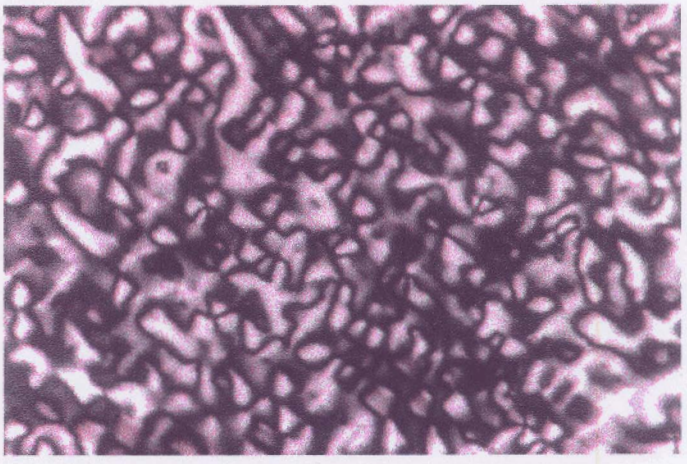

(b)

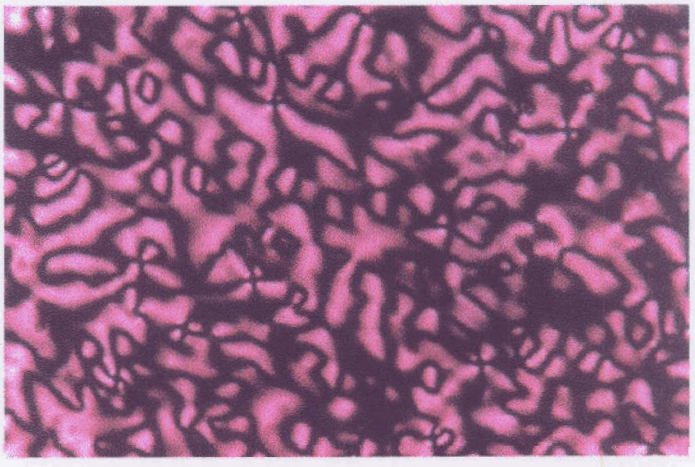

Fig. 621. Photomicrographs obtained for compound 6.F.8, (a) schlieren texture in the phase and (b) higher birefringent schlieren texture in the SmX phase.

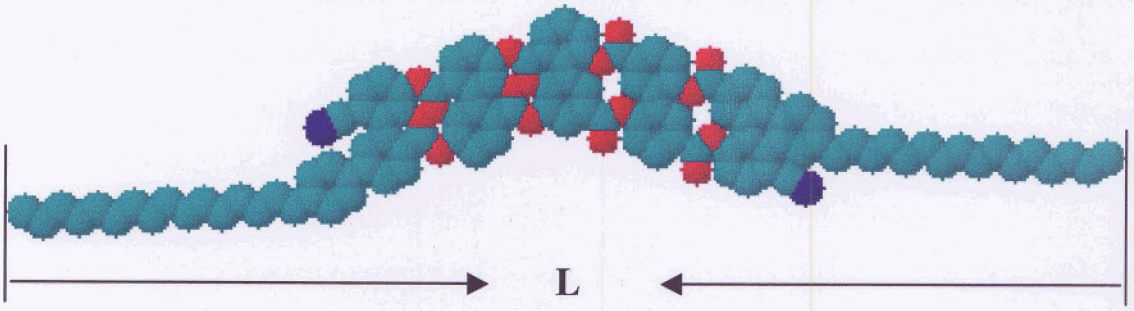

Fig. 6.22 A space-tilling model of the antiparallel arrangement of strongly polar molecules used to measure the length of the partial bilayer structure.

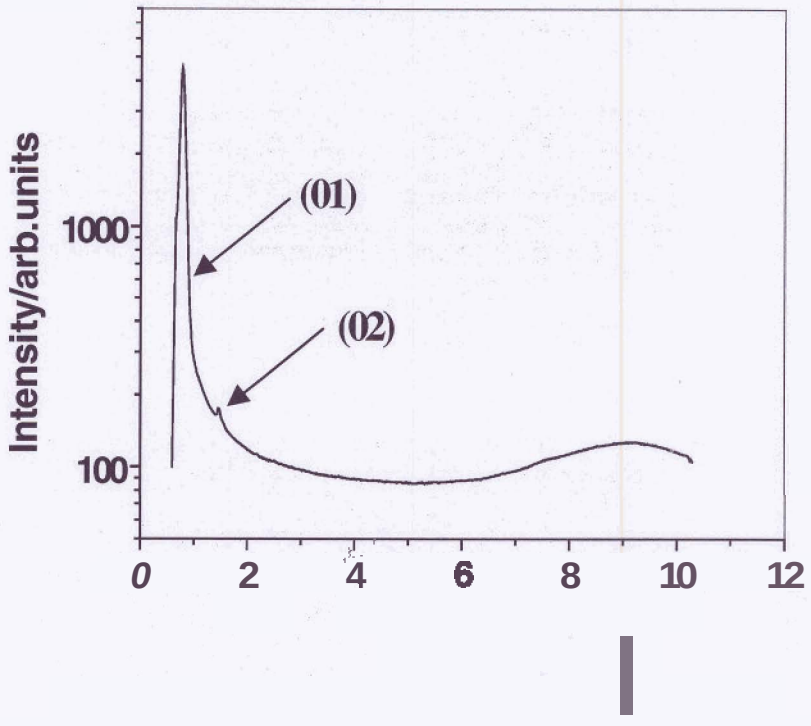

Fig. 6.23. Intensity profile of the X-ray diffraction pattern in the $SmA_{db}P_A$ phase of compound 6.F.8 obtained at 166°C as a function of the Bragg angle θ. The sharp reflection corresponds to a layer spacing of 58.8 Å. A very weak second order reflection (24.4 Å) can also be seen. The diffuse maximum corresponds to 4.7 Å, which is typical for intermolecular separation in the liquid-like layers.

The current was measured across 1 kΩ resistance and the polarization value works out to be 140 nC cm^{-2}. As described in Part-**I**, no switchable domains could be observed due to the absence of layer chirality and only a focal-conic texture was observed which was also independent of the polarity of the applied field. On lowering the temperature further into the SmX phase, the polarization value gradually increases and a saturated value obtained is about 250 nC cm^{-2} and the current response trace obtained is shown in figure **6.24b**. However, from the available data, it is difficult to speculate the exact nature of the lower temperature SmX phase. As explained earlier, the increase in birefringence and also the polarization value indicate a tilt of the molecules in the lower temperature SmX phase, which could not be determined from XRD studies.

Table 6.8. The layer spacings d obtained from XRD, for the smectic phases of several compounds investigated and the molecular length L, measured in the most extended form with an all *trans* conformation of the chain.

Compound	d/Å		L/Å
	First order	Second order	
6.D.3	48.6	24.3	45.2
6.D.5	51.3	-	47.7
6.D.8	58.8	29.4	54.5
6.E.5	52.0	-	47.7
6.E.8	57.8	28.9	54.5
6.F.5	54.4	-	47.7
6.F.8	58.8	29.4	54.5
6.F.9	61.7	30.8	57

Plots of the transition temperatures against the number of carbon atoms in the n-alkyl chain for the compounds of series **6.IV**, **6.V** and **6.VI** are shown in figure **6.25** (**a**,**b** and **c**). It can be seen that N-I transition temperature curve falls gradually while the SmA_d - I transition temperature curve rises on increasing the chain length for all the three series of compounds. The transition temperature curve obtained for the $SmA_{db}P_A$ - SmA_d phases rises initially and

then levels off gradually and a rising trend could be seen for the SmX phase obtained in only two compounds of series **6.VI**. For all the three series of compounds, the mesophase-mesophase and mesophase-isotropic transition temperatures fall on smooth curves indicating the phase similarity.

As a comparison between the compounds with and without fluorine substituent the following observations can be made. The introduction of fluorine at *ortho* position (series **6.V**) reduces the clearing temperatures by about 10° while the melting points are marginally increased. It can also be seen in figure **6.25b** that both SmA_d and $SmA_{db}P_A$ phase thermal ranges are reduced by a fluorine substituent at *ortho* position. However, in the case of *meta* fluorine substituted compounds, both melting and clearing transition temperatures are reduced by about 5-10°. Interestingly, an additional unknown smectic mesophase (SmX) has been induced which shows antiferroelectric switching behaviour.

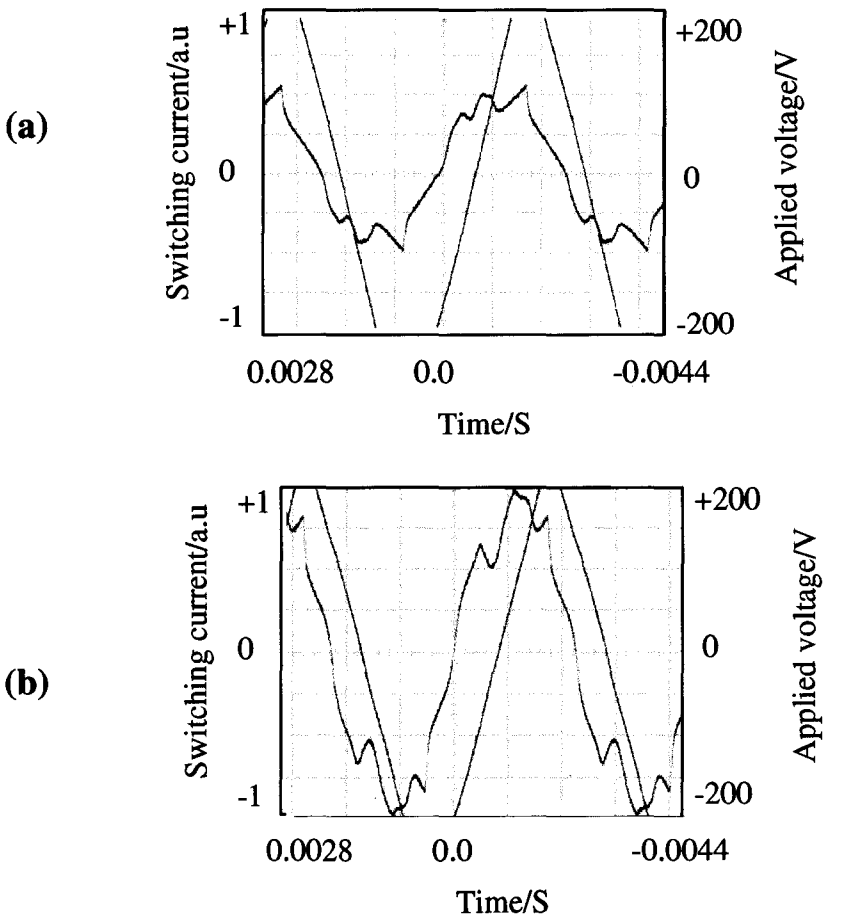

Fig. 6.24. Switching current response obtained by applying a triangular-wave voltage of about ± 280 V at 1kHz (a) in $SmA_{db}P_A$ phase at 170°C; polarization value, P ≈ 140 nC cm^{-2} and (b) in SmX phase at 152°C; polarization value, P ≈ 250 nC cm^{-2} exhibited by compound 6.F.9. Cell thickness 18 *μm*.

(a)

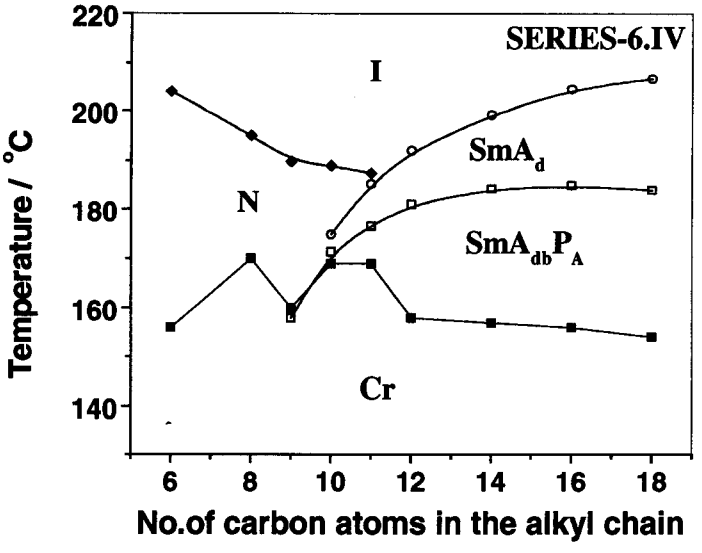

(b)

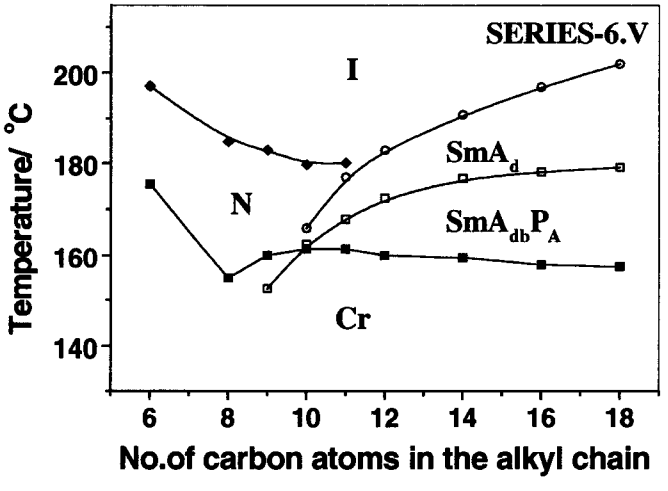

(c)

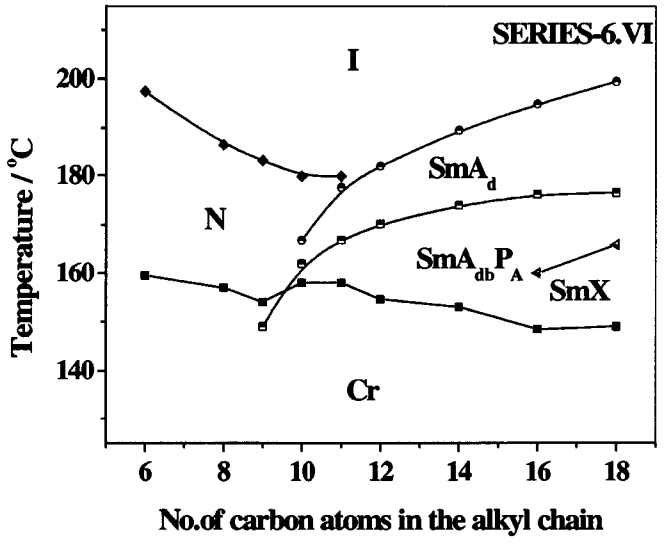

Fig. 6.25. Plots of transition temperatures as a function of the number of carbon atoms in the n-alkyl chain obtained for compounds of (a) series 6.IV, (b) series 6.V and (c) series 6.VI.

Comparison between the mesophases of compounds of structure 6.1 and 6.2:

The compounds of structure **6.1** contain five phenyl rings while the compounds of structure **6.2** contain six phenyl rings and hence the melting as well as the clearing transition temperatures increase in the latter. Also, the thermal range of the mesophases increases by about 10 to 20° depending on the n-alkyl chain length as well as the position of the fluorine substituent. More interestingly, a nematic phase is induced for shorter chain compounds of structure **6.2** and hence a direct transition from a uniaxial nematic phase to a polar biaxial smectic A_d phase has been observed for the first time.

Experimental

4-Cyanophenyl-4-benzyloxybenzoate, (6.1)

4-Cyanophenol, (5g, 42 mmol) and 4-benzyloxybenzoic acid, (9.58g, 42 mmol) were dissolved in dry chloroform (100ml). After the addition of N, N' - dicyclohexylcarbodiimide (DCC), (10g, 48 mmol) and a catalytic amount of 4-(N,N dimethylamino)pyridine (DMAP), the mixture was stirred at room temperature for about 15 hours. The dicyclohexylurea which precipitated was filtered off and the filtrate diluted with an excess of chloroform. This combined solution was washed with 2% aqueous acetic acid solution (3 X 100 ml) and 5% ice-cold aqueous sodium hydroxide solution (3 X 100 ml) and finally washed with water and dried (anhydrous Na_2SO_4). The solid residue obtained after removal of solvent was chromatographed on silica gel using chloroform as an eluent. Removal of solvent from the eluate afforded a white material which was crystallized from a mixture of chloroform and acetonitrile. Yield, 11.2g (81%); m.p. 179.5-180°C; ν_{max} (KBr):3099, 3064, 2231, 1728, 1685, 1604, 1508, 1225, 1163, 1070 cm^{-1}; δ_H: 8.14 (d, ^{3}J8.8 Hz, 2H, Ar-H), 7.72 (d, ^{3}J8.7 Hz, 2H, Ar-H), 7.4-7.33 (m, 7H, Ar-H), 7.07 (d, ^{3}J8.8 Hz, 2H, Ar-H), 5.17 (s, 2H, $ArCH_2O$-). Elemental analysis: C_{21} H_{15} NO_3 requires, C, 76.58; H, 4.59; N, 4.25%; found, C, 77.0; H, 4.53; N, 4.20%.

4-Cyanophenyl-4-hydroxybenzoate, (6.2)

Compound **6.1** (11.0g) was dissolved in 1,4-dioxane (100ml) and 5% Pd-C catalyst (2.2g) was added to it. The mixture was stirred at 55°C in an atmosphere of hydrogen till the required quantity of hydrogen was absorbed. This was filtered hot and the solvent removed under reduced pressure. The solid material so obtained was chromatographed on silica gel and eluted using a mixture of 5% acetone in chloroform. Removal of solvent from the eluate gave a product, which was crystallized from a mixture of 1,4-dioxane and petroleum ether (b.p 60-80°C). Yield, 6g (75%); m.p. 205-206°C; ν_{max} (KBr):3352, 3103, 3060, 2237, 1733, 1685, 1612, 1595, 1496, 1271, 1068 cm^{-1}; δ_H: 8.1 (d, ^{3}J7.6Hz, 2H, Ar-H), 7.73 (d, ^{3}J7.7 Hz, 2H, Ar-H), 7.35 (d, ^{3}J7.6 Hz, 2H, Ar-H), 6.94 (d, ^{3}J7.7 Hz, 2H, Ar-H), 5.73 (s, 1H, Ar-OH, exchangeable with D_2O). Elemental analysis: C_{14} H_9 NO_3 requires, C, 70.29; H, 3.79; N, 5.85%; found, C, 70.29; H, 3.7; N, 6.05%.

4-Cyanophenyl-4-(3-benzyloxybezoyloxy)benzoate, (6.3)

This was synthesized following a procedure described for the preparation of compound **6.1.** Yield, 72%; m.p. 146-147°C; ν_{max} (KBr):3100, 3066, 2227, 1726, 1602, 1581, 1508, 1485, 1417, 1270, 1016 cm^{-1}; δ_H: 8.28 (d, ^{3}J8.5 Hz, 2H, Ar-H), 7.84-7.74 (m, 4H,Ar-H), 7.47-7.26 (m, 11H, Ar-H), 5.16 (s, 2H, $ArCH_2O$). Elemental analysis: C_{28} H_{19} NO_3 requires, C, 74.82; H, 4.26; N, 3.11%; found, C, 74.53; H, 4.20; N, 3.12%.

4-Cyanophenyl-4-(3-hydroxybenzoyloxy)benzoate, (6.4)

This was synthesized following a procedure described for the preparation of compound **6.2.** Yield, 75%; m.p. 211-213°C; ν_{max} (KBr):3298, 3105, 3068, 2245, 1730, 1600, 1589, 1508, 1487, 1270, 1170, 1058 cm^{-1}; δ_H: 9.13 (s, 1H, Ar-OH, exchangeable with D_2O), 8.31 (d, ^{3}J8.8 Hz, 2H, Ar-H) 7.94 (d, ^{3}J8.8 Hz, 2H, Ar-H), 7.7-7.2 (m, 8H, Ar-H). Elemental analysis: C_{21} H_{13} NO_5 requires, C, 70.19; H, 3.64; N, 3.89%; found, C, 69.89; H, 3.53; N, 4.09%.

4-Cyanophenyl-4-[3-(4-benzyloxybenzoyloxy)benzoyloxy]benzoate, (6.5)

This was synthesized following a procedure used for the preparation of compound **6.1.** Yield, 70%; m.p. 167-168°C; ν_{max} (KBr):3101, 3072, 2231, 1740, 1730, 1602, 1502, 1444, 1250, 1056 cm^{-1}; δ_H: 8.28 (d, ^{3}J8.4 Hz, 2H, Ar-H), 8.18-8.06 (m, 4H, Ar-H), 7.75 (d, ^{3}J8.3Hz, 2H, Ar-H), 7.62-7.34 (m, 11H, Ar-H), 7.08(d, ^{3}J8.6 Hz, 2H, Ar-H), 5.17 (s, 2H, $ArCH_2O$-). Elemental analysis: C_{35} H_{23} NO_7 requires C, 73.8; H, 4.07; N, 2.46%; found, C, 74.15; H, 3.97; N, 2.32%.

4-Cyanophenyl-4-[3-(4-hydroxybenzoyloxy)benzoyloxy]benzoate, (6.6)

This was synthesized following a procedure used for the preparation of compound **6.2.** Yield, 71%; m.p. 206-207°C; ν_{max} (KBr):3385, 3101, 3066, 2237, 1738, 1600, 1500, 1413, 1250, 1163, 1060 cm^{-1}; δ_H: 9.4 (s, 1H, Ar-OH, exchangeable with D_2O), 8.32 (d, ^{3}J8.6 Hz, 2H, Ar-H), 8.15-8.09 (m, 4H, Ar-H), 7.94 (d, ^{3}J8.5Hz, 2H, Ar-H), 7.76-7.6 (m, 6H, Ar-H), 7.03 (d, ^{3}J8.6 Hz, 2H, Ar-H). Elemental analysis: C_{28} H_{17} NO_7 requires, C, 70.14; H, 3.57; N, 2.92%; found, C, 69.8; H, 3.59; N, 2.60%.

4-Cyanophenyl-4-[3-(2-fluoro-4-benzyloxybenzoyloxy)benzoyloxy]benzoate, (6.7)

This was synthesized following a procedure used for the preparation of compound **6.1.** Yield, 72%; m.p. 173-174°C; ν_{max} :2924, 2854, 2231, 1740, 1728, 1618, 1454, 1246, 1045 cm^{-1}; δ_H: 8.29-8.27(d, 2H, ^{3}J8.68 Hz, Ar-H), 8.13-8.06 (m, 3H, Ar-H), 7.77-7.75 (d, 2H, ^{3}J8.64 Hz, Ar-

H), 7.62-7.37 (m, 11H, Ar-H), 6.89-6.87(d, 1H, ^{3}J8.6 Hz, Ar-H), 6.82-6.78(dd, 1H, ^{3}J12.58 Hz, ^{4}J2.04 Hz, Ar-H), 5.15 (s, 2H, $ArCH_2O$-).

4-Cyanophenyl-4-[3-(2-fluoro-4-hydroxybenzoyloxy)benzoyloxy]benzoate, (6.8)

This was synthesized following a procedure used for the preparation of compound **6.2.** Yield, 86%; m.p. 210-212°C; ν_{max} :3389, 2924, 2854, 2228, 1751, 1740, 1724, 1616, 1591, 1460, 1255, 1128 cm^{-1}; δ_H: 9.85(s, 1H, Ar-OH, exchangeable with D_2O), 8.34-8.32(d, 2H, ^{3}J8.68 Hz, Ar-H), 8.16-8.05 (m, 3H, Ar-H), 7.96-7.94(d, 2H, ^{3}J8.64 Hz, Ar-H), 7.76-7.67 (m, 2H, Ar-H), 7.63-7.60(d, 4H, ^{3}J8.6 Hz, Ar-H), 6.89-6.87(dd, 1H, ^{3}J8.72 Hz, ^{4}J2.32 Hz, Ar-H), 6.8-6.76(dd, 1H, ^{3}J12.78 Hz, ^{4}J2.32 Hz, Ar-H).

4-Cyanophenyl-4-[3-(3-fluoro-4-benzyloxybenzoyloxy)benzoyloxy]benzoate, (6.9).

This was synthesized following a procedure used for the preparation of compound **6.1.** Yield, 75%; m.p. 164-165°C; ν_{max} :2924, 2854, 2231, 1742, 1730, 1610, 1458, 1246, 1045 cm^{-1}; δ_H: 8.29-8.27(d, 2H, ^{3}J8.56 Hz, Ar-H), 8.14-7.92 (m, 4H, Ar-H), 7.77-7.75 (d, 2H, ^{3}J8.36 Hz, Ar-H), 7.63-7.59 (t, 1H, ^{3}J7.96 Hz, Ar-H), 7.53-7.34(m, 10H, Ar-H), 7.13-7.09(t, 1H, ^{3}J8.6 Hz, Ar-H), 5.26 (s, 2H, $ArCH_2O$-).

4-Cyanophenyl-4-[3-(3-fluoro-4-hydroxybenzoyloxy)benzoyloxy]benzoate, (6.10)

This was synthesized following a procedure used for the preparation of compound **6.2.** Yield, 89%; m.p. 221-223°C; ν_{max} :3313, 2924, 2854, 2243, 1738, 1620, 1601, 1434, 1261, 1128 cm^{-1}; δ_H: 9.9(s, 1H, Ar-OH, exchangeable with D_2O), 8.47-8.45(d, 2H, ^{3}J8.08 Hz, Ar-H), 8.3-8.25 (m, 2H, Ar-H), 8.09-8.05(m, 4H, Ar-H), 7.9-7.82 (m, 2H, Ar-H), 7.75-7.73(d, 4H, ^{3}J8.32 Hz, Ar-H), 7.36-7.33(m, 1H, Ar-H).

4-Cyanophenyl-4-[3-{4-(4-n-octyloxybenzoyloxy)benzoyloxy}benzoyloxy]benzoate, (6.A.1)

This was synthesized following a procedure used for the preparation of compound **6.1.** Yield, 60%; m.p. 140.5°C; ν_{max}: 2918, 2852, 2237, 1736, 1605, 1591, 1278, 1080 cm^{-1}; δ_H: 8.24-8.21 (m, 4H, Ar-H), 8.1-8.02 (m, 4H, Ar-H), 7.7-7.68 (d, 2H, ^{3}J8.72 Hz, Ar-H), 7.58-7.47 (m, 2H, Ar-H), 7.36-7.3 (m, 6H, Ar-H), 6.93-6.91(d, 2H, ^{3}J8.92 Hz, Ar-H), 4.0-3.97(t, 2H, ^{3}J6.56 Hz, Ar-OCH_2-), 1.8-1.73(quin, 2H, ^{3}J6.72 Hz, Ar-OCH_2-$C\underline{H}_2$-), 1.53-1.23 (m, 10H, 5 × -CH_2-), 0.84-0.81 (t, 3H, ^{3}J6.64 Hz, 1 × -CH_3). Elemental analysis: C_{43} H_{37} NO_9 requires, C, 72.56; H, 5.24; N, 1.97%; found, C, 72.45; H, 5.27; N, 1.95%.

4-Cyanophenyl-4-[3-{4-(4-n-decyloxybenzoyloxy)benzoyloxy}benzoyloxy]benzoate, (6.A.2)

Yield, 58%; m.p. 133.5°C; ν_{max}: 2920, 2852, 2240, 1736, 1606, 1594, 1278, 1080 cm^{-1}; δ_H: 8.24-8.21 (m, 4H, Ar-H), 8.1-8.02 (m, 4H, Ar-H), 7.7-7.68 (d, 2H, ^{3}J8.56 Hz, Ar-H), 7.58-7.48 (m, 2H, Ar-H), 7.38-7.3 (m, 6H, Ar-H), 6.93-6.91(d, 2H, ^{3}J8.88 Hz, Ar-H), 4.0-3.97(t, 2H, ^{3}J6.52 Hz, Ar-OCH_2-), 1.8-1.73(quin, 2H, ^{3}J6.72 Hz, Ar-OCH_2-$C\underline{H}_2$-), 1.53-1.21 (m, 14H, 7 × -CH_2-), 0.84-0.80 (t, 3H, ^{3}J6.56 Hz, 1 × -CH_3). Elemental analysis: C_{45} H_{41} NO_9 requires, C, 73.06; H, 5.59; N, 1.89%; found, C, 72.95; H, 5.68; N, 1.92%.

4-Cyanophenyl-4-[3-{4-(4-n-undecyloxybenzoyloxy)benzoyloxy}benzoyloxy]benzoate, (6.A.3)

Yield, 57%; m.p. 131°C; ν_{max}:2916, 2852, 2243, 1736, 1602, 1280, 1080 cm^{-1}; δ_H: 8.31-8.28 (m, 4H, Ar-H), 8.16-8.09 (m, 4H, Ar-H), 7.77-7.75 (d, 2H, ^{3}J8.72 Hz, Ar-H), 7.63-7.54 (m, 2H, Ar-H), 7.43-7.37 (m, 6H, Ar-H), 7.0-6.98(d, 2H, ^{3}J8.92 Hz, Ar-H), 4.07-4.04(t, 2H, ^{3}J6.56 Hz, Ar-OCH_2-), 1.86-1.80(quin, 2H, ^{3}J6.72 Hz, Ar-OCH_2-$C\underline{H}_2$-), 1.48-1.28 (m, 16H, 8 × -CH_2-), 0.9-0.87 (t, 3H, ^{3}J6.72 Hz, 1 × -CH_3). Elemental analysis: C_{46} H_{43} NO_9 requires, C, 73.29; H, 5.75; N, 1.86%; found, C, 73.06; H, 5.82; N, 1.79%.

4-Cyanophenyl-4-[3-{4-(4-n-dodecyloxybenzoyloxy)benzoyloxy}benzoyloxy]benzoate, (6.A.4)

Yield, 61%; m.p. 129.5°C; ν_{max}:2924, 2854, 2230, 1740, 1600, 1252, 1080 cm^{-1}; δ_H: 8.31-8.28 (m, 4H, Ar-H), 8.16-8.09 (m, 4H, Ar-H), 7.77-7.75 (d, 2H, ^{3}J8.56 Hz, Ar-H), 7.65-7.55 (m, 2H, Ar-H), 7.43-7.37 (m, 6H, Ar-H), 7.0-6.98(d, 2H, ^{3}J8.88 Hz, Ar-H), 4.07-4.04(t, 2H, ^{3}J6.56 Hz, Ar-OCH_2-), 1.86-1.80(quin, 2H, ^{3}J6.68 Hz, Ar-OCH_2-$C\underline{H}_2$-), 1.48-1.27 (m, 18H, 9 × -CH_2-), 0.9-0.87 (t, 3H, ^{3}J6.6 Hz, 1 × -CH_3). Elemental analysis: C_{47} H_{45} NO_9 requires, C, 73.52; H, 5.90; N, 1.82%; found, C, 73.46; H, 5.85; N, 1.81%.

4-Cyanophenyl-4-[3-{4-(4-n-tridecyloxybenzoyloxy)benzoyloxy}benzoyloxy]benzoate, (6.A.5)

Yield, 59%; m.p. 129°C; ν_{max}:2918, 2852, 2241, 1736, 1600, 1252, 1080 cm^{-1}; δ_H: 8.31-8.28 (m, 4H, Ar-H), 8.16-8.09 (m, 4H, Ar-H), 7.77-7.75 (d, 2H, ^{3}J8.64 Hz, Ar-H), 7.65-7.55 (m, 2H, Ar-H), 7.43-7.37 (m, 6H, Ar-H), 7.0-6.98(d, 2H, ^{3}J8.88 Hz, Ar-H), 4.07-4.04(t, 2H, ^{3}J6.56 Hz, Ar-OCH_2-), 1.86-1.80(quin, 2H, ^{3}J6.68 Hz, Ar-OCH_2-$C\underline{H}_2$-), 1.48-1.27 (m, 20H,

10 × -CH_2-), 0.9-0.87 (t, 3H, ^{3}J6.68 Hz, 1 × -CH_3). Elemental analysis: C_{48} H_{47} NO_9 requires, C, 73.73; H, 6.06; N, 1.79%; found, C, 73.64; H, 6.09; N, 1.55%.

4-Cyanophenyl-4-[3-{4-(4-n-tetradecyloxybenzoyloxy)benzoyloxy}benzoyloxy]benzoate, (6.A.6)

Yield, 60%; m.p. 129.5°C; ν_{max}(KBr):2916, 2851, 2243, 1736, 1603, 1279, 1255, 1078 cm^{-1}; δ_H: 8.31-8.28 (m, 4H, Ar-H), 8.16-8.09 (m, 4H, Ar-H), 7.77-7.75 (d, 2H, ^{3}J8.64 Hz, Ar-H), 7.65-7.55 (m, 2H, Ar-H), 7.43-7.37 (m, 6H, Ar-H), 7.0-6.98(d, 2H, ^{3}J8.92 Hz, Ar-H), 4.07-4.04(t, 2H, ^{3}J6.56 Hz, Ar-OCH_2-), 1.86-1.80(quin, 2H, ^{3}J6.68 Hz, Ar-OCH_2-C$\underline{H}_2$-), 1.48-1.27 (m, 22H, 11 × -CH_2-), 0.9-0.87 (t, 3H, ^{3}J6.64 Hz, 1 × -CH_3). Elemental analysis: C_{49} H_{49} NO_9 requires, C, 73.94; H, 6.21; N, 1.76%; found, C, 73.66; H, 6.27; N, 1.35%.

4-Cyanophenyl-4-[3-{4-(4-n-pentadecyloxybenzoyloxy)benzoyloxy}benzoyloxy] benzoate, (6.A.7)

Yield, 56%; m.p. 129.5°C; ν_{max}:2916, 2851, 2241, 1736, 1603, 1256, 1078 cm^{-1}; δ_H: 8.31-8.28 (m, 4H, Ar-H), 8.17-8.09 (m, 4H, Ar-H), 7.77-7.75 (d, 2H, ^{3}J8.68 Hz, Ar-H), 7.65-7.55 (m, 2H, Ar-H), 7.43-7.37 (m, 6H, Ar-H), 7.0-6.98(d, 2H, ^{3}J8.84 Hz, Ar-H), 4.07-4.04(t, 2H, ^{3}J6.48 Hz, Ar-OCH_2-), 1.85-1.79(quin, 2H, ^{3}J6.96 Hz, Ar-OCH_2-C$\underline{H}_2$-), 1.48-1.27 (m, 24H, 12 × -CH_2-), 0.9-0.86 (t, 3H, ^{3}J6.64 Hz, 1 × -CH_3). Elemental analysis: C_{50} H_{51} NO_9 requires, C, 74.15; H, 6.35; N, 1.73%; found, C, 74.48; H, 6.14; N, 1.71%.

4-Cyanophenyl-4-[3-{4-(4-n-hexadecyloxybenzoyloxy)benzoyloxy}benzoyloxy]benzoate, (6.A.8)

Yield, 58%; m.p. 130°C; ν_{max}(KBr):2916, 2851, 2247, 1736, 1605, 1256, 1074 cm^{-1}; δ_H: 8.31-8.28 (m, 4H, Ar-H), 8.17-8.09 (m, 4H, Ar-H), 7.77-7.75 (d, 2H, ^{3}J8.72 Hz, Ar-H), 7.65-7.55 (m, 2H, Ar-H), 7.43-7.37 (m, 6H, Ar-H), 7.0-6.98(d, 2H, ^{3}J8.92 Hz, Ar-H), 4.07-4.04(t, 2H, ^{3}J6.56 Hz, Ar-OCH_2-), 1.86-1.80(quin, 2H, ^{3}J6.68 Hz, Ar-OCH_2-C$\underline{H}_2$-), 1.48-1.26 (m, 24H, 12 × -CH_2-), 0.9-0.87 (t, 3H, ^{3}J6.64 Hz, 1 × -CH_3). Elemental analysis: C_{51} H_{53} NO_9 requires, C, 74.34; H, 6.48; N, 1.7%; found, C, 74.08; H, 6.54; N, 1.56%.

4-Cyanophenyl-4-[3-{4-(4-n-octadecyloxybenzoyloxy)benzoyloxy}benzoyloxy]benzoate, (6.A.9)

Yield, 56%; m.p. 129.5°C; ν_{max}: 2916, 2851, 2247, 1734, 1605, 1256, 1082 cm^{-1}; δ_H: 8.31-8.28 (m, 4H, Ar-H), 8.17-8.09 (m, 4H, Ar-H), 7.77-7.75 (d, 2H, ^{3}J8.48 Hz, Ar-H), 7.65-7.55 (m, 2H, Ar-H), 7.43-7.37 (m, 6H, Ar-H), 7.0-6.98(d, 2H, ^{3}J8.72 Hz, Ar-H), 4.07-4.04(t, 2H,

^{3}J6.44 Hz, Ar-OCH_2-), 1.85-1.80(quin, 2H, ^{3}J6.88 Hz, Ar-OCH_2-$C\underline{H}_2$-), 1.48-1.26 (m, 28H, 14 × -CH_2-), 0.9-0.86 (t, 3H, ^{3}J6.24 Hz, 1 × -CH_3). Elemental analysis: C_{53} H_{57} NO_9 requires, C, 74.71; H, 6.74; N, 1.64%; found, C, 74.48; H, 6.72; N, 1.34%.

4-Cyanophenyl-4-[3-{4-(4-n-dodecyloxybenzoyloxy)2-fluorobenzoyloxy}benzoyloxy] benzoate, (6.B.1)

Yield, 60%; m.p. 130°C; ν_{max}:2924, 2854, 2241, 1740, 1732, 1607, 1251, 1080 cm^{-1}; δ_H: 8.3-8.1 (m, 7H, Ar-H), 7.77-7.75 (d, 2H, ^{3}J8.52 Hz, Ar-H), 7.65-7.56 (m, 2H, Ar-H), 7.43-7.38 (m, 4H, Ar-H), 7.22-7.2 (m, 2H, Ar-H), 7.0-6.98(d, 2H, ^{3}J8.8 Hz, Ar-H), 4.07-4.04(t, 2H, ^{3}J6.44 Hz, Ar-OCH_2-), 1.86-1.80(quin, 2H, ^{3}J6.52 Hz, Ar-OCH_2-$C\underline{H}_2$-), 1.48-1.27 (m, 18H, 9 × -CH_2-), 0.9-0.87 (t, 3H, ^{3}J6.24 Hz, 1 × -CH_3).

4-Cyanophenyl-4-[3-{4-(4-n-tetradecyloxybenzoyloxy)2-fluorobenzoyloxy}benzoyloxy] benzoate, (6.B.2)

Yield, 58%; m.p. 132°C; ν_{max}:2924, 2854, 2241, 1740, 1736, 1610, 1603, 1252, 1080 cm^{-1}; δ_H: 8.3-8.1 (m, 7H, Ar-H), 7.77-7.75 (d, 2H, ^{3}J8.68 Hz, Ar-H), 7.65-7.56 (m, 2H, Ar-H), 7.43-7.38 (m, 4H, Ar-H), 7.22-7.2 (m, 2H, Ar-H), 7.0-6.98(d, 2H, ^{3}J8.84 Hz, Ar-H), 4.07-4.04(t, 2H, ^{3}J6.52 Hz, Ar-OCH_2-), 1.85-1.81(quin, 2H, ^{3}J6.52 Hz, Ar-OCH_2-$C\underline{H}_2$-), 1.48-1.27 (m, 22H, 11 × -CH_2-), 0.9-0.86 (t, 3H, ^{3}J6.28 Hz, 1 × -CH_3).

4-Cyanophenyl-4-[3-{4-(4-n-hexadecyloxybenzoyloxy)2-fluorobenzoyloxy}benzoyloxy] benzoate, (6.B.3)

Yield, 61%; m.p. 131.5°C; ν_{max}:2924, 2854, 2240, 1740, 1735, 1610, 1603, 1254, 1080 cm^{-1}; δ_H: 8.3-8.1 (m, 7H, Ar-H), 7.77-7.75 (d, 2H, ^{3}J8.72 Hz, Ar-H), 7.65-7.56 (m, 2H, Ar-H), 7.43-7.38 (m, 4H, Ar-H), 7.22-7.2 (m, 2H, Ar-H), 7.0-6.98(d, 2H, ^{3}J8.88 Hz, Ar-H), 4.07-4.04(t, 2H, ^{3}J6.52 Hz, Ar-OCH_2-), 1.85-1.81(quin, 2H, ^{3}J6.58 Hz, Ar-OCH_2-$C\underline{H}_2$-), 1.48-1.26 (m, 26H, 13 × -CH_2-), 0.9-0.86 (t, 3H, ^{3}J6.44 Hz, 1 × -CH_3).

4-Cyanophenyl-4-[3-{4-(4-n-octadecyloxybenzoyloxy)2-fluorobenzoyloxy}benzoyloxy] benzoate, (6.B.4)

Yield, 62%; m.p. 131°C; ν_{max}: 2924, 2854, 2240, 1740, 1732, 1610, 1603, 1254, 1080 cm^{-1}; δ_H: 8.3-8.1 (m, 7H, Ar-H), 7.77-7.75 (d, 2H, ^{3}J8.64 Hz, Ar-H), 7.65-7.56 (m, 2H, Ar-H), 7.43-7.38 (m, 4H, Ar-H), 7.22-7.2 (m, 2H, Ar-H), 7.0-6.98(d, 2H, ^{3}J8.88 Hz, Ar-H), 4.07-4.04(t, 2H, ^{3}J6.52 Hz, Ar-OCH_2-), 1.85-1.81(quin, 2H, ^{3}J6.50 Hz, Ar-OCH_2-$C\underline{H}_2$-), 1.48-1.26 (m, 30H, 15 × -CH_2-), 0.89-0.86 (t, 3H, ^{3}J6.50 Hz, 1 × -CH_3).

4-Cyanophenyl-4-[3-{4-(4-n-hexyloxybenzoyloxy)3-fluorobenzoyloxy}benzoyloxy] benzoate, (6.C.1)

Yield, 56%; m.p. 161°C; ν_{max}: 2924, 2854, 2224, 1750, 1742, 1607, 1278, 1128, 1080 cm^{-1}; δ_H: 8.3-8.28 (d, 2H, ^{3}J8.64 Hz, Ar-H), 8.17-8.05 (m, 6H, Ar-H), 7.77-7.75 (d, 2H, ^{3}J8.6 Hz, Ar-H), 7.66-7.54 (m, 2H, Ar-H), 7.48-7.37 (m, 5H, Ar-H), 7.01-6.97(d, 2H, ^{3}J8.84 Hz, Ar-H), 4.08-4.05(t, 2H, ^{3}J6.56 Hz, Ar-OCH_2-), 1.87-1.79(quin, 2H, ^{3}J6.64 Hz, Ar-OCH_2-$C\underline{H}_2$-), 1.51-1.22 (m, 6H, 3 × -CH_2-), 0.94-0.9 (t, 3H, ^{3}J7.04 Hz, 1 × -CH_3).

4-Cyanophenyl-4-[3-{4-(4-n-dodecyloxybenzoyloxy)3-fluorobenzoyloxy}benzoyloxy] benzoate, (6.C.2)

Yield, 58%; m.p. 119.5°C; ν_{max}:2922, 2852, 2233, 1745, 1736, 1608, 1278, 1124, 1080 cm^{-1}; δ_H: 8.3-8.28 (d, 2H, ^{3}J8.64 Hz, Ar-H), 8.17-8.05 (m, 6H, Ar-H), 7.77-7.75 (d, 2H, ^{3}J8.56 Hz, Ar-H), 7.66-7.54 (m, 2H, Ar-H), 7.48-7.38 (m, 5H, Ar-H), 7.01-6.99(d, 2H, ^{3}J8.76 Hz, Ar-H), 4.08-4.04(t, 2H, ^{3}J6.44 Hz, Ar-OCH_2-), 1.85-1.79(quin, 2H, ^{3}J6.88 Hz, Ar-OCH_2-$C\underline{H}_2$-), 1.48-1.27 (m, 18H, 9 × -CH_2-), 0.9-0.87 (t, 3H, ^{3}J6.2 Hz, 1 × -CH_3).

4-Cyanophenyl-4-[3-{4-(4-n-tridecyloxybenzoyloxy)3-fluorobenzoyloxy}benzoyloxy] benzoate, (6.C.3)

Yield, 55%; m.p. 120°C; ν_{max}:2924, 2854, 2234, 1745, 1738, 1608, 1278, 1125, 1080 cm^{-1}; δ_H: 8.3-8.28 (d, 2H, ^{3}J8.76 Hz, Ar-H), 8.17-8.06 (m, 6H, Ar-H), 7.77-7.75 (d, 2H, ^{3}J8.72 Hz, Ar-H), 7.66-7.54 (m, 2H, Ar-H), 7.48-7.38 (m, 5H, Ar-H), 7.01-6.99(d, 2H, ^{3}J8.92 Hz, Ar-H), 4.08-4.04(t, 2H, ^{3}J6.52 Hz, Ar-OCH_2-), 1.86-1.79(quin, 2H, ^{3}J6.72 Hz, Ar-OCH_2-$C\underline{H}_2$-), 1.55-1.27 (m, 20H, 10 × -CH_2-), 0.9-0.87 (t, 3H, ^{3}J6.52 Hz, 1 × -CH_3).

4-Cyanophenyl-4-[3-{4-(4-n-tetradecyloxybenzoyloxy)3-fluorobenzoyloxy}benzoyloxy] benzoate, (6.C.4)

Yield, 57%; m.p. 120.5°C; ν_{max}:2924, 2854, 2234, 1747, 1732, 1608, 1260, 1122, 1068 cm^{-1}; δ_H: 8.3-8.28 (d, 2H, ^{3}J8.64 Hz, Ar-H), 8.17-8.06 (m, 6H, Ar-H), 7.77-7.75 (d, 2H, ^{3}J8.52 Hz, Ar-H), 7.66-7.54 (m, 2H, Ar-H), 7.48-7.38 (m, 5H, Ar-H), 7.01-6.99(d, 2H, ^{3}J8.76 Hz, Ar-H), 4.08-4.04(t, 2H, ^{3}J6.48 Hz, Ar-OCH_2-), 1.85-1.81(quin, 2H, ^{3}J6.72 Hz, Ar-OCH_2-$C\underline{H}_2$-), 1.55-1.27 (m, 22H, 11 × -CH_2-), 0.9-0.86 (t, 3H, ^{3}J6.4 Hz, 1 × -CH_3).

4-Cyanophenyl-4-[3-{4-(4-n-pentadecyloxybenzoyloxy)3-fluorobenzoyloxy}benzoyloxy] benzoate, (6.C.5)

Yield, 54%; m.p. 121°C; ν_{max}: 2924, 2854, 2243, 1747, 1736, 1608, 1253, 1124, 1068 cm^{-1}; δ_H: 8.3-8.28 (d, 2H, ^{3}J8.6 Hz, Ar-H), 8.17-8.06 (m, 6H, Ar-H), 7.77-7.75 (d, 2H, ^{3}J8.56 Hz, Ar-H), 7.66-7.54 (m, 2H, Ar-H), 7.48-7.38 (m, 5H, Ar-H), 7.01-6.99(d, 2H, ^{3}J8.76 Hz, Ar-H), 4.08-4.04(t, 2H, ^{3}J6.52 Hz, Ar-OCH_2-), 1.85-1.81(quin, 2H, ^{3}J6.72 Hz, Ar-OCH_2-C$\underline{H}_2$-), 1.55-1.27 (m, 24H, 12 × -CH_2-), 0.9-0.86 (t, 3H, ^{3}J6.4 Hz, 1 × -CH_3).

4-Cyanophenyl-4-[3-{4-(4-n-hexadecyloxybenzoyloxy)3-fluorobenzoyloxy}benzoyloxy] benzoate, (6.C.6)

Yield, 55%; m.p. 121°C; ν_{max}:2920, 2851, 2243, 1738, 1701, 1610, 1605, 1253, 1124, 1076 cm^{-1}; δ_H: 8.3-8.28 (d, 2H, ^{3}J8.72 Hz, Ar-H), 8.17-8.06 (m, 6H, Ar-H), 7.77-7.75 (d, 2H, ^{3}J8.6 Hz, Ar-H), 7.66-7.54 (m, 2H, Ar-H), 7.48-7.38 (m, 5H, Ar-H), 7.01-6.99(d, 2H, ^{3}J8.92 Hz, Ar-H), 4.08-4.04(t, 2H, ^{3}J6.52 Hz, Ar-OCH_2-), 1.86-1.81(quin, 2H, ^{3}J6.72 Hz, Ar-OCH_2-C$\underline{H}_2$-), 1.55-1.27 (m, 26H, 13 × -CH_2-), 0.9-0.86 (t, 3H, ^{3}J6.44 Hz, 1 × -CH_3).

4-Cyanophenyl-4-[3-{4-(4-n-octadecyloxybenzoyloxy)3-fluorobenzoyloxy}benzoyloxy] benzoate, (6.C.7)

Yield, 57%; m.p. 120°C; ν_{max}: 2918, 2852, 2243, 1736, 1610, 1603, 1254, 1120, 1076 cm^{-1}; δ_H: 8.3-8.28 (d, 2H, ^{3}J8.64 Hz, Ar-H), 8.17-8.06 (m, 6H, Ar-H), 7.77-7.75 (d, 2H, ^{3}J8.52 Hz, Ar-H), 7.66-7.54 (m, 2H, Ar-H), 7.48-7.38 (m, 5H, Ar-H), 7.01-6.99(d, 2H, ^{3}J8.88 Hz, Ar-H), 4.08-4.04(t, 2H, ^{3}J6.56 Hz, Ar-OCH_2-), 1.85-1.81(quin, 2H, ^{3}J7.07 Hz, Ar-OCH_2-C$\underline{H}_2$-), 1.55-1.26 (m, 30H, 15 × -CH_2-), 0.9-0.86 (t, 3H, ^{3}J6.44 Hz, 1 × -CH_3).

4-Cyanophenyl-4-[3-{4-(4-n-hexylbiphenyl-4-carbonyloxy)benzoyloxy}benzoyloxy] benzoate, (6.D.1)

Yield, 56%; m.p. 156°C; ν_{max}: 2922, 2854, 2243, 1736, 1605, 1591, 1275, 1080 cm^{-1}; δ_H: 8.27-8.03 (m, 7H, Ar-H), 7.7-7.48 (m, 9H, Ar-H), 7.38-7.19 (m, 8H, Ar-H), 2.62-2.59(t, 2H, ^{3}J7.6 Hz, Ar-CH_2-), 1.61-1.56(quin, 2H, ^{3}J6.88 Hz, Ar-CH_2-C$\underline{H}_2$-), 1.5-1.27 (m, 6H, 3 × -CH_2-), 0.85-0.81 (t, 3H, ^{3}J6.96 Hz, 1 × -CH_3). Elemental analysis: C_{47} H_{37} NO_8 requires, C, 75.9; H, 5.01; N, 1.88%; found, C, 75.46; H, 4.98; N, 1.86%.

4-Cyanophenyl-4-[3-{4-(4-n-octylbiphenyl-4-carbonyloxy)benzoyloxy}benzoyloxy] benzoate, (6.D.2)

Yield, 53%; m.p. 170°C; ν_{max}:2920, 2852, 2243, 1736, 1605, 1273, 1080 cm^{-1}; δ_H: 8.27-8.03 (m, 7H, Ar-H), 7.7-7.49 (m, 9H, Ar-H), 7.38-7.19 (m, 8H, Ar-H), 2.62-2.59(t, 2H, ^{3}J7.6 Hz, Ar-CH_2-), 1.61-1.56(quin, 2H, ^{3}J6.8 Hz, Ar-CH_2-C$\underline{H}_2$-), 1.55-1.21 (m, 10H, 5 × -CH_2-), 0.83-0.8 (t, 3H, ^{3}J6.64 Hz, 1 × -CH_3). Elemental analysis: C_{49} H_{41} NO_8 requires, C, 76.25; H, 5.35; N, 1.81%; found, C, 76.41; H, 5.24; N, 1.75%.

4-Cyanophenyl-4-[3-{4-(4-n-nonylbiphenyl-4-carbonyloxy)benzoyloxy}benzoyloxy] benzoate, (6.D.3)

Yield, 55%; m.p. 160°C; ν_{max}:2920, 2852, 2243, 1738, 1605, 1273, 1080 cm^{-1}; δ_H: 8.27-8.03 (m, 7H, Ar-H), 7.7-7.48 (m, 9H, Ar-H), 7.38-7.19 (m, 8H, Ar-H), 2.62-2.58(t, 2H, ^{3}J7.64 Hz, Ar-CH_2-), 1.59-1.57(quin, 2H, ^{3}J6.82 Hz, Ar-CH_2-C$\underline{H}_2$-), 1.57-1.21 (m, 12H, 6 × -CH_2-), 0.83-0.8 (t, 3H, ^{3}J6.64 Hz, 1 × -CH_3). Elemental analysis: C_{50} H_{43} NO_8 requires, C, 76.42; H, 5.52; N, 1.78%; found, C, 76.08; H, 5.46; N, 1.63%.

4-Cyanophenyl-4-[3-{4-(4-n-decylbiphenyl-4-carbonyloxy)benzoyloxy}benzoyloxy] benzoate, (6.D.4)

Yield, 58%; m.p. 169°C; ν_{max}:2922, 2852, 2243, 1736, 1605, 1275, 1080 cm^{-1}; δ_H: 8.27-8.03 (m, 7H, Ar-H), 7.7-7.48 (m, 9H, Ar-H), 7.38-7.19 (m, 8H, Ar-H), 2.62-2.58(t, 2H, ^{3}J7.68 Hz, Ar-CH_2-), 1.59-1.57(quin, 2H, ^{3}J6.86 Hz, Ar-CH_2-C$\underline{H}_2$-), 1.57-1.21 (m, 14H, 7 × -CH_2-), 0.83-0.8 (t, 3H, ^{3}J6.68 Hz, 1 × -CH_3). Elemental analysis: C_{51} H_{45} NO_8 requires, C, 76.58; H, 5.67; N, 1.75%; found, C, 76.68; H, 5.56; N, 1.73%.

4-Cyanophenyl-4-[3-{4-(4-n-undecylbiphenyl-4-carbonyloxy)benzoyloxy}benzoyloxy] benzoate, (6.D.5)

Yield, 54%; m.p. 169°C; ν_{max}:2920, 2852, 2243, 1736, 1605, 1273, 1080 cm^{-1}; δ_H: 8.27-8.03 (m, 7H, Ar-H), 7.7-7.49 (m, 9H, Ar-H), 7.38-7.19 (m, 8H, Ar-H), 2.62-2.58(t, 2H, ^{3}J7.52 Hz, Ar-CH_2-), 1.59-1.57(quin, 2H, ^{3}J6.8 Hz, Ar-CH_2-C$\underline{H}_2$-), 1.57-1.2 (m, 16H, 8 × -CH_2-), 0.83-0.8 (t, 3H, ^{3}J6.52 Hz, 1 × -CH_3). Elemental analysis: C_{52} H_{47} NO_8 requires, C, 76.73; H, 5.82; N, 1.72%; found, C, 77.09; H, 5.81; N, 1.32%.

4-Cyanophenyl-4-[3-{4-(4-n-dodecylbiphenyl-4-carbonyloxy)benzoyloxy}benzoyloxy] benzoate, (6.D.6)

Yield, 56%; m.p. 158°C; ν_{max}: 2918, 2851, 2243, 1736, 1728, 1605, 1275, 1080 cm^{-1}; δ_H: 8.27-8.03 (m, 7H, Ar-H), 7.7-7.49 (m, 9H, Ar-H), 7.38-7.19 (m, 8H, Ar-H), 2.62-2.58(t, 2H, ^{3}J7.56 Hz, Ar-CH_2-), 1.61-1.55(quin, 2H, ^{3}J6.92 Hz, Ar-CH_2-$C\underline{H}_2$-), 1.27-1.2 (m, 18H, 9 × -CH_2-), 0.83-0.8 (t, 3H, ^{3}J6.64 Hz, 1 × -CH_3). Elemental analysis: C_{53} H_{49} NO_8 requires, C, 76.88; H, 5.97; N, 1.69%; found, C, 76.43; H, 5.82; N, 1.76%.

4-Cyanophenyl-4-[3-{4-(4-n-tetradecylbiphenyl-4-carbonyloxy)benzoyloxy}benzoyloxy] benzoate, (6.D.7)

Yield, 59%; m.p. 157°C; ν_{max}:2918, 2851, 2243, 1736, 1605, 1273, 1080 cm^{-1}; δ_H: 8.27-8.03 (m, 7H, Ar-H), 7.7-7.48 (m, 9H, Ar-H), 7.38-7.19 (m, 8H, Ar-H), 2.62-2.58(t, 2H, ^{3}J7.64 Hz, Ar-CH_2-), 1.59-1.57(quin, 2H, ^{3}J6.92 Hz, Ar-CH_2-$C\underline{H}_2$-), 1.27-1.19 (m, 22H, 11 × -CH_2-), 0.83-0.79 (t, 3H, ^{3}J6.68 Hz, 1 × -CH_3). Elemental analysis: C_{55} H_{53} NO_8 requires, C, 77.17; H, 6.24; N, 1.64%; found, C, 77.4; H, 6.18; N, 1.7%.

4-Cyanophenyl-4-[3-{4-(4-n-hexadecylbiphenyl-4-carbonyloxy)benzoyloxy}benzoyloxy] benzoate, (6.D.8)

Yield, 57%; m.p. 156°C; ν_{max}:2918, 2851, 2243, 1736, 1605, 1273, 1080 cm^{-1}; δ_H: 8.27-8.03 (m, 7H, Ar-H), 7.7-7.48 (m, 9H, Ar-H), 7.38-7.19 (m, 8H, Ar-H), 2.62-2.58(t, 2H, ^{3}J7.64 Hz, Ar-CH_2-), 1.59-1.57(quin, 2H, ^{3}J6.96 Hz, Ar-CH_2-$C\underline{H}_2$-), 1.27-1.15 (m, 28H, 14 × -CH_2-), 0.83-0.79 (t, 3H, ^{3}J6.64 Hz, 1 × -CH_3). Elemental analysis: C_{57} H_{57} NO_8 requires, C, 77.44; H, 6.5; N, 1.58%; found, C, 77.43; H, 6.44; N, 1.62%.

4-Cyanophenyl-4-[3-{4-(4-n-octadecylbiphenyl-4-carbonyloxy)benzoyloxy}benzoyloxy] benzoate, (6.D.9)

Yield, 58%; m.p. 154°C; ν_{max}:2916, 2851, 2243, 1738, 1605, 1273, 1080 cm^{-1}; δ_H: 8.27-8.03 (m, 7H, Ar-H), 7.7-7.49 (m, 9H, Ar-H), 7.38-7.19 (m, 8H, Ar-H), 2.62-2.58(t, 2H, ^{3}J7.64 Hz, Ar-CH_2-), 1.59-1.57(quin, 2H, ^{3}J6.96 Hz, Ar-CH_2-$C\underline{H}_2$-), 1.27-1.15 (m, 32H, 16 × -CH_2-), 0.83-0.79 (t, 3H, ^{3}J6.64 Hz, 1 × -CH_3). Elemental analysis: C_{59} H_{61} NO_8 requires, C, 77.69; H, 6.74; N, 1.54%; found, C, 77.32; H, 6.67; N, 1.22%.

4-Cyanophenyl-4-[3-{4-(4-n-octadecylbiphenyl-4-carbonyloxy)benzoyloxy}benzoyloxy] benzoate, (6.D.10)

Yield, 58%; m.p. 154°C; ν_{max}:2916, 2851, 2243, 1738, 1605, 1273, 1080 cm^{-1}; δ_H: 8.27-8.03 (m, 7H, Ar-H), 7.7-7.49 (m, 9H, Ar-H), 7.38-7.19 (m, 8H, Ar-H), 2.62-2.58(t, 2H, ^{3}J7.64 Hz, Ar-CH_2-), 1.59-1.57(quin, 2H, ^{3}J6.96 Hz, Ar-CH_2-C$\underline{H}_2$-), 1.27-1.15 (m, 32H, 16 × -CH_2-), 0.83-0.79 (t, 3H, ^{3}J6.64 Hz, 1 × -CH_3). Elemental analysis: C_{59} H_{61} NO_8 requires, C, 77.69; H, 6.74; N, 1.54%; found, C, 77.32; H, 6.67; N, 1.22%.

4-Cyanophenyl-4-[3-{4-(4-n-hexylbiphenyl-4-carbonyloxy)2-fluorobenzoyloxy} benzoyloxy]benzoate, (6.E.1)

Yield, 50%; m.p. 175.5°C; ν_{max}:2924, 2855, 2237, 1740, 1734, 1610, 1587, 1245, 1050 cm^{-1}; δ_H: 8.3-8.11 (m, 6H, Ar-H), 7.77-7.58 (m, 9H, Ar-H), 7.43-7.24 (m, 8H, Ar-H), 2.7-2.66(t, 2H, ^{3}J7.48 Hz, Ar-CH_2-), 1.68-1.62(quin, 2H, ^{3}J7.0 Hz, Ar-CH_2-C$\underline{H}_2$-), 1.3-1.27 (m, 6H, 3 × -CH_2-), 0.91-0.88 (t, 3H, ^{3}J6.64 Hz, 1 × -CH_3).

4-Cyanophenyl-4-[3-{4-(4-n-octylbiphenyl-4-carbonyloxy)2-fluorobenzoyloxy} benzoyloxy]benzoate, (6.E.2)

Yield, 52%; m.p. 155°C; ν_{max}:2922, 2853, 2243, 1736, 1605, 1590, 1260, 1074 cm^{-1}; δ_H: 8.3-8.04 (m, 6H, Ar-H), 7.77-7.58 (m, 9H, Ar-H), 7.43-7.24 (m, 8H, Ar-H), 2.7-2.66(t, 2H, ^{3}J7.52 Hz, Ar-CH_2-), 1.67-1.64(quin, 2H, ^{3}J7.0 Hz, Ar-CH_2-C$\underline{H}_2$-), 1.3-1.28 (m, 10H, 5 × -CH_2-), 0.91-0.88 (t, 3H, ^{3}J6.64 Hz, 1 × -CH_3).

4-Cyanophenyl-4-[3-{4-(4-n-nonylbiphenyl-4-carbonyloxy)2-fluorobenzoyloxy} benzoyloxy]benzoate, (6.E.3)

Yield, 55%; m.p. 160°C; ν_{max}: 2920, 2852, 2243, 1736, 1605, 1593, 1259, 1074 cm^{-1}; δ_H: 8.23-8.04 (m, 6H, Ar-H), 7.7-7.51 (m, 9H, Ar-H), 7.36-7.16 (m, 8H, Ar-H), 2.62-2.58(t, 2H, ^{3}J7.68 Hz, Ar-CH_2-), 1.61-1.55(quin, 2H, ^{3}J7.56 Hz, Ar-CH_2-C$\underline{H}_2$-), 1.27-1.2 (m, 12H, 6 × -CH_2-), 0.83-0.8 (t, 3H, ^{3}J6.64 Hz, 1 × -CH_3).

4-Cyanophenyl-4-[3-{4-(4-n-decylbiphenyl-4-carbonyloxy)2-fluorobenzoyloxy} benzoyloxy]benzoate, (6.E.4)

Yield, 57%; m.p. 161.5°C; ν_{max}:2920, 2852, 2243, 1736, 1605, 1593, 1259,1074 cm^{-1}; δ_H: 8.23-8.04 (m, 6H, Ar-H), 7.7-7.51 (m, 9H, Ar-H), 7.36-7.16 (m, 8H, Ar-H), 2.62-2.58(t, 2H,

^{3}J7.68 Hz, Ar-CH_2-), 1.61-1.55(quin, 2H, ^{3}J7.52 Hz, Ar-CH_2-C$\underline{H}_2$-), 1.27-1.2 (m, 14H, 7 × -CH_2-), 0.83-0.8 (t, 3H, ^{3}J6.6 Hz, 1 × -CH_3).

4-Cyanophenyl-4-[3-{4-(4-n-undecylbiphenyl-4-carbonyloxy)2-fluorobenzoyloxy} benzoyloxy]benzoate, (6.E.5)

Yield, 55%; m.p. 161.5°C; ν_{max}:2920, 2851, 2243, 1736, 1605, 1593, 1259,1074 cm^{-1}; δ_H: 8.23-8.04 (m, 6H, Ar-H), 7.7-7.51 (m, 9H, Ar-H), 7.36-7.16 (m, 8H, Ar-H), 2.62-2.58(t, 2H, ^{3}J7.52 Hz, Ar-CH_2-), 1.61-1.55(quin, 2H, ^{3}J6.92 Hz, Ar-CH_2-C$\underline{H}_2$-), 1.27-1.2 (m, 16H, 8 × -CH_2-), 0.83-0.8 (t, 3H, ^{3}J6.64 Hz, 1 × -CH_3).

4-Cyanophenyl-4-[3-{4-(4-n-dodecylbiphenyl-4-carbonyloxy)2-fluorobenzoyloxy} benzoyloxy]benzoate, (6.E.6)

Yield, 57%; m.p. 160°C; ν_{max}:2920, 2851, 2243, 1736, 1603, 1593, 1259,1074 cm^{-1}; δ_H: 8.23-8.04 (m, 6H, Ar-H), 7.7-7.51 (m, 9H, Ar-H), 7.36-7.16 (m, 8H, Ar-H), 2.62-2.58(t, 2H, ^{3}J7.64 Hz, Ar-CH_2-), 1.6-1.57(quin, 2H, ^{3}J6.9 Hz, Ar-CH_2-C$\underline{H}_2$-), 1.27-1.2 (m, 18H, 9 × -CH_2-), 0.83-0.79 (t, 3H, ^{3}J6.64 Hz, 1 × -CH_3).

4-Cyanophenyl-4-[3-{4-(4-n-tetradecylbiphenyl-4-carbonyloxy)2-fluorobenzoyloxy} benzoyloxy]benzoate, (6.E.7)

Yield, 56%; m.p. 159.5°C; ν_{max}:2920, 2851, 2243, 1736, 1603, 1593, 1259,1074 cm^{-1}; δ_H: 8.23-8.04 (m, 6H, Ar-H), 7.7-7.51 (m, 9H, Ar-H), 7.36-7.16 (m, 8H, Ar-H), 2.62-2.58(t, 2H, ^{3}J7.6 Hz, Ar-CH_2-), 1.59-1.57(quin, 2H, ^{3}J6.9 Hz, Ar-CH_2-C$\underline{H}_2$-), 1.27-1.19 (m, 22H, 11 × -CH_2-), 0.83-0.79 (t, 3H, ^{3}J6.6 Hz, 1 × -CH_3).

4-Cyanophenyl-4-[3-{4-(4-n-hexadecylbiphenyl-4-carbonyloxy)2-fluorobenzoyloxy} benzoyloxy]benzoate, (6.E.8)

Yield, 58%; m.p. 158°C; ν_{max}:2920, 2852, 2243, 1736, 1603, 1593, 1259,1074 cm^{-1}; δ_H: 8.23-8.04 (m, 6H, Ar-H), 7.7-7.51 (m, 9H, Ar-H), 7.36-7.16 (m, 8H, Ar-H), 2.62-2.58(t, 2H, ^{3}J7.56 Hz, Ar-CH_2-), 1.59-1.57(quin, 2H, ^{3}J6.86 Hz, Ar-CH_2-C$\underline{H}_2$-), 1.27-1.15 (m, 26H, 13 × -CH_2-), 0.83-0.79 (t, 3H, ^{3}J6.6 Hz, 1 × -CH_3).

4-Cyanophenyl-4-[3-{4-(4-n-octadecylbiphenyl-4-carbonyloxy)2-fluorobenzoyloxy} benzoyloxy]benzoate, (6.E.9)

Yield, 55%; m.p. 157.5°C; ν_{max}:2922, 2852, 2243, 1736, 1603, 1593, 1259,1074 cm^{-1}; δ_H: 8.23-8.04 (m, 6H, Ar-H), 7.7-7.51 (m, 9H, Ar-H), 7.36-7.16 (m, 8H, Ar-H), 2.62-2.58(t, 2H,

^{3}J7.8 Hz, Ar-CH_2-), 1.59-1.57(quin, 2H, ^{3}J6.82 Hz, Ar-CH_2-$C\underline{H}_2$-), 1.27-1.15 (m, 30H, 15 × -CH_2-), 0.83-0.79 (t, 3H, ^{3}J6.68 Hz, 1 × -CH_3).

4-Cyanophenyl-4-[3-{4-(4-n-hexylbiphenyl-4-carbonyloxy)3-fluorobenzoyloxy} benzoyloxy]benzoate, (6.F.1)

Yield, 52%; m.p. 159.5°C; ν_{max}:2924, 2855, 2239, 1736, 1603, 1263, 1068 cm^{-1}; δ_H: 8.3-8.08 (m, 8H, Ar-H), 7.77-7.75 (d, 4H, ^{3}J8.72 Hz, Ar-H), 7.66-7.38 (m, 9H, Ar-H), 7.32-7.30 (d, 2H, ^{3}J8.12 Hz, Ar-H), 2.7-2.66(t, 2H, ^{3}J7.68 Hz, Ar-CH_2-), 1.66-1.64(quin, 2H, ^{3}J6.82 Hz, Ar-CH_2-$C\underline{H}_2$-), 1.34-1.25 (m, 6H, 3 × -CH_2-), 0.92-0.88 (t, 3H, ^{3}J7.0 Hz, 1 × -CH_3).

4-Cyanophenyl-4-[3-{4-(4-n-octylbiphenyl-4-carbonyloxy)3-fluorobenzoyloxy} benzoyloxy]benzoate, (6.F.2)

Yield, 55%; m.p. 157°C; ν_{max}:2922, 2852, 2241, 1736, 1603, 1273, 1076 cm^{-1}; δ_H: 8.3-8.08 (m, 8H, Ar-H), 7.77-7.75 (d, 4H, ^{3}J8.12 Hz, Ar-H), 7.66-7.38 (m, 9H, Ar-H), 7.32-7.30 (d, 2H, ^{3}J8.2 Hz, Ar-H), 2.69-2.65(t, 2H, ^{3}J7.64 Hz, Ar-CH_2-), 1.66-1.64(quin, 2H, ^{3}J6.8 Hz, Ar-CH_2-$C\underline{H}_2$-), 1.34-1.22 (m, 10H, 5 × -CH_2-), 0.89-0.87 (t, 3H, ^{3}J7.04 Hz, 1 × -CH_3).

4-Cyanophenyl-4-[3-{4-(4-n-nonylbiphenyl-4-carbonyloxy)3-fluorobenzoyloxy} benzoyloxy]benzoate, (6.F.3)

Yield, 58%; m.p. 154°C; ν_{max}:2922, 2852, 2241, 1736, 1603, 1273, 1076 cm^{-1}; δ_H: 8.3-8.08 (m, 8H, Ar-H), 7.77-7.75 (d, 4H, ^{3}J8.8 Hz, Ar-H), 7.66-7.38 (m, 9H, Ar-H), 7.32-7.30 (d, 2H, ^{3}J8.08 Hz, Ar-H), 2.69-2.65(t, 2H, ^{3}J7.56 Hz, Ar-CH_2-), 1.66-1.64(quin, 2H, ^{3}J6.82 Hz, Ar-CH_2-$C\underline{H}_2$-), 1.34-1.22 (m, 12H, 6 × -CH_2-), 0.9-0.87 (t, 3H, ^{3}J6.72 Hz, 1 × -CH_3).

4-Cyanophenyl-4-[3-{4-(4-n-decylbiphenyl-4-carbonyloxy)3-fluorobenzoyloxy} benzoyloxy]benzoate, (6.F.4)

Yield, 57%; m.p. 158°C; ν_{max}:2922, 2852, 2241, 1738, 1603, 1273, 1076 cm^{-1}; δ_H: 8.3-8.08 (m, 8H, Ar-H), 7.77-7.75 (d, 4H, ^{3}J8.8 Hz, Ar-H), 7.66-7.38 (m, 9H, Ar-H), 7.32-7.30 (d, 2H, ^{3}J8.08 Hz, Ar-H), 2.69-2.65(t, 2H, ^{3}J7.64 Hz, Ar-CH_2-), 1.66-1.64(quin, 2H, ^{3}J6.82 Hz, Ar-CH_2-$C\underline{H}_2$-), 1.34-1.22 (m, 14H, 7 × -CH_2-), 0.9-0.87 (t, 3H, ^{3}J6.68 Hz, 1 × -CH_3).

4-Cyanophenyl-4-[3-{4-(4-n-undecylbiphenyl-4-carbonyloxy)3-fluorobenzoyloxy} benzoyloxy]benzoate, (6.F.5)

Yield, 59%; m.p. 158°C; ν_{max}:2924, 2855, 2241, 1736, 1603, 1273, 1076 cm^{-1}; δ_H: 8.3-8.08 (m, 8H, Ar-H), 7.77-7.75 (d, 4H, ^{3}J8.76 Hz, Ar-H), 7.66-7.38 (m, 9H, Ar-H), 7.32-7.30 (d,

2H, ^{3}J8.08 Hz, Ar-H), 2.69-2.65(t, 2H, ^{3}J7.56 Hz, Ar-CH_2-), 1.66-1.64(quin, 2H, ^{3}J6.8 Hz, Ar-CH_2-$C\underline{H}_2$-), 1.34-1.25 (m, 16H, 8 × -CH_2-), 0.9-0.87 (t, 3H, ^{3}J6.72 Hz, 1 × -CH_3).

4-Cyanophenyl-4-[3-{4-(4-n-dodecylbiphenyl-4-carbonyloxy)3-fluorobenzoyloxy} benzoyloxy]benzoate, (6.F.6)

Yield, 56%; m.p. 154.5°C; ν_{max}: 2924, 2852, 2241, 1736, 1603, 1273, 1074 cm^{-1}; δ_H: 8.3-8.08 (m, 8H, Ar-H), 7.77-7.75 (d, 4H, ^{3}J8.76 Hz, Ar-H), 7.66-7.38 (m, 9H, Ar-H), 7.32-7.30 (d, 2H, ^{3}J8.08 Hz, Ar-H), 2.69-2.65(t, 2H, ^{3}J7.84 Hz, Ar-CH_2-), 1.66-1.64(quin, 2H, ^{3}J6.72 Hz, Ar-CH_2-$C\underline{H}_2$-), 1.34-1.25 (m, 18H, 9 × -CH_2-), 0.9-0.87 (t, 3H, ^{3}J6.24 Hz, 1 × -CH_3).

4-Cyanophenyl-4-[3-{4-(4-n-tetradecylbiphenyl-4-carbonyloxy)3-fluorobenzoyloxy} benzoyloxy]benzoate, (6.F.7)

Yield, 59%; m.p. 153°C; ν_{max}:2920, 2851, 2243, 1736, 1605, 1273, 1074 cm^{-1}; δ_H: 8.3-8.08 (m, 8H, Ar-H), 7.77-7.75 (d, 4H, ^{3}J8.0 Hz, Ar-H), 7.66-7.38 (m, 9H, Ar-H), 7.32-7.30 (d, 2H, ^{3}J8.2 Hz, Ar-H), 2.69-2.65(t, 2H, ^{3}J7.76 Hz, Ar-CH_2-), 1.66-1.64(quin, 2H, ^{3}J6.7 Hz, Ar-CH_2-$C\underline{H}_2$-), 1.34-1.26 (m, 22H, 11 × -CH_2-), 0.9-0.86 (t, 3H, ^{3}J6.64 Hz, 1 × -CH_3).

4-Cyanophenyl-4-[3-{4-(4-n-hexadecylbiphenyl-4-carbonyloxy)3-fluorobenzoyloxy} benzoyloxy]benzoate, (6.F.8)

Yield, 61%; m.p. 148.5°C; ν_{max}: 2920, 2851, 2243, 1736, 1603, 1273, 1074 cm^{-1}; δ_H: 8.3-8.07 (m, 8H, Ar-H), 7.77-7.75 (d, 4H, ^{3}J8.16 Hz, Ar-H), 7.66-7.38 (m, 9H, Ar-H), 7.32-7.30 (d, 2H, ^{3}J8.16 Hz, Ar-H), 2.69-2.65(t, 2H, ^{3}J7.6 Hz, Ar-CH_2-), 1.66-1.64(quin, 2H, ^{3}J6.56 Hz, Ar-CH_2-$C\underline{H}_2$-), 1.34-1.26 (m, 26H, 13 × -CH_2-), 0.9-0.86 (t, 3H, ^{3}J6.64 Hz, 1 × -CH_3).

4-Cyanophenyl-4-[3-{4-(4-n-octadecylbiphenyl-4-carbonyloxy)3-fluorobenzoyloxy} benzoyloxy]benzoate, (6.F.9)

Yield, 60%; m.p. 149°C; ν_{max}:2920, 2851, 2243, 1736, 1605, 1273, 1074 cm^{-1}; δ_H: 8.3-8.08 (m, 8H, Ar-H), 7.77-7.75 (d, 4H, ^{3}J8.76 Hz, Ar-H), 7.66-7.38 (m, 9H, Ar-H), 7.32-7.30 (d, 2H, ^{3}J8.08 Hz, Ar-H), 2.69-2.65(t, 2H, ^{3}J7.6 Hz, Ar-CH_2-), 1.66-1.64(quin, 2H, ^{3}J6.52 Hz, Ar-CH_2-$C\underline{H}_2$-), 1.34-1.26 (m, 30H, 15 × -CH_2-), 0.89-0.86 (t, 3H, ^{3}J6.68 Hz, 1 × -CH_3).

Chapter-7

Synthesis and mesomorphic properties of

(i) **[R]-[+]-7-[4-(4-n-Tetradecyloxybenzoyloxy)3-fluorobenzoyloxy]2-naphthyl-2-[4-{4-(4-n-tetradecyloxybenzoyloxy)3-fluorobenzoyloxy} phenyloxy] propionate, (Compound 7.A.1)**

(ii) **[R]-[+]-7-[4-(E-4-n-Octadecyloxycinnamoyloxy)3-fluorobenzoyloxy] 2-naphthyl-2-[4-{4-(E-4-n-octadecyloxycinnamoyloxy)3-fluoro-benzoyloxy}phenyloxy]propionate, (Compound 7.B.1)**

(iii) **[R]-[+]-7-[4-(E-4-n-Alkoxy-α-methylcinnamoyloxy)3-fluoro-benzoyloxy]2-naphthyl-2-[4-{4-(E-4-n-alkoxy-α-methyl-cinnamoyloxy)3-fluorobenzoyloxy}phenyloxy]propionates, (Compounds 7.C.1 and 7.C.2)**

(iv) **[S]-[+]-4-[4-(1-Methylheptyloxy)benzoyloxy]phenyl-3-[4-(4-n-alkyl-biphenyl-4-carbonyloxy)benzoyloxy]benzoates, (Compounds 7.D.1 to 7.D.4)**

(v) **[S]-[+]-4-[4-(1-Methylheptyloxy)benzoyloxy]phenyl-3-[4-(4-n-dodecyloxybiphenyl-4-carbonyloxy)benzoyloxy]benzoate, (Compound 7.E.1)**

Chiral compounds exhibiting ferro- and / antiferro-electric phases.

Molecular chirality is an important factor in liquid crystals, which manifests in the form of helical ordering of the constituent molecules in the mesophase. The cholesteric phase [1] and the other blue phases (BP) [131,132] with helical structure and the discovery of ferro- and antiferro-electricity in chiral calamitic compounds stimulated the growth of the study of liquid crystals due to their potential practical applications. After a century of the discovery of the first liquid crystal, a new chiral phase namely the helical SmA^* phase (twist grain boundary smectic A phase) was discovered [9, 10]. Generally, compounds exhibiting the antiferroelectric smectic C^* (SmC^*_A) phase shows the sub phases such as the SmC^*_α and the ferrielectric (SmC^*_γ) phases. For a clear understanding of the correlation between the molecular structure and the appearance of these phases and phase sequences, a number of chiral rod-like compounds have been synthesized and investigated by several groups [133].

Until recently, it was thought to be a general rule that in order to produce chiral or polar structures in fluid phases it is necessary to incorporate chirality at the molecular level. In 1996, Niori *et al.* [20] reported a ferroelectric polar order in achiral banana-shaped molecules. Careful experiments on this mesophase by Link *et al.* [28] established that the phase is actually antiferroelectric with possible chiral and racemic structures. However, it has been possible to obtain a homogeneously chiral state by the addition of a chiral dopant to this phase [28]. In order to investigate the influence of a chiral group in banana-shaped molecules, Nakata *et al.* [90] studied the chiral analogues of achiral bent-core molecules. The ferroelectric phase obtained had a racemic ground state structure ($SmC_AP_F^*$) though the compound was composed of chiral molecules. This observation violates a rule that the handedness of chiral structure in fluid phases is determined by the molecular chirality. A brilliant approach by Walba *et al.* [54] was based on the knowledge that the ferroelectric structure requires an anticlinic interlayer correlation in bent-core molecules and he chose racemic (±) 2-octanol to satisfy this requirement (known to exhibit SmC_a structure in calamitics) and reported ferroelectric switching behaviour in banana liquid crystals.

Results and discussion

We have investigated a few bent-core compounds containing chiral moieties and the preliminary results obtained are reported here. The chiral group is present either within the rigid bent-core structure or is part of the aliphatic chain. The mesophases obtained were investigated by the classical techniques of polarizing microscopy, DSC, XRD and electro-optical investigations for switchable mesophases. These compounds exhibit blue phase, cholesteric, TGB_A, ferro-, antiferro- and ferri-electric phases.

The central cores used were 2,7-dihydroxynaphthalene and 3-hydroxybenzoic acid while the chiral materials used were [R]-[–]-octan-2-ol and [S]-[–]-ethyl lactate and were all commercial compounds. The synthesis of 3-fluoro-4-benzyloxybenzoic acid and 4-n-alkoxybenzoic acids are described in Chapter-**2**. E-4-n-Alkoxycinnamic acids and E-4-n-alkoxy-α-methylcinnamic acids were prepared as described in Chapter-**3**. 4-n-Alkylbiphenyl-4-carboxylic acids were prepared as described in Chapter-**5**. 4-n-Dodecyloxybiphenyl-4-carboxylic acid was prepared following a procedure described in the literature [134]. 3-Benzyloxybenzoic acid was prepared as described in Chapter-**6**. 7-Benzyoxy-2-hydroxynaphthalene, **7.1** was obtained by reacting 1:1 equivalents of 2,7-dihydroxynaphthalene and benzyl chloride in the presence of anhydrous potassium carbonate in butan-2-one. [R]-[+]-2-[4-(Benzyloxy)phenyloxy]propionic acid (**7.3**) was prepared by Mitsunobu reaction [135] of 4-benzyloxyphenol with [S]-[–]-ethyl lactate in the presence of triphenylphosphine and diethylazodicarboxylate followed by hydrolysis using aqueous alkali. Compound **7.3** was esterified with **7.1** in the presence of DCC, DMAP and dry CH_2Cl_2, the resultant material obtained was subjected to hydrogenolysis to yield bis-phenol **7.5**. This was further esterified using two equivalents of 3-fluoro-4-benzyloxybenzoic acid to yield dibenzyloxy ester **7.6** which was subjected to hydrogenolysis to obtain the bis-phenol **7.7**. Compounds **7.A.1**, **7.B.1**, **7.C.1** and **7.C.2** were obtained by esterifying the bis-phenol **7.7** with an appropriate acid as shown in scheme **7.1**.

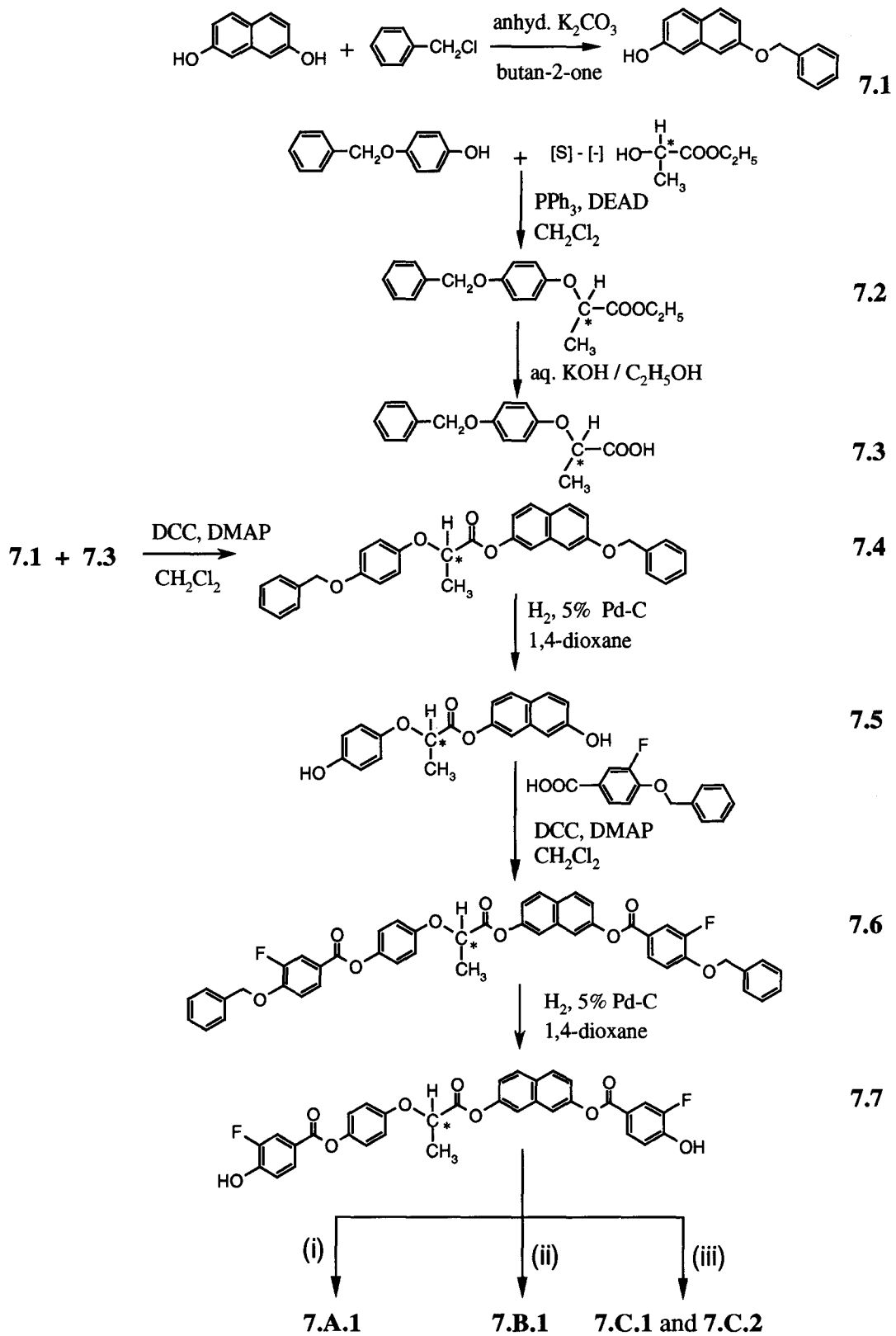

Reagents and conditions: (i) 4-n-tetradecyloxybenzoic acid, DCC, DMAP, dry CH_2Cl_2; (ii) E-4-n-octadecyloxycinnamic acid, DCC, DMAP, dry CH_2Cl_2 and (iii) E-4-n-tridecyloxy- or E-4-n-octadecyloxy-α-methylcinnamic acid, DCC, DMAP, dry CH_2Cl_2.

Scheme 7.1. Synthetic pathway used to obtain the unsymmetrical mesogens from 2,7-dihydroxynaphthalene.

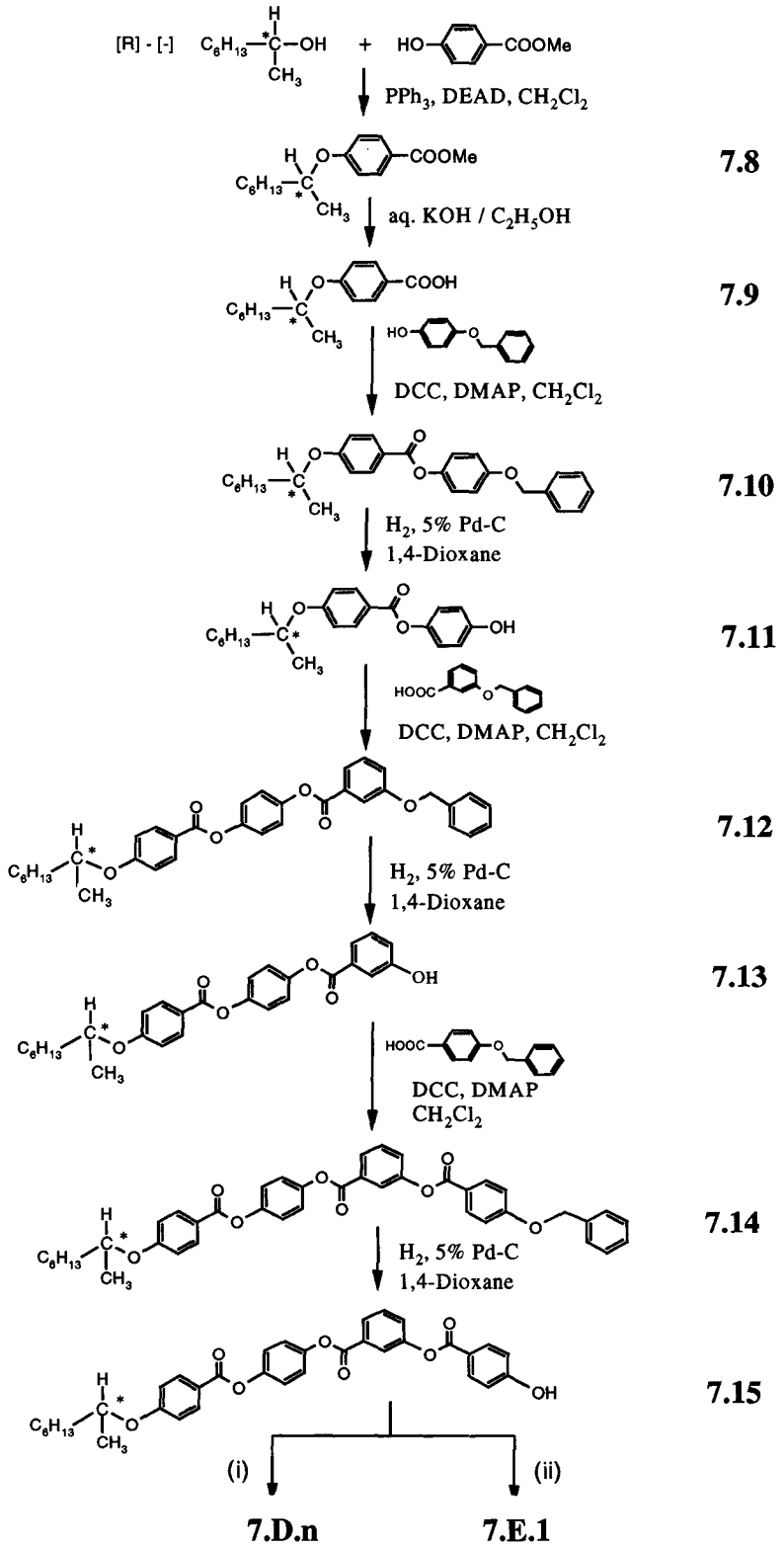

Reagents and conditions: (i) 4-n-alkylbiphenyl-4-carboxylic acids, DCC, DMAP, dry CH_2Cl_2 and (ii) 4-n-dodecyloxybiphenyl-4-carboxylic acid, DCC, DMAP, dry CH_2Cl_2.

Scheme 7.2. Synthetic pathway used to obtain the unsymmetrical mesogens from 3-hydroxybenzoic acid.

[S]-[+]-4-(1-methylheptyloxy)benzoic acid was prepared by etherification reaction of methyl-4-hydroxybenzoate with [R]-[–]-octan-2-ol as described above and the resultant compound obtained was hydrolyzed using aqueous alkali. The acid so obtained was esterified using 4-benzyloxyphenol and the benzyloxy ester obtained was subjected to hydrogenolysis. [S]-[–]-4-[4-(1-methylheptyloxy)benzoyloxy]phenyl-3-(4-hydroxybenzoyloxy)benzoate **7.15** was obtained by a subsequent DCC coupling and hydrogenolysis reactions as shown in scheme **7.2**. The required phenol **7.15** obtained was further esterified as shown (scheme **7.2**) using 4-n-alkylbiphenyl-4-carboxylic acids or 4-n-dodecyloxybiphenyl-4-carboxylic acid to obtain the target compounds (**7.D.1** - **7.D.4** and **7.E.1**).

The mesomorphic properties of compound 7.A.1:

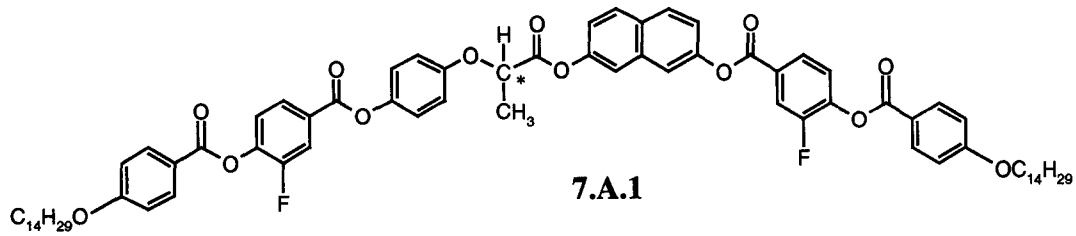

7.A.1

Cr 130.5 N^* 162.0[d] BP 163.2 I

37.0 *1.25*

d: enthalpy denoted is the sum of both I to BP and BP to N^* phase transitions.

On heating a thin film of the sample sandwiched between a glass slide and a cover slip and viewing under a polarizing microscope, cholesteric phase appears as oily streaks with a blue colour background as shown in figure **7.1**. On increasing or decreasing the temperature the background colour changes. However, on very slow cooling of the isotropic liquid, a texture with blue and yellow colours with a short temperature range (about 1^o) appears and has been characterized as a blue phase. The optical photomicrograph of this texture is shown in figure **7.2**. On cooling the blue phase, a polygonal planar texture appears which is typical of the cholesteric phase. The clearing enthalpy obtained is about 1.2 $kJmol^{-1}$ which is the sum of both the phase transitions (ie, I to BP and BP to N^*). On lowering the temperature further, below the melting point, crystallization takes place.

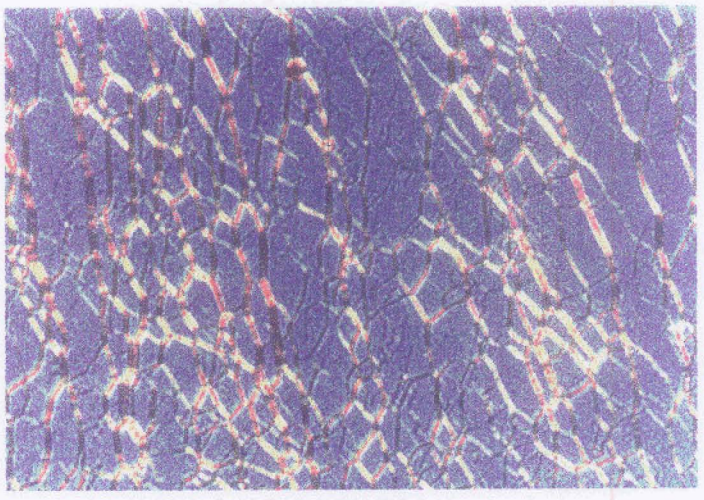

Fig. 7.1. Optical photomicrograph of the cholesteric phase of compound 7.A.1 at 152°C.

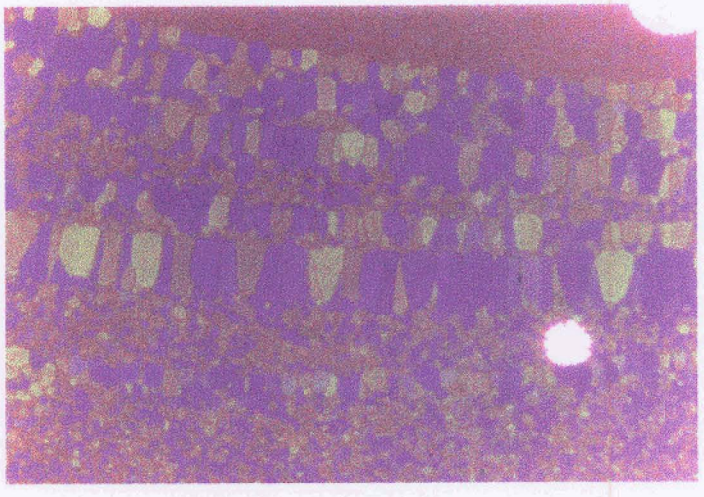

Fig. 7.2. Optical photomicrograph of the blue phase of compound 7.A.1 close to the isotropic phase.

The mesomorphic properties of compound 7.B.1:

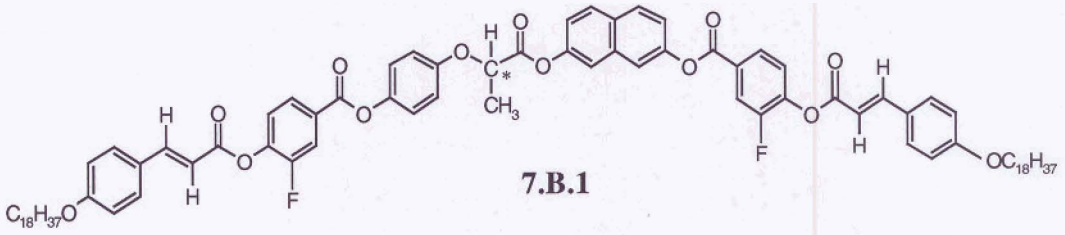

7.B.1

Cr 142.0 (SmA 134.0)[a] (TGB_A 135.0) N^* 176.0[d] BP 177.5 I

85.0 *1.04* *1.58*

a: transition enthalpy could not be determined as the sample crystallizes immediately.

d: enthalpy denoted is the sum of both I to BP and BP to N^* phase transitions.

As described for compound 7.A.1, compound 7.B.1 also shows the characteristic features of the cholesteric phase as .shown in figure 7.3. On slow cooling the isotropic liquid, a short range of blue phase (about 1.5°) appears and a typical texture of this phase is shown in figure 7.4. *On* cooling further below the cholesteric phase to a temperature of 134°C, the field of view becomes dark until the sample crystallizes. However, on heating the dark regions, a filamentary growth pattern as shown in figure 7 5 appears. These observations indicate that the lower temperature homeotropic texture is due to the SmA phase and the filamentary growth pattern is due to the twist grain boundary A (TGB_A) phase. The SmA phase obtained is highly metastable and invariably the TGB_A phase crystallizes directly.

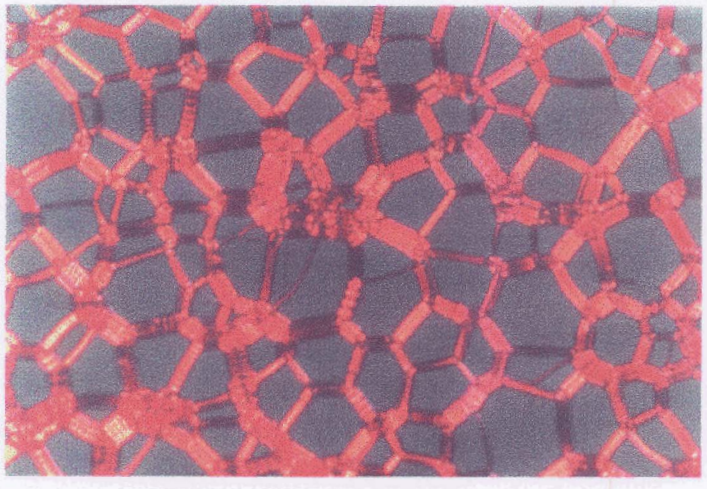

Fig. 7.3. Optical photomicrograph of the cholesteric phase of compound 7.B.1 at 155°C.

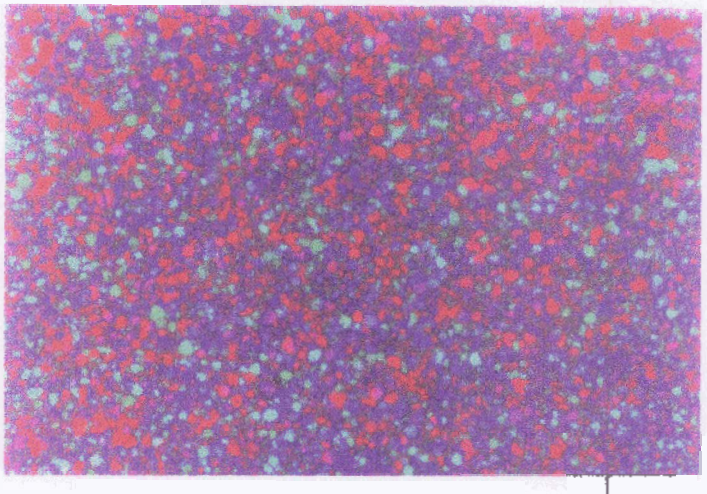

Fig. 7.4. Optical photomicrograph of the blue phase of compound 7.B.1 close to the isotropic phase.

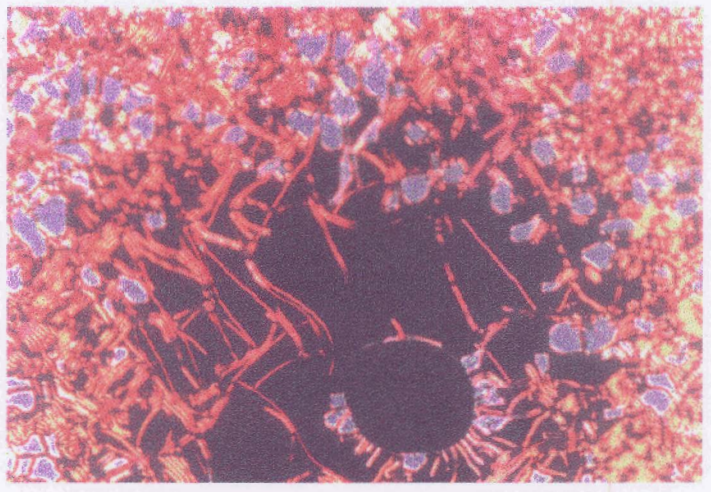

Fig. 7.5. Optical photomicrograph of compound 7.B.1 showing a filamentary texture of TGB_A phase originating from the homeotropic regions of the SmA phase.

The mesomorphic properties of compounds 7.C.1 and 7.C.2:

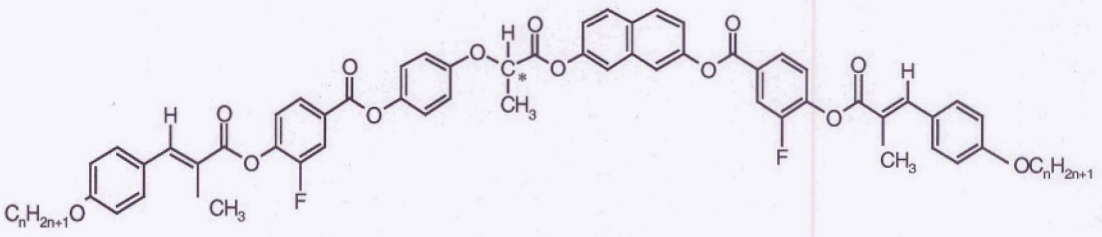

7.C.1	n=13,	Cr 123.5 N^* 147.5[d] BP 148.5 I	
		50.0	*0.95*
7.C.2	n=18,	Cr 127.0 (TGB_A 124.0) N^* 141.0[d] BP 142.0 I	
		63.1	*1.78*

d: enthalpy denoted is the sum of both I to BP and BP to N*phase transitions.

As described for compound 7.A.1, compound 7.C.1 also shows BP and N^* phases on lowering the temperature from the isotropic phase. On increasing the chain length, for example, n-octadecyloxy homologue (7.C.2) shows TGB_A phase in addition to N*and BP phases.

The mesomorphic properties of compounds of series 7.I:

The transition temperatures and the associated enthalpies for compounds 7.D.1 to 7.D.4 are shown in table 7.1. On slow cooling a thin film of the isotropic liquid of compound 7.D.1, both schlieren and planar textures typical of the cholesteric phase appear. On further cooling,

Table 7.1: Transition temperatures (°C) and enthalpies (kJmol^{-1}) for the compounds of series 7.I.

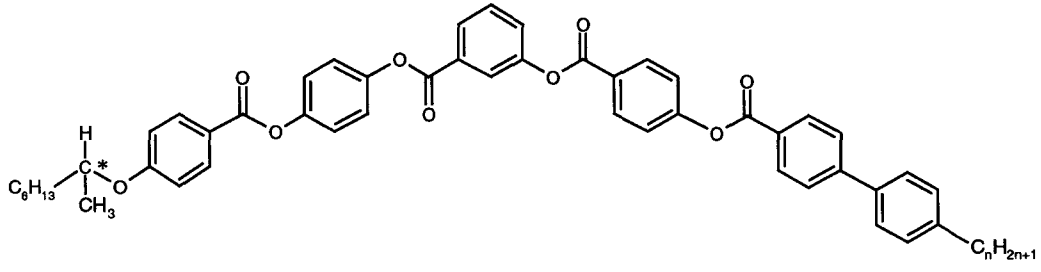

Compound	n	Cr		SmC*		SmA		TGB_A		N*		I
7.D.1	10	.	117.0	.	124.5[a]	.	125.0[a]	.	125.7	.	126.0	.
			22.3						*0.55*		*1.9*	
7.D.2	11	.	120.0	.	126.9	.	127.2[e]	.	127.9	-		.
			25.0				*0.92*		*2.3*			
7.D.3	12	.	122.5	.	127.9	.	128.3	.	128.6[f]	-		.
			26.2						*4.0*			
7.D.4	14	.	122.5	.	129.8	-		.	130.0[g]	-		.
			26.9						*4.4*			

a: enthalpy could not be determined.

e: enthalpy denoted is the sum of both SmC* to SmA and SmA to TGB_A phase transitions

f: enthalpy denoted is the sum of SmC* to SmA, SmA to TGB_A and TGB_A to isotropic phase transitions.

g: enthalpy denoted is the sum of both SmC* to TGB_A and TGB_A to isotropic phase transitions.

multiple domains begin to develop on the schlieren texture, which transform to a homeotropic texture as the temperature is lowered further. This homeotropic texture is characteristic of the SmA phase. When the SmA phase is cooled, a pseudohomeotropic texture is obtained for the SmC^* phase. On shearing the homeotropic regions of the SmC^* phase, a schlieren texture could be obtained. When the sample was heated from the homeotropically aligned SmA phase, straight filaments develop and finally coalesce to an undefined texture as shown in figure 7.5 for compound 7.B.1. It can be seen in table 7.1 that TGB_A and SmA phases appear simultaneously for a short temperature range (about 1°) on lowering the temperature. In a planar alignment of the sample, SmC^* phase exhibits a banded focal-conic texture and a cloudy like texture was obtained in a homeotropically aligned cell on cooling the SmA phase. The ferroelectric nature of the SmC^* phase was confirmed by electto-optical studies.

On increasing the chain length, compounds 7.D.2 and 7.D.3 were obtained in which N^* phase gets eliminated and only TGB_A, SmA and SmC^* phases were observed. The presence of TGB_A phase could be determined as it appears with the characteristic features under a polarizing microscope. A photomicrograph of the appearance of the TGB_A phase on cooling the isotropic liquid of compound 7.D.3 is shown in figure 7.6.

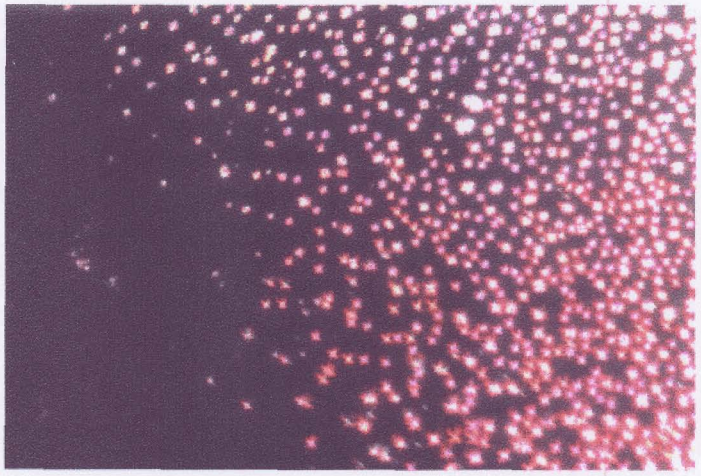

Fig. 7.6. Optical photomicrograph showing the appearance of TGB_A phase of compound 7.D.3 on cooling the isotropic liquid.

Compound 7D.4 shows only TGB_A and SmC^* phases. The first order layer spacing obtained in the SmC^* phase at 125°C is 46.3 Å. The calculated tilt angle is about 39°. A photomicrograph obtained at the transition from TGB_A to SmC^* phase is shown in figure 7.7.

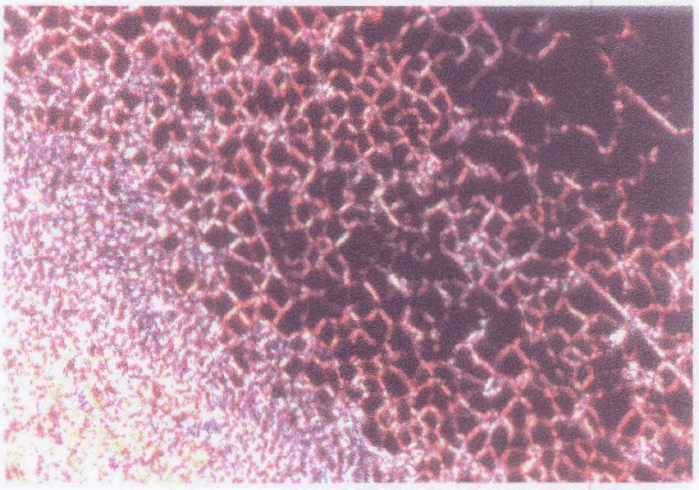

Fig. 7.7. Optical photomicrograph of compound 7.D.4 showing the transition from TGB_A phase to the SmC^* phase.

Electro-optical switching characteristics were carried out in the SmC^* phase as follows. Compound 7.D.4 was taken in a cell which was constructed for planar alignment and having a thickness of about 14 μm. By applying a triangular-wave electric field of about ± 85 V and at a frequency of 40 Hz, a single polarization current peak could be observed for each half period indicating the ferroelectric switching behaviour for the mesophase. The current was measured across 10 kΩ resistance. The calculated polarization value is about 23 nC cm^{-2} which is very small when compared with the polarization value observed for an achiral banana-shaped compound. The current response trace obtained in the SmC^* phase of compound 7.D.4 is shown in figure 7.8.

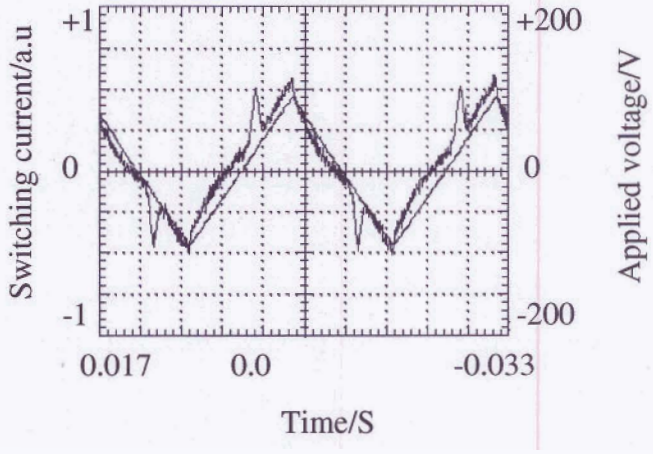

Fig. 7.8. Switching current response obtained by applying a triangular-wave voltage of about ± 85 V and at a frequency of 40Hz in the SmC phase of compound 7.D.4 at 124°C. Cell thickness, 14 μm; polarization value, $P_S \approx 23$ nC cm^{-2}.

The mesomorphic properties of compound 7.E.1:

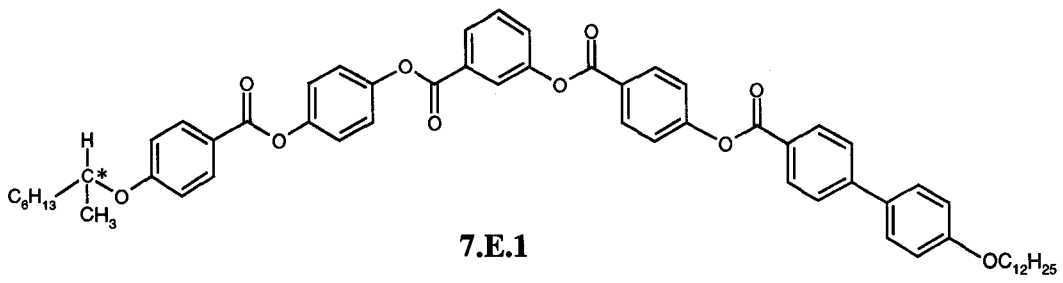

7.E.1

Cr		X_{AF}		SmC^*_γ		SmC^*		SmC^*_α		I
	28.6		*7.86*		*0.06*		-		*4.8*	

A preliminary investigation was carried out on the mesophases exhibited by compound **7.E.1** under a polarizing microscope. On cooling the isotropic liquid of a thin film of a sample sandwiched between a glass slide and a cover a slip, a schlieren texture was obtained which is characteristic of the SmC^*_α phase. On further cooling a pseudo homeotropic texture could be obtained. This texture was similar to the one observed for the SmC^* phase of compound **7.D.4**. On decreasing the temperature further to 140°C, a weak birefringent plate-like texture was obtained. The characteristic feature of this phase is that the texture is dynamic even at a constant temperature. This type of texture has been observed for SmC^*_γ phase and hence the mesophase of this compound has been identified as ferrielectric. On further decreasing the temperature to 118°C, a drastic change in the texture could be observed. The textural features observed appears to be different from the mesophases known so far. Hence, the mesophase has been designated as X_{AF} (unidentified antiferroelectric mesophase) due to the antiferroelectric switching behaviour it exhibits. The optical photomicrograph obtained in this mesophase is shown in figure **7.9**.

In order to establish the identity of the mesophases, the sample was examined in different cells coated for homogeneous and homeotropic alignments. When the sample was cooled in a homogeneously aligned cell, a focal-conic texture was obtained for the SmC^*_α phase. On further cooling, sharp lines appeared parallel to the focal-conics (banded focal-conic texture). This feature is characteristic of SmC^* phase with a short pitch value. The optical photomicrograph obtained in the SmC^* phase is shown in figure **7.10**. On cooling the isotropic liquid of the same compound in a homeotropically aligned cell, below the SmC^* phase, a weak birefringent plate-like texture was obtained which showed strong fluctuations in intensity indicating a SmC^*_γ phase and the same is shown in figure **7.11**.

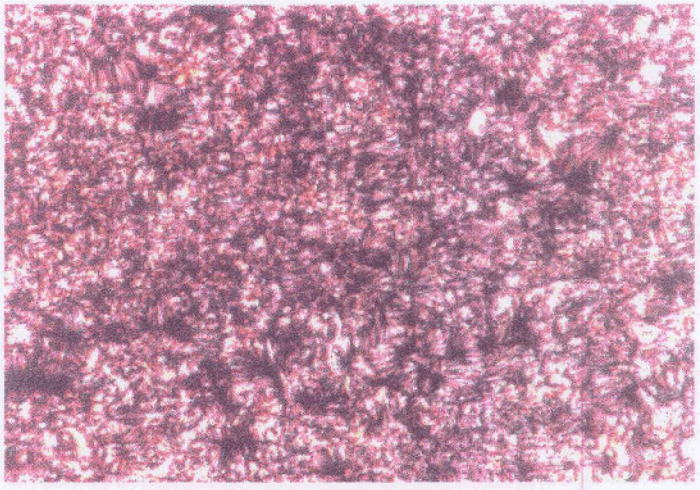

Fig. 7.9. Optical photomicrograph obtained in the X_{AF} phase of compound 7.E.1 at 116°C.

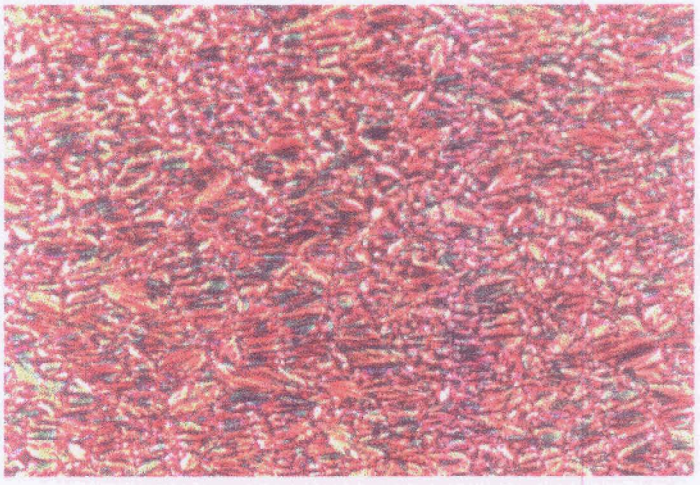

Fig. 7.10. Optical photomicrograph obtained in the SmC^* phase of compound 7.E.1 at 144°C.

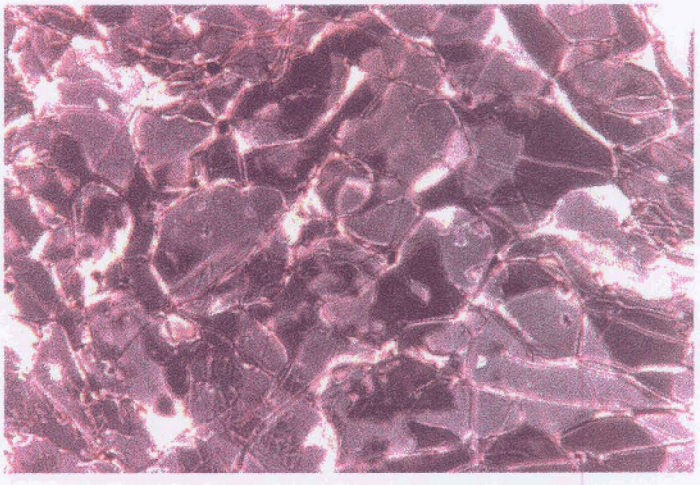

Fig. 7.11. Optical photomicrograph obtained in the SmC^*_γ phase of compound 7.E.1 at 125°C.

The phase sequence in this compound was further confirmed by XRD and electro-optical studies. Compound **7.E.1** showed the following XRD pattern. In the small angle region, the first order reflection was obtained with d=45.6 Å in the SmC^* phase (at 144°C). The calculated tilt angle was about 39°. On lowering the temperature to 130°C, the first order layer spacing was obtained with d=46.2 Å in the SmC^*_γ phase. On further decreasing the temperature, an X_{AF} phase was obtained which shows the following XRD pattern. In the small angle region, three sharp reflections were obtained at d_1=44.5 Å,d_2=30.2 Å and d_3=22.3 Å. The first and third reflections obtained indicate the lamellar periodicity and the second reflection indicates that the phase must have a two-dimensional ordering of the molecules. In all the three phases (SmC^*, SmC^*_γ and X_{AF}), a wide-angle diffuse peak at about 4.6 Å was obtained indicating the fluidity of the alkyl chains.

Finally, electro-optical studies were carried out in SmC^*, SmC^*_γ and X_{AF} phases in order to prove the characteristic features of ferro-, ferri- and antiferro-electric properties. Compound **7.E.1** was taken in a cell which was constructed for planar alignment having a thickness of about 8.9 *μm*. The sample was cooled under a triangular-wave electric field of about ±195 V and a frequency of 300 Hz. A single polarization current peak could be observed in the SmC^* phase as expected. The calculated P_S value was about 12 nC cm^{-2}. A current-time response trace obtained is shown in figure **7.12.** On lowering the temperature further under the same conditions, the P_S value increased marginally in the SmC^*_γ phase and was about 20 nC cm^{-2}. On lowering the temperature further into the columnar X_{AF} phase, the polarization value increased drastically and was about 230 nC cm^{-2}.

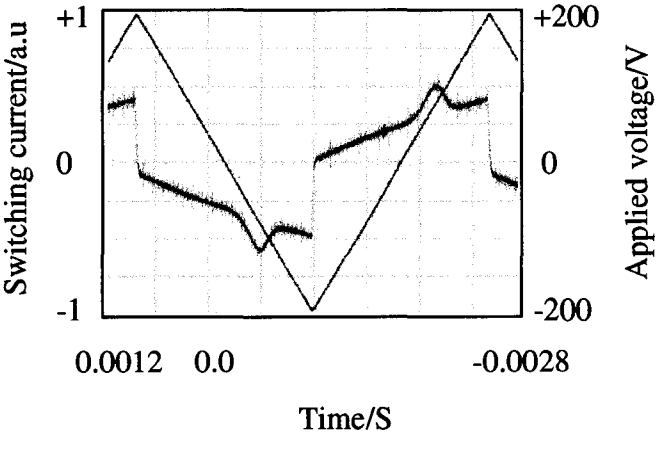

Fig. 7.12. Switching current response obtained by applying a triangular-wave voltage of about ± 195 V and at a frequency of 300Hz in the SmC^* phase of compound 7.E.1 at 143°C. Cell thickness, 8.9 *μm*; polarization value, $P_S \approx 12$ nC cm^{-2}.

The observation of two polarization current peaks as shown in figure **7.13** confirms the antiferroelectric ground state structure of the lowest temperature columnar phase. The current was measured across 1 kΩ resistance. Further experiments are necessary to unambiguously arrive at the structure of this interesting phase.

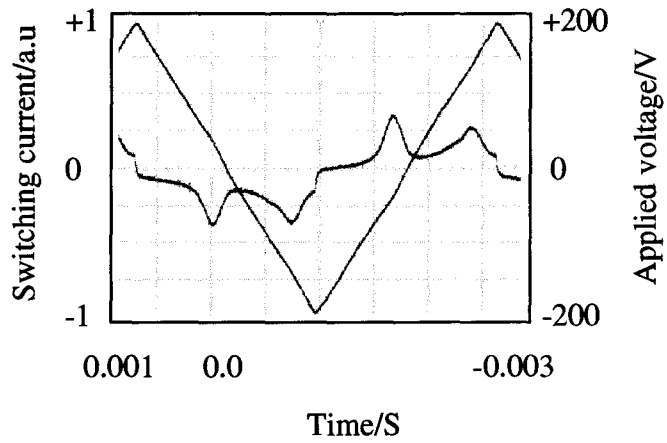

Fig. 7.13. Switching current response obtained by applying a triangular-wave voltage of about ± 195 V and at a frequency of 300Hz in the X_{AF} phase of compound 7.E.1 at 115°C. Cell thickness, 8.9 *μm*; polarization value, $P_S \approx 230$ nC cm^{-2}.

Experimental

7-Benzyloxy-2-hydroxynaphthalene, (7.1)

To a mixture of 2,7-dihydroxynaphthalene (5g, 31.25 mmol), benzyl chloride(4.0g, 31.62 mmol) and butan-2-one (100 ml) anhydrous potassium carbonate(13.0g, 93.75mmol)was added slowly with stirring under anhydrous conditions. The reaction mixture was refluxed for about 25 hours with stirring using a magnetic stirrer. Excess butan-2-one was distilled off and the reaction mixture was poured into ice-cold water and hydrochloric acid and extracted with ether (3 × 50 ml). The combined organic solution was thoroughly washed with water and dried over anhydrous sodium sulphate. The crude compound obtained after the removal of solvent was passed through a column of silica gel using 2% acetone in chloroform as eluent and the product isolated was crystallized from toluene. Yield, 4.2g(54%); m.p. 151-152°C. ν_{max}:3200, 2924, 2855, 1628, 1608 cm^{-1}; δ_H: 8.72(s, 1H, Ar-OH, exchangeable with D_2O), 7.84-7.80(m, 2H, Ar-H), 7.67.65 (d, ^{3}J7.4 Hz, 2H, Ar-H), 7.56-7.45(m, 3H, Ar-H), 7.34-7.33 (d, ^{4}J2.4 Hz, 1H, Ar-H), 7.26-7.25 (d, ^{4}J2.32 Hz, 1H, Ar-H), 7.16-7.10 (m, 2H, Ar-H), 5.33 (s, 2H, $ArCH_2O$-).

[R]-[+]-Ethyl-2-[4-(benzyloxy)phenyloxy]propionate, (7.2)

This was prepared using a procedure described by Mitsunobu *et al.* [135]. A solution of 4-benzyloxyphenol(10g, 50 mmol), [S]-[-]-ethyl lactate(7.0g, 60 mmol), triphenylphosphine (TPP) (14.2g, 55 mmol)and dry dichloromethane (100 ml)was cooled in ice and a solution of diethylazodicarboxylate (DEAD) (9.6 g, 55 mmol)in CH_2Cl_2(10 ml) was added dropwise over a period of about 1 hour with stirring. Then the stirring was continued for 10 hours at room temperature. Then, dichloromethane (50 ml) was distilled off, and the reaction mixture cooled in an ice-bath, the solid separated was filtered off and washed with petroleum-ether (b.p. 60-80°C). The residue obtained after the removal of solvent from the combined filtrate was chromatographed using a mixture of chloroform and petroleum-ether (b.p. 60-80°C) as eluent. The product thus obtained was crystallized from a mixture of ethanol and water. Yield, 10.5 g (70%); m.p. 50-51°C; $[\alpha]_D^{25}$ = +25.4°; ν_{max}: 2924, 2855, 1742, 1618, 1456, 1209, 1132 cm^{-1}.

[R]-[+]-2-[4-(Benzyloxy)phenyloxy]propionic acid, (7.3)

Ethyl-2-[4-(benzyloxy)phenyloxy]propionate(10g) and alcoholic 10% potassium hydroxide solution was refluxed for about 5 hours. Excess ethanol was distilled off and the reaction mixture was poured into a mixture of ice-cold water and hydrochloric acid. The precipitated

solid was separated by filtration and washed with water several times until it was free from acid and dried. This compound was crystallized from a mixture of toluene and petroleum ether. Yield, 7.5g (83%); m.p. 96-97°C; $[\alpha]_D^{25}$ = +10.6°; ν_{max}: 3684, 3009, 2855, 1720, 1676, 1601, 1456, 1130 cm^{-1}; δ_H: 7.43-7.30(m, 5H, Ar-H), 6.92-6.84 (m, 4H, Ar-H), 5.02(s, 2H, Ar-CH_2O-), 4.73-4.68(q, ^{3}J6.8 Hz, 1H, Ar-O-C<u>H</u>(CH_3)-), 1.65-1.63(d, ^{3}J6.8 Hz, 3H, Ar-O-CH(C<u>H</u>$_3$)-).

[R]-[+]-7-(Benzyloxy)-2-naphthyl-2-[4-(benzyloxy)phenyloxy]propionate, (7.4)

Compound **7.1** (4g, 16 mmol) and compound **7.3** (4.35g, 16 mmol) were dissolved in dry dichloromethane (75ml). After the addition of N, N^1 - dicyclohexylcarbodiimide (DCC), (4g, 18.5 mmol) and a catalytic amount of 4-(N, N-dimethylamino)pyridine (DMAP), the mixture was stirred at room temperature for about 12 hours. The dicyclohexylurea which precipitated was filtered off and the filtrate diluted with chloroform. This solution was washed with 2% aqueous acetic acid solution (3 ×100 ml) and 5% ice-cold sodium hydroxide solution (3 × 100 ml) and finally washed with water and dried over anhydrous sodium sulphate. The crude residue obtained after removal of solvent was chromatographed on silica gel using chloroform as an eluent. Removal of solvent from the eluate afforded a white material which was crystallized from a mixture of chloroform and alcohol. Yield, 5.7g (71%); m.p. 83-85°C; $[\alpha]_D^{25}$ = +55.5°; ν_{max}: 2922, 2854, 1767, 1630, 1605, 1456, 1244 cm^{-1}; δ_H: 7.76-6.68(m, 20H, Ar-H), 5.16(s, 2H, Ar-CH_2O-), 5.04(s, 2H, Ar-CH_2O-), 4.98-4.88(q, ^{3}J6.8 Hz, 1H, Ar-O-C<u>H</u>(CH_3)-), 1.81-1.80(d, ^{3}J6.8 Hz, 3H, Ar-O-CH(C<u>H</u>$_3$)-).

[R]-[+]-7-Hydroxy-2-naphthyl-2-(4-hydroxyphenyloxy)propionate, (7.5)

Compound **7.4** (5.0g) was dissolved in 1,4-dioxane (50ml) and 5% Pd-C catalyst (1.0g) was added to it. The mixture was stirred at 50°C in an atmosphere of hydrogen till the required quantity of hydrogen was absorbed. The mixture was filtered hot and the solvent removed under reduced pressure. The residue was chromatographed on silica gel and eluted with a mixture of 5% acetone in chloroform. Removal of solvent from the eluate gave the required product as a gummy material, which was directly used for further reaction. Yield, 2.8g (89%); $[\alpha]_D^{25}$ = +27.2°; ν_{max}: 3450, 3296, 2924, 2854, 1732, 1715, 1620, 1601, 1456, 1250 cm^{-1}; δ_H: 8.78(s, 1H, Ar-OH, exchangeable with D_2O), 8.06(s, 1H, Ar-OH, exchangeable with D_2O), 7.97-7.92(m, 2H, Ar-H), 7.43-7.29(d, 1H, ^{4}J2.16 Hz, Ar-H), 7.39-6.82(m, 7H, Ar-H), 5.08-5.03(q, ^{3}J6.76 Hz, 1H, Ar-O-C<u>H</u>(CH_3)-), 1.86-1.84(d, ^{3}J6.76 Hz, 3H, Ar-O-CH(C<u>H</u>$_3$)-).

[R]-[+]-7-(3-Fluoro-4-benzyloxybenzoyloxy)-2-naphthyl-2-[4-(3-fluoro-4-benzyl-oxybenzoyloxy)phenyloxy]propionate, (7.6)

This was synthesized following a procedure described for the preparation of compound **7.4** using [R]-[+]-7-Hydroxy-2-naphthyl-2-(4-hydroxyphenyloxy)propionate and 3-fluoro-4-benzyloxybenzoic acid. Yield, 68%; m.p. 185-186°C; $[\alpha]_D^{25}$ = + 41.2°; ν_{max}: 2924, 2854, 1776, 1730, 1716, 1616, 1458, 1298 cm^{-1}; δ_H: 7.99-6.77(m, 26H, Ar-H), 5.26(s, 2H, Ar-CH_2O-), 5.24(s, 2H, Ar-CH_2O-), 5.05-4.96(q, ^{3}J6.72 Hz, 1H, Ar-O-C<u>H</u>(CH_3)-), 1.86-1.84(d, ^{3}J6.72 Hz, 3H, Ar-O-CH(C<u>H</u>$_3$).

[R]-[+]-7-(3-Fluoro-4-hydroxybenzoyloxy)-2-naphthyl-2-[4-(3-fluoro-4-hydroxy-benzoyloxy)phenyloxy]propionate, (7.7)

This was prepared following a procedure similar to that described for compound **7.5.** Yield, 85%; m.p. 156-158 °C; $[\alpha]_D^{25}$ = + 34.3°; ν_{max}: 3329(br), 2924, 2854, 1772, 1757, 1732, 1616, 1446, 1284 cm^{-1}; δ_H: 9.9(s, 1H, Ar-OH, exchangeable with D_2O), 8.19-7.95(m, 7H, Ar-H), 7.81-7.80(d, 1H, ^{4}J2.16 Hz, Ar-H), 7.61-7.58(d, 1H, ^{3}J8.88 Hz, ^{4}J2.32 Hz, Ar-H), 7.46-7.27(m, 7H, Ar-H), 5.44-5.39(q, ^{3}J6.76 Hz, 1H, Ar-O-C<u>H</u>(CH_3)-), 1.97-1.95(d, ^{3}J6.76 Hz, 3H, Ar-O-CH(C<u>H</u>$_3$).

[S]-[+]-Methyl-4-(1-methylheptyloxy)benzoate, (7.8)

This was synthesized following a procedure described for the preparation of compound **7.2** using [R]-[-]-2-octanol and methyl-4-hydroxybenzoate.

Yield, 78%; $[\alpha]_D^{25}$ = + 7.0°; ν_{max}: 2932, 2858, 1720, 1605, 1435, 1253, 1168 cm^{-1}.

[S]-[+]-4-(1-methylheptyloxy)benzoic acid, (7.9)

This was prepared following a procedure similar to that described for the preparation of compound **7.3.** Yield, 88%; m.p. 64-65°C; $[\alpha]_D^{25}$ = +17.4°; ν_{max}: 3423, 2932, 2856, 1688, 1605, 1425, 1254, 1172 cm^{-1}; δ_H: 8.95(s, 1H, Ar-COO<u>H</u>, exchangeable with D_2O), 8.13-8.09(d, 2H, ^{3}J8.88 Hz, Ar-H), 7.12-7.08(d, 2H, ^{3}J8.88 Hz, Ar-H), 4.74-4.68(m, 1H, Ar-O-C<u>H</u>(CH_3)-), 1.5-1.4(m, 13H, 5 × -CH_2- ,1 × -CH_3), 1.02-0.98(t, 3H, ^{3}J6.76 Hz, 1 × -CH_3). Elemental analysis: C_{15} H_{22} O_3 requires, C, 71.97; H, 8.86%; found, C, 71.79; H, 8.7%.

[S]-[+]-4-(Benzyloxy)phenyl-4-(1-methylheptyloxy)benzoate, (7.10)

This was synthesized following a procedure described for the preparation of compound **7.4** using [S]-[+]-4-(1-methylheptyloxy)benzoic acid and 4-benzyloxyphenol. Yield, 72%; m.p.

60-61°C; $[\alpha]_D^{25}$ = +11.2°; ν_{max}: 2924, 2854, 1730, 1605, 1454, 1252 cm^{-1}; δ_H: 8.13-8.10(d, 2H, ^{3}J8.9 Hz, Ar-H), 7.45-7.32(m, 5H, Ar-H), 7.12-7.09(d, 2H, ^{3}J9.04 Hz, Ar-H), 7.02-6.99(d, 2H, ^{3}J9.04 Hz, Ar-H), 6.95-6.93(d, 2H, ^{3}J8.9 Hz, Ar-H), 5.07(s, 2H, Ar-CH_2O-), 4.5-4.45(m, 1H, Ar-O-C<u>H</u>(CH_3)-), 1.37-1.29(m, 13H, 5 × -CH_2- ,1 × -CH_3), 0.9-0.87(t, 3H, ^{3}J6.68 Hz, 1 × -CH_3). Elemental analysis: C_{28} H_{32} O_4 requires, C, 77.75; H, 7.46%; found, C, 78.19; H, 7.55%.

[S]-[+]-4-Hydroxyphenyl-4-(1-methylheptyloxy)benzoate, (7.11)

This was prepared following a procedure is similar to that described for the preparation of compound **7.5.** Yield, 87%; m.p. 103-104°C; $[\alpha]_D^{25}$ = +13.3°; ν_{max}: 3447, 2924, 2854, 1705, 1605, 1456, 1259 cm^{-1}; δ_H: 8.56(s, 1H, Ar-OH, exchangeable with D_2O), 8.23-8.21(d, 2H, ^{3}J8.76 Hz, Ar-H), 7.42-7.19(m, 4H, Ar-H), 7.04-7.0(d, 2H, ^{3}J8.8 Hz, Ar-H), 4.8-4.45(m, 1H, Ar-O-C<u>H</u>(CH_3)-), 1.5-1.4(m, 13H, 5 × -CH_2- ,1 × -CH_3), 1.03-0.99(t, 3H, ^{3}J6.56 Hz, 1 × -CH_3). Elemental analysis: C_{21} H_{26} O_4 requires, C, 73.66; H, 7.65%; found, C, 73.95; H, 7.89%.

[S]-[+]-4-[4-(1-Methylheptyloxy)benzoyloxy]phenyl-3-(benzyloxy)benzoate,(7.12)

This was synthesized following a procedure described for the preparation of compound **7.4.** Yield, 72%; m.p. 99-100°C; $[\alpha]_D^{25}$ = + 16.1°; ν_{max}: 2924, 2854, 1732, 1605, 1458,1261 cm^{-1}; δ_H: 8.16-8.13(d, 2H, ^{3}J8.9 Hz, Ar-H), 7.84-7.80(m, 2H, Ar-H), 7.48-7.33(m, 6H, Ar-H), 7.27-7.25(m, 5H, Ar-H), 6.98-6.95(d, 2H, ^{3}J8.9 Hz, Ar-H), 5.15(s, 2H, Ar-CH_2O), 4.5-4.45(m, 1H, Ar-O-C<u>H</u>(CH_3)-), 1.82-1.3(m, 13H, 5×-CH_2-, 1 × -CH_3), 0.9-0.87(t, 3H, ^{3}J6.68 Hz, 1 × -CH_3). Elemental analysis: C_{35} H_{36} O_6 requires, C, 76.06; H, 6.57%; found, C, 75.6; H, 6.53%.

[S]-[+]-4-[4-(1-Methylheptyloxy)benzoyloxy]phenyl-3-hydroxybenzoate, (7.13)

This was prepared following a procedure similar to that described for the preparation of compound **7.5.** Yield, 85%; m.p. 108-109°C; $[\alpha]_D^{25}$ = + 8.2°; ν_{max}:3445, 2924, 2854, 1730, 1715, 1709, 1605, 1456, 1292 cm^{-1}; δ_H: 8.99(s, 1H, Ar-OH, exchangeable with D_2O), 8.28-8.25(d, 2H, ^{3}J8.6 Hz, Ar-H), 7.83-7.78(m, 2H, Ar-H), 7.59-7.51(m, 5H, Ar-H), 7.34-7.32(d, 1H, ^{3}J8.0 Hz, Ar-H), 7.25-7.23(d, 2H, ^{3}J8.6 Hz, Ar-H), 4.8-4.77(m, 1H, Ar-O-C<u>H</u>(CH_3)-), 1.56-1.44(m, 13H, 5 × -CH_2- ,1 × -CH_3), 1.01-0.98(t, 3H, ^{3}J6.92 Hz, 1 × -CH_3). Elemental analysis: C_{28} H_{30} O_6 requires, C, 72.71; H, 6.54%; found, C, 73.05; H, 6.69%.

[S]-[+]-4-[4-(1-Methylheptyloxy)benzoyloxy]phenyl-3-(4-benzyloxybenzoyloxy) benzoate, (7.14)

This was synthesized following a procedure described for the preparation of compound **7.4.** Yield, 70%; m.p. 125-126°C; $[\alpha]_D^{25}$ = +13.9°; ν_{max}: 2924, 2854, 1730, 1607, 1458,1261cm^{-1}; δ_H: 8.19-8.04(d, 5H, Ar-H), 7.6-7.56(t, 1H, ^{3}J7.96 Hz, Ar-H), 7.51-7.26(m, 10H, Ar-H), 7.09-7.07(d, 2H, ^{3}J8.8 Hz, Ar-H), 6.96-6.94(d, 2H, ^{3}J8.8 Hz, Ar-H), 5.17(s, 2H, Ar-CH_2O-), 4.51-4.46(m, 1H, Ar-O-C<u>H</u>(CH_3)-), 1.94-1.3(m, 13H, 5 × -CH_2- ,1 × -CH_3), 0.9-0.87(t, 3H, ^{3}J6.52 Hz, 1 × -CH_3). Elemental analysis: C_{42} H_{40} O_8 requires, C, 74.98; H, 5.99%; found, C, 74.98; H, 6.19%.

[S]-[+]-4-[4-(1-Methylheptyloxy)benzoyloxy]phenyl-3-(4-hydroxybenzoyloxy)benzoate, (7.15)

This was synthesized following a procedure similar to that described for the preparation of compound **7.5.** Yield, 87%; m.p. 163-164°C; $[\alpha]_D^{25}$ = + 5.1°; ν_{max}: 3385, 2930, 2854, 1734, 1709, 1701, 1605, 1458, 1290 cm^{-1}; δ_H: 9.57(s, 1H, Ar-OH, exchangeable with D_2O), 8.27-8.20(d, 6H, Ar-H), 7.87-7.78(m, 2H, Ar-H), 7.58-7.50(m, 4H, Ar-H), 7.25-7.23(d, 2H, ^{3}J8.8 Hz, Ar-H), 7.18-7.15(d, 2H, ^{3}J8.68 Hz, Ar-H), 4.81-4.77(m, 1H, Ar-O-C<u>H</u>(CH_3)-), 1.91-1.44(m, 13H, 5 × -CH_2- ,1 × -CH_3), 1.01-0.98(t, 3H, ^{3}J6.96 Hz, 1 × -CH_3). Elemental analysis: C_{35} H_{34} O_8 requires, C, 72.15; H, 5.88%; found, C, 72.28; H, 5.98%.

[R]-[+]-7-[4-(4-n-Tetradecyloxybenzoyloxy)3-fluorobenzoyloxy]-2-naphthyl-2-[4-{4-(4-n-tetradecyloxybenzoyloxy)3-fluorobenzoyloxy}phenyloxy]propionate, (7.A.1)

This was synthesized following a procedure described for the preparation of compound **7.4.** Yield, 65%; m.p. 130.5°C; $[\alpha]_D^{25}$ = + 32.2°; ν_{max}: 2924, 2854, 1750, 1740, 1608, 1510, 1256, 1169 cm^{-1}; δ_H: 8.15-8.0(m, 8H, Ar-H), 7.91-7.86(t, 2H, ^{3}J9.56 Hz, Ar-H), 7.666-7.661(d, 1H, ^{4}J2.04 Hz, Ar-H), 7.48-7.32(m, 4H, Ar-H), 7.19-7.16(m, 3H, Ar-H), 7.07-7.05(d, 2H, ^{3}J9.04 Hz, Ar-H), 6.98-6.96(d, 4H, ^{3}J8.84 Hz, Ar-H), 5.04-5.0(q, ^{3}J6.70 Hz, 1H, Ar-O-C<u>H</u>(CH_3)-), 4.05-4.02(t, 4H, ^{3}J5.52 Hz, 2 × Ar-OCH_2-), 1.99-1.77(m, 7H, 1 × Ar-O-CH(C<u>H</u>$_3$), 2 × Ar-OCH_2-C<u>H</u>$_2$-), 1.49-1.25(m, 44H, 22 × -CH_2-), 0.88-0.86(t, 6H, ^{3}J6.52 Hz, 2 × -CH_3).

[R]-[+]-7-[4-(E-4-n-Octadecyloxycinnamoyloxy)3-fluorobenzoyloxy]-2-naphthyl-2-[4-{4-(E-4-n-octadecyloxycinnamoyloxy)3-fluorobenzoyloxy}phenyloxy]propionate, (7.B.1)

Yield, 69%; m.p. 142°C; $[\alpha]_D^{25}$ = + 24.4°; ν_{max}: 2920, 2851, 1759, 1738, 1637, 1604, 1510, 1254, 1176 cm^{-1}; δ_H: 8.09-8.01(m, 4H, Ar-H), 7.92-7.87(m, 4H, Ar-H), 7.674-7.673(d, 1H,

^{4}J1.96 Hz, Ar-H), 7.67-7.5(m, 5H, Ar-H), 7.42-7.34(m, 3H, Ar-H), 7.20-7.18(m, 3H, Ar-H), 7.09-7.06(d, 2H, ^{3}J8.88 Hz, Ar-H), 6.94-6.92(d, 4H, ^{3}J8.44 Hz, Ar-H), 6.53-6.49(d, 2H, ^{3}J15.88 Hz, Ar-H), 5.07-5.02(q, ^{3}J6.76 Hz, 1H, Ar-O-C<u>H</u>(CH_3)-), 4.02-3.99(t, 4H, ^{3}J6.36 Hz, 2 × Ar-OCH_2-), 1.87-1.77(m, 7H, 1 × Ar-O-CH(C<u>H</u>$_3$), 2 × Ar-OCH_2-C<u>H</u>$_2$-), 1.46-1.11(m, 60H, 30 × -CH_2-), 0.89-0.86(t, 6H, ^{3}J6.4 Hz, 2 × -CH_3).

[R]-[+]-7-[4-(E-4-n-Tridecyloxy-α-methylcinnamoyloxy)3-fluorobenzoyloxy]-2-naphthyl-2-[4-{4-(E-4-n-tridecyloxy-α-methylcinnamoyloxy)3-fluorobenzoyloxy} phenyloxy]propionate, (7.C.1)

Yield, 75%; m.p. 123.5°C; $[\alpha]_D^{25}$ = + 16.1°; ν_{max}: 2922, 2852, 1759, 1734, 1635, 1605, 1508, 1248, 1176 cm^{-1}; δ_H: 8.1-8.01(m, 4H, Ar-H), 7.93-7.88(m, 4H, Ar-H), 7.675-7.670(d, 1H, ^{4}J2.04 Hz, Ar-H), 7.50-7.34(m, 8H, Ar-H), 7.2-7.18(m, 3H, Ar-H), 7.09-7.06(d, 2H, ^{3}J8.96 Hz, Ar-H), 6.96-6.94(d, 4H, ^{3}J7.72 Hz, Ar-H), 5.07-5.02(q, ^{3}J6.6 Hz, 1H, Ar-O-C<u>H</u>(CH_3)-), 4.02-3.99(t, 4H, ^{3}J6.44 Hz, 2 × Ar-OCH_2-), 2.285-2.282(d, 6H, ^{4}J1.16 Hz, 2 × -CH=C(C<u>H</u>$_3$)COO-), 1.89-1.77(m, 7H, 1 × Ar-O-CH(C<u>H</u>$_3$), 2 × Ar-OCH_2-C<u>H</u>$_2$-), 1.47-1.26(m, 40H, 20 × -CH_2-), 0.89-0.87(t, 6H, ^{3}J6.36 Hz, 2 × -CH_3).

[R]-[+]-7-[4-(E-4-n-Octadecyloxy-α-methylcinnamoyloxy)3-fluorobenzoyloxy]-2-naphthyl-2-[4-{4-(E-4-n-octadecyloxy-α-methylcinnamoyloxy)3-fluorobenzoyloxy} phenyloxy]propionate, (7.C.2)

Yield, 72%; m.p. 127°C; $[\alpha]_D^{25}$ = + 24.4°; ν_{max}: 2920, 2852, 1757, 1736, 1635, 1607, 1508, 1256, 1176 cm^{-1}; δ_H: 8.1-8.01(m, 4H, Ar-H), 7.94-7.88(m, 4H, Ar-H), 7.68-7.67(d, 1H, ^{4}J2.12 Hz, Ar-H), 7.51-7.34(m, 8H, Ar-H), 7.2-7.17(m, 3H, Ar-H), 7.09-7.07(d, 2H, ^{3}J9.08 Hz, Ar-H), 6.96-6.94(d, 4H, ^{3}J7.36 Hz, Ar-H), 5.06-5.04(q, ^{3}J6.8 Hz, 1H, Ar-O-C<u>H</u>(CH_3)-), 4.02-3.99(t, 4H, ^{3}J6.32 Hz, 2 × Ar-OCH_2-), 2.284-2.281(d, 6H, ^{4}J1.32 Hz, 2 × -CH=C(C<u>H</u>$_3$)COO-), 1.87-1.77(m, 7H, 1 × Ar-O-CH(C<u>H</u>$_3$), 2 × Ar-OCH_2-C<u>H</u>$_2$-), 1.47-1.26(m, 60H, 30 × -CH_2-), 0.89-0.86(t, 6H, ^{3}J6.6 Hz, 2 × -CH_3).

[S]-[+]-4-[4-(1-Methylheptyloxy)benzoyloxy]phenyl-3-[4-(4-n-decylbiphenyl-4-carbonyloxy)benzoyloxy]benzoate, (7.D.1)

Yield, 60%; m.p. 117°C; $[\alpha]_D^{25}$ = + 33.0°; ν_{max}: 2922, 2852, 1734, 1710, 1701, 1603, 1508,1256, 1163 cm^{-1}; δ_H: 8.32-8.31(d, 2H, ^{3}J8.76 Hz, Ar-H), 8.27-8.24(d, 2H, ^{3}J8.52 Hz, Ar-H), 8.14-8.06(m, 4H, Ar-H), 7.75-7.72(d, 2H, ^{3}J8.52 Hz, Ar-H), 7.62-7.51(m, 5H, Ar-H), 7.42-7.40(d, 2H, ^{3}J8.76 Hz, Ar-H), 7.30-7.24(m, 5H, Ar-H), 6.95-6.93(d, 2H, ^{3}J8.92 Hz, Ar-

H), 4.49-4.45(m, 1H, Ar-O-C<u>H</u>(CH_3)-), 2.67-2.63(t, 2H, ^{3}J7.6 Hz, 1 × Ar-CH_2-), 1.79-1.25(m, 29H, 13 × -CH_2- , 1 × -CH_3), 0.88-0.83(m, 6H, 2 × -CH_3). Elemental analysis: C_{58} H_{68} O_9 requires, C, 77.14; H, 6.92%; found, C, 77.33; H, 6.98%.

[S]-[+]-4-[4-(1-Methylheptyloxy)benzoyloxy]phenyl-3-[4-(4-n-undecylbiphenyl-4-carbonyloxy)benzoyloxy]benzoate, (7.D.2)

Yield, 63%; m.p. 120°C; $[\alpha]_D^{25}$ = + 40.3°; ν_{max}: 2922, 2854, 1740, 1732, 1716, 1700, 1603, 1506,1257, 1163 cm^{-1}; δ_H: 8.32-8.30(d, 2H, ^{3}J8.72 Hz, Ar-H), 8.27-8.24(d, 2H, ^{3}J8.48 Hz, Ar-H), 8.14-8.06(m, 4H, Ar-H), 7.75-7.72(d, 2H, ^{3}J8.48 Hz, Ar-H), 7.62-7.51(m, 5H, Ar-H), 7.42-7.40(d, 2H, ^{3}J8.76 Hz, Ar-H), 7.30-7.24(m, 5H, Ar-H), 6.95-6.93(d, 2H, ^{3}J8.96 Hz, Ar-H), 4.49-4.45(m, 1H, Ar-O-C<u>H</u>(CH_3)-), 2.67-2.63(t, 2H, ^{3}J7.68 Hz, 1 × Ar-CH_2-), 1.79-1.25(m, 31H, 14 × -CH_2- , 1 × -CH_3), 0.88-0.83(m, 6H, 2 × -CH_3). Elemental analysis: C_{59} H_{70} O_9 requires, C, 77.27; H, 7.03%; found, C,76.8; H, 7.11%.

[S]-[+]-4-[4-(1-Methylheptyloxy)benzoyloxy]phenyl-3-[4-(4-n-dodecylbiphenyl-4-carbonyloxy)benzoyloxy]benzoate, (7.D.3)

Yield, 65%; m.p. 122.5°C; $[\alpha]_D^{25}$ = + 36.7°; ν_{max}: 2922, 2852, 1742, 1734, 1715, 1701, 1605, 1506, 1257, 1163 cm^{-1}; δ_H: 8.32-8.30(d, 2H, ^{3}J8.68 Hz, Ar-H), 8.27-8.24(d, 2H, ^{3}J8.36 Hz, Ar-H), 8.14-8.06(m, 4H, Ar-H), 7.75-7.72(d, 2H, ^{3}J8.36 Hz, Ar-H), 7.62-7.51(m, 5H, Ar-H), 7.42-7.40(d, 2H, ^{3}J8.72 Hz, Ar-H), 7.30-7.24(m, 5H, Ar-H), 6.95-6.93(d, 2H, ^{3}J8.92 Hz, Ar-H), 4.49-4.46(m, 1H, Ar-O-C<u>H</u>(CH_3)-), 2.67-2.63(t, 2H, ^{3}J7.64 Hz, 1 × Ar-CH_2-), 1.79-1.25(m, 33H, 15 × -CH_2- , 1 × -CH_3), 0.88-0.82(m, 6H, 2 × -CH_3). Elemental analysis: C_{60} H_{72} O_9 requires, C, 77.39; H, 7.14%; found, C, 77.85; H, 7.23%.

[S]-[+]-4-[4-(1-Methylheptyloxy)benzoyloxy]phenyl 3-[4-(4-n-tetradecylbiphenyl-4-carbonyloxy)benzoyloxy]benzoate, (7.D.4)

Yield, 62%; m.p. 122.5°C; $[\alpha]_D^{25}$ = + 55.7°; ν_{max}: 2924, 2854, 1742, 1734, 1712, 1701, 1605, 1506, 1257, 1163 cm^{-1}; δ_H: 8.32-8.30(d, 2H, ^{3}J8.8 Hz, Ar-H), 8.27-8.24(d, 2H, ^{3}J8.52 Hz, Ar-H), 8.14-8.06(m, 4H, Ar-H), 7.75-7.72(d, 2H, ^{3}J8.52 Hz, Ar-H), 7.62-7.51(m, 5H, Ar-H), 7.42-7.40(d, 2H, ^{3}J8.76 Hz, Ar-H), 7.30-7.24(m, 5H, Ar-H), 6.95-6.93(d, 2H, ^{3}J8.92 Hz, Ar-H), 4.49-4.46(m, 1H, Ar-O-C<u>H</u>(CH_3)-), 2.67-2.63(t, 2H, ^{3}J7.68 Hz, 1 × Ar-CH_2-), 1.79-1.24(m, 37H, 17 × -CH_2- , 1 × -CH_3), 0.88-0.83(m, 6H, 2 × -CH_3). Elemental analysis: C_{62} H_{76} O_9 requires, C, 77.63; H, 7.36%; found, C, 77.34; H, 7.43%.

[S]-[+]-4-[4-(1-Methylheptyloxy)benzoyloxy]phenyl 3-[4-(4-n-dodecyloxybiphenyl-4-carbonyloxy)benzoyloxy]benzoate, (7.E.1)

Yield, 68%; m.p. 114.5°C; $[\alpha]_D^{25}$ = + 25.7°; ν_{max}: 2922, 2852, 1738, 1720, 1705, 1605, 1510, 1252, 1175 cm^{-1}; δ_H: 8.32-8.30(d, 2H, ^{3}J8.64 Hz, Ar-H), 8.25-8.23(d, 2H, ^{3}J8.36 Hz, Ar-H), 8.14-8.06(m, 4H, Ar-H), 7.71-7.69(d, 2H, ^{3}J8.32 Hz, Ar-H), 7.61-7.51(m, 5H, Ar-H), 7.42-7.40(d, 2H, ^{3}J8.64 Hz, Ar-H), 7.30-7.22(m, 3H, Ar-H), 7.0-6.98(d, 2H, ^{3}J8.72 Hz, Ar-H), 6.95-6.93(d, 2H, ^{3}J8.84 Hz, Ar-H), 4.48-4.45(m, 1H, Ar-O-C<u>H</u>(CH_3)-), 4.02-4.38(t, 2H, ^{3}J6.56 Hz, 1 × Ar-OCH_2-), 1.82-1.25(m, 33H, 15 × -CH_2- , 1 × -CH_3), 0.88-0.84(m, 6H, 2 × -CH_3). Elemental analysis: C_{60} H_{72} O_{10} requires, C, 76.09; H, 7.02%; found, C, 76.29; H, 7.14%.

REFERENCES

[1] F. Reinitzer, *Monatsh. Chem.*, **9**, 4221 (1888).

[2] "Molecular Structure and the Properties of Liquid Crystals" by G. W. Gray, Academic Press, London and New York (1962).

[3] "Thermotropic Liquid Crystals" by G. W. Gray (Society of Chemical Industry, John Wiley and Sons, 1987).

[4] Handbook of Liquid Crystals, Vol. 1: Fundamentals; Vol. 2A: Low Molecular Weight Liquid Crystals I; Vol. 2B: Low Molecular Weight Liquid Crystals II; and Vol. 3: High Molecular Weight Liquid Crystals, Edited by D. Demus, J. Goodby, G. W. Gray, H. W. Spiess and V. Vill (Wiley-VCH, 1998)

[5] R.B.Meyer, L.Liebert, L.Strzelecki and P.Keller, *J. de Phys. Lett.*, **36**, L-69 (1975).

[6] A. Fukuda, Y. Takanishi, T. Ishikawa and H. Takezoe, *J. Mater. Chem.*, **4**, 997 (1994).

[7] A.D.L.Chandani, E.Gorecka, Y.Ouchi, H.Takezoe and A.Fukuda, *Jpn. J. Appl. Phys.*, **28**, L1265, (1989).

[8] E.Gorecka, A.D.L.Chandani, Y.Ouchi, H.Takezoe and A.Fukuda, *Jpn. J. Appl. Phys.*, **29**, 131, (1990).

[9] P.G.de Gennes, *Solid State Commun.*, **10**, 753 (1972).

[10] (a) S. R. Renn and T. C. Lubensky, *Phys. Rev. A.*, **38**, 2132 (1988).
(b) J.W.Goodby, M.A.Waugh, S.M.Stein, E.Chin, R.Pindak and J.S. Patel, *Nature*, London, **337**,449 (1989).

[11] S. Chandrasekar, B. K. Sadashiva and K. A. Suresh, *Pramana,* **9**, 471 (1977).

[12] D. Vorlander, *Ber. Dtsch. Chem. Ges.*, **39**, 803 (1906).

[13] G. Pelzl, I. Wirth and W. Weissflog, *Liq. Cryst.*, **28**, 969 (2001).

[14] D. Vorlander and A. Apel, *Ber. Dtsch. Chem. Ges.*, **65**, 1101(1932).

[15] D. Vorlander, *Ber. Dtsch. Chem. Ges.*, **62**, 2831(1929).

[16] D. Demus, *Liq. Cryst.*, **5**, 75 (1989).

[17] M. Kuboshita, Y.Matsunaga and M.Matsuzaki, *Mol. Cryst. Liq. Cryst.*, **199**, 319 (1991).

[18] M. Matsuzaki and M. Kuboshita, *Liq. Cryst.*, **14**, 105 (1993).

[19] T.Akutagawa, Y.Matsunaga and K.Yashubara, *Liq. Cryst.*, **17**, 659 (1994).

[20] T.Niori, T.Sekine, J.Watanabe, T.Furukawa and H.Takezoe, *J. Mater. Chem.*, **6**, 1231 (1996).

[21] R. B. Meyer, *Mol. Cryst. Liq. Cryst.*, **40**, 33 (1977).

[22] T.Sekine, Y.Takanishi, T.Niori, J.Watanabe and H.Takezoe, *Jpn. J. Appl. Phys.*, **36**,

L1201 (1997).

[23] T.Sekine, T.Niori, M.Sone, J.Watanabe, S.W.Choi, Y.Takanishi and H.Takezoe, *Jpn. J. Appl. Phys.*, **36**, 6455 (1997).

[24] T.Sekine, T.Niori, J.Watanabe, T.Furukawa, S.W.Choi and H.Takezoe, *J. Mater. Chem.*, **7**,1307 (1997).

[25] T.Niori, T.Sekine, J.Watanabe, T.Furukawa and H.Takezoe, *Mol. Cryst. Liq. Cryst.*, **301**, 337 (1997).

[26] D. Shen, S. Diele, I. Wirth and C. Tschierske, *Chem. Commun.*, 2573(1998).

[27] A. Jakli, CH. Lischka, W. Weissflog, S. Rauch and G. Heppke, *Mol. Cryst. Liq. Cryst.*, **328**, 299 (1999).

[28] D. R. Link, G. Natale, R. Shao, J. E. Maclennan, N. A. Clark, E. Körblova and D. M. Walba, *Science*, **278**, 1924 (1997).

[29] G. Heppke, D. Krüerke, C. Löhning, D. Lötzsch, S. Rauch and N. K. Sharma, Freiburger Arbeitstagung *Flüssige Kristalle*, Freiburg, Germany, Poster P 70 (1997).

[30] W. Weissflog, C. Lischka, I. Benne, T. Scharf, G. Pelzl, S. Diele and H. Kruth, *Proc. SPIE: Int. Soc. Opt. Eng.*, **3319**, 14 (1998).

[31] H. R. Brand, P. E. Cladis and H. Pleiner, *Eur. J. Phys. (B).*, **6**, 347 (1998).

[32] G. Pelzl, S. Diele and W. Weissflog, *Adv. Mater.*, **11**, 707 (1999).

[33] J.Watanabe, T.Niori, T.Sekine and H.Takezoe, *Jpn. J. Appl. Phys.*, **37**, L139 (1998).

[34] D. Shen, A. Pegenau, S. Diele, I. Wirth and C. Tschierske, *J. Am. Chem. Soc.*, **122**, 1593 (2000).

[35] B. K. Sadashiva, *Pramana,* **53**, 231 (1999).

[36] B. K. Sadashiva, V. A. Raghunathan and R. Pratibha, *Ferroelectrics*, **243**, 29 (2000).

[37] S. Diele, S.Grande, H.Kruth, C.Lischka, G.Pelzl, W.Weissflog and I.Wirth, *Ferroelectrics*, **212**, 169 (1998).

[38] J. P. Bedel, J. C. Rouillon, J. P. Marcerou, M. Laguerre, H. T. Nguyen and M. F. Achard, *J. Mater. Chem.*, **12,** 2214 (2002)

[39] G. Heppke and D. Moro, *Science*, **279**, 1872 (1998).

[40] H. R. Brand, P. E. Cladis and H. Pleiner, *Macromolecules*, **25**, 7223 (1992).

[41] H. Nadasi, W. Weissflog, A. Eremin, G. Pelzl, S. Diele, B. Das and S. Grande, *J. Mater. Chem.*, **12**, 1316 (2002).

[42] D. Shen, S. Diele, G. Pelzl, I. Wirth and C. Tschierske, *J. Mater. Chem.*, **9**, 661 (1999).

[43] J. C. Rouillon, J. P. Marcerou, M. Laguerre, H. T. Nguyen and M. F. Achard, *J. Mater.*

Chem., **11**, 2946 (2001).

[44] G. Pelzl, S. Diele, A. Jakli, C. Lischka, I. Wirth and W. Weissflog, *Liq. Cryst.*, **26**, 135 (1999).

[45] A. Jakli, CH. Lischka, W. Weissflog, G. Pelzl and A. Saupe, *Liq. Cryst.*, **27**,1405 (2000).

[46] P. G. de Gennes, *The Physics of Liquid Crystals* (Oxford: Clarendon Press, 1975).

[47] P. E. Cladis, H. Pleiner and H. R. Brand, in Abstracts of the 7 th International Conference on Ferroelectric Liquid Crystals, Darmstadt, Germany, pp. 2-3 (1999).

[48] W. Weissflog, H. Nadasi, U. Dunemann, G. Pelzl, S. Diele, A. Eremin and H. Kresse, *J. Mater. Chem.*, **11**, 2748 (2001).

[49] N. A. Clark, D. R. Link, D. Coleman, W. G. Jang, J. Fernsler, C. Boyer, J. Zasadzinski, D. M. Walba, E. Korblova and W. Weissflog, Book of abstracts, 19 th International Liquid Crystal Conference, 30 June-5 July, Edinburgh, U. K., C5 (2002).

[50] J. P. Bedel, J. C. Rouillon, J. P. Marcerou, M. Laguerre, H. T. Nguyen and M. F. Achard, *Liq. Cryst.*, **28**, 1285 (2001).

[51] J. P. Bedel, J. C. Rouillon, J. P. Marcerou, M. Laguerre, H. T. Nguyen and M. F. Achard, *Liq. Cryst.*, **27**, 1411 (2000).

[52] H. T. Nguyen, J. C. Rouillon, J. P. Marcerou, J. P. Bedel, P. Barois and S. Sarmento, *Mol. Cryst. Liq. Cryst.*, **328**, 177 (1999).

[53] A. Eremin, I. Wirth, S. Diele, G. Pelzl, H. Schmalfuss, H. Kresse, H. Nadasi, K. Fodor-Csorba, E. Gacs-Baitz and W. Weissflog, *Liq. Cryst.*, **29**, 775 (2002).

[54] D. M. Walba, E. Korblova, R. Shao, J. E. Maclennan, D. R. Link, M. A. Glaser and N. A. Clark, *Science*, **288** (2000).

[55] G. Heppke, D. D. Parghi and H. Sawade, *Liq. Cryst.*, **27**, 313 (2000).

[56] C. K. Lee, A. Primak, A. Jakli, E. J. Choi, W. C. Zin and L. C. Chien, *Liq. Cryst.*, **28**, 1293 (2001).

[57] I. Dierking, H. Sawade and G. Heppke, *Liq. Cryst.*, **28**,1767 (2001).

[58] A. Jakli, G. G. Nair, C. K. Lee, R. Sun, and L. C. Chien, *Phys. Rev. E.*, 63, 061710 (2001).

[59] J. P. Bedel, J. C. Rouillon, J. P. Marcerou, M. Laguerre, M. F. Achard, and H. T. Nguyen *Liq. Cryst.*, **27**, 103 (2000).

[60] H. Dehne, M. Potter, S. Sokolowski, W. Weissflog, S. Diele, G. Pelzl, I. Wirth, H. Kresse, H. Schmalfuss and S. Grande, *Liq. Cryst.*, **28**, 1269 (2001).

[61] H. N. Shreenivasa Murthy and B. K. Sadashiva, *Liq. Cryst.*, **29**, 1223 (2002).

[62] L. Kovalenko, W. Weissflog, S. Grande, S. Diele, G. Pelzl and I. Wirth, *Liq. Cryst.*, **27**,

683 (2000).

[63] J. Thisayukta, H. Kamee, S. Kawauchi and J. Watanabe, *Mol. Cryst. Liq. Cryst.*, **346**, 63 (2000).

[64] J. Thisayukta, Y. Nakayama and J. Watanabe, *Liq. Cryst.*, **27**, 1129 (2000).

[65] J. Thisayukta, H. Niwano, H. Takezoe and J. Watanabe, *J. Mater. Chem.*, **11**, 2717 (2001).

[66] B. K. Sadashiva, H. N. Shreenivasa Murthy and Surajit Dhara, *Liq. Cryst.*, **28,** 483 (2001).

[67] I. Wirth, S. Diele, A. Eremin, G. Pelzl, S. Grande, L. Kovalenko, N. Pancenko and W. Weissflog, *J. Mater. Chem.*, **11**, 1642 (2001).

[68] G. Heppke, D. D. Parghi and H. Sawade, *Ferroelectrics,* **243**, 269 (2000).

[69] C. K. Lee and L. C. Chien, *Ferroelectrics,* **243**, 231 (2000).

[70] C. K. Lee and L. C. Chien, *Liq. Cryst.*, **26,** 609 (1999).

[71] A. Eremin, S. Diele, G. Pelzl, H. Kresse, S. Grande, H. Nadasi and W. Weissflog, Book of Abstracts, 19th International Liquid Crystal Conference, 30 June - 5 July, Edinburgh, U.K., C5 (2002).

[72] G. H. Brown, (ed.), Liquid Crystals, Vol. 2, part-I, Synopsis of Panel Discussion on Applications, pp. 217-232, Gordon and Breach, New York (1969).

[73] A. Jakli, L. C. Chien, D. Kruerke, H. Sawade and G. Heppke, *SID Intl. Digest Tech. Papers*, (2001).

[74] P. E. Cladis, H. R. Brand and H. Pleiner, *Liq. Cryst. Today,* Vol. 9, No. **3/4** (1999).

[75] J. Prost and P. Barois, *J. Chim. Phys.*, **80**, 65 (1983).

[76] R. G. Petschek and K. M. Wiefling, *Phys. Rev. Lett.*, **59**, 343 (1987).

[77] F. Tournilhac, L. M. Blinov, J. Simon and S. V. Yablonsky, *Nature,* **359**, 621 (1992).

[78] J. Watanabe, Y. Nakata and K. Shimizu, *J. Phys. II (France).*, **4**, 581 (1994).

[79] J. Thisayukta, Y. Nakayama, S. Kawauchi, H. Takezoe and J. Watanabe, *J. Am. Chem. Soc.*, **122**, 7441 (2000).

[80] N. Kasthuraiah, B. K. Sadashiva, S. Krishnaprasad and G. G. Nair, *Liq. Cryst.*, **24,** 639 (1998).

[81] S. M. Kelly, *Helv. Chim. Acta.*, **67**, 1572 (1984).

[82] G. W. Gray, C. Hogg and D. Lacey, *Mol. Cryst. Liq. Cryst.*, **67**, 1 (1981).

[83] C. Weygand and R. Gabler, *Z. Phys. Chem.*, **B46**, 270 (1940).

[84] G. W. Gray and B. Jones, *J. Chem. Soc.*, 4179 (1953).

[85] G. W. Gray and B. Jones, *J. Chem. Soc.*, 2556 (1954).

[86] M. F. Nabor, H. T. Nguyen, C. Destrade, J. P. Marcerou and R. J. Twieg, *Liq. Cryst.*, **10,** 785 (1991).

[87] H. T. Nguyen, A. Babeau, J. C. Rouillon, G. Sigaud, N. Isaert and F. Bougrioua, *Ferroelectrics*, **179**, 33 (1996).

[88] W. Weissflog, CH. Lischka, S. Diele, I. Wirth and G. Pelzl, *Liq. Cryst.*, **27**, 43 (2000).

[89] W. Weissflog, I. Wirth, S. Diele, G. Pelzl and H.Schmalfuss, *Liq. Cryst.*, **28**, 1603 (2001).

[90] M. Nakata, D. R. Link, F. Araoka, J. Thisayukta, Y. Takanishi, K. Ishikawa, J.Watanabe and H. Takezoe, *Liq. Cryst.*, **28**, 1301 (2001).

[91] S. Rauch, P. Bault, H. Sawade, G. Heppke, G. G. Nair and A. Jakli, *Phys. Rev. E.*, **66**, 021706 (2002).

[92] C. K. Lee, S. S. Kwon, S. T. Shin, E. Choi, S. Lee and L. C. Chien, *Liq. Cryst.*, **29**, 1007 (2002).

[93] G. Dantlgraber, A. Eremin, S. Diele, A. Hauser, H. Kresse, G. Pelzl and C. Tschierske, *Angew. Chem., Int. Ed.* **13**, 41 (2002).

[94] G. Dantlgraber, D. Shen, S. Diele and C. Tschierske, *Chem. Mater.*, **14**, 1149 (2002).

[95] J. Matraszek, J. Mieczkowski, J. Szydlowska and E. Gorecka, *Liq. Cryst.*, **27**, 429(2000).

[96] G. W. Gray and B. Jones, *J. Chem. Soc.*, 1467 (1954).

[97] J. R. Johnson, " *Organic Reactions*", Vol. 1, Eds. R. Adams, W. E. Bachmann, L. F. Fieser, J. R. Snyder, John Wiley & Sons, New York, p.210 (1942).

[98] B. K. Sadashiva, *Mol. Cryst. Liq. Cryst.*, **35**, 205 (1976).

[99] K. Wang, A. Jakli, H. Li, Y. Yang and J. Wen, *Liq. Cryst.*, **28**, 1705(2001).

[100] A. Jakli, D. Kruerke, H. Sawade and G. Heppke, *Phys. Rev. Lett.*, **25**, 5715 (2001).

[101] J. Mieczkowski, J. Szydlowska, J. Matraszek, D. Pociecha, E. Gorecka, B. Donnio and D. Guillon, *J. Mater. Chem.*, **12**, 3392 (2002).

[102] K. Fodor-Csorba, A. Vajda, G. Galli, A. Jakli, D. Demus, S. Holly, E. Gacs-Baitz, *Macromol. Chem. Phys.*, **203**, 1556 (2002).

[103] G. Dantlgraber, U. Baumeister, S. Diele, H. Kresse, B. Luhmann, H. Lang and C. Tschierske, *J. Am. Chem. Soc.*, **124**, 14852 (2002).

[104] G. Pelzl, S. Diele, S. Grande, A. Jakli, C. Lischka, H. Kresse, H. Schmalfuss, I. Wirth and W. Weissflog, *Liq. Cryst.*, **26**, 401 (1999).

[105] W. Weissflog, C. Lischka, S. Diele, G. Pelzl and I. Wirth, *Mol. Cryst. Liq. Cryst.*, **328**, 101 (1999).

[106] W. Weissflog, C. Lischka, S. Diele, G. Pelzl, I. Wirth, S. Grande, H. Kresse, H.

Schmalfuss, H. Hartung and A. Stettler, *Mol. Cryst. Liq. Cryst.*, **333**, 203 (1999).

[107] D. S. Shankar Rao, G. G. Nair, S. Krishna Prasad, S. Anita Nagamani and C. V. Yelamaggad, *Liq. Cryst.*, **28**, 1239 (2001).

[108] D. M. Walba, E. Korblova, R. Shao and N. A. Clark, *J. Mater. Chem.*, **11**, 2743 (2001).

[109] (a) Chemical Index, D-05321 and D-05324; (b) Commercial compound
(c) F. Juncai, L. Bin, L. Yang and L. Changchuan, *Synth. Commun.*, **26**, 4545-4548 (1996).

[110] D. S. Kemp, D. D. Cox and K. G. Paul, *J. Am. Chem. Soc.*, **25**, 7312 (1975).

[111] B. K. Sadashiva and G. S. R. Subba Rao, *Mol. Cryst. Liq. Cryst.*, **38**, 703 (1977).

[112] F. Jones, Ph. D. Thesis, Harvard University (1972); P. G. de Gennes, The Physics of Liquid Crystals, p. 304 (Oxford University Press, Oxford, 1974).

[113] H. N. Shreenivasa Murthy and B. K. Sadashiva, Book of Abstracts, 19th International Liquid Crystal Conference, 30 June - 5 July, Edinburgh, U.K., P 422 (2002).

[114] N. A. Clark, D. R. Link, D. Coleman, W. G. Jang, J. Fernsler, C. Boyer, J. Zasadzinski, D. M. Walba, E. Korblova and W. Weissflog, Book of Abstracts, 19th International Liquid Crystal Conference, 30 June - 5 July, Edinburgh, U.K., C5 (2002).

[115] P. G. de Gennes, "*The Physics of Liquid Crystals*", Clarendon Press, Oxford (1974).

[116] P. G. de Gennes, *The Physics of Liquid Crystals*, Clarendon Press, Oxford, 3rd ed. (1982).

[117] W. L. McMillan, *Phys. Rev. A4.*, 1238 (1971).

[118] W. L. McMillan, *Phys. Rev. A8.*, 1921 (1973).

[119] H. R. Brand, P. E. Cladis and H. Pleiner, *Macromolecules*, **25**, 7223, (1992).

[120] H.F. Leube and H.Finkelmann, *Makromol. Chem.*, **192**, 1317 (1991).

[121] K. J. K. Semmler, T. J. Dingemans and E. T. Samulski, *Liq. Cryst.*, **24**, 799 (1998).

[122] T. Hegmann, J. Kain, S. Diele, G. Pelzl and C. Tschierske, *Angew. Chem., Int. Ed.* **40**, 887 (2001).

[123] R. Pratibha, N.V. Madhusudana and B.K. Sadashiva, *Science,* **288**, 2184 (2000); R. Pratibha, N.V. Madhusudana and B.K. Sadashiva, *Mol.Cryst.Liq.Cryst.*, **365**, 755 (2001).

[124] B. K. Sadashiva, *Mol.Cryst.Liq.Cryst.*, **55**, 135 (1979).

[125] M. Prehm, X. H. Cheng, S. Diele, M. K. Das, and C. Tschierske, *J. Am. Chem. Soc.*, **124**,12072 (2002).

[126] M. Prehm, S. Diele, M. K. Das, and C. Tschierske, *J. Am. Chem. Soc.*, **125**, 614 (2003).

[127] A. Eremin, S. Diele, G. Pelzl, H. Nadasi, W. Weissflog, J. Salfetnikova and H. Kresse, *Phys. Rev., E,* **64**, 51707 (2001).

[128] M. W. Schroder, S. Diele, N. Pancenko, W. Weissflog and G. Pelzl, , *J. Mater. Chem.,* **12**, 1331 (2002).

[129] N.V. Madhusudana and S.Chandrasekhar, *Pramana Supplement,* **1**, 57 (1975).

[130] A.J. Leadbetter, J.C. Prost, J.P. Gaughan, G.W. Gray and A. Mosley, *J.Phys.*, **40**, 375 (1979).

[131] D.Coates and G.W.Gray, *Phys. Lett.*, **45A**, 115 (1973).

[132] D.W.Berreman, *Liquid Crystals and Ordered Fluids*, Plenum Press, New York, **4**, 925 (1984).

[133] A. Fukuda, Y. Takanishi, T. Isozaki, K. Ishikawa and H. Takezoe, *J. Mater. Chem.,* **4**, 997 (1994).

[134] G. W. Gray, J. B. Hartly and B. Jones, *J. Chem. Soc.,* 1412 (1955).

[135] O. Mitsunobu and M. Eguchi, *Bull. Chem. Soc.,* Japan, **44**, 3427, (1971).